THE UNIVERSITY *of* EDINBURGH

Ecological genetics of the invasive tree pathogen *Phytophthora austrocedri* and its native host juniper

Daisy Crowson

A thesis submitted for the degree of Doctor of Philosophy

Institute of Ecology and Evolution

The University of Edinburgh

2025

Abstract

Invasive tree pathogens are a growing threat to natural and managed ecosystems, causing severe ecological and economic impacts. The outcome of novel plant-pathogen interactions depends on a complex suite of evolutionary and ecological processes that are unique to each system. Understanding these interactions therefore requires taking diverse and complementary approaches: quantitative genetics can be employed to address questions regarding host resistance; population genetics and genomics can be used to explore key pathogen traits and evolutionary history; and molecular analyses can provide a mechanistic insight into the host-pathogen interaction. This thesis integrates these approaches to investigate the evolutionary and ecological dynamics of the invasive oomycete pathogen *Phytophthora austrocedri* and its UK-native host juniper (*Juniperus communis*). In Chapter 1, I outline the framework of my research by introducing the background of the rising problem of invasive plant pathogens, discussing the evolutionary-ecology of novel host-pathogen interactions and describing the pathosystem. Chapter 2 investigates the presence and nature of any resistance to the pathogen in natural host populations. By means of a progeny-provenance inoculation trial I show that: resistance in juniper is a heritable genetic trait; juniper has both qualitative and quantitative variation in resistance; and *P. austrocedri* is imposing natural selection on juniper populations, with a higher frequency of resistant juniper individuals found in populations previously exposed to the pathogen. In Chapter 3, I present new, high-quality reference genomes for each of the two distinct geographical lineages of *P. austrocedri*, establishing the first genomic resources for this species. In Chapter 4, I explore large-scale genome evolution, population genomics, and genetic diversity in the pathogen. I use flow cytometry and whole-genome sequence data to show that *P. austrocedri* is a tetraploid, but that variation in genome size and evidence of large genomic deletions suggest diploidisation and triploidisation is occurring in some isolates. I confirm that *P. austrocedri* is of hybrid origin, with the hybridisation event likely predating the divergence of the two lineages. I also show that levels of genome-wide genetic diversity and within-subgenome heterozygosity in the pathogen are very low, suggesting a history of self-fertilisation, but that the hybrid nature of the pathogen allows it to maintain high levels of between-subgenome heterozygosity. Chapter 5 investigates the molecular basis of resistance in the host and of virulence in the pathogen using dual RNAseq of the host-pathogen interaction. I show that a successful defence response in juniper is characterised by rapid induction of ethylene signalling and associated production of secondary metabolites and pathogenesis-related proteins, and I identify a candidate transmembrane receptor that may underlie this rapid

response. I also show that increased virulence in the pathogen appears linked to enhanced suppression and evasion of host defences, which may also allow an extended biotrophic phase, and I identify candidate genes that may be driving these differences. Finally, in Chapter 6, I synthesise the findings of the previous chapters and set them within the broader context of research into the evolutionary ecology of novel host-pathogen interactions. I conclude by outlining some practical recommendations for managing the juniper-*P. austrocedri* pathosystem that arise from the results presented in this thesis. In summary, this research integrates quantitative genetics, genomics, and molecular analyses to advance our understanding of the evolutionary dynamics underlying novel plant-pathogen interactions.

Lay summary

Invasive tree pathogens are becoming an increasing threat to forests and natural landscapes around the world. Tree pathogens can have particularly devastating ecological and economic impacts when they are introduced into a new geographical area and are presented with the opportunity to infect a new host species. The outcome of these new plant-pathogen interactions depends on many factors, including the genetics of any resistance found in tree populations, the biology and evolution of the pathogen, and the molecular basis of the interaction between them. To understand and manage these new diseases, we therefore need to study both sides of the plant-pathogen interaction, using a range of scientific approaches. This thesis combines genetic, ecological and molecular methods to investigate the invasive pathogen *Phytophthora austrocedri* and its UK-native host juniper (*Juniperus communis*). The results show that some juniper individuals are naturally resistant to infection, and that this resistance has a genetic basis that can be inherited. In areas where the disease has been present for longer, resistant trees are more common, suggesting that natural selection is already favouring them. On the pathogen side, new genome data reveal that *P. austrocedri* has a complex evolutionary history: it is a hybrid species with four copies of each chromosome, and seems to mostly be reproducing through self-fertilisation. Despite low levels of genetic diversity, the hybrid nature of the pathogen may allow it to maintain high levels of evolutionary potential. Finally, by studying juniper trees infected with *P. austrocedri* on a molecular level, this thesis identifies important determinants of disease resistance and susceptibility. Resistant juniper individuals rapidly recognise the pathogen and activate chemical defences and signalling pathways that help to limit infection, while more aggressive strains of the pathogen appear better able to avoid or suppress these defences. The thesis concludes by outlining some practical management advice to mitigate the impact of *P. austrocedri* on UK juniper populations that arises from these findings. Overall, this research integrates the genetics of disease resistance in trees, the evolutionary history of pathogens, and the molecular interaction between them to improve our understanding of the evolution of novel plant-pathogen interactions.

Acknowledgements

First, I would like to thank my supervisors: Stephen Cavers, Joan Cottrell, Richard Ennos and Sarah Green. I list them alphabetically, because each contributed uniquely while demonstrating an exceptional ability to work collaboratively as true co-supervisors. Their guidance, advice and input has been invaluable to the work presented in this thesis, and their unhesitating support and understanding through a few tough times has been deeply appreciated. I have learned so much from their wealth of knowledge and from their approach to doing research, and I owe a large part of the enjoyment, satisfaction and enthusiasm I have felt while doing this PhD to them.

I would like to thank members of the Forest Research and CEH teams who helped and advised me in the lab and greenhouse, including Carolyn Riddell (advice and support), Heather Dun (juniper watering), Maria Stanisz-Migal (extractions), Debbie Frederickson-Matika (zoospores), Stuart A'Hara (juniper genotyping) and Annika Perry (flow cytometry).

Thank you to Graham Stone for his insightful and good-natured contributions to my thesis in his role as committee chair. Also Jarrod Hadfield, to whom I owe most of my understanding of random effects and link functions.

Thank you to everyone at the E4 DTP for giving me this incredible opportunity, and for providing such a welcoming and encouraging start to my PhD programme.

I have to give a shout-out to the marvellous crew of people who inhabit Ashworth and make it such a special place to work. And among that already special crowd, I would like to give an extra thanks to Hend: a kindred spirit who helped keep me sane during Edinburgh winters and happy during Edinburgh summers.

I would like to thank my mum and dad for supporting me with their unconditional love and understanding, and for all those encouraging postcards that felt like hugs. Also my sister, whose casual conquering of a PhD with two toddlers in tow was a constant source of inspiration for me, and whose unique combination of practical wisdom and irreverent humour is the best tonic for the vicissitudes of (graduate student) life.

Finally, I am so full of gratitude toward Stuart. I would like to thank him for all the thoughtful advice he has offered; for his willingness to discuss the various methodological, statistical and bioinformatic hurdles I have faced along the way; and for the encouraging words, Michelin-worthy meals, and glasses of thesis wine that helped me over the finish line. Most of all, I thank him for the love and support he has shown me on every step of this journey, and for his unswerving belief in me. He always thought I could do this; I know I could not have done it without him.

Table of Contents

List of Figures

List of Tables

CHAPTER 1:
Introduction

1.1 The problem of invasive plant pathogens

Invasive plant pathogens pose a significant threat to both natural and managed ecosystems. In agriculture, pathogens are routinely implicated in reduced crop yield and quality, threatening global food security (Strange and Scott 2005; Oerke 2006; Ristaino et al. 2021). In forestry, tree pathogens can lead to wide-scale decimation of important timber trees, with major economic and environmental costs (Lovett et al. 2016; Kenis et al. 2017). Finally, invasive pathogens can also have disastrous ecological effects, with landscape-wide devastation and even extirpation of keystone species (Garbelotto and Gonthier 2022; D'Amato et al. 2023).

The costs associated with invasive plant pathogens are difficult to quantify – while pathogens of major global agricultural or forestry crops can cause damages worth billions of dollars in yield losses alone (Pimentel et al. 2005; Tyler 2007; Pennisi 2010), economic costs of pathogens will also encompass management, research, surveillance, and loss of social and environmental value (Downey et al. 2025). For example, ash dieback has been estimated to cost the UK £888 million annually (Hill et al. 2019; Eschen et al. 2023), despite ash not representing a commercially important timber species. Beyond economic costs, invasive pathogens can also disrupt ecosystems, have severe knock-on ecological impacts, and cause major and irreversible shifts in culturally and environmentally significant landscapes (Lovett et al. 2016; Garbelotto and Gonthier 2022; D'Amato et al. 2023). Diseases such as sweet chestnut blight, Dutch elm disease or ash dieback have effects so far-reaching that they have become well-known concerns to the general public, and routinely reach national-level news (e.g., Briggs 2019; Kinver 2020; Carrington 2025). Altogether, the hugely significant economic, ecological and societal impacts of invasive plant pathogens are undeniable.

Human action is increasingly moving species outside their native ranges (van Kleunen et al. 2015), both deliberately and accidentally. Continually expanding global trade networks have been shown to be responsible for the incidental introduction of plant pathogens into new areas (Banks et al. 2015; Chapman et al. 2017), and plant nurseries and the ornamental trade have repeatedly been associated with the introduction and spread of a wide range of plant pathogens (Jones and Baker 2007; Puertolas et al. 2021). This accidental transportation of pathogens can occur through the movement of packaging, bark, wood products, seeds,

cuttings or flowers, as well as live plants and associated soil (Liebhold et al. 2012; Santini et al. 2013). Meanwhile, the changing climate is shifting the ranges of both hosts (Pecl et al. 2017) and pathogens (Bebber et al. 2013; Dudney et al. 2021), bringing together new host-pathogen combinations. Milder winters may also allow more pathogen inocula to overwinter, which could lead to more frequent and severe disease outbreaks (Velásquez et al. 2018). Finally, climate change is also likely to cause abiotic stress to host plants (Chaudhry and Sidhu 2021), making them less able to tolerate and resist infection (Desprez-Loustau et al. 2006). The threat posed by invasive plant pathogens is therefore ever-increasing.

1.2 Evolutionary-ecology of novel host-pathogen interactions

Plant pathogens have a profound impact on the ecology and evolution of their hosts, driving host population dynamics (Jeger et al. 2014; Zhan et al. 2021), influencing community composition and succession (Hansen and Goheen 2000; Mordecai 2011), and exerting major selective pressures that are implicated in processes as fundamental as the maintenance of genetic diversity in populations (Delph and Kelly 2014) and of sexual reproduction in species (Levin 1975; Busch et al. 2004). Pathogens impose selection on plants for increased resistance, and host plants in turn exert selective pressure on pathogens to overcome host defences, resulting in a classic co-evolutionary relationship; indeed, the first use of the term "co-evolution" was in relation to plant-pathogen interactions (Mode 1958). These systems are characterised by negative frequency-dependent selection, spatial and temporal heterogeneity in disease prevalence, and the cost of resistance and virulence (Burdon and Thrall 2009; Brown and Tellier 2011; Burdon and Laine 2019), factors that keep the interactions dynamic and ensure neither side emerges completely victorious. In natural populations, host-pathogen interactions are thus expected to develop into intimate, dynamically stable co-evolutionary relationships, where each party responds to the ever-changing selective pressures imposed by the other (Brown and Tellier 2011; Ennos 2015).

When this co-evolutionary history between host and pathogen is absent, however – for instance, in the case of newly introduced plant pathogens or hosts – the outcome of these host-pathogen encounters becomes difficult to predict, and will depend on a complex set of interacting ecological and evolutionary processes (Parker and Gilbert 2004; Ennos 2015; Desprez-Loustau et al. 2016). In most cases, the introduced pathogen will fail to cause any infection due to either an unfavourable environment or a lack of susceptible hosts (Agrios 2005; Parker and Gilbert 2004). However, in cases where by chance the pathogen does

encounter a suitable host, the lack of a shared co-evolutionary relationship means that the susceptible host is likely to be almost *universally* susceptible, as alleles that confer resistance are not expected to be segregating at high frequencies in the population (Ennos 2015). These novel host-pathogen encounters can therefore sometimes result in a catastrophic collapse of the host population (e.g., Ristaino 2002; Rigling and Prospero 2018).

Some resistance to the novel pathogen may, however, already be present in the host population at low frequencies, either arising by chance through random mutation or due to prior exposure to a pathogen with a similar mode of action, resulting in some degree of preadaptation (Parker and Gilbert 2004). As the pathogen spreads through the population, any resistance alleles would be strongly selected for, which could result in evolutionary rescue (Carlson et al. 2014). Under this process, following an initial large decrease in size due to high mortality among susceptible genotypes, the population would recover through preferential survival and reproduction of resistant genotypes, thereby avoiding extinction.

However, evolutionary rescue is a concept usually applied in the context of abiotic stress (but see Searle and Christie 2021). When dealing with biotic stress such as an invading pathogen, the dynamics are more complex, because the pathogen can in turn respond to any adaptation in the host population. For instance, a new pathogen variant may arise that is able to infect the previously resistant host genotype. This could be particularly likely in the case of an epidemic situation with a booming pathogen population spreading rapidly through a mostly susceptible host. Under such conditions, the pathogen population would be large and growing, and evolution would favour it to overwhelm any host resistance (Ennos 2015). Conversely, if the pathogen has low levels of genetic diversity and limited dispersal ability, the balance may shift in favour of the host, particularly when host populations harbour substantial standing genetic variation. Given the right circumstances, these novel pathosystems could therefore develop over time into the kind of sustainable co-evolutionary relationship that characterises the interaction between long-established pathogens and their native hosts (Figure 1.1).

The durability of resistance and the eventual outcome for the host population will thus depend on a range of complex eco-evolutionary factors, including: i) the nature of host resistance, where complete (qualitative) resistance mediated by a single gene is less robust than partial (quantitative) resistance governed by multiple genes (Brown 2015); ii) the population size, reproductive strategy and mode of transmission of the pathogen, where rapid

dispersal and properties that give rise to high genetic diversity will increase the probability of the pathogen overwhelming host resistance (Parker and Gilbert 2004; Ennos 2015); and iii) the ecology and life history of the host, where small populations, long generation times and low regeneration rates will make the host more vulnerable, and put them at a disadvantage compared to the pathogen (Gilbert 2002; Ennos 2015).

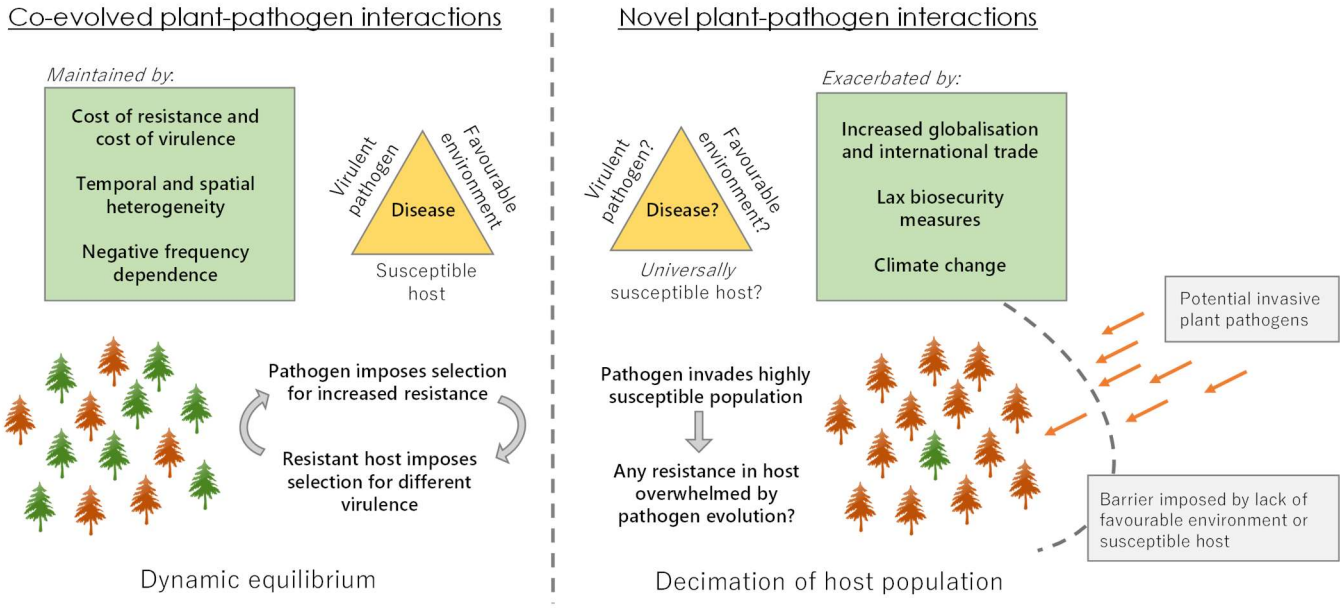

Figure 1.1. Comparison between the expectation of dynamic equilibrium for co-evolved plant-pathogen interactions, and the problem of introduced plant pathogens, which can result in the decimation of the novel host's population. Although the chance of any one introduced pathogen causing disease is low, as the number of incidents increases the probability of one succeeding increases. The lack of a co-evolutionary relationship means the susceptible host may be (almost) universally susceptible.

1.3 Understanding novel host-pathogen interactions requires diverse approaches

Novel host-pathogen interactions are complex systems to study, with a broad suite of ecological and evolutionary processes governing their dynamics on both sides of the interaction. Understanding these systems therefore requires a combination of complementary approaches, each providing a distinct but interconnected perspective on the interaction.

The host side is often best explored through quantitative genetics, which can reveal the presence, frequency, and nature of resistance within natural populations. This typically involves carrying out experiments that look at the phenotype of related individuals grown in a common

environment to determine the amount of genetic variation that exists for a trait (for example, resistance). Although this approach does not identify the specific genes or molecular mechanisms underlying resistance, it provides crucial information about the heritability of resistance (e.g., Frampton et al. 2018; Xu et al. 2021; de la Mata et al. 2024), which is a key parameter underlying the adaptive potential of the host population. In addition, these experiments can also provide insight into the genetic architecture of resistance traits based on the distribution of resistance phenotypes within and among families (Sniezko et al. 2019). Importantly, quantitative genetics requires no prior genomic resources, making it a particularly useful tool when studying trees such as conifers, which have extremely large and highly repetitive genomes that make genome sequencing and assembly a difficult task, even with modern sequencing technologies (de la Torre et al. 2014). Thus, quantitative genetics has a strong history of being used in tree-breeding programmes, contributing to the development of durable resistance in several commercially important forest species (Sniezko et al. 2014; Sniezko and Nelson 2022).

On the other hand, factors influencing the pathogen side of the interaction are often better suited to being studied through population genetics and genomics. Analysing the distribution of alleles and genotypes in pathogen populations can reveal the pathogen's evolutionary and population history, genetic diversity and divergence of lineages, signatures of positive selection, and evidence of rapid adaptation (Everhart et al. 2021). In addition, whole-genome approaches can provide insights into large genome structure and the distribution of diversity across the genome, which can be used to understand major pathogen evolutionary processes, such as polyploidy, hybridisation and the rapid proliferation of virulence-related genes. These approaches have been used to determine a pathogen's origin (Jung et al. 2021; Tsykun et al. 2022), date of introduction (Winkworth et al. 2021), mode of reproduction (Capador et al. 2020), hybridisation events (Goss et al. 2011; Van Poucke et al. 2021), ploidy (Morales-Cruz et al. 2020), and number and distribution of virulence-related proteins (Haas et al. 2009; Lee et al. 2021), all key factors on the pathogen side of the interaction.

Finally, plant pathology has a strong history of taking a functional molecular approach, which can be used to identify the specific genes, proteins and pathways underlying resistance and virulence, and can provide a mechanistic understanding of the interaction between host and pathogen on a molecular level. This work has led to the formulation of the zig-zag model of plant defence (Jones and Dangl 2006), which divides plant immunity into pattern-triggered

immunity (mediated through transmembrane receptors that recognise conserved pathogen molecules) and effector-triggered immunity (mediated through intracellular receptors that recognise highly variable virulence-related effector proteins). Much of the work in this area has been carried out using model organisms (e.g., *Arabidopsis* and various crops), where the availability of extensive genomic resources, genetic engineering techniques and mutant lines allows for sophisticated experiments that identify the exact role played by specific genes in host defence and pathogen virulence (e.g., Falk et al. 1999; Gómez-Gómez and Boller 2000; Liang et al. 2021; Zhao et al. 2022). However, more recently, transcriptomic approaches have provided a way to explore these molecular processes in species that have limited or no genomic resources (e.g., Carrasco et al. 2017; Dun et al. 2022; Fernandes et al. 2024), allowing the development of a mechanistic understanding of defence in non-model organisms.

Integrating these complementary approaches – quantitative genetics, population genomics, and molecular analysis – provides a comprehensive framework for studying both sides of the host-pathogen interaction, allowing us to link genetic variation, evolutionary processes, and molecular mechanisms to understand how resistance and virulence arise and persist. Such an integrated perspective will also strengthen our ability to predict the outcomes of novel host-pathogen encounters, and to design informed strategies for managing the impacts of invasive plant pathogens.

1.4 *Phytophthora* plant pathogens

Phytophthora is a large genus of over 200 described species, including many highly destructive plant pathogens notorious for causing huge economic losses, major ecological disruption, and significant societal impacts (Erwin and Ribeiro 1996; Hansen 2015; Brasier et al. 2022). For example, *P. sojae* causes root and stem rot in soybean, and results in $1-2 billion annual losses worldwide (Tyler 2007); *P. cinnamomi* is pathogenic to a wide range of woody and herbaceous species, and has caused extensive dieback and mortality in eucalyptus forests in Australia and Fagaceae forests in the US and Europe (Hardham and Blackman 2018; Jung et al. 2018); and *P. infestans* is the cause of potato late blight, a disease which resulted in mass famine and migration in Ireland in the 1840s, and which is still a threat to global food security (Turner 2005; Yuen 2021).

Once thought to be members of the Kingdom Fungi due to superficial resemblance in morphology and behaviour, *Phytophthora* actually belong to the phylum *Oomycota*, which are members of the Stramenopiles, a very distant branch of the phylogenetic tree that also

includes diatoms and brown algae (Beakes et al. 2012; Burki 2014). Unlike fungi, which are haploid or dikaryotic for most of their lifecycle, the main lifecycle stages of *Phytophthora* are diploid. *Phytophthora* can spread through asexual motile zoospores produced in structures called sporangia, as well as by means of highly resilient sexual oospores (Drenth et al. 1995; Goodwin 1997) (Figure 1.2). Some *Phytophthora* species have two distinct mating types (heterothallic), while other *Phytophthora* species have just one mating type (homothallic) and can produce oospores through self-fertilisation (Goodwin 1997; Judelson 2009). Most *Phytophthora* are considered hemibiotrophs, with an initial biotrophic phase in the infection, during which the pathogen feeds on living host cells, followed by a necrotrophic phase, during which infected host cells are killed (Boevink et al. 2020). Typically, *Phytophthora* cause root and stem disease, and are soil-borne or water-borne, although aerially-dispersing species that cause aerial stem lesions and/or leaf blight do also exist (Brasier et al. 2022).

Phytophthora often form clonal lineages that show little genetic structure by population (Cooke et al. 2005; Schoebel et al. 2014; Mullet et al. 2024), demonstrating that in many cases sexual reproduction is limited. This raises the question of how these pathogens can so successfully respond and adapt to novel environments and hosts, as asexual reproduction will limit the efficacy of selection due to interference between loci (Hill and Robertson 1966; Keightley and Otto 2006). One way *Phytophthora* may be able to overcome this limitation is by having dynamic genomes that can undergo rapid expansion of gene families (Morales-Cruz et al. 2020; Lee et al. 2021; Cox et al. 2022) and whole-genome duplication events resulting in polyploidy (Bertier et al. 2013; Morales-Cruz et al. 2020; Ayala-Usma et al. 2021). Hybrid polyploids (allopolyploids) have also been reported in *Phytophthora* across multiple different clades (Brasier et al. 1999; Bertier et al. 2013; Van Poucke et al. 2021). The ability to tolerate the large changes in genome structure involved in polyploidy and hybridisation may give *Phytophthora* enhanced adaptive potential in the face of novel or evolving hosts. In particular, whole or partial genome duplication could increase the arsenal of effector proteins in the genome, allowing these virulence-related proteins to proliferate and diversify (Morales-Cruz et al. 2020). By bringing together divergent lineages into a single genome, hybridisation is also thought to enhance adaptive potential, and has been shown to result in broader host ranges (Érsek et al. 1995), or in some cases even the ability to infect hosts not associated with either parental species (Brasier et al. 1999; Man in 't Veld et al. 2007; Bertier et al. 2013). This plastic, adaptable nature of *Phytophthora* genomes could therefore be key in their success as plant pathogens.

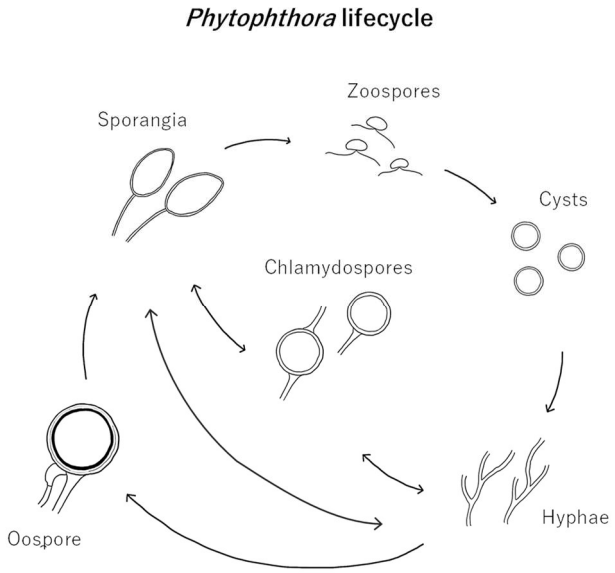

Figure 1.2. Key stages of the *Phytophthora* lifecycle. Zoospores are asexual, motile spores. Oospores are resilient, sexual spores. Adapted from: © Forest Phytophthoras of the World 2025

1.5 The juniper-*Phytophthora austrocedri* pathosystem

Juniper (*Juniperus communis*) is an evergreen dioecious conifer (Cupressaceae) that grows as small trees or shrubs throughout the Northern Hemisphere (Thomas et al. 2007). As one of only three native conifers in the UK (Johnson and More 2015), juniper plays an important ecological role in UK landscapes, and has a rich community of associated native flora and fauna (Hall et al. 2004; Ward 1977). Although juniper remains geographically widespread in the UK (Figure 1.3), populations are often small and isolated, with limited gene flow and significant genetic differentiation between populations (Baker et al. 2025a; Baker et al. 2025b). Additionally, juniper populations consist of individuals with an increasing age profile due to low rates of natural regeneration (Thomas et al. 2007). Consequently, *J. communis* is included in the list of priority species for conservation in the UK (BRIG 2007), and juniper populations are likely to be vulnerable to new threats.

Phytophthora austrocedri was first described in 2007 as the causal agent of widespread dieback and mortality in Chilean cedar (*Austrocedrus chilensis*) in the Patagonian Andean forests of Argentina (Greslebin et al. 2007; Greslebin and Hansen 2010). Subsequently, *P. austrocedri* was also identified as the cause of extensive mortality of juniper in populations across northern England and Scotland, UK (Green et al. 2012; Green et al. 2014). Elsewhere, it

has been detected causing isolated cases of disease in nurseries and urban parks in the UK, Germany, Iran and the USA, affecting *J. communis* and several other members of the cypress family, including *J. horizontalis*, *Cupressus sempervirens* and *Callitropsis nootkatensis* (Werres et al. 2014; Green et al. 2016; Mahdikhani et al. 2017; Kipp 2024). The only cases of *P. austrocedri* causing widespread infections in natural populations are in Argentina and the UK. The pathogen is believed to be invasive in both countries, although its origin remains unknown (Henricot et al. 2017).

Phytophthora austrocedri is in clade 8d of the *Phytophthora* genus, alongside fellow tree pathogens *P. obscura* and *P. syringae* (Greslebin et al. 2007; Yang et al. 2017). Like many *Phytophthora* species, *P. austrocedri* is soil-borne and water-borne, infecting the roots and basal stem of juniper trees, and forming visible lesions in the phloem (Green et al. 2012). Above-ground symptoms in juniper trees include foliar bronzing, dieback of the crown, and eventual mortality once the lesion girdles the stem (Green et al. 2012). The presence of *P. austrocedri* has now been confirmed (through isolation, sequencing and/or qPCR of lesion tissue from symptomatic trees) in multiple juniper populations across northern England and Scotland (Green et al. 2014; Donald et al. 2020; Donald et al. 2021) (Figure 1.3). In the most heavily affected areas, the majority of juniper trees in the population show symptoms (Green et al. 2014; Donald et al. 2020). One such population in Glen Artney (Perthshire, Scotland) has long-dead juniper trees that appear to predate the discovery of *P. austrocedri* in the UK (S. Green, personal communication). It is therefore likely that the pathogen had been present in the UK for a considerable time before its discovery.

Juniper is highly susceptible to *P. austrocedri*, and the threat posed by this invasive pathogen is therefore considerable. However, many of the key features that govern the outcome of novel host-pathogen interactions remain unknown for this pathosystem, limiting our ability to make short- and long-term predictions. On the host side, there is evidence for some degree of natural resistance within juniper populations, with different juniper clones developing lesions of varying size when inoculated with *P. austrocedri*, and with some clones seemingly capable of preventing infection altogether (Green et al. 2020). However, we do not know the prevalence of resistance in natural juniper populations, or the extent to which resistance is due to heritable genetic variation, which is a requirement for adaptive change to occur.

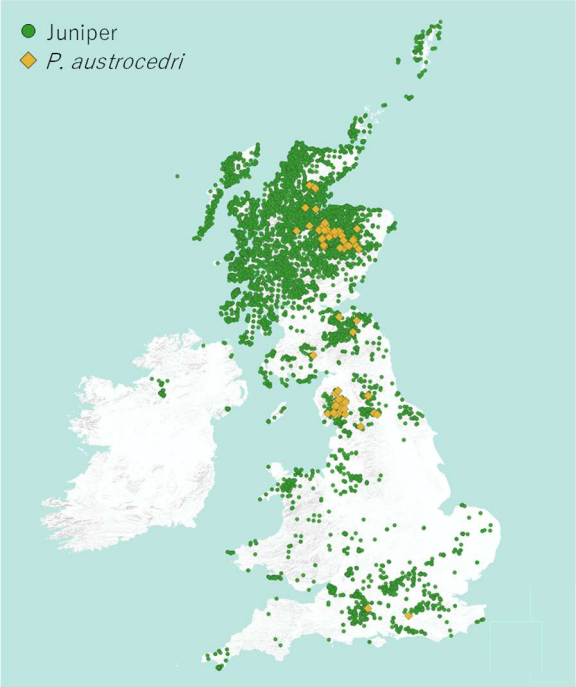

Figure 1.3. Map of the United Kingdom showing the distribution of juniper and records of *Phytophthora austrocedri*. Source of juniper distribution data: NBN Atlas. Source of *P. austrocedri* data: Flora Donald.

On the pathogen side, as *P. austrocedri* is soil-borne and requires moisture to grow and spread (Riddell et al. 2020), this should slow the spread of the disease compared to airborne pathogens both within and between populations. In addition, *P. austrocedri* is thought to disperse primarily via asexual zoospores (Henricot et al. 2017), which may limit genetic diversity and restrict adaptive potential (Charlesworth and Charlesworth 2010). However, the rate of pathogen spread across the UK, and levels of genetic diversity within and between populations, are still unknown. One study suggested that all *P. austrocedri* isolates found in the UK may be clones (Henricot et al. 2017); however, this inference was based on a small number of housekeeping genes, which might be expected to show low levels of variation. Moreover, there is variation between *P. austrocedri* isolates in their morphology and levels of virulence (Henricot et al. 2017; Green et al. 2020), which suggests they are not all genetically identical.

Gaining a deeper understanding of this pathosystem is therefore critical, in order to predict how the interaction may develop over time, inform effective strategies for conserving juniper populations, and optimally manage the ongoing impact of *P. austrocedri* on a vulnerable native tree.

1.6 Thesis overview and aims

Invasive tree pathogens can have devastating effects on natural, urban and managed forests, making them critically important systems to study. By improving our understanding of the ecological and evolutionary factors influencing the dynamics of novel pathosystems, we can gain greater ability to predict, manage and mitigate the impacts of current and future pathogen invasions. Beyond their applied importance, novel host-pathogen systems also provide unique opportunities to investigate key evolutionary processes, such as response to selection, rapid adaptation to new environments, and co-evolution. Although evolution is often considered a slow process, in these dynamic systems evolutionary change can occur over short timescales. The arrival of a pathogen in a naïve host population creates a natural experiment in which we can observe how pathogens adapt to new hosts and environments, and in turn impose strong selection on their novel hosts. Invasive pathogens thus represent valuable models for understanding fundamental evolutionary processes.

Studying a wide variety of different pathosystems will broaden our understanding of the processes governing host-pathogen dynamics, and allow generalisations to be made about how these systems evolve. At the same time, the dynamics of every pathosystem will be unique, shaped by the individual eco-evolutionary characteristics of both host and pathogen. These key factors are often poorly characterised for invasive pathogens, particularly when they form novel associations with new hosts, as in the case of the juniper-*P. austrocedri* system. Making specific predictions and management recommendations will therefore always be best served by basing them on detailed study of the specific pathosystem in question.

The overarching aims of this thesis are therefore two-fold:

1) To use evolutionary and ecological approaches to investigate a novel host-pathogen interaction, in order to advance our understanding of the processes that drive the evolution and dynamics of these systems; and

2) To explore the biology, ecology and dynamics of the specific juniper-*P. austrocedri* interaction, in order to provide evidence-based recommendations for the management of this invasive pathogen and the conservation of its vulnerable host.

To achieve these aims, this thesis examines both sides of the interaction in this novel host-pathogen system, using a combination of quantitative genetic, genomic, and molecular approaches to provide an integrated understanding of host defence, pathogen evolution, and the molecular dialogue between the two.

In Chapter 2, I address the host side of the interaction by investigating the presence, prevalence and nature of resistance in juniper populations. By means of two inoculation trials and a quantitative genetic framework, I demonstrate that resistance to *P. austrocedri* is present in many UK juniper populations, that it has a heritable genetic basis, and that populations exposed to the pathogen show evidence of ongoing selection for resistance. These findings reflect positively on juniper's adaptive potential in the face of the threat posed by *P. austrocedri*.

Chapter 3 and Chapter 4 focus on the pathogen side of the interaction. In Chapter 3, I present new, high-quality genomic resources for *P. austrocedri*, a necessary first step for addressing questions about pathogen population history, evolution and adaptive potential. Chapter 4 then explores the population genomics and large-scale genome evolution of *P. austrocedri*, with an emphasis on exploring the factors underlying its success as an invasive pathogen. I show that *P. austrocedri* is of hybrid origin, and that most isolates are tetraploid, although some isolates show evidence of triploidisation and diploidisation. I then discuss how hybridisation followed by self-fertilisation may be a highly effective evolutionary strategy, as it allows the maintenance of high levels of between-genome heterozygosity despite repeated rounds of self-fertilisation reducing within-genome heterozygosity to extremely low levels.

Chapter 5 examines both sides of the host-pathogen interaction by exploring the molecular basis of disease resistance in the host and of virulence in the pathogen. I carry out a dual RNAseq inoculation trial using two juniper genotypes (one more resistant, one highly susceptible) and two *P. austrocedri* isolates (one more virulent, one less virulent). I show that resistance to *P. austrocedri* in juniper is characterised by rapid pathogen detection followed by a sustained defence response mediated through the ethylene signalling pathway. This effective defence response appears to depend on both pathogen factors (likely the expression of particular effector proteins and/or elicitors) as well as host factors (possibly the presence of a particular transmembrane pattern-recognition receptor), resulting in a genotype-by-genotype interaction that determines infection outcome.

Finally, in Chapter 6 I synthesise the findings presented in the preceding chapters, discussing them within the broader context of the evolutionary ecology of novel host-pathogen interactions. I then outline some practical management recommendations for the juniper-*P. austrocedri* pathosystem based directly on these results. I conclude by identifying key avenues for future research that will build on this work to further unravel the dynamics of invasive plant pathogens.

CHAPTER 2:
Vulnerable juniper populations show adaptive potential in the face of a highly damaging invasive tree pathogen

Abstract

Invasive tree pathogens pose a significant and increasing threat to natural ecosystems. The outcome of these novel host-pathogen interactions depends largely on the presence and nature of resistance in host populations, which will govern the host's potential to respond through natural selection and adaptation to the new threat. This study assessed the adaptive potential of juniper (*Juniperus communis*) in the face of the invasive tree pathogen *Phytophthora austrocedri* through two inoculation experiments: an excised-shoot trial using six different *P. austrocedri* isolates, and a progeny-provenance trial that inoculated whole trees with a single highly virulent isolate. We found evidence for both qualitative and quantitative resistance in juniper populations, with lesion length (quantitative resistance) showing moderate to high heritability and lesion development (qualitative resistance) showing very high heritability. There was a significant genotype-by-genotype interaction between pathogen isolate and host genotype, lowering the estimate of heritability to moderate values when calculated across six different isolates. Finally, we found evidence that *P. austrocedri* is imposing natural selection on juniper populations, with individuals originating from highly exposed populations having a lower predicted probability of developing a lesion. Based on the results of this study, we recommend that the most effective management strategy for vulnerable UK juniper populations is to promote natural regeneration within populations, making use of existing genetic diversity in resistance within natural populations without risking the introduction of new *P. austrocedri* genotypes through the planting of nursery-grown juniper.

2.1 Introduction

Invasive tree pathogens are a threat to natural, managed and urban forests, causing major economic losses and significant ecosystem disruption (Budde et al. 2016; Lovett et al. 2016; D'Amato et al. 2023). In novel host-pathogen interactions between a non-native pathogen and a previously unexposed host, individuals in the host population are likely to be almost universally susceptible to the new pathogen, because the lack of a past co-evolutionary relationship means that alleles that confer disease resistance are not expected to be segregating at high frequencies in the host population (Ennos 2015). At worst, invasive tree pathogens can cause decimation of the host population across its entire range (e.g., Kinloch 2003; Harwood et al. 2011; Rigling and Prospero 2018).

Some initial resistance to a novel pathogen could, however, already be present within naïve host populations at low frequencies, arising either by chance through random mutation, or due to prior exposure to a pathogen with a similar mode of action, resulting in a degree of preadaptation (Parker and Gilbert 2004). This may be particularly true in tree species, which often have large effective population sizes and maintain high levels of standing genetic variation (Petit and Hampe 2006; Kremer et al. 2025). As the pathogen spreads through the population, any resistance alleles will experience strong positive selection, which could result in the host responding to the new threat through adaptation (Cavers and Cottrell 2015). However, whether such adaptation through natural selection occurs will depend on multiple factors, including the initial frequency of resistant genotypes in the host population, the heritability of resistance, and the durability of resistance.

The extent to which resistance to a pathogen is due to heritable genetic variation is crucial for determining the host's adaptive potential (Telford et al. 2015). The heritability of a trait – defined as the proportion of total variation that is explained by additive genetic variance (Falconer and Mackay 1996) – is a fundamental measure in predicting evolutionary response, as it governs the efficacy of natural or artificial selection (Roff 1997). The heritability of resistance will be influenced by the genetic basis of the trait, as well as by the stability of resistance across different environments and pathogen genotypes. High levels of heritability in disease resistance will allow more efficient selection and will thus increase the adaptive potential of the host.

The nature of disease resistance in plants can be divided into qualitative (complete) resistance and quantitative (incomplete) resistance (Agrios 2005). Qualitative resistance is often attributed to being the result of a single gene of large effect (R gene), while quantitative resistance is usually considered to arise from multiple genes of smaller effect (St. Clair 2010). Because resistance mediated by a single gene is expected to be less robust to pathogen evolution than resistance governed by multiple genes, qualitative resistance is predicted to be less durable than quantitative resistance (McDonald and Linde 2002; Brown 2015). However, some have argued that a strict separation into qualitative vs. quantitative is too simplistic, and that resistance is better seen as a continuum (Poland et al. 2009). In fact, while there are cases in which quantitative resistance has been shown to have a basis distinct from major-gene-associated qualitative resistance (Poland et al. 2009), in other cases they may share the same underlying mechanism (Kamoun et al. 1999). Phenotypic patterns of resistance alone may therefore tell us little about the underlying genetic architecture of the trait, and hence its durability.

The outcome of novel plant-pathogen interactions ultimately depends on the presence and nature of resistance within the host population. Host resistance has been successfully exploited in large-scale tree breeding programmes (Sniezko and Nelson 2022) that have artificially selected resistant genotypes, particularly in commercially important tree species (Sniezko et al. 2014; Sniezko et al. 2019). In non-commercial tree species, the resources for a large-scale breeding programme may not be available; however, knowledge of host resistance and adaptive potential is essential for informing conservation and management strategies designed to mitigate the impact of invasive pathogens.

Juniper (*Juniperus communis*) is an evergreen, dioecious conifer (Cupressaceae) that plays an important ecological role in UK landscapes as one of only three native conifer species (Johnson and More 2015). Although juniper remains geographically widespread in the UK, it is considered vulnerable due to forming small, isolated populations with low levels of natural regeneration (Thomas et al. 2007; Broome et al. 2017). Consequently, *J. communis* is listed as a priority species for conservation (BRIG 2007). Juniper is now under further threat from the invasive oomycete pathogen *Phytophthora austrocedri* (Green et al. 2014). First detected in the UK in 2010 (Green et al. 2012), *P. austrocedri* is causing extensive mortality in juniper populations across northern England and Scotland (Green et al. 2014). Elsewhere, *P. austrocedri* is also the causal agent of widespread dieback and mortality of Chilean cedar (*Austrocedrus*

chilensis) in the Patagonian Andean forests of Argentina (Greslebin et al. 2007; Greslebin and Hansen 2010). The pathogen is thought to be invasive in both the UK and Argentina, but its origin is still unknown (Henricot et al. 2017). Previous work has shown there is evidence of resistance to *P. austrocedri* in some juniper individuals (Green et al. 2020); however, the nature of the resistance and the extent to which it is due to heritable genetic variation that could allow adaptation is not known.

This study aims to assess the adaptive potential of UK juniper populations in response to the threat posed by *P. austrocedri* by addressing the following questions: 1) To what extent is resistance to *P. austrocedri* a heritable genetic trait in juniper? 2) What is the nature of disease resistance (qualitative vs. quantitative) in juniper? and 3) Is there evidence that natural selection is already operating in juniper populations as a response to *P. austrocedri*? Addressing these questions will provide the foundation for evidence-based management and conservation of this vulnerable native tree.

2.2 Methods

2.2.1 Excised shoot inoculation trial

An initial excised shoot-based inoculation trial was carried out in order to i) screen *P. austrocedri* isolates to assess relative virulence and ii) get an estimate of broad-sense heritability of juniper host resistance by making use of within-genotype replication. Six *P. austrocedri* isolates were chosen for screening, representing different populations and isolated in different years (Table 2.1). Older isolates had recently been passed through the host to restore virulence.

We collected 190 shoots from 10 juniper individuals from an isolated population that remains free of any symptoms of *P. austrocedri* (Lammermuir Hills, Scotland; Table 2.2), allowing for three replicates per isolate/genotype combination and one negative control per juniper genotype. We processed the shoots to ensure all were approximately equal in length (35-40 cm), and dipped cut ends in wax to prevent desiccation. Excised shoots were inoculated as described in Green et al. (2020). Briefly, mycelial plugs (4 mm diameter) were taken from the edge of *P. austrocedri* cultures actively growing on V8 agar. A sterile cork borer (4 mm diameter) was used to remove a piece of bark in the middle of the shoot, and the mycelial plug was placed on the exposed cambium layer. The area was covered with cotton wool thoroughly moistened with sterilised distilled water, before wrapping with parafilm and tin foil.

Negative controls were inoculated in the same way with plugs taken from a sterile V8 agar plate. Shoots were processed over three days, with each day forming one block and with one replicate of each genotype/isolate combination inoculated per day in a fully randomised block design. Shoots were harvested five weeks after inoculation and lesion length measured by careful removal of the outer bark to expose the lesion underneath (Figure S2.1). Shoot width at the point of inoculation was also recorded.

2.2.2 Progeny-provenance whole-tree inoculation trial

Open-pollinated seed was collected from 54 mother trees from 13 natural populations across the UK (Table 2.2) in autumn 2015. Seed was germinated as described in Baker et al. (2025a). Trees were grown in a common environment in greenhouse conditions in a randomised block design, with each block containing one member of a family, and potted up as needed. The experiment was carried out in autumn and winter 2023/2024 when the trees were approximately six years old. At the time of inoculation median tree height was 90 cm and all trees were in 3L pots. Most families were represented by six individuals per maternal tree (half-siblings or full-siblings), but the loss of some of these trees meant that a few families were only represented by four or five individuals (Table 2.2). The trial included a total of 306 trees, plus six positive and six negative controls.

Trees were inoculated at the stem base following the mycelial plug method described for whole plants in Green et al. (2020) using only one *P. austrocedri* isolate (GA7; Table 2.1). Mycelial plugs (4 mm diameter) were taken from the edge of *P. austrocedri* cultures actively growing on V8 agar. A sterile cork borer (4 mm diameter) was used to remove a piece of bark at the base of the stem, and the mycelial plug was placed on the exposed cambium layer. The area was covered with cotton wool thoroughly moistened with sterilised distilled water, before wrapping with parafilm and tin foil. Inoculations were carried out in six fully randomised blocks, with one member of each family present in each block, along with a positive and negative control. Controls were trees of a genotype known to be highly susceptible based on previous inoculation trials (Green, unpublished data) that were inoculated either as described above with a mycelial plug (positive control) or as described above but instead using a sterile plug of V8 agar (negative control).

The trial ran over a period of five months, as only two blocks could fit concurrently in the greenhouse. Blocks one and two were inoculated in October 2023, blocks three and four were inoculated in December 2023, and blocks five and six were inoculated in January 2024.

Temperature in the greenhouse was set to 15°C, temperature and humidity were recorded using data loggers, and trees were kept well watered. Six plugs from each colony used in the inoculations were plated on V8 agar to confirm all plugs produced actively growing colonies in greenhouse conditions. Trees were harvested five weeks after inoculation. Bark surrounding the inoculation point was removed using a scalpel to expose the lesion beneath (Figure 2.1). Lesion length and width were recorded, along with tree height and stem width at the inoculation point.

To confirm lesion formation was due to *P. austrocedri,* re-isolation was attempted from a randomly chosen subset of 56 trees across all blocks by plating small pieces of phloem/cambium tissue taken from the leading edge of the lesion on *Phytophthora* selective medium (synthetic mucor agar; Brasier et al. 2005). Resulting colonies were identified as *P. austrocedri* based on its distinctive coralloid hyphae (Greslebin et al. 2007). *Phytophthora austrocedri* infection was also confirmed by qPCR in a random subset of 30 trees (five trees per block). Tissue was collected from the edge of lesions and freeze dried prior to DNA extraction using the DNeasy Plant Pro Kit (Qiagen) following the manufacturer's instructions. The presence of *P. austrocedri* DNA in lesion tissue was confirmed using qPCR assays following the protocol described in Mulholland et al. (2013).

Table 2.1. Location and date of isolation for the *Phytophthora austrocedri* isolates used in the inoculation trials. The host in all cases was juniper (*Juniperus communis*). Source of isolates: Forest Research Northern Research Station, Roslin, Midlothian, Scotland.

Isolate name	Location	Latitude (°)	Longitude (°)	Isolation date
BF207	Blowick Fell, Cumbria, England	54.551	-2.311	February 2015
GA10-SG	Glen Artney, Perthshire, Scotland	56.334	-4.012	May 2021
GA510	Glen Artney, Perthshire, Scotland	56.339	-4.017	May 2021
GA7	Glen Artney, Perthshire, Scotland	56.337	-4.050	October 2018
SS2	Bridge of Brown, Highland, Scotland	57.266	-3.522	October 2012
TDJ3	Teesdale, County Durham, England	54.645	-2.169	November 2011

Table 2.2. Location of the population, number of families and individuals included in the seed-grown progeny-provenance trial, and whether the population was classified as high exposure to *Phytophthora austrocedri* (extensive mortality already taken place) or low exposure to *P. austrocedri* (no evidence of mortality associated with the pathogen).

Population	Country	Latitude (°)	Longitude (°)	Number of families	Number of individuals	Level of exposure
Argyll (AG)	Scotland	56.605	-6.123	4	22	Low
Arran (AR)	Scotland	55.550	-5.202	4	22	Low
Balnaguard Glen (BG)	Scotland	56.644	-3.730	5	30	Low
Blowick Fell (BF)	England	54.558	-2.931	8	48	High
Bulford Hill (BH)	England	51.204	-1.700	1	6	Low
Blea Tarn (BT)	England	54.426	-3.088	4	20	High
Glen Artney (GA)	Scotland	56.340	-3.996	5	30	High
Invernaver (IN)	Scotland	58.521	-4.256	1	6	Low
Lammermuir (LM)	Scotland	55.853	-2.710	6	31	Low
Morrone Birkwood (MB)	Scotland	56.998	-3.426	2	11	Low
Thwaites Fell (TF)	England	54.302	-3.262	7	39	High
Tynron (TY)	Scotland	55.214	-3.846	1	5	Low
Whitewell (WW)	Scotland	57.155	-3.796	6	36	High

2.2.3 Data analysis and estimation of heritability

2.2.3.1 Excised shoot inoculation trial analysis

As lesion length showed a strong positive skew in distribution, the measurements were log-transformed for subsequent analysis using linear mixed-effects models. Log lesion length was modelled using the R package lme4 (Bates et al. 2015), with *Tree* and *Isolate* fitted as random effects and *Block* fitted as a fixed effect. *Shoot width* (mm) was initially included as a covariate, but was subsequently removed from the model due to no evidence of any effect (β = -0.02 [-0.06-0.02], p=0.25), and the simpler model without shoot width providing a better fit (lower AIC and BIC scores). Confidence intervals around estimated parameters and ratios of variances were generated using parametric bootstrapping. Significance of individual model terms fitted as random effects was tested using likelihood ratio tests of nested models.

A second model with an added *Tree:Isolate* interaction term was also fitted to get a measure of broad-sense heritability within isolates (see below). The interaction term was

excluded from other analyses due to its poor performance in parametric bootstrapping, suggesting an overly-complex random effect structure for the sample size.

2.2.3.2 Estimation of broad-sense heritability

Broad-sense heritability (H^2), the proportion of phenotypic variance explained by genotypes, was estimated using two approaches. First, H^2 was estimated across all *P. austrocedri* isolates (using the model without a *Tree:Isolate* interaction term) by using the variance among juniper trees (V_{tree}), isolates ($V_{isolate}$), blocks (V_{block}) and residual variance (V_{res}) as follows:

$$H^2 = V_G/V_P = V_{tree} / (V_{tree} + V_{isolate} + V_{block} + V_{res})$$

Second, H^2 was estimated for the case when inoculated with the same *P. austrocedri* isolate (using the model with a *Tree:Isolate* interaction term) by excluding $V_{isolate}$ from the denominator and adding the *Tree:Isolate* interaction term ($V_{t:i}$) to the numerator as follows:

$$H^2 = V_G/V_P = (V_{tree} + V_{t:i})/ (V_{tree} + V_{t:i} + V_{block} + V_{res})$$

The amount of variation explained by fixed effects was extracted from the model using the R package insight (Lüdecke et al. 2019).

2.2.3.3 Progeny-provenance whole tree inoculation trial analysis

Lesion length showed a bimodal distribution, with a group of trees showing no lesion or very little lesion development and a larger group of trees showing an approximately normally distributed lesion length centred around a larger mean (Figure 2.2). In order to analyse these data, lesion development was separated into two response variables: 1) presence/absence of lesion development and 2) length of lesion if developed. In all trees the inoculation process itself resulted in discoloration, even if there was no subsequent lesion development (even negative controls had a discoloured "lesion" that was 4-6 mm long; see Figure 2.1). This means the threshold for classifying a tree as having lesion development cannot be the absence of any discoloration. Therefore, a lesion was classified as "development present" if lesion length was more than 15 mm. This threshold is unavoidably somewhat arbitrary, but was chosen to best fit the distribution of the data (Figure 2.2): there was a large spike of trees with lesions below this size, while the remaining trees exhibited a distribution of lesion lengths that can reasonably be modelled using a Gaussian distribution. Moreover, the analysis was not sensitive to the exact threshold, as rerunning the analysis based on different thresholds (from 10 mm to 20 mm) had only small effects on the estimated parameter values and would have no impact on their interpretation (Table S2.1).

The two traits (presence/absence of lesion development and lesion length when present) were analysed using multivariate generalised linear mixed models implemented in the Bayesian R package MCMCglmm (Hadfield 2010). Presence/absence of lesion development was modelled for all data using the threshold model, which assumes there is a latent liability trait that underlies the binary trait of interest and uses a probit link function (Falconer and Mackay 1996; de Villemereuil et al. 2016). Lesion development occurs when a certain threshold in the latent trait is exceeded. For the subset of trees that developed a lesion, lesion length was modelled assuming a Gaussian distribution. *Family*, *Population* and *Block* were fitted as random effects. We investigated whether tree size has an effect on lesion development by fitting *Stem width* (mm) or *Tree height* (cm) as covariates, then controlled for tree size by fitting *Tree height* as a random slope allowed to vary by population.

Priors were defined following the recommendations in Hadfield (2019). Parameter expanded priors were used for (co)variances of random effects (specification: V=1, nu=2, alpha.mu=0, alpha.V=1000), an inverse Wishart prior was used for the residual variance of lesion length (specification: V=1, nu=0.002) and default diffuse normal priors with large variances were used for fixed effects. The residual variance of the binary trait (lesion development present/absent) was fixed at 1. We set the MCMC thinning interval to 100 after a burn-in period of 30,000, and let the chain run for enough iterations to obtain a minimum effective sampling size >2,000 for all parameters. Convergence was assessed by visual inspection of trace plots and by checking that autocorrelation between successive stored samples was <0.1.

2.2.3.4 Estimation of narrow-sense heritability

Narrow-sense heritability (h^2) is the proportion of total phenotypic variance explained by additive genetic variance. In a half-sibling family design, additive genetic variance is equal to four times the amount of variation explained by family, whereas in a full-sibling design it is equal to twice the amount of variation explained by family, although this latter estimate would be inflated due to shared dominance effects (Falconer and Mackay 1996). The open-pollination design of this trial means our families are likely to include a mixture of both half-siblings and full-siblings. We therefore approximated a roughly equal proportion of full- and half-sibling, and multiplied the variance attributed to family by three to get an estimate of additive genetic variance. Narrow-sense heritability was then calculated using estimates of variance attributed

to *Family* (V_{fam}), *Population* (V_{pop}), *Tree_height:Population*(V_{hgt}), *Block* (V_{block}) and residual variance (V_{res}) as follows:

$$h^2 = V_a/V_p = 3 \times V_{fam} / (V_{fam} + V_{pop} + V_{hgt} + V_{block} + V_{res})$$

We also calculated the proportion of total variation explained by *Population*, *Block* and *Tree_height:Population* and report this as the intraclass correlation coefficient (ICC).

For the binary threshold trait (lesion presence/absence), h^2 was estimated on both the latent trait scale and the observed data scale. Heritability on the latent scale can be interpreted as the heritability of a theoretical latent trait that underlies the susceptibility to developing the lesion, whereas heritability on the observed data scale refers to the heritability of the probability of developing a lesion. Quantitative genetic parameters on the observed data scale were extracted from the model using the R package QGglmm (de Villemereuil et al. 2016).

To investigate the effect of previous exposure at the population source site to *Phytophthora austrocedri*, a separate model was fitted that included level of exposure of the population as a fixed effect. Populations were classified as either High Exposure (*P. austrocedri* presence confirmed and substantial mortality already occurred) or Low Exposure (no evidence of mortality associated with *P. austrocedri*), based on data from Green et al. (2014) and Donald et al. (2021) (Table 2.2).

Figure 2.1. Representative pictures of different degrees of lesion development. Length of lesion in each case is indicated in the bottom right the picture. A standardised scale bar is shown in the bottom left of each picture. A: Negative control, the discoloration is just a result of the inoculation process. B: Inoculated tree that is visually indistinguishable from the negative control. C: Slight extension of discoloration beyond inoculation point. D: Clear lesion development, but the lesion is relatively small in size. E: Large lesion, but not large enough to girdle the stem. F: Very large lesion that girdles the stem. We classified B and C as "lesion development absent" and D, E, and F as "lesion development present".

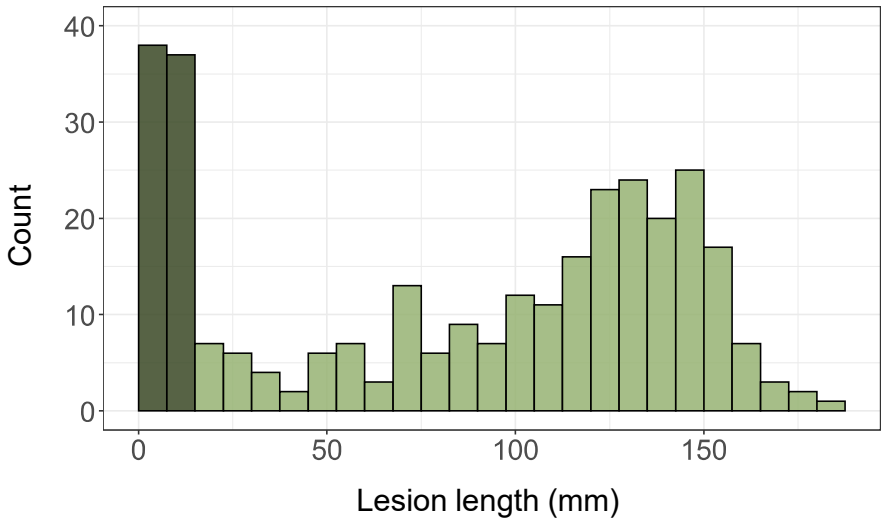

Figure 2.2. Histogram showing the bimodal distribution of lesion lengths in the progeny-provenance whole tree trial. Dark green bars represent the trees that were classified as "lesion development absent" (lesion length ≤15 mm), while the light green bars represent trees that were classified as "lesion development present" (lesion length > 15 mm).

2.3 Results

2.3.1 Excised shoot inoculation trial

2.3.1.1 Variation in virulence among Phytophthora austrocedri isolates

Phytophthora austrocedri isolates varied significantly in the size of lesions produced (LRT $\chi^2_{(1)}$ = 28.3, p < 0.001; Figure 2.3). The estimated variance in log lesion length associated with pathogen isolate was 0.020 (0.0016-0.052), which accounted for 14.1% (1.1-33.9%) of total variance in lesion length.

Of the six isolates used in the trial, only two isolates (GA10-SG and GA7) were able to form at least small lesions on all juniper genotypes tested (Figure 2.3). The same two isolates also had positive conditional modes, indicating that their predicted log lesion size was larger than the average prediction across all isolates (Figure S2.2). These results suggest isolates GA10-SG and GA7 are more virulent than the other four isolates, and would be good candidates for use in future inoculation trials. We chose isolate GA7 for further work for practical reasons, as its rate of growth when cultured in laboratory conditions was considerably faster than GA10-SG.

2.3.1.2 Broad-sense heritability of disease resistance in juniper

Juniper shoots showed a range of lesion lengths, from little/no lesion development through to large lesions, with the largest lesion measuring 176 mm (Figure 2.3). There was significant

variation between juniper genotypes in log lesion length (LRT $\chi^2_{(1)}$ = 66.7, p < 0.001), with the estimated variance in log lesion associated with tree genotype being 0.048 (0.013-0.11). Broad-sense heritability of lesion length across all *P. austrocedri* isolates was estimated as 0.35 (0.13-0.57) (Table 2.3).

When added to the model, the *Tree:Isolate* interaction term explained a significant amount of variation (LRT $\chi^2_{(1)}$ = 11.4, p < 0.001). However, the parametric bootstrapping performed poorly on individual estimates for this model, suggesting insufficient data for the complex random effect structure. Nevertheless, the joint proportion of variation explained by both the *Tree* and *Tree:Isolate* terms was more stable, and the broad-sense heritability of lesion length when individuals were infected by the same *P. austrocedri* isolate could therefore be estimated as 0.54 (0.33-0.71) (Table 2.3).

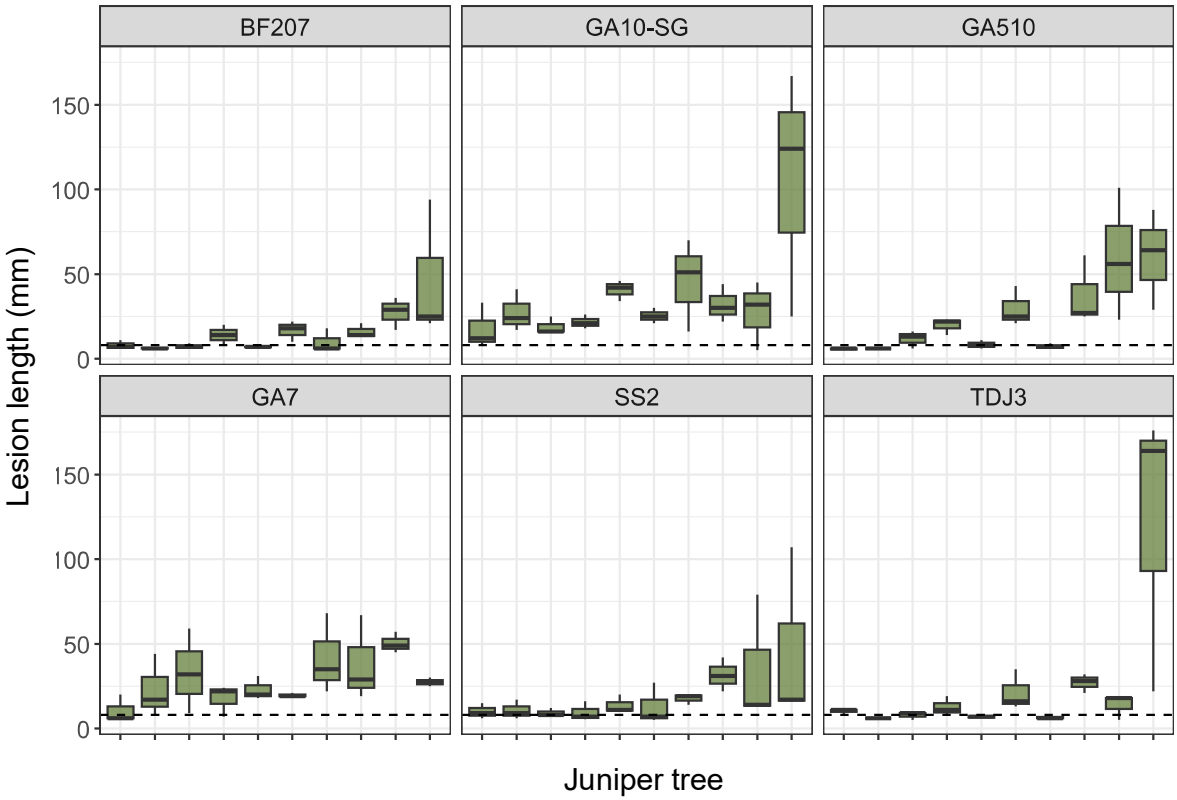

Figure 2.3. Results of the excised shoot trial showing the distribution of lesion lengths for each *Phytophthora austrocedri* isolate and juniper tree combination, with each panel representing a different pathogen isolate. Dashed line indicates the size of the discoloration on the negative controls that was due to the inoculation process itself. Lesion sizes overlapping the dashed line were therefore visually indistinguishable from the negative controls.

2.3.2 Progeny-provenance trial

There was considerable variation between juniper trees in lesion size five weeks after inoculation, from little/no lesion development through to large lesions (Figure 2.4), with the largest lesion being 182 mm long. Of the 306 trees included in the trial, 231 (75.5%) were classified as "lesion present" (lesion length > 15 mm) while 75 trees (24.5%) were classified as "lesion absent" (lesion length ≤ 15 mm). Mean lesion length for "lesion present" trees was 112 mm, and median lesion length was 123 mm. Mean lesion length for "lesion absent" trees was 8 mm and the median was 7 mm.

The negative controls included in the trial did not develop lesions, and all positive controls developed large lesions (≥98 mm). *Phytophthora austrocedri* is notoriously difficult to isolate even from active infections; however, a subset of re-isolation attempts (29/56 = 52%) were successful. Furthermore, qPCR assays confirmed the presence of *P. austrocedri* DNA in all of the subset of 30 inoculated trees tested (Table S2.2).

2.3.2.1 Effect of tree size

There was no evidence that stem width (mm) had an effect on either the probability of lesion development (β = 0.0004 [-0.068-0.061], p=0.99) or the length of lesion (mm) if present (β = -0.26 [-1.9-1.4], p=0.74), and its inclusion increased the model's DIC, suggesting a poorer fit. Stem width was therefore excluded from the model. Similarly, there was no evidence that tree height (cm) affected the probability of lesion development (β = -0.001 [-0.002-0.0004], p=0.28). However, there was a significant positive association between tree height and lesion length (β = 0.31 [0.07-0.57], p=0.014).

There was no significant variation in tree height between families after accounting for population and block (LRT $\chi^2_{(1)}$=0.19, p=0.66); however, populations did vary significantly in tree height (LRT $\chi^2_{(1)}$=31.9, p<0.001). This difference is particularly driven by the inclusion in the trial of juniper trees from Arran, which belong to a different subspecies (*Juniperus communis* ssp. *nana*) that has a small, procumbent growth form (Thomas et al. 2007). Because of these clear differences in growth form between populations, the effect of tree height was allowed to vary between populations by fitting a random slopes model.

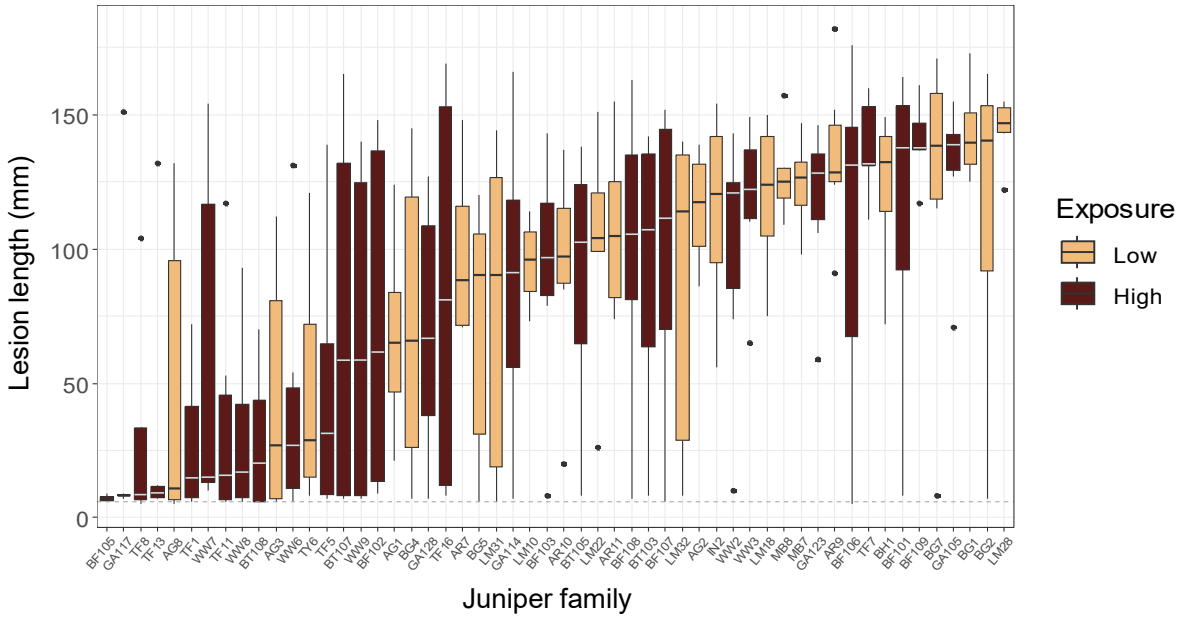

Figure 2.4. Results of the whole tree progeny-provenance trial showing the distribution of lesion size by family. Boxplots are colour-coded according to the level of previous exposure to *Phytophthora austrocedri* in the population: high exposure to *P. austrocedri*, meaning extensive mortality has already taken place at the population site, or low exposure to *P. austrocedri*, meaning no evidence of mortality associated with the pathogen. Dashed line indicates the size of the discoloration on the negative controls that is due to the inoculation process itself.

2.3.2.2 Estimates of intraclass correlation coefficients and narrow-sense heritability

The estimates of the variance components and ICC for all random effects included in the model are shown in Table 2.4. The posterior distributions of both *Block* and *Population* showed strongly skewed distributions bordering zero, which is reflected in how the confidence intervals for these parameter estimations approach zero (Table 2.4). In view of the fact that estimates of variances cannot be negative, this can be interpreted as a lack of evidence of *Block* or *Population* explaining a significant amount of variation in the probability of lesion development or in lesion length if present. In contrast, the posterior distributions of *Family* were clearly removed from zero, suggesting *Family* does explain a significant amount of variation in both the probability of lesion development and the length of lesions.

Estimates of h^2 were significantly above zero for both traits: 0.44 (0.08-0.86) for lesion length and 0.92 (0.24-1.6) for lesion development presence on the latent trait scale. The estimate of h^2 for the probability of developing a lesion (the observed data scale) was 0.43 (0.10-0.80). A comparison of the various estimates of heritability is shown in Table 2.3.

Table 2.3. Estimates of different kinds of heritability of resistance to *Phytophthora austrocedri* in juniper. For the excised shoot trial, the estimates were generated by maximum likelihood and the parentheses show 95% confidence intervals generated by parametric bootstrapping. For the progeny-provenance trial estimates are medians of the posterior distribution and parentheses show 95% credible intervals.

Trial description	Type of heritability	Pathogen isolates	Trait	Estimate of heritability
Excised shoot with six isolates	Broad-sense (H^2)	Across isolates	Log lesion length	0.35 (0.13-0.57)
		Within isolates		0.54 (0.33-0.71)
Progeny-provenance whole tree	Narrow-sense (h^2)	Single isolate	Lesion length	0.44 (0.08-0.86)
			Lesion presence/absence (latent scale)	0.92 (0.24-1.6)
			Lesion presence/absence (observed scale)	0.43 (0.10-0.80)

Table 2.4. Results of the model estimating variance components and intraclass correlation coefficients (ICC) in the progeny-provenance trial. Estimates are the medians of the posterior distributions. Parentheses show the 95% credible intervals. Estimates for lesion presence/absence are on the latent scale.

	Lesion presence/absence		Lesion length	
	Variance	**ICC**	**Variance**	**ICC**
Family	0.58 (0.14-1.3)	0.30 (0.08-0.52)	234 (33-519)	0.15 (0.03-0.28)
Population	0.30 ($6x10^{-8}$-2.0)	0.16 ($2x10^{-8}$-0.55)	22 ($3x10^{-6}$-200)	0.014 ($2x10^{-9}$-0.11)
Tree_height:Pop	10^{-5} (10^{-11}-10^{-4})	$6x10^{-6}$ ($3x10^{-12}$-$5x10^{-5}$)	0.006 ($2x10^{-9}$-0.04)	$4x10^{-6}$ (10^{-12}-$2x10^{-5}$)
Block	0.02 (10^{-8}-0.29)	0.01 ($6x10^{-9}$-0.13)	64 ($4x10^{-5}$-398)	0.04 ($3x10^{-8}$-0.21)
Residual	1	NA	1261 (967-1501)	NA

2.3.2.3 Genetic covariance between traits

The best estimate for within-family covariance between the probability of lesion development (on the latent scale) and the length of lesion if present was positive (6.1 [-1.4-15.1]). However, as the 95% credible intervals overlap zero, we cannot be confident in this positive association between the two traits. Similarly, the genetic correlation between the two traits was estimated to be 0.50 (-0.03-0.97). Although this suggests there may be a positive genetic correlation between the probability of developing a lesion and the length of lesion if present, there is considerable uncertainty in this estimate, as the confidence intervals are very wide and overlap zero.

2.3.2.4 Effect of previous exposure to Phytophthora austrocedri

There was a significant difference in the probability of lesion development between populations with high levels of previous exposure to *P. austrocedri* versus populations with no evidence of exposure to *P. austrocedri* (β = 1.0 [0.23-1.9], p=0.017). However, there was no difference between high exposure versus low exposure populations in the length of lesion when present (β = 5.8 [-9.1-22.9], p=0.44). Figure 2.5 shows the predicted values for the two variables in high vs. low exposure populations after marginalizing all random effects.

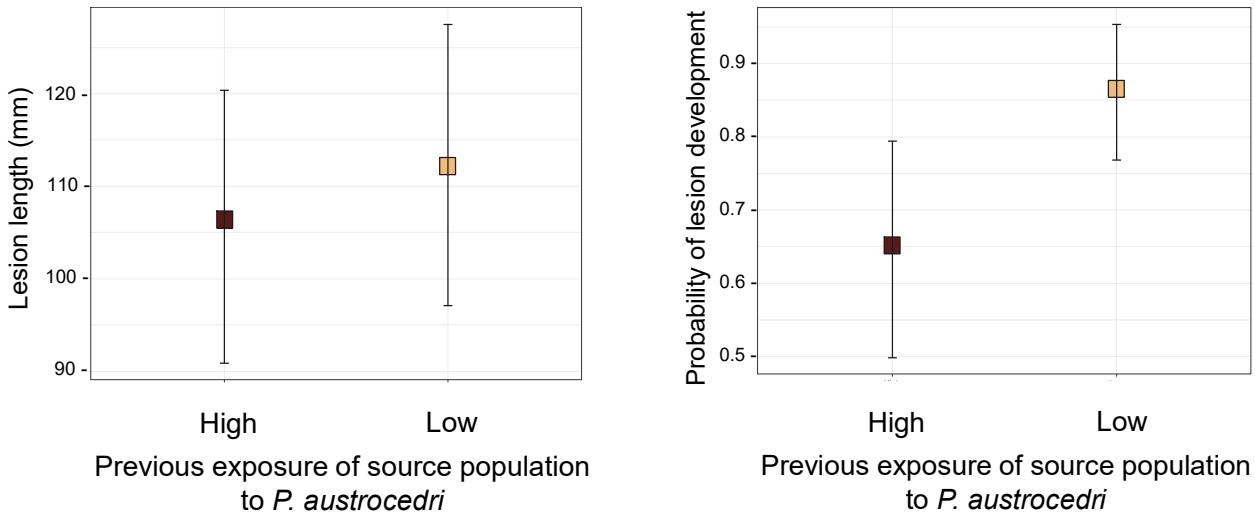

Figure 2.5. Predicted values for lesion length (left) and probability of lesion development on the observed data scale (right), depending on the level of previous exposure to *Phytophthora austrocedri* in the population. High exposure was defined as extensive mortality having already taken place at the population site; low exposure was defined as there being no evidence of mortality associated with the pathogen. Predictions were made after marginalizing all random effects. There was a significant difference in the probability of lesion development between high exposure and low exposure populations, but no difference in lesion length if present.

2.4 Discussion

2.4.1 Evidence for both qualitative and quantitative resistance

The distribution of lesion lengths across all individuals suggests both qualitative and quantitative resistance to *P. austrocedri* may be present in UK juniper populations (Figure 2.2). While most trees developed lesions, variation in lesion length indicated that some susceptible trees were able to slow down the rate of pathogen spread to some extent (quantitative or incomplete resistance). Meanwhile, a subset of trees showed little or no lesion development, suggesting they were able to prevent pathogen establishment altogether (qualitative or complete resistance).

The presence of both qualitative and quantitative resistance has also been reported in the closely related pathosystem of *P. lateralis* and Port-Orford-cedar (*Chamaecyparis lawsoniana)* (Sniezko et al. 2020). In that study, qualitative resistance was proposed to result from a single major gene, based on Mendelian segregation patterns in progeny survival (Sniezko et al. 2020). However, in our case the number of progeny per family was insufficient to test for Mendelian segregation patterns.

Some inferences could potentially be made from the positive within-family covariance between the two resistance traits, which could indicate that the probability of lesion development shares an underlying genetic basis with length of lesion when present. However, a positive covariance between resistance traits could also indicate co-occurrence of these traits in genotypes for other reasons; for example, selection imposed by *P. austrocedri* could increase the frequency of both types of resistance in the same families. Furthermore, the 95% credible intervals of the estimated covariance overlap with zero, meaning we cannot be confident in the positive association between the two resistance traits.

Overall, while the results presented here show a distinction between qualitative vs. quantitative resistant phenotypes in juniper, further work is needed before any conclusions can be drawn about the underlying genetic architecture of resistance in this pathosystem.

2.4.2 Heritability of resistance

The best estimate of narrow-sense heritability for lesion length was moderate to high (0.44), while the best estimate for lesion presence (on the latent scale) was very high (0.92). To put these values in context, Graham et al. (2018) reviewed genetic variation in *Phytophthora* resistance across multiple tree pathosystems and reported heritability estimates ranging from

0.34 to 0.9 for resistance to pathogens affecting roots and shoots. More recently, the heritability of survival in eastern white pine inoculated with *P. cinnamomi* was estimated at 0.44 (Frampton et al. 2018), and the heritability of survival of alder inoculated with either *P. uniformis* or *P. x alni* was estimated to be 0.32 and 0.1, respectively (Redondo et al. 2020).

The estimate of heritability of lesion presence on the observed data scale reflects the heritability of the probability of developing a lesion. This estimate was lower than the estimate on the latent scale, which is always expected to be the case (de Villemereuil et al. 2016). Although the transformation onto the observed data scale provides insight into how much variation in the phenotypic (observed) trait is attributable to additive genetic variance, this estimate is likely to be a poor predictor of response to selection (de Villemereuil et al. 2016). By contrast, the latent-scale estimate of heritability can be used for such evolutionary predictions (de Villemereuil et al. 2016), and is therefore more relevant for assessing juniper's adaptive potential.

Several caveats should be considered when interpreting the estimates of heritability of resistance traits presented here. First, the experiments were conducted under controlled glasshouse conditions, which substantially reduces environmental variation compared to natural settings. Because heritability reflects the proportion of total phenotypic variance attributable to genetic factors, any additional variation in phenotypic resistance caused by variation in the environment would result in lower heritability estimates if measured in natural populations. Secondly, in this study heritability was calculated across multiple populations, whereas in natural systems, it is the heritability within populations that is the parameter most relevant for predicting evolutionary response to selection. This distinction is important because differences among populations can inflate estimates of genetic variance and, consequently, heritability (Falconer and Mackay 1996).

Finally, the 95% credible intervals on the estimates of heritability were relatively wide, demonstrating there is considerable uncertainty surrounding these estimates. This is a reflection of the complexity of the random effects structure relative to the available sample sizes; precise estimates of quantitative genetic parameters typically require thousands rather than hundreds of individuals. Nevertheless, it is worth noting that the estimates of heritability of lesion length in the two separate inoculation trials (when estimated for a single isolate) were similar, providing an independent corroboration of the result.

Ultimately, many of these limitations are inherent to studying ecologically important but experimentally challenging tree-pathogen systems. The absence of a reliable, scalable inoculation method and the long generation times of woody hosts like juniper impose practical constraints that make large-scale quantitative genetic studies difficult. However, despite these challenges, the primary aim of this study was not to obtain highly precise estimates of quantitative genetic parameters, but rather to determine whether resistance to *P. austrocedri* that had previously been observed in juniper (Green et al. 2020) has a heritable genetic basis. The results presented here provide strong evidence that it does.

2.4.3 Genotype-by-genotype interaction between host and pathogen

In addition to *P. austrocedri* isolates varying in virulence across juniper genotypes, there was also a significant genotype-by-genotype (GxG) interaction between pathogen isolate and host genotype. For example, isolate TDJ3 failed to produce lesions on many of the more resistant genotypes, but caused the largest lesions on a particularly susceptible genotype (Figure 2.3). Such GxG interactions are expected under the gene-for-gene model of R-gene-mediated resistance (Flor 1971; Dodds, 2023), but they have also been reported in cases of partial, quantitative resistance (e.g., Flier et al. 2003; Darvishzadeh et al. 2007).

An important consequence of the significant GxG interaction between isolate and genotype is a reduction in the estimate of heritability to resistance when measured across multiple pathogen isolates. Frampton et al. (2018) found that the interaction between *P. cinnamomi* isolate and pine host family was so strong that estimated heritability dropped from 0.44-0.57 to almost zero when calculated across just two pathogen isolates. The effect in the present study was less extreme, with still moderate levels of heritability maintained across six *P. austrocedri* isolates (Table 2.3). Nevertheless, this still suggests juniper may be less able to respond to *P. austrocedri* through adaptation if multiple pathogen genotypes are present within one host population.

2.4.4 Evidence for natural selection in juniper populations

The difference in predicted probability of developing a lesion between juniper populations that have been highly exposed to *P. austrocedri* and those with no evidence of exposure (Figure 2.5) is likely a result of extensive mortality in exposed populations causing a shift in the relative frequency of resistant genotypes due to the removal of more susceptible genotypes. Thus, this is evidence that the invasive *P. austrocedri* is imposing rapid natural selection on juniper

populations. This is an important result that suggests that, despite being previously naïve to *P. austrocedri*, juniper populations are demonstrating resilience through standing genetic variation in resistance that is effective enough to significantly increase their probability of survival in natural populations.

Evidence of natural selection in response to an invasive tree pathogen is rare, but has been reported in other systems. For example, Redondo et al. (2020) found significant differences in the frequency of resistance between exposed and unexposed alder populations in the case of *P. uniformis,* although not in the case of *P. x alni* (Redondo et al. 2020). Heritability of resistance in the latter case was low, which may explain the lack of evidence of natural selection. Several studies have also reported natural selection to be occurring in ash trees in response to *Hymenoscyphus fraxineus*, the causal agent of ash dieback, showing increased reproductive success in more resistant ash trees compared to more susceptible ash trees (Semizer-Cuming et al. 2019; Semizer-Cuming et al. 2021), and an age-related shift in frequency of multiple alleles putatively associated with resistance (Stocks et al. 2019; Metheringham et al. 2025).

By contrast, no significant difference in predicted values between exposed and unexposed populations was seen in the case of lesion length (Figure 2.5). There are several possible explanations for this. Firstly, variation in lesion length detected over a five-week inoculation trial may have little relevance to long-term survival on timescales relevant to juniper. This would mean that, although some juniper genotypes appear to have some degree of quantitative resistance by slowing down the progression of *P. austrocedri*, they do still succumb to the pathogen, resulting in no measurable increase in the relative frequency of genotypes with more quantitative resistance. Alternatively, the lack of evidence of selection on lesion length could reflect differences in the temporal dynamics between the two resistance traits, as the lower heritability of lesion length could result in slower, less efficient selection. In this case, quantitative resistance would still be expected to increase in frequency over time in populations exposed to *P. austrocedri*.

2.4.5 Implications for the conservation of vulnerable juniper populations in the face of *Phytophthora austrocedri*

Based on the results presented here, we suggest the best management strategy for the conservation of juniper in the UK is to promote and enhance natural regeneration within each population, giving juniper populations the best chance to respond to the threat posed by *P.*

austrocedri through natural selection and adaptation. Unfortunately, rates of natural regeneration are known to be very low in many UK juniper populations, and developing reliable methods to enhance regeneration remains a major challenge (Thomas et al. 2007; Broome et al. 2017). Despite these practical difficulties, we make this recommendation for the following reasons:

1) Resistant genotypes are present in most populations. Resistant juniper individuals were detected in nearly all populations where more than two families were sampled, indicating that most populations possess standing genetic variation in disease resistance without the need for introducing resistant genotypes from other sources. The only exception was juniper sampled from the Isle of Arran, which belong to a different subspecies (*J. communis* ssp. *nana*) and which, based on the results of this study, may be universally susceptible. Fortunately, *P. austrocedri* has not yet been detected on Arran, and every effort should be made to prevent its introduction.

2) Both qualitative and quantitative resistance are present and heritable. Juniper populations contain heritable genetic variation for both qualitative and quantitative resistance, providing the raw materials necessary for adaptation to *P. austrocedri*. Although further work is required to determine the genetic architecture underlying these resistance phenotypes, the coexistence of both types of resistance may also enhance its durability and robustness against pathogen evolution (McDonald and Linde 2002; Brown 2015; Sniezko and Liu 2023).

3) There is evidence that natural selection is occurring. The significant difference in predicted probability of developing a lesion between populations based on levels of prior exposure to *P. austrocedri* suggests natural selection is already acting in exposed populations, and that resistance is effective at increasing the probability of host survival in natural field conditions.

4) Not all *P. austrocedri* genotypes are equal. Not only do *P. austrocedri* isolates vary in virulence, but there is also a significant GxG interaction between host and pathogen that reduces estimates of heritability of resistance when calculated across multiple pathogen isolates. This means that it is important not to transport *P. austrocedri* within and between sites, even in exposed populations, as juniper genotypes resistant to one genotype of *P. austrocedri* may be less resistant or even fully susceptible to a different pathogen genotype. *Phytophthora austrocedri* is soil- or water-borne, and therefore has limited natural dispersal capacity (Riddell et al. 2020). However, many *Phytophthora* species, including *P. austrocedri*, are frequently detected in nurseries and nursery-grown plants (Parke et al. 2014; Prigigallo et

al. 2015; Green et al. 2025). Active planting of nursery-grown resistant juniper genotypes therefore carries a real risk of introducing *P. austrocedri* into unexposed populations or introducing new *P. austrocedri* genotypes into already-affected populations (Donald et al. 2021).

In summary, the conservation of juniper in the UK will be best served by promoting natural regeneration within populations while limiting the spread of *P. austrocedri* between populations, giving juniper the greatest opportunity to respond to the pathogen through natural selection and adaptation.

CHAPTER 3:
High-quality reference genomes for two lineages of the oomycete tree pathogen *Phytophthora austrocedri*

Note: This chapter has been written to be submitted as a Genome Resource Paper and is therefore intentionally very succinct.

Abstract

Phytophthora austrocedri is an oomycete pathogen known to cause disease in several tree species within the cypress family (Cupressaceae). First described as the causal agent of widespread dieback and mortality of Chilean cedar (*Austrocedrus chilensis*) in Argentina, *P. austrocedri* was subsequently also identified as the cause of extensive mortality of juniper (*Juniperus communis*) in the UK. Isolates of *P. austrocedri* from Argentina and the UK form genetically distinct lineages. Despite the importance of the genus as highly destructive plant pathogens, chromosome-level assemblies of *Phytophthora* are still scarce, and there are currently no genomic resources available for *P. austrocedri*. Here, we used high-coverage PacBio long-read sequencing and Hi-C data to generate high-quality, near-chromosome-level assemblies for one isolate from each of the two major lineages. The UK isolate (TDJ3) yielded a 154 Mb assembly across 24 scaffolds; the Argentinian isolate (PHY-211) yielded a 173 Mb assembly across 25 contigs. These high-quality reference genomes for both lineages of *P. austrocedri* will be a valuable resource for further research into the virulence, genome evolution and population history of both *P. austrocedri* and other *Phytophthora* pathogens.

3.1 Introduction

Phytophthora austrocedri is an oomycete pathogen known to cause disease in several tree species within the cypress family (Cupressaceae). First described as the causal agent of widespread dieback and mortality of Chilean cedar (*Austrocedrus chilensis*) in the Patagonian Andean forests of Argentina (Greslebin et al. 2007; Greslebin and Hansen 2010), *P. austrocedri* was subsequently also identified as the cause of extensive mortality of juniper (*Juniperus communis)* in populations across northern England and Scotland, UK (Green et al. 2012; Green et al. 2014). The pathogen is believed to be invasive in both regions, although its geographic origin remains unknown (Henricot et al. 2017). Beyond natural ecosystems, *P. austrocedri* has also been detected causing isolated cases of disease in nurseries and urban parks in the UK, Germany, Iran and the USA, affecting *J. communis* and several other members of the cypress family, including *J. horizontalis*, *Cupressus sempervirens* and *Callitropsis nootkatensis* (Werres et al. 2014; Green et al. 2016; Mahdikhani et al. 2017; Kipp 2024).

Previous work has shown isolates of *P. austrocedri* from Argentina and the UK form genetically distinct lineages, although there appears to be little genetic diversity within each lineage (Vélez et al. 2014; Henricot et al. 2017). Here, we present the first genomic resources for this highly damaging tree pathogen in the form of high-quality, near-chromosome-level assemblies representing one isolate from each of the two major lineages.

3.2 Methods

3.2.1 Sample preparation

Two *P. austrocedri* isolates were used in this study, one representing the UK lineage (TDJ3; Green et al. 2014) and one representing the Argentinian lineage (PHY-211; Vélez et al. 2014) (Table 2.1). Cultures of *P. austrocedri* were grown in V8 broth until approximately 2-3 cm in diameter, and were then ground in liquid nitrogen. To achieve high molecular weight DNA, extractions were carried out using a modified protocol based on Zelaya-Molina et al. (2011) and Schwessinger and Rathjen (2017) (see Supplementary Methods for full description of protocol). Extractions underwent quality control to ensure all samples had good 260/280 nm absorbance ratios (Infinite F Nano+, Tecan; NanoPhotometer NP80, Implen), DIN scores above eight (Tapestation 2200, Agilent Technologies) and DNA concentrations above 40 ng/µl (Qubit 2.0, Thermo Fisher Scientific). PacBio HiFi sequencing was carried out using the PacBio Sequel IIe system (TDJ3 isolate) and the PacBio Revio system (PHY-211 isolate), with one SMRT cell used per isolate.

Tissue from one isolate (TDJ3) was also subjected to Hi-C sequencing. For this, fresh mycelial tissue was ground in liquid nitrogen, followed by tissue fixation and library preparation using the Arima High Coverage HiC kit, according to the manufacturer's instructions. Sequencing (150 bp paired-end reads) was carried out on the Illumina NovaSeq X platform.

To annotate the genome, three replicate colonies of TDJ3 were flash frozen and ground in liquid nitrogen for RNA extraction using the Monarch Total RNA Miniprep Kit (New England Biolabs), following the manufacturer's instructions. RNA extractions underwent quality control to ensure all samples had good 260/280 nm absorbance ratios (Infinite F Nano+, Tecan), RNA concentrations above 50 ng/µl (Qubit 2.0, Thermo Fisher Scientific) and RIN scores above eight (Tapestation 2200, Agilent Technologies). Poly(A) enriched RNA sequencing (150 bp paired-end reads) was carried out on the Illumina NovaSeq 6000 platform.

3.2.2 Genome assembly

After retaining only Q20 reads or higher, PacBio sequencing generated 1.5 million HiFi reads for TDJ3 and 3.8 million HiFi reads for PHY-211. To explore genome properties prior to assembly, we carried out k-mer analyses using kmc v3.2.1 (Kokot et al. 2017) followed by Genomescope v2.0 (Ranallo-Benavidez et al. 2020). The estimated k-mer coverage was 74 for TDJ3 and 183 for PHY-211, and the k-mer distributions suggested *P. austrocedri* is likely a tetraploid (Figure S3.1).

Reads shorter than 5 kb were filtered out, and any reads containing adapter sequences were removed using Cutadapt v2.6 (Martin 2011). Remaining reads were then subsampled to achieve homozygous coverage of 50x and assembled using HiFiasm v0.19.5 (Cheng et al. 2021). Hi-C reads were used in the TDJ3 assembly process to help phase the assembly. Mitochondrial contigs were removed from the assembly using Tiara v1.0.3 (Karlicki et al. 2022), then assembled separately into one circularised contig using MitoHiFi v3.2.2 (Uliano-Silva et al. 2023). Contigs representing haplotypic duplication in the assembly (haplotigs) were identified and removed using purge_dups v1.2.6 (Guan et al. 2020). Completeness of the assembly was assessed using Busco v5.4.7 (Simão et al. 2015), and the assembly was checked for contamination using BlobToolKit v4.1.5 (Challis et al. 2020).

To scaffold the TDJ3 assembly, HiC reads were trimmed to remove adapters and low-quality sequences using Skewer v0.2.2 (Jiang et al. 2014). Automated scaffolding tools introduced scaffolding errors in the assembly, probably due to the polyploid nature of *P.*

austrocedri. The assembly was therefore curated manually using the sanger-tol/curationpretext pipeline v1.4.0 (DOI: 10.5281/zenodo.12773958) and PretextView v0.2.5 (Harry 2021).

To annotate the TDJ3 genome, RNAseq reads were trimmed to remove adapters and low-quality sequences using Skewer v0.2.2 (Jiang et al. 2014) and mapped to the final assemblies using STAR v2.7.11 (Dobin et al. 2013). Repetitive regions were first modelled using RepeatModeler v2.0.5 (Flynn et al. 2020), then soft masked using RepeatMasker v4.1.5 (Smit et al. 2015). Finally, annotation was carried out using the BRAKER3 pipeline v3.0.8 (Gabriel et al. 2024).

3.3 Results and discussion

The statistics of the final genome assemblies are shown in Table 3.1. Both *P. austrocedri* isolates generated high-quality, highly contiguous assemblies. The assembly sizes (154 Mb and 173 Mb; Table 3.1) are large for *Phytophthora*, which typically have genome sizes of 40–100 Mb when diploid (e.g., Thorpe et al. 2021; Cox et al. 2022; Kronmiller et al. 2023). Along with the genomic DNA k-mer spectra (Figure S3.1), this supports the idea that *P. austrocedri* is likely a tetraploid. The UK isolate (TDJ3) was assembled into 24 scaffolds, with >99% of the assembly contained in 19 scaffolds >2Mb in length. The Argentinian isolate (PHY-211) was assembled into 25 contigs, with >99% of the assembly contained in 24 contigs >2Mb in length. Based on the number of chromosomes identified in other tetraploid *Phytophthora* species (18-24; Sansome et al. 1991; Brasier et al. 1999), these statistics suggest at least near-chromosome-level assemblies.

Figure 3.1A shows the high level of synteny between the two *P. austrocedri* assemblies. Figure 3.1B shows the synteny between TDJ3 and the chromosome-level assembly of *P. agathidicida* (Cox et al. 2022). Note that because *P. austrocedri* is tetraploid, most regions of the diploid *P. agathidicida* genome demonstrate sequence similarity with two regions of the *P. austrocedri* genome.

In summary, we present the first genomic resources available for *P. austrocedri* in the form of near-chromosome level assemblies for two isolates, representing two distinct lineages of this pathogen. Despite the ecological and economic importance of the genus as highly destructive plant pathogens, chromosome-level assemblies of *Phytophthora* are still scarce. These high-quality reference genomes for both the UK and Argentinian lineages of *P. austrocedri* will therefore be a valuable resource for further research into the virulence, genome evolution and population history of both *P. austrocedri* and other *Phytophthora* pathogens.

Table 3.1. Summary statistics for genome assemblies of two *Phytophthora austrocedri* isolates representing different lineages. FR-NRS = Forest Research Northern Research Station, Roslin, Midlothian, Scotland; CIEFAP = Centro de Investigación y Extensión Forestal, Andino Patagónico, Esquel, Chubut, Argentina.

		ISOLATE	
		TDJ3	**PHY-211**
ISOLATE INFORMATION	**Origin**	County Durham, UK	Chubut Province, Argentina
	Host	*Juniperus communis*	*Austrocedrus chilensis*
	Isolation date	November 2011	January 2010
	Source	FR-NRS	CIEFAP
GENOME ASSEMBLY STATISTICS	**Assembly size**	154 Mb	173 Mb
	No. of scaffolds /contigs	24	25
	N50	9.28 Mb	8.26 Mb
	N90	5.47 Mb	4.21 Mb
	L50	7	8
	L90	16	19
	GC content	51.9%	51.8%
	Busco completeness score	100% (88% duplicated)	100% (90% duplicated)
	No. of genes	15,157	N/A
	Repetitive DNA content	39.2%	42.4 %
	Accession number	*Pending*	*Pending*
MITOGENOME STATISTICS	**Assembly size**	39,968 bp	39,977 bp
	No. of contigs	1	1
	GC content	21.4%	21.4%

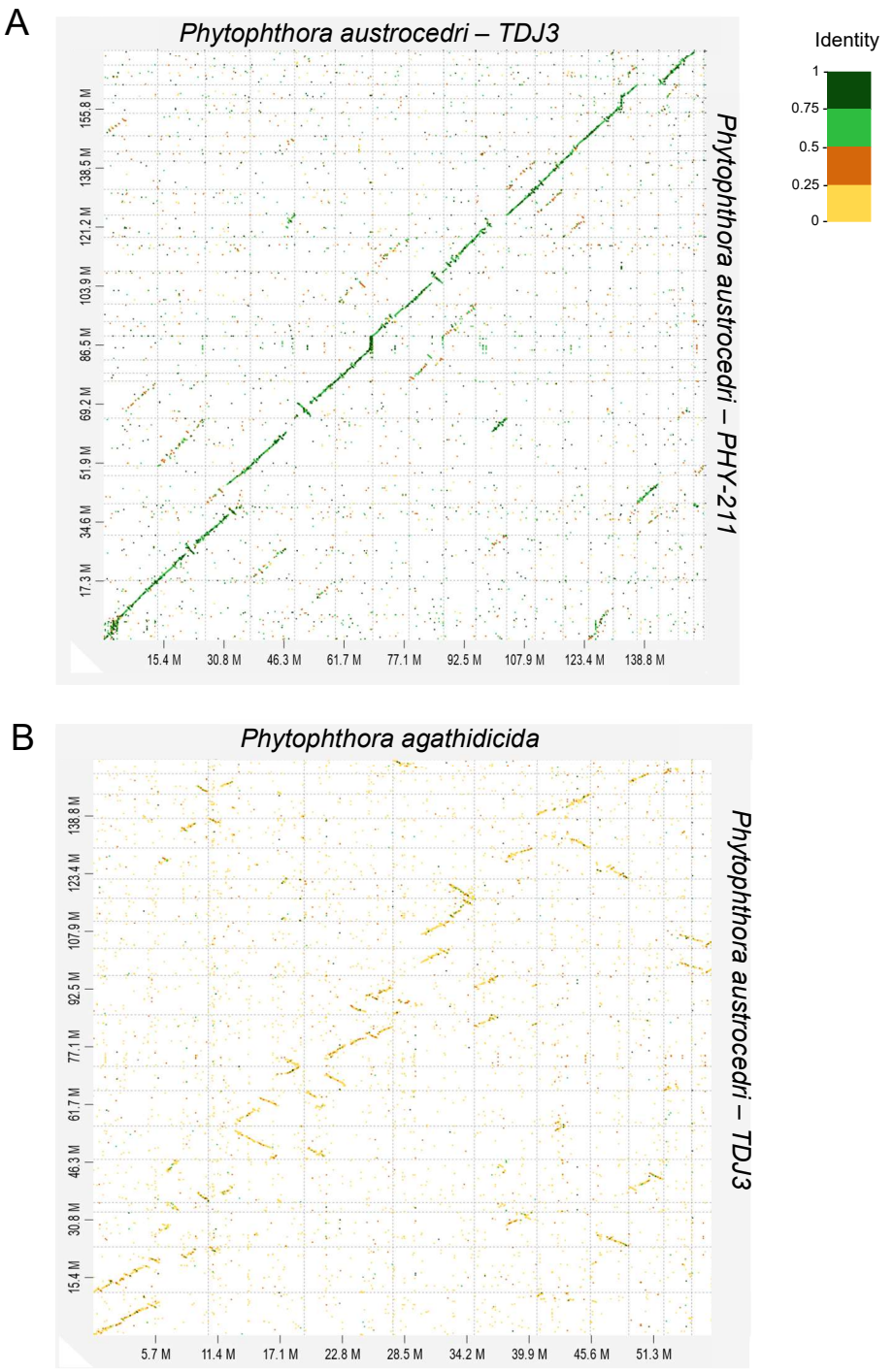

Figure 3.1. Synteny between the assemblies of the two *Phytophthora austrocedri* lineages (TDJ3 and PHY-211; A) and between *P. austrocedri* (TDJ3) and a chromosome-level assembly of *P. agathidicida* (B). Synteny dot plots were produced using D-GENIES v1.5.0 (Cabanettes and Klopp 2018). The grey lines delineate individual contigs/scaffolds, and the colour coding represents alignment identity between contigs/scaffolds. The best matching contigs/scaffolds between the two assemblies are shown along the diagonal. There is a high level of synteny and sequence similarity between the two *P. austrocedri* assemblies, and moderate synteny between *P. austrocedri* and *P. agathidicida*. Because *Phytophthora austrocedri* is tetraploid and *P. agathidicida* is diploid, most regions of the *P. agathidicida* genome show sequence similarity with two regions of the *P. austrocedri* genome.

CHAPTER 4:
Low genetic diversity but high between-subgenome heterozygosity in the invasive hybrid tree pathogen *Phytophthora austrocedri*

Abstract

The genus *Phytophthora* includes many important plant pathogens that are often particularly destructive when they are introduced into a new environment, gain the opportunity to infect a novel host, and become invasive. Key features of *Phytophthora* biology may contribute to their success as invasive plant pathogens, including polyploidy and hybridisation. One successful invasive *Phytophthora* species is *P. austrocedri*, which is causing extensive mortality in two tree species of the cypress family in two different geographical regions (UK and Argentina). This study uses flow cytometry combined with high-coverage, whole-genome sequencing of 17 *P. austrocedri* isolates representing both geographical lineages to characterise the pathogen's ploidy, genome composition, genetic diversity and divergence within and between lineages, with an emphasis on exploring the factors underlying its success as an invasive plant pathogen. We show that most *P. austrocedri* isolates are tetraploid, but based on k-mer analyses and pronounced variation in coverage, triploidisation and diploidisation appears to be in progress in some isolates. We confirm that *P. austrocedri* is of hybrid origin (allotetraploid), and that the hybridisation event likely occurred before the two geographical lineages diverged. Levels of genome-wide genetic diversity and within-subgenome heterozygosity are very low, suggesting a history of self-fertilisation. However, the hybrid nature of the pathogen means it maintains high levels of between-subgenome heterozygosity. This particular combination of allotetraploidy and self-fertilisation makes use of highly resilient oospores while maintaining high levels of between-subgenome heterozygosity, which may represent a particularly advantageous strategy for a plant pathogen colonising novel environments.

4.1 Introduction

The genus *Phytophthora* includes many highly destructive plant pathogens that pose a significant threat to agriculture, forestry and natural ecosystems (Hansen 2015; Brasier et al. 2022). Most of the over 200 *Phytophthora* species are pathogenic, and *Phytophthora* disease affects all kinds of plants, from annual herbaceous crops through to large trees (Agrios 2005). Some *Phytophthora* have a wide host range, while others appear to be limited to a small number of closely related hosts (Agrios 2005). As is the case for many pathogens, *Phytophthora* are often particularly destructive when they are introduced into a new environment, gain the opportunity to infect a new host and become invasive (Garbelotto and Gonthier 2022; D'Amato et al. 2023). There are several infamous examples of invasive *Phytophthora* species causing extensive economic, environmental and societal damage, including *P. cinnamomi*, which has caused extensive mortality in eucalyptus forests in Australia and Fagaceae forests in the US and Europe (Hardham and Blackman 2018; Jung et al. 2018), and *P. infestans*, the causal agent of potato late blight, which was responsible for mass famine and migration in Ireland in the 1840s and which remains a threat to global food security to this day (Turner 2005; Yuen 2021).

Superficially resembling filamentous fungi, *Phytophthora* actually belong to the phylum *Oomycota*, which are members of the Stramenopiles, a clade that also includes diatoms and brown algae (Beakes et al. 2012; Burki 2014). There are several features of *Phytophthora* biology that are thought to contribute to their success as plant pathogens. To begin with, *Phytophthora* can reproduce through either large numbers of motile, asexual zoospores or by means of sexual oospores. The latter have been shown to be highly resilient, able to tolerate temperatures well below freezing (Drenth et al. 1995) and to survive for months or even years in soil under natural field conditions (Turkensteen et al. 2000; Babadoost and Pavon 2013). As many *Phytophthora* species are obligate plant pathogens, having highly resistant oospores provides greater flexibility in their lifecycle, allowing them to survive temporary absences of suitable hosts. These long-lived sexual spores are thus likely to provide an important mechanism through which *Phytophthora* can colonise new areas.

Some *Phytophthora* species have two distinct mating types (heterothallic) and are not typically able to self-fertilise, while other *Phytophthora* species have just one mating type (homothallic) and readily produce oospores through self-fertilisation (Goodwin 1997; Judelson 2009). When it comes to invading a new geographical area, being able to reproduce through self-fertilisation is likely to be advantageous, as this circumvents the need for two mating types

to be introduced into the same area at the same time by chance. In the absence of both mating types, heterothallic *Phytophthora* can also make use of asexual reproduction through zoospores – indeed, early epidemics of the heterothallic *P. infestans* were all caused by clonal lineages of the pathogen, due to the absence of one of the mating types (Fry et al. 1992). Both strategies have their disadvantages, however: self-fertilisation reduces levels of heterozygosity by half every generation, eroding genetic diversity (Goodwin 1997), while asexual reproduction will reduce adaptive potential, as the lack of recombination will result in reduced efficacy of selection due to interference between loci (Hill and Robertson 1966; Keightley and Otto 2006). Furthermore, in both cases introduced lineages will experience greatly reduced genetic diversity compared to ancestral states, due to the genetic bottleneck imposed by founder effects (Meffert 2006).

Low genetic diversity is likely to be a disadvantage for a pathogen invading a new geographical area, as it means reduced evolutionary potential to adapt to the novel environment and novel hosts. One way *Phytophthora* species may overcome a lack of genetic diversity is by having flexible genomes that can undergo rapid duplication events leading to expansion of gene families (Morales-Cruz et al. 2020; Lee et al. 2021; Cox et al. 2022), as well as whole-genome duplication events resulting in polyploidy. Polyploidy has been reported in multiple *Phytophthora* species in different clades (e.g., Bertier et al. 2013; Morales-Cruz et al. 2020; Ayala-Usma et al. 2021), and it has even been speculated that a whole-genome duplication event forms part of the history of *Phytophthora* species, with signals of ancient polyploidisation being detected in three *Phytophthora* species that are now considered to be diploid (Martens and Van de Peer 2010). Polyploidy has been shown to enhance adaptation to specific environments in plants (Ramsey 2011), and has been speculated to do so in *Phytophthora* (Sansome 1977). Increased ploidy has also been shown to be associated with larger families of virulence effectors (Morales-Cruz et al. 2020), which could allow for more rapid adaptation to novel or evolving hosts.

In some cases, polyploidy in *Phytophthora* can also involve a hybridisation event, as whole genome duplication can restore fertility when the diverged chromosomes of a hybrid are otherwise unable to pair effectively during meiosis (Charron et al. 2019). *Phytophthora* hybrids have been detected in natural populations (Brasier et al. 1999; Goss et al. 2011; Bertier et al. 2013; Van Poucke et al. 2021) and have also been created artificially in laboratory environments (Érsek et al. 1995; Donahoo and Lamour 2008). By bringing together divergent lineages, hybridisation immediately increases the genetic diversity and levels of heterozygosity in the

hybrid relative to the parental species. In plants and animals, hybridisation has repeatedly been shown to increase fitness in the form of hybrid vigour or heterosis (Birchler et al. 2006; Nicholas et al. 2016). In *Phytophthora*, hybrids have in some cases been shown to inherit the host range of both parental species, broadening the number of hosts a species can infect (Érsek et al. 1995), or even to cause disease in novel hosts that are not associated with either parental species (Brasier et al. 1999; Man in 't Veld et al. 2007; Bertier et al. 2013). By enhancing genetic diversity and evolutionary potential, hybridisation may thus facilitate successful invasions into novel environments and new hosts.

One successful invasive *Phytophthora* species is the tree pathogen *P. austrocedri*. Of unknown origin, *P. austrocedri* has become invasive in two widely separated geographical locations, where it is causing extensive mortality in two different hosts: juniper (*Juniperus communis*) in the UK (Green et al. 2012; Green et al. 2014) and Chilean cedar (*Austrocedrus chilensis*) in Argentina (Greslebin et al. 2007; Greslebin and Hansen 2010). Based on new reference genomes for both lineages (Chapter 3 of this thesis), *P. austrocedri* is thought to be a tetraploid, but different isolates of the same *Phytophthora* species can vary in their ploidy (Brasier et al. 2004; Bertier et al. 2013). *Phytophthora austrocedri* is known to be self-fertile (homothallic; Greslebin et al. 2007; Henricot et al. 2017), and analyses based on molecular markers have suggested both the UK and Argentinian lineages show low levels of genetic diversity (Vélez et al. 2014; Henricot et al. 2017). Previously it has been speculated that these lineages may reproduce entirely clonally, based on fixed patterns of heterozygosity (Henricot et al. 2017). However, these inferences were made based on an analysis of DNA sequences from a small number of genes, and many of the key features regarding *P. austrocedri*'s genetics and evolution remain unknown. This study uses flow cytometry combined with high-coverage, whole-genome sequencing of 17 *P. austrocedri* isolates representing both geographical lineages to characterise the pathogen's ploidy, genome composition, genetic diversity and divergence within and between lineages, with an emphasis on exploring the factors underlying its success as an invasive pathogen.

4.2 Methods

4.2.1 *Phytophthora austrocedri* isolates

There are two geographical lineages of *P. austrocedri*, one found in Argentina (ARG) and one found in the UK (Henricot et al. 2017). Each lineage has its own reference genome assembly (isolate TDJ3 for the UK lineage and isolate PHY-211 for the ARG lineage; see Table 4.1), and in both cases the assemblies suggest *P. austrocedri* is a tetraploid (Chapter 3 of this thesis). This study uses 17 *P. austrocedri* isolates in total: 13 isolates originating from four different populations in the UK, three isolates originating from Argentina, and one isolate that was discovered in a nursery in Germany, and that has previously been reported to belong to the ARG lineage (Henricot et al. 2017). Full details of the isolates included in this study are shown in Table 4.1.

Table 4.1. Details of the *P. austrocedri* isolates used in this study. Source of UK isolates: Forest Research Northern Research Station, Roslin, Midlothian, Scotland. Source of Argentinian isolates: Centro de Investigación y Extensión Forestal, Andino Patagónico, Esquel, Chubut, Argentina. Source of German isolate: Julius Kühn-Institut, Federal Research Centre for Cultivated Plants, Institute for Plant Protection in Horticulture and Forests, Braunschweig, Germany. *The two isolates from which reference genomes were generated are marked with an asterisk.

Isolate	Lineage	Population	Latitude, longitude (°)	Isolation date
BBA	ARG	Plant nursery, Germany		2001
BF207	UK	Cumbria, UK	54.551, -2.311	February 2015
BT3	UK	Cumbria, UK	54.422, -3.085	November 2012
GA3	UK	Perthshire, UK	56.336, -4.010	February 2012
GA7	UK	Perthshire, UK	56.337, -4.050	October 2018
GA10-SG	UK	Perthshire, UK	56.338, -4.012	May 2021
GA197	UK	Perthshire, UK	56.336, -3.999	February 2015
GA510	UK	Perthshire, UK	56.339, -4.017	May 2021
GAT6	UK	Perthshire, UK		February 2012
GK2	UK	Grampian, UK	57.375, -3.956	October 2012
SS2	UK	Grampian, UK	57.266, -3.522	October 2012
***TDJ3**	UK	Durham, UK	54.645, -2.169	November 2011
TDJ6	UK	Durham, UK	54.648, -2.204	March 2012
TDJ20	UK	Durham, UK	54.644, -2.168	November 2011
***PHY-211**	ARG	Chubut, Argentina	-42.775, -71.536	Jan 2010
PHY-215	ARG	Chubut, Argentina	-42.775, -71.536	Jan 2010
PHY-257	ARG	Neuquén, Argentina	-40.676, -71.312	May 2008

4.2.2 Flow cytometry sample preparation and analysis

Phytophthora austrocedri cultures were grown in Petri dishes containing V8 broth for 2-3 weeks. Actively growing edges of the mycelial tissue were excised, rinsed in sterilised distilled water and kept on ice while samples were prepared for analysis. The samples were processed using the CyStain PI Absolute P kit (Sysmex) following the manufacturer's recommendations. Leaf material from the plant *Raphanus sativus L. 'Saxa'* was used as an internal standard (Doležel et al. 2007). Mycelial tissue was co-chopped with the plant standard using a sharp razor in nuclei extraction buffer and filtered through a 10 µm filter (CellTrics, Sysmex), before adding the staining buffer, propidium iodide and RNAse. Samples were analysed using the CyFlow Ploidy Analyser (Sysmex) following the manufacturer's recommendations. Three biological replicates (different cultures) were prepared for each isolate on three different days. Measurements on the flow cytometer were repeated three times for each sample preparation, forming three technical replicates for each biological replicate.

Flow cytometry measures total DNA content of nuclei, and genome size can then be estimated based on the position of fluorescence peaks relative to an internal standard of known genome size. In this case the standard (*R. sativus L. 'Saxa'*) had a 2C DNA content of 1.11 pg (Doležel et al. 2007). The estimated DNA content in pg can then be multiplied by 978 to convert to Mb (Doležel et al. 2003), and divided by two in order to get the more commonly used estimate of 1C genome size in Mb. Flow cytometry data were analysed using the R package flowPloidy, which uses non-linear regression to objectively identify the different peaks in flow cytometry fluorescence histograms (Smith et al. 2018). Each sample histogram was then inspected manually to ensure good model fit, correct identification of peaks, and to identify the standard peak.

4.2.3 DNA extraction for whole-genome sequencing

Cultures of *P. austrocedri* were grown in V8 broth for two to three weeks until individual colonies were approximately 2-3 cm in diameter. Colonies were then rinsed with sterilised distilled water, blotted dry on filter paper, and cut into smaller pieces using aseptic techniques. The mycelial pieces were placed in Eppendorf tubes with two small ball bearings, frozen in liquid nitrogen, and then disrupted using the TissueLyser II (Qiagen) until the mycelium was reduced to a fine powder. DNA was extracted using the NucleoSpin Tissue kit (Macherey-Nagel) following manufacturer's recommendations. Extractions underwent quality control to ensure all samples had good 260/280 nm absorbance ratios (Infinite F Nano+, Tecan) and

suitable DNA concentrations (Qubit, ThermoFisher Scientific), before normalisation and sequencing (150 bp paired-end reads) on the Illumina NovaSeq 6000 platform.

4.2.4 Analyses of genome structure

Raw reads were trimmed to remove adapters and low-quality sequences using Skewer (Jiang et al. 2014). To explore genome properties, k-mers (k=21) were counted using kmc (Kokot et al. 2017), counting up to a coverage of 10^6 to ensure repetitive regions of the genome were not excluded from the analysis. K-mer spectra were then explored for each isolate using Genomescope 2.0 (Ranallo-Benavidez et al. 2020), initially fitting tetraploid models and subsequently attempting to fit diploid and triploid models if the tetraploid model was a poor fit. Genome size can be estimated from k-mers based on the total number of k-mers and the k-mer coverage (Hesse 2023). For polyploid genomes, Genomescope reports monoploid genome size; to get estimated 1C genome size for a tetraploid, this estimate was therefore multiplied by two. The ploidy of each isolate was further explored using Smudgeplot, which uses coverage ratios of heterozygous k-mer pairs to make inferences about ploidy (Ranallo-Benavidez et al. 2020). An initial estimate of monoploid coverage (or k-mer coverage) was calculated based on the total amount of Illumina sequencing data (number of reads multiplied by read length) for each isolate divided by individual estimated genome size based on the flow cytometry results, and these values were used as an input for both Genomescope and Smudgeplot to specify monoploid coverage.

Reads for all isolates were mapped to both reference genomes (UK and ARG lineages) using bwa (Li and Durbin 2009). Genome-wide coverage patterns were then explored using deepTools (Ramírez et al. 2016). For each isolate, we calculated the $\log_2$ ratio of normalised coverage relative to the corresponding reference isolate mapped to its own reference genome in 50 bp windows across the genome. Normalisation between samples was performed using a global scaling factor derived from the total number of mapped reads in each library. Comparing each isolate to the reference in this way helps control for systematic biases associated with the reference assembly (e.g. misassemblies or repetitive regions), allowing differences in coverage to more directly reflect underlying differences in genome composition between isolates.

In addition, SAMtools (Li et al. 2009) was used to calculate percentage genome coverage for each isolate. Here, coverage was defined as the proportion of positions with at least one aligned read, calculated within bins across scaffolds/contigs.

4.2.5 Analyses of genetic diversity and divergence

SNPs were called using BCFtools (Danecek et al. 2021), making no assumptions of Hardy-Weinberg equilibrium across samples. SNPs were then filtered based on various quality parameters, excluding any SNPs with quality score <27, mapping quality bias MQBZ <-8, read position bias RPBZ <-5 or >5, or genotype quality score <27. An initial analysis showed that heterozygous calls were very sensitive to coverage (Figure S4.1), possibly due to the flexible nature of *Phytophthora* genomes, which can undergo duplication events. Two approaches were therefore taken to filter SNPs based on coverage depth.

Firstly, to explore genetic clustering between isolates, a moderately strict across-sample coverage depth filter was implemented to exclude sites with a coverage more than 1.5 times the median coverage, or below an average of 20x coverage per sample. This approach is likely to result in a significant number of "false" heterozygous calls that arise from paralogs rather than true heterozygous sites; however, these false heterozygous sites still represent real genomic variation, and there is no reason why these variants cannot therefore be used for genetic clustering based on similarity. This dataset of filtered SNPs was then pruned using vcftools (Danecek et al. 2011) to retain only those SNPs that were more than 10 kb apart. A principal component analysis (PCA) was then carried out on the pruned SNP dataset using Adegenet (Jombart 2008).

Secondly, to explore genetic diversity across the genome, it is more important to get an accurate assessment of true heterozygous variants in the genome. To achieve this, an individual depth filter was imposed on each sample individually, excluding sites with a depth of coverage more than 1.5 times the median coverage expected for true heterozygous SNPs for each sample. This method should result in a more sensitive screening of regions with unusual coverage within each isolate. However, this approach does result in many more missing sites in the dataset, which could result in a downwardly biased estimate of genetic diversity (Korunes and Samuk 2021). To account for this, nucleotide diversity (π) and divergence (d_{XY}) were calculated using pixy (Korunes and Samuk 2021), which generates unbiased estimates in the presence of missing data. Nucleotide diversity and divergence were calculated in a sliding window analysis using 100 kb non-overlapping windows. Diversity within lineages was measured by using all isolates mapped to their own reference (UK isolates mapped to the UK reference and ARG isolates mapped to the ARG reference). Thus, this represents nucleotide diversity within the lineage rather than within populations, an approach that was justified due to the limited sample sizes in each population. Genetic divergence

between lineages was estimated by mapping all isolates to the UK reference, then calculating average pairwise differences between isolates from different lineages.

Mitochondrial sequences were analysed separately by mapping reads to the relevant reference mitogenome for each lineage and calling SNPs using BCFtools (Danecek et al 2021), assuming a haploid genotype. BCFtools was then used to generate a consensus mitogenome for each isolate. These whole-mitogenome sequences were aligned using MAFFT (Katoh and Standley 2013) and a network analysis was implemented and visualised in SplitsTree (Huson and Bryant 2024), using the NeighborNet method based on p-distance between sequences (Bryant and Huson 2023). The average number of nucleotide differences within and between lineages was calculated using MEGA (Tamura et al. 2021).

4.2.6 Phylogenetic analysis of homologs

To investigate genetic divergence between lineages further, and explore a possible hybrid origin of *P. austrocedri*, we analysed the phylogenetic relationship between homologous genes within and between the two *P. austrocedri* lineages and other *Phytophthora* species. We downloaded reference genomes for 17 other species of *Phytophthora* from NCBI (Table S4.1), and used BUSCO (Simão et al. 2015) to identify genes expected to be present in all *Phytophthora* genomes in a single copy (Stramenopiles odb10). The dataset consisted of 100 genes in total. Gene sequences were extracted from the genome assemblies using SAMtools (Li et al. 2009). Most of the genes were present twice in the *P. austrocedri* assemblies, as would be expected in a tetraploid genome.

Gene sequences (representing orthologs across *Phytophthora* species as well as the two homologous gene copies present within each *P. austrocedri* assembly) were aligned using MAFFT (Katoh and Standley 2013). Aligned sequences could not be concatenated to build a single overall phylogenetic tree, due to the unknown pairing between different homologous genes within the two *P. austrocedri* lineages. Maximum likelihood trees were therefore constructed for each gene separately using RAxML-NG (Kozlov et al. 2019), using the GTR+GAMMA model with default parameters. Each individual gene tree was then inspected using Phylo.io (Robinson et al. 2016) to determine the topology of the homologs within and between the two *P. austrocedri* lineages. Pairwise distances between all sequences were calculated using MEGA (Tamura et al. 2021), using maximum likelihood and assuming gamma distributed rate variation among sites.

4.3 Results

4.3.1 Genome size estimates

There was considerable variation between *P. austrocedri* isolates in their genome size estimated by flow cytometry, ranging from 131 Mb to 249 Mb (Figure 4.1; Table 4.2). Mean genome size was 198 Mb and median genome size was 196 Mb. The average coefficient of variation between technical replicates was 1.3%, which is considered an acceptable amount of error (Loureiro et al. 2023). The average coefficient of variation between biological replicates (using the mean value across technical replicates) was 2.7%, demonstrating there are consistent differences between isolates in genome size. Isolates originating from outside the UK (ARG lineage) had the most extreme values in genome size, including both the largest and smallest values (Figure 4.1). Estimates of genome sizes for UK isolates ranged from 171 Mb to 213 Mb.

Genome size estimates based on k-mer analysis were in all cases smaller than estimates from flow cytometry (by an average of 34 Mb, or 17%), ranging from 101 Mbp to 198 Mbp (Table 4.2). There was a significant positive correlation between the genome sizes estimated using the two different methods for each isolate ($r_{(15)}$ = 0.76, $p<0.001$), showing general concordance between the methods. However, the normalised estimates of genome size between the two methods did not align for all isolates, with some isolates showing distinct differences in estimated genome size between the two methods (Figure 4.2).

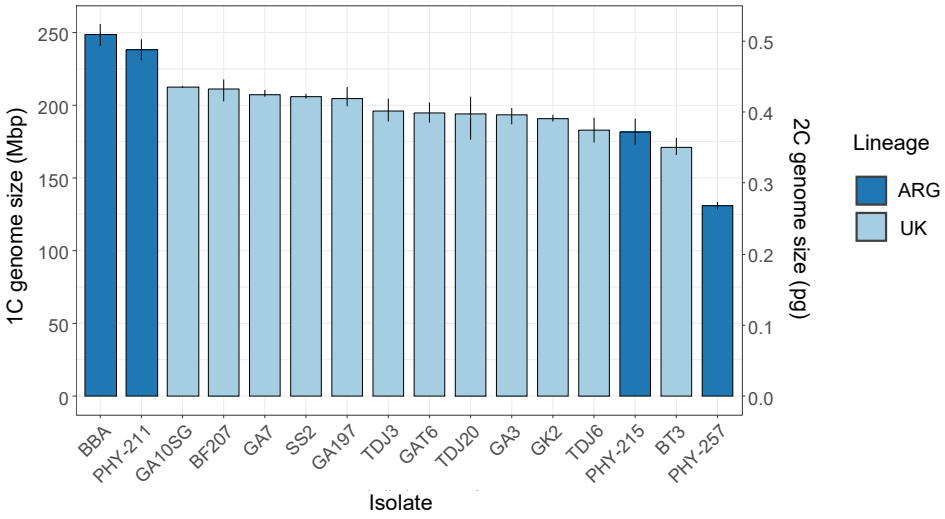

Figure 4.1. Comparison of genome size estimated using flow cytometry across *Phytophthora austrocedri* isolates. Shade of blue represents geographical lineage, with dark blue indicating ARG and light blue indicating UK. Error bars represent total range between the highest and lowest estimates for each isolate across three biological replicates.

Table 4.2. Estimated genome size (Mb) for *Phytophthora austrocedri* isolates using flow cytometry and k-mer analysis. For the flow cytometry data, the mean is reported with brackets showing the lowest and highest values recorded for each isolate across three biological replicates. Flow cytometry data are missing for one isolate (grey box). Estimates were generally concordant between the two methods, but in all cases estimated genome size was larger when using flow cytometry. Estimated monoploid coverage was calculated based on the total length of sequencing data divided by estimated 2C genome size. *The two isolates that represent the reference genomes are marked with an asterisk.

Isolate	Lineage	Population	Genome size (flow cytometry)	Genome size (k-mer analysis)	Estimated monoploid coverage
BBA	ARG	Germany	249 (241-256)	198	27
BF207	UK	Cumbria	211 (203-218)	177	35
BT3	UK	Cumbria	171 (166-178)	162	38
GA10SG	UK	Perthshire	213 (212-213)	175	37
GA197	UK	Perthshire	205 (199-213)	164	43
GA3	UK	Perthshire	193 (187-198)	172	39
GA510	UK	Perthshire		168	
GA7	UK	Perthshire	208 (206-210)	167	35
GAT6	UK	Perthshire	195 (188-202)	159	43
GK2	UK	Grampian	191 (189-193)	185	42
SS2	UK	Grampian	206 (205-208)	182	37
TDJ20	UK	Durham	194 (177-206)	170	38
***TDJ3**	UK	Durham	196 (189-204)	163	37
TDJ6	UK	Durham	183 (175-192)	164	33
***PHY-211**	ARG	Chubut	238 (231-245)	178	30
PHY-215	ARG	Chubut	182 (173-191)	106	34
PHY-257	ARG	Neuquén	131 (128-134)	101	51

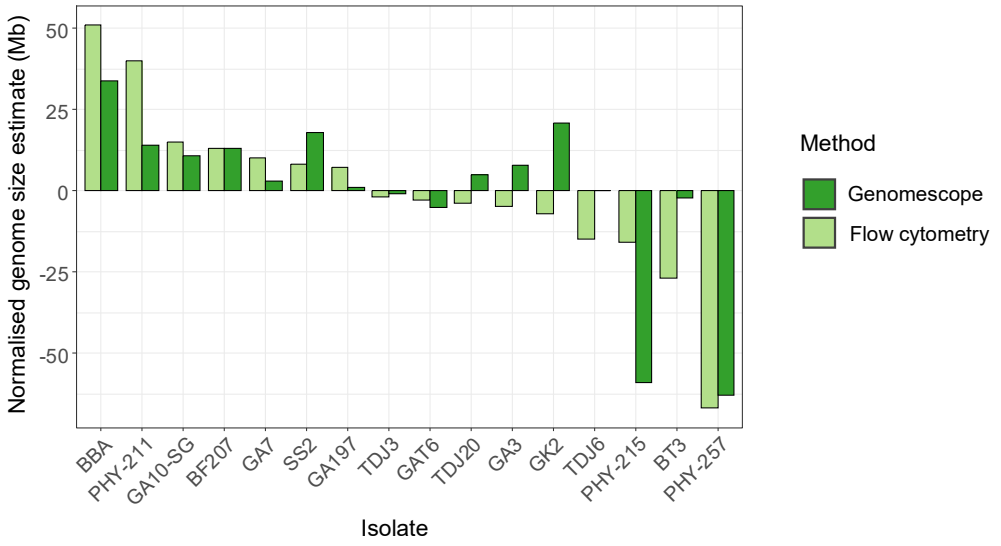

Figure 4.2. Comparison between the two methods for estimating genome size. Estimates were normalised around zero, then deviations from the mean were plotted for each method and each isolate. Shade of green represents the estimation method, with light green indicating flow cytometry and dark green indicating k-mer analysis using Genomescope. Methods were fairly concordant in their deviations from the mean for each isolate in most, but not all, cases.

4.3.2 Evidence of variation in ploidy levels between isolates

Based on the analysis of k-mer spectra using Genomescope and analyses of heterozygous k-mers using Smudgeplot, most *P. austrocedri* isolates appear to be tetraploid (Figure 4.3). However, there was variation in genome structure between isolates, which has been summarised into the four patterns described in Figure 4.3.

Firstly, in some cases tetraploidy was clear based on a distinct 1x peak in the k-mer spectra (demonstrating the true monoploid coverage value), combined with a clear high abundance of AABB heterozygous k-mer pairs in the Smudgeplot analysis, which shows that the most frequent heterozygous k-mer pairs were present at 4x monoploid coverage, rather than the 2x coverage that would be expected in a diploid genome (Figure 4.3A).

The k-mer spectra in Genomescope can also be used to make inference about whether a tetraploid is of hybrid origin (allopolyploidy), based on the assumption that recombination is expected to happen preferentially within, rather than between, hybrid subgenomes (Ranallo-Benavidez et al. 2020). Allotetraploids are therefore expected to have genomes in which nucleotide heterozygosity exhibits a high proportion of an *aabb* pattern and a low proportion of an *aaab* pattern, while tetraploids of non-hybrid origin (autotetraploids) are expected show the opposite pattern (*aaab* > *aabb*) (Ranallo-Benavidez et al. 2020). In this case, the k-mer spectra had *aabb* > *aaab* (Figure 4.3A), which suggests *P. austrocedri* may be an allotetraploid.

A second distinct pattern showed no clear 1x peak in the k-mer spectra (Figure 4.3B), and tetraploidy was inferred based on the predicted k-mer coverage as calculated from the estimated genome size (using flow cytometry) and the amount of sequence data. In these cases, the large 2x peak was in the correct position based on the predicted 1x peak, suggesting the estimation method is accurate and the 1x peak is simply not visible. As above, these kmer spectra had a higher proportion of *aabb* k-mers, and the frequency of *aaab* was very low, suggesting allopolyploidy.

Thirdly, two isolates (PHY-215 and PHY-257) had a very large 1x peak that, if tetraploid, would be indicative of very high frequency of heterozygosity in the *aabb* pattern, and even higher values of *aaab* (Figure 4.3C). However, the Smudgeplot of heterozygous k-mer pairs suggests these isolates are actually diploid, with most heterozygous k-mer pairs clearly being at 2x the monoploid coverage. Furthermore, diploid and triploid Genomescope models both fit similarly well compared to the tetraploid model (Figure S4.2A), although it should be noted that the diploid model requires very high levels of genome heterozygosity (3%). These isolates

could represent an ancestral diploid state with high levels of heterozygosity. Alternatively, these isolates may have undergone the tetraploidy event, followed by large genomic deletions resulting in diploidisation of large parts of the genome.

Finally, two isolates (BT3 and TDJ6) showed unusual k-mer spectra that were not a good fit to any ploidy level (Figure 4.3D). These isolates were predicted to be triploid by Smudgeplot, based on a relatively high count of AAB heterozygous k-mers; that is, heterozygous k-mers showing 3x monoploid coverage, and with a ratio of 2:1 of major to minor k-mer coverage. However, no good fit to the data could be found using Genomescope for either triploid or diploid models (Figure S4.2B). These unusual k-mer spectra are possibly a result of large deletions in the genome following the tetraploidy event, resulting in some regions of the genome being effectively triploid, while others remain tetraploid.

4.3.3 Evidence of large genomic deletions and duplications

A comparison of coverage across the genome relative to the appropriate reference *P. austrocedri* isolate revealed large regions in the genome that appear to have undergone either duplication or deletion events in some *P. austrocedri* isolates (Figure 4.4). In some cases, these duplications or deletions represented entire chromosomes, while in other cases they involved smaller regions. The deletions reduced coverage to roughly half that of the reference, which is consistent with the loss of a single copy of the region. In no case was coverage reduced to zero, indicating that no region has been completely lost. These duplication or deletion events were often shared between multiple isolates, particularly those originating from the same populations. Notably, the two UK isolates with unusual k-mer spectra (BT3 and TDJ6), speculated above as being due to partial triploidy, do show the largest number of deletions relative to the reference, including multiple whole chromosomes (Figure 4.4).

ARG isolates also exhibited evidence of duplication or deletion events, although in many cases the ratio of coverage did not reach the expected half or twofold difference compared to the reference, especially in isolate PHY-215. Interestingly, isolate PHY-257 did not show evidence of extensive deletion events, despite having a genome size approximately half that of the reference (Figure 4.1). Together with the k-mer analyses, this suggests this isolate may be close to fully diploid. In this case, the coverage ratio would remain fairly uniform across the genome, as all regions would be present in half the number of copies in the diploid genome relative to the tetraploid reference.

Despite clear evidence of deletions or duplications, all isolates covered >99% (often 100%) of the reference genome from their respective lineage when coverage was assessed as the proportion of bases with at least one mapped read. Thus, although isolates differ in the number of copies of each chromosome present in their genome, there is no evidence that any isolate has completely lost all copies of any large region of the genome.

A summary of the k-mer analyses, coverage analyses and the proposed explanation of the observed patterns for each of the 17 isolates included in this study are shown in Table 4.3.

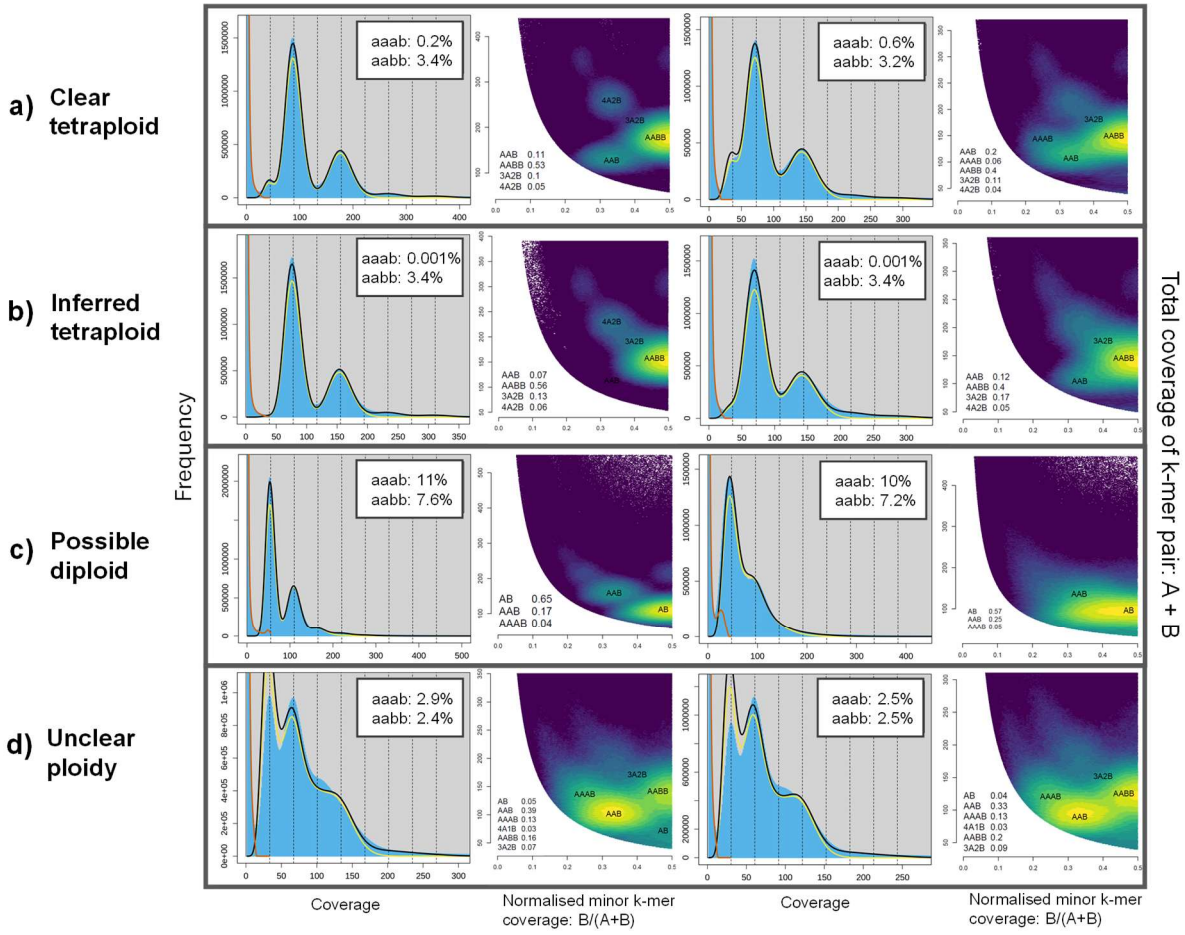

Figure 4.3. Four patterns (a-d) of genome structure based on k-mer spectra analysis (Genomescope) and analysis of heterozygous k-mer pairs (Smudgeplot). Each pair of images (k-mer spectrum on the left and Smudgeplot on the right) represents one isolate. Two isolates have been shown to represent each pattern, although the number of isolates exhibiting each pattern varied. a) Clear tetraploidy. There is a distinct 1x peak in the k-mer spectrum, and a clear high frequency of AABB heterozygous k-mer pairs in the Smudgeplot analysis, demonstrating that the most frequent heterozygous k-mer pairs were present at 4x monoploid coverage, rather than the 2x monoploid coverage that would be expected in a diploid genome. This pattern is seen in 7/17 isolates. b) Inferred tetraploidy. There is no distinct 1x peak in the k-mer spectrum, but its position is inferred from genome size data (flow cytometry). The high abundance of AABB heterozygous k-mers in the Smudgeplot also suggests tetraploidy. This pattern is seen in 6/17 isolates. c) Possible diploid. A very large 1x peak, and diploid, triploid or tetraploid Genomescope models fit similarly well. Here we present the results for the tetraploid fit for consistency between isolates; other ploidy fits are shown in Figure S4.2A. Smudgeplot suggests these isolates are diploid, based on most heterozygous k-mers having 2x monoploid coverage. This pattern is observed in 2/17 isolates. d) Unclear ploidy. Unusual k-mer spectra that were not a good fit to any ploidy level. Smudgeplot suggests triploidy based on a relatively high count of AAB heterozygous k-mers, showing 3x monoploid coverage with a normalised minor k-mer coverage ratio of ~0.3. However, no good fit to the data could be found using Genomescope for either triploid or diploid models (Figure S4.2B). This pattern is observed in 2/17 isolates. The frequency of nucleotide heterozygosity patterns *aaab* vs *aabb* in Genomescope is also shown in each case, which can be used to make inferences about the nature of the tetraploidy. Specifically, *aabb*>*aaab* suggests a hybrid origin (allopolyploidy), whereas *aabb*<*aaab* would suggest a non-hybrid origin (autopolyploidy).

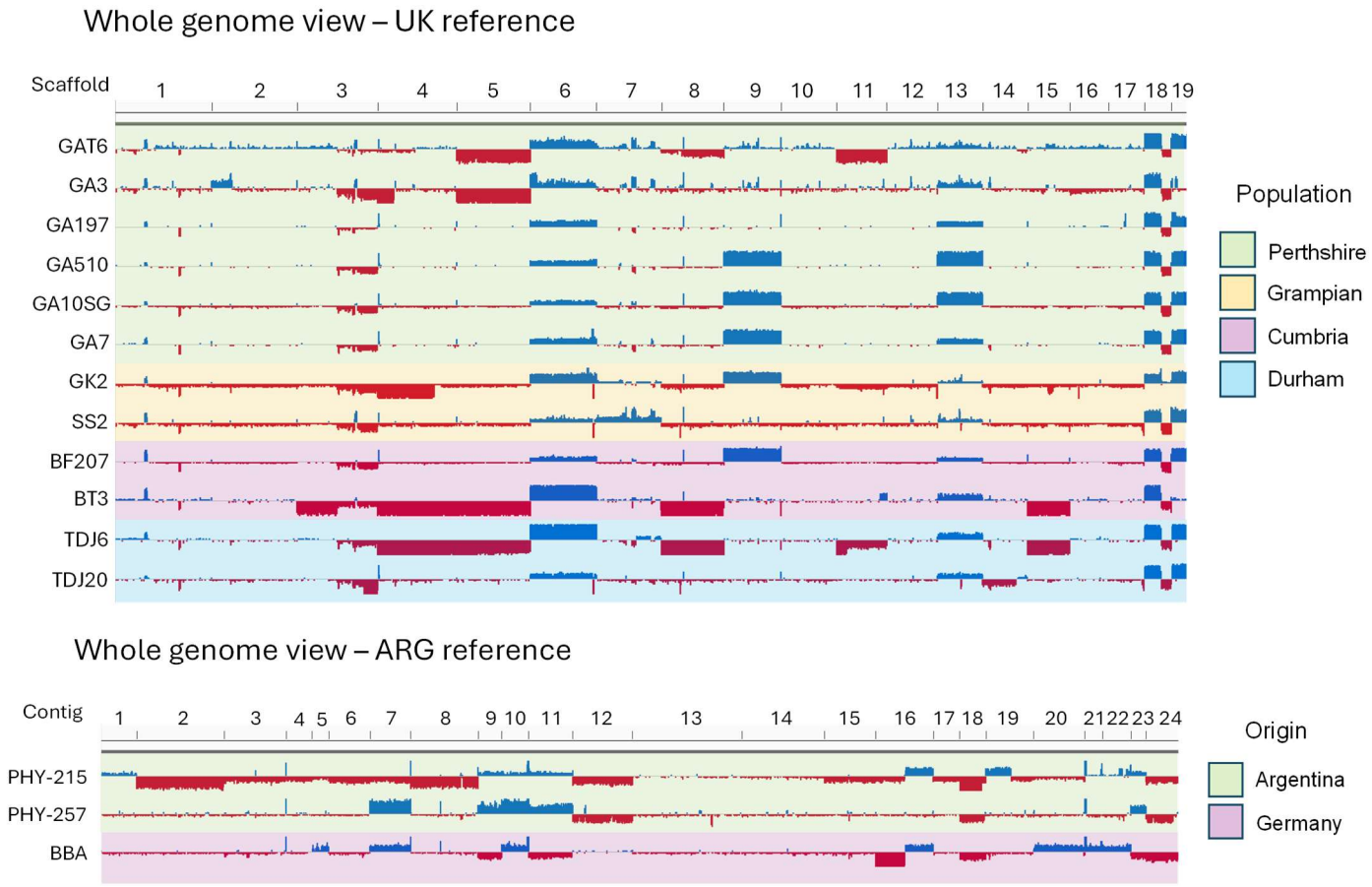

Figure 4.4. Variation in coverage between isolates across the whole genome. Above is UK isolates relative to the UK reference; below is ARG isolates relative to the ARG reference. Bars represent the $\log_2$ fold change ($\log_2$FC) of coverage between each isolate and the reference isolate mapped to itself in 50 bp windows across the genome. Red indicates a negative number (lower coverage in the isolate compared to the reference) and blue indicates a positive number (higher coverage in the isolate compared to the reference). The scale for each goes from $\log_2$FC-1 (half the coverage) to $\log_2$FC 1 (twice the coverage). The highest and lowest bars in the graph (for example, scaffold 4, 5, 6 and 8 in isolates BT3 and TDJ6) reach those values. These areas therefore represent regions where coverage was twice or half that of the reference. The shorter bars represent smaller differences in $\log_2$FC coverage. Background colours represent population or country of origin. There appear to be multiple examples of whole-scaffold deletions or duplication in the UK isolates, often shared between multiple isolates. However, these deletions appear to represent only a single copy of the chromosome/region in the genome. Thus, coverage is reduced to half the value of the reference, but every chromosome/region is still present in all isolates. In the case of ARG isolates, the duplications or deletions are less apparent, as they rarely reach values of twice or half the coverage. For example, contig 2 in isolate PHY-215 and contig 12 in PHY-215 and PHY-257 have coverage ratio of ~0.6 rather than 0.5 that of the reference.

Table 4.3. Summary of the various analyses addressing genome composition and ploidy for all isolates, showing the inferences made by Genomescope k-mer spectra, Smudgeplot heterozygous k-mer pairs, whether there was a clear 1x (monoploid) k-mer peak, and whether the distribution of coverages across the genome shows evidence of large duplications or deletions. The ratio of coverage had to be close to ~2x or ~0.5x over an entire scaffold/contig in order to be considered evidence of a deletion or duplication event. The proposed explanation for the observed patterns is also given for each isolate.

Isolate	Lineage	Population	Genomescope best fit	Smudgeplot inference	Clear 1x peak?	Large deletions?	Large duplications?	Proposed explanation
BBA	ARG	Germany	Tetraploid	Tetraploid	Yes	No	No	Clear tetraploid
BF207	UK	Cumbria	Tetraploid	Tetraploid	No	No	Yes	Tetraploid with low levels of heterozygosity
BT3	UK	Cumbria	No good fit	Triploid	Yes	Yes	Yes	Triploidisation in progress
GA10SG	UK	Perthshire	Tetraploid	Tetraploid	No	No	Yes	Tetraploid with low levels of heterozygosity
GA197	UK	Perthshire	Tetraploid	Tetraploid	Yes	No	No	Clear tetraploid
GA3	UK	Perthshire	Tetraploid	Tetraploid	Yes	Yes	No	Clear tetraploid
GA510	UK	Perthshire	Tetraploid	Tetraploid	No	No	Yes	Tetraploid with low levels of heterozygosity
GA7	UK	Perthshire	Tetraploid	Tetraploid	No	No	Yes	Tetraploid with low levels of heterozygosity
GAT6	UK	Perthshire	Tetraploid	Tetraploid	Yes	Yes	No	Clear tetraploid
GK2	UK	Grampian	Tetraploid	Tetraploid	No	Yes	Yes	Tetraploid with low levels of heterozygosity
SS2	UK	Grampian	Tetraploid	Tetraploid	Yes	No	No	Clear tetraploid
TDJ20	UK	Durham	Tetraploid	Tetraploid	Yes	No	No	Clear tetraploid
TDJ3	UK	Durham	Tetraploid	Tetraploid	Yes	Reference	Reference	Clear tetraploid
TDJ6	UK	Durham	No good fit	Triploid	Yes	Yes	Yes	Triploidisation in progress
PHY-211	ARG	Chubut	Tetraploid	Tetraploid	No	Reference	Reference	Tetraploid with low levels of heterozygosity
PHY-215	ARG	Chubut	Diploid, triploid or tetraploid	Diploid	Yes	Yes	No	Diploid or diploidisation in progress
PHY-257	ARG	Neuquén	Diploid, triploid or tetraploid	Diploid	Yes	Partial	Partial	Diploid or diploidisation in progress

4.3.4 Genetic clustering of isolates

After applying quality filters and pruning, there were ~14,000 SNPs across all isolates (mapped to the UK reference) and ~3,200 SNPs within the UK lineage alone. A PCA including all isolates clearly separated UK isolates from non-UK isolates along the first axis, which explained the vast majority of variation (Figure 4.5A). The second axis accounted for only a small fraction of the total variation, and separated the ARG isolates from each other, while all UK isolates remained very closely clustered. Although the number of ARG isolates is small, there was no clear clustering by population of origin in Argentina, with two isolates from different populations clustering very closely, while the third isolate was separated along the second axis despite sharing a population of origin with one of the other isolates (Figure 4.5A).

A second PCA based on the UK isolates alone showed that, unlike ARG isolates, UK isolates mostly clustered closely by region (Figure 4.5B). The only exception was a Durham isolate that clustered closely with the two isolates from Grampian. There was no signal of time in the clustering: the UK isolates were collected over a ten-year period (Table 4.1), but did not cluster by isolation date.

4.3.5 Genetic diversity across the genome

After applying quality filters and individual-level depth filtering there were ~39,000 SNPs within UK isolates (mapped to the UK reference) and ~23,000 SNPs within ARG isolates (mapped to the ARG reference). The number of SNPs was considerably larger when reads were mapped between lineages (~2.1 million SNPs when all isolates were mapped to the UK reference), indicating substantial divergence between the lineages.

On average, nucleotide diversity was very low: the mean value across the genome was $3.1x10^{-5}$ in the UK lineage and $3.4.x10^{-5}$ in the ARG lineage. However, certain genomic regions showed elevated diversity, with maximum nucleotide diversity within a 100 kb window reaching 0.0014 in both lineages. Notably, these maximum estimates of nucleotide diversity were found on homologous chromosomes in both lineages (Figure 4.6). Average pairwise nucleotide divergence between lineages was 0.015 across sliding windows and reached a maximum of 0.038 in the same region of the genome that showed elevated within-lineage nucleotide diversity (Figure 4.6).

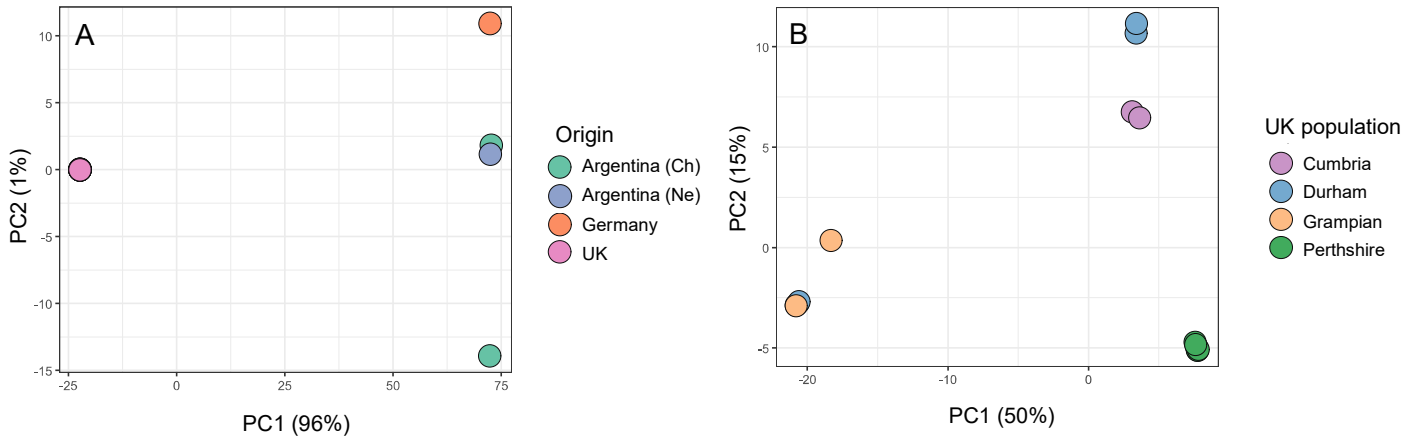

Figure 4.5. Principal component analysis (PCA) showing the genetic clustering among *Phytophthora austrocedri* isolates. A: When all isolates from both lineages were analysed together, the PCA clearly separated UK from ARG isolates along the main axis, which explained the vast majority of variation. The second axis explained only a small amount of the variation, and separated the four ARG isolates. Isolates from Argentina did not cluster by population of origin, with one of the isolates from Chubut (Ch) clustering closely with the isolate from Neuquén (Ne) instead of with the second isolate from Chubut. B: PCA of only UK isolates. Isolates clustered by population, with one exception: one isolate collected in Durham clustered with isolates from Grampian.

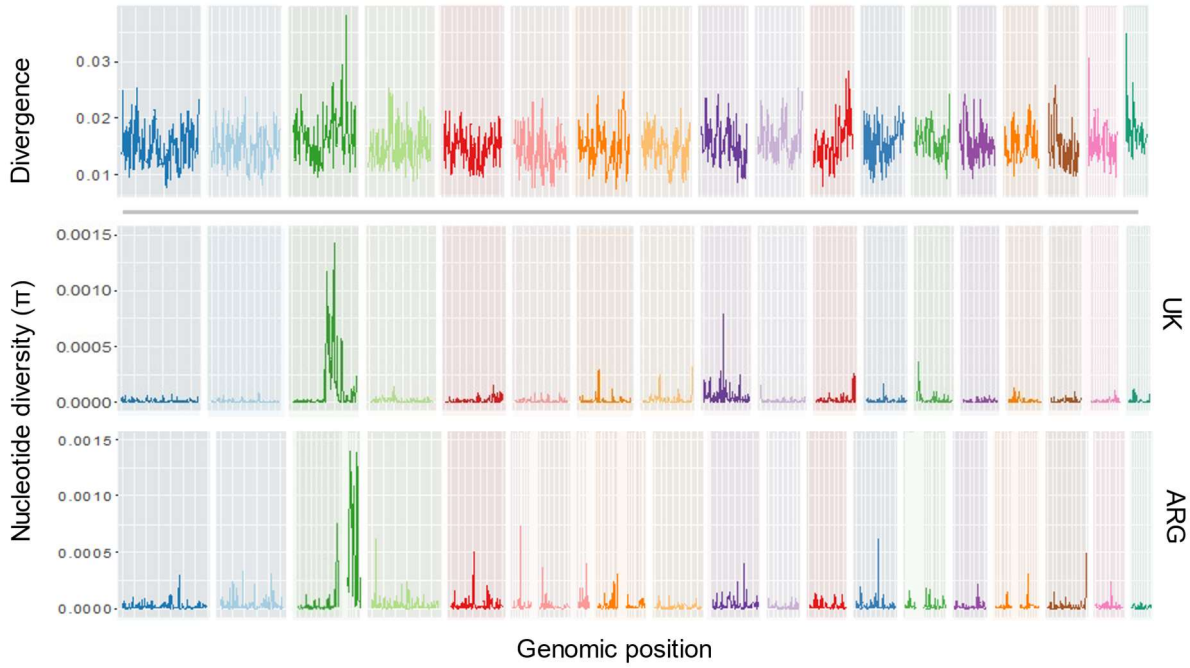

Figure 4.6. Genetic diversity (below) and divergence (above) across the *Phytophthora austrocedri* genome. Nucleotide diversity was calculated across all isolates within each lineage mapped to their own reference. Divergence was calculated as the average pairwise differences between isolates between lineages, with all isolates mapped to the UK reference. Colours represent different scaffolds. The contigs in the ARG reference have been ordered and coloured to show homology compared to the UK reference based on alignment using D-GENIES (Cabanettes and Klopp 2018). Diversity is generally very low, but some genomic regions show elevated diversity and divergence.

4.3.6 Mitochondrial analysis

Very few SNPs were detected in the mitochondrial genome within either lineage of *P. austrocedri*. No SNPs were identified when reads from the UK reference isolate were mapped to its own reference mitogenome, demonstrating good accuracy in the method. Two SNPs were called when reads from the reference ARG isolate were mapped to its own reference, but these were subsequently removed from the analysis, as they were uniformly called as alternate alleles across all four ARG isolates and therefore most likely reflected an error in the assembly.

The average number of pairwise nucleotide differences in the mitogenome between UK isolates was only 3.0, and in some cases multiple isolates had identical haplotypes (Figure 4.7). Similarly, the average number of pairwise nucleotide differences between ARG isolates was 3.3. In contrast, there was considerable divergence between the two lineages, with an average of 914 nucleotide differences detected between isolates in different lineages (Figure 4.7). The average pairwise p-distance between lineages was 0.023.

4.3.7 Analysis of homologous genes

Additional evidence for the hybrid nature of *P. austrocedri* was found in the analysis of homologous genes within and between the two lineages. If *P. austrocedri* were an autotetraploid (that is, derived from whole-genome duplication without hybridisation), divergence between duplicated gene copies would be expected to remain low within the genome, due to recombination between multiple homologous chromosomes during meiosis (Xu et al. 2015; He et al. 2018). Even if *P. austrocedri* reproduced mostly clonally, very occasional sexual cycles would still result in reduced divergence between gene copies within lineages compared to between lineages.

On the other hand, if *P. austrocedri* were an allotetraploid (that is, of hybrid origin), homologous chromosomes would be expected to pair within rather than between subgenomes during recombination events (Wu et al. 2002; Xu et al. 2015), and homologous genes would therefore remain diverged between the two subgenomes. In this case, the two gene copies within each reference genome would represent *homoeologs*, defined as homologous genes that diverged during a speciation event and were then brought back together into the same genome by hybridisation (Glover et al. 2016). If the UK and ARG lineages diverged after the hybridisation event, this would result in pairs of homologous genes being more closely related between lineages than within lineages.

Of the 100 BUSCO genes analysed, 95 were present in duplicate in at least one of the *P. austrocedri* reference assemblies, allowing an analysis of the relationship between homologs within and between lineages. Of those, 91 genes displayed a tree topology consistent with a hybrid origin (clustering between *P. austrocedri* lineages), while just four were indicative of a non-hybrid origin (clustering within *P. austrocedri* lineages) (Figure 4.8).

Mean genetic distance between homologs within *P. austrocedri* lineages (i.e., divergence between homoeologs) was 0.0136 (±0.0007) in the ARG reference genome and 0.0128 (±0.0006) in the UK reference genome. Meanwhile, the average distance between the least diverged pairs of homologs for each gene between the two *P. austrocedri* assemblies was significantly lower (0.0070 ±0.0002). Average genetic distance between the more diverged pairs of homologs for each gene between the two reference genomes was similar to the within-lineage distance between homoeologs (0.0132 ±0.0005). Note that these calculations are based on the assumption that all pairs of least-diverged and all pairs of most-diverged homologs share an origin, but it should be noted that the two subgenomes in *P. austrocedri* have not been separated.

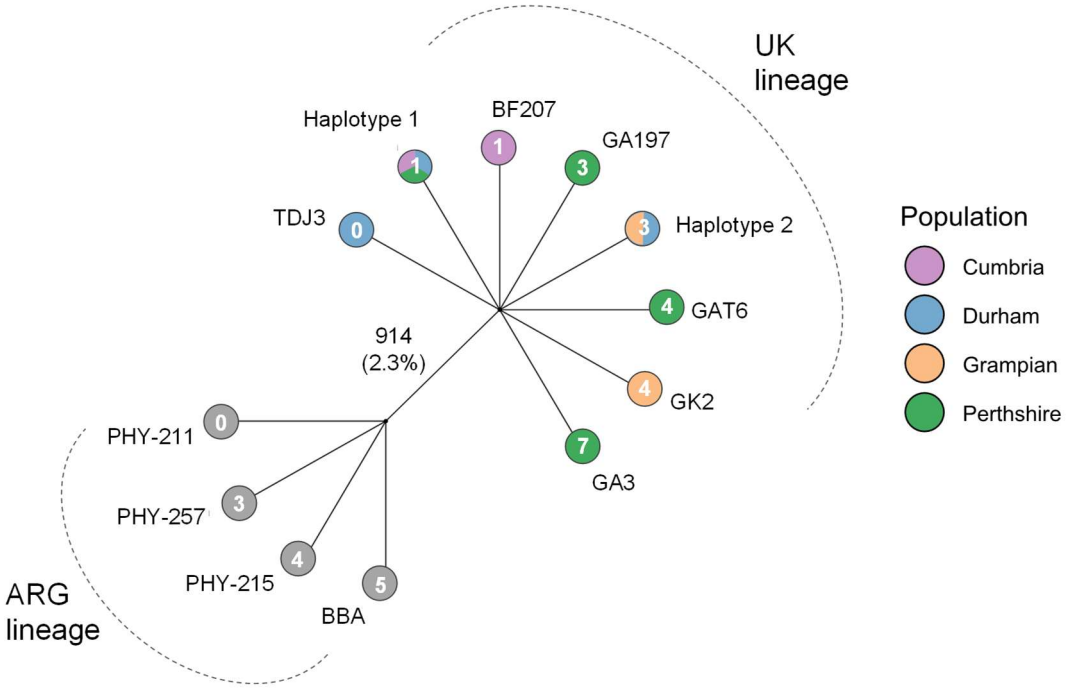

Figure 4.7. Clustering network of whole mitogenome sequences. Within lineages sequences are highly similar, and the only detectable clustering structure is between lineages. Numbers inside the circles represent the number of differences (SNPs) between each isolate and the relevant reference isolate (TDJ3 for the UK lineage and PHY-211 for the ARG lineage). Some isolates had identical haplotypes in the UK lineage: Haplotype 1 represents five isolates and Haplotype 2 represents two isolates. In the case of the UK lineage, the colour of the circle represents the population of origin. There is no apparent clustering by population, with identical haplotypes being found in different populations. The numbers on the branch between lineages represents the average pairwise number of differences between isolates from different lineages and the proportion of sites that are different as a percentage.

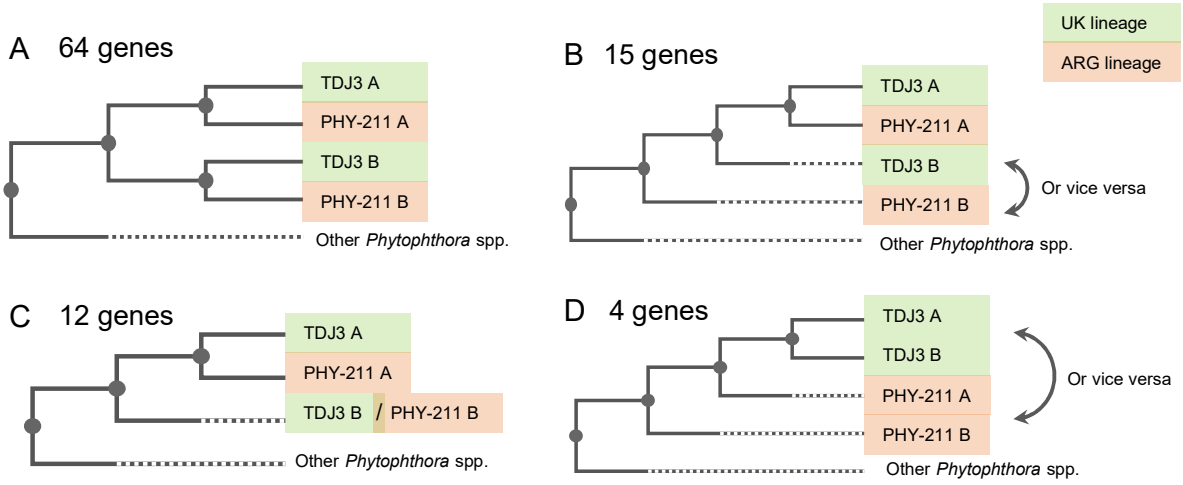

Figure 4.8. Summary of the different gene tree topologies for the 95 BUSCO genes that were present twice in at least one of the *Phytophthora austrocedri* reference genome assemblies. TDJ3 is the UK reference isolate; PHY-211 is the ARG reference isolate. Tree topologies A, B and C support a hybrid origin, as homologs cluster between lineages. Tree topology D supports a non-hybrid origin, as homologs cluster within lineages. The number of genes showing each topology is indicated above the tree.

4.4 Discussion

4.4.1 Genome size and ploidy variation

The average 1C genome size across *P. austrocedri* isolates as measured by flow cytometry was 198 Mb. This is comparatively large for a *Phytophthora* species, with the usual range being 60–100 Mb when diploid (Vercauteren et al. 2011; Bertier et al. 2013; Van Poucke et al. 2021). Suspected or known polyploid *Phytophthora* species have been reported to have similarly large genome sizes, or in some cases even larger (Bertier et al. 2013; Jung et al. 2017; Van Poucke et al. 2021). Combined with the k-mer spectra (Figure 4.3), these results suggest that *P. austrocedri* is a polyploid. More specifically, most *P. austrocedri* isolates appear to be tetraploid, with the excess of *aabb* k-mers suggesting a hybrid origin (allotetraploid).

The estimated genome sizes using the k-mer based analysis were in all cases smaller than those estimated by flow cytometry. There are several reasons why the estimates might differ between methods. Firstly, although flow cytometry is usually considered the gold standard when it comes to estimating genome size, sources of variation and biases can arise from choice of protocol, choice of reference standard or interference from secondary metabolites (Doležel et al. 2007; Loureiro et al. 2023). On the other hand, k-mer based methods can also be subject to biases, which can arise due to sequencing errors, a biased representation of the genome in the sequencing data, or high repeat content in the genome (Hesse 2023). There have been several studies showing deviations in genome size estimates between the two methods, although there is no consistency in terms of which method gives a higher estimate (e.g., Guo et al. 2015; Al-Qurainy et al. 2021; Dai et al. 2022). In the case of this study, the flexible nature of *Phytophthora* genomes may make it difficult to get accurate estimates based on k-mer analyses, as models fitted by Genomescope do not account for the possibility of uneven chromosome copy number, which may be occurring in some of the isolates due to the deletion of a single copy of some chromosomes.

Although most *P. austrocedri* isolates appear to be tetraploid, there is a wide range of genome sizes, varying by almost two-fold (from 131 Mb to 249 Mb), which suggests isolates may vary in their ploidy. Furthermore, in some cases the results of the k-mer analyses do not fit neatly with tetraploidy. Firstly, two UK isolates (BT3 and TDJ6) appear to be undergoing triploidisation, as they have comparatively small genome size estimates (Figure 4.1), many heterozygous k-mers at 3x monoploid coverage (Figure 4.3d), and evidence of large deletions of individual copies of chromosomes (Figure 4.4). Secondly, two ARG isolates (PHY-215 and

PHY-257) appear to be near-diploids, based on their small genome size (Figure 4.3) and distinct k-mer spectra (Figure 4.3c). These isolates could possibly represent an ancestral diploid state prior to tetraploidy. However, based on their very high levels of estimated heterozygosity (Figure S4.2A) and the fact that all regions of the genome are present in these isolates (Figure 4.4), they would have to represent an ancestral diploid hybrid, rather than one of the two parental species that formed the polyploid hybrid. Overall, and in the absence of genome size estimates from a larger number of ARG isolates, it is perhaps more likely that these isolates are instead undergoing a process of diploidisation following the tetraploidy event. In this case, the isolates appear to have retained the two hybrid subgenomes in just one single copy, resulting in a diploid genome with very high levels of heterozygosity.

A similar process of loss of copies of chromosomes in a tetraploid resulting in near diploidisation of the genome has previously been observed in *P. alni*, where the "standard" variant (*P. alni* subsp. *alni*) is considered to be tetraploid or near-tetraploid (18-22 chromosomes), but where there are several other variants with chromosome counts ranging from 12-17 (Brasier et al. 2004). Similarly, although generally considered to be a diploid, many successful clonal lineages of *P. infestans* are triploid, a state that is speculated to have arisen through triploidisation following tetraploidy (Li et al. 2017). Furthermore, triploid *P. infestans* isolates have also been shown to revert to a diploid state under stressful conditions (Li et al. 2017). Thus, it appears that the ploidy variation and loss of chromosomes resulting in triploidisation or diploidisation shown here to be occurring in *P. austrocedri* may be a common *Phytophthora* trait.

It is worth noting that knowledge of the pathogen's genome size provided by flow cytometry was critical when carrying out the genome profiling of the *P. austrocedri* isolates, as it provided essential information regarding expected monoploid coverage. In the absence of knowledge of *P. austrocedri*'s genome size, it would have been easy to conclude mistakenly that many of these isolates were diploid, due to the absence of any monoploid (1x) coverage peak in the k-mer spectra. Thus, despite the overall ease and accuracy of k-mer based methods, flow cytometry remains a critical tool when carrying out genome profiling, particularly in the case of organisms with genomes as apparently flexible as those of *Phytophthora*.

4.4.2 Divergence between lineages and evidence of shared hybridisation event

The two geographical lineages of *P. austrocedri* (ARG and UK) were genetically very distinct, with an average divergence of ~2.3% across the mitogenome and ~1.5% divergence when averaged over a whole-genome sliding window analysis (Figure 4.6). Divergence in BUSCO genes between the lineages was lower, at an average of ~0.7%; however, this difference is not surprising given that BUSCO genes represent a set of highly conserved genes, which would be expected to have a slower evolutionary rate. Other *Phytophthora* species with distinct inter-continental lineages have also been shown to be highly diverged: the different lineages of *P. ramorum*, for example, are genetically very distinct and are estimated to have diverged 0.75-1.3 million years ago (Dale et al. 2019).

Despite this substantial divergence between *P. austrocedri* lineages, the hybridisation event was likely shared between them. Although it is theoretically possible that hybridisation took place more recently and independently in both lineages, involving the same parental species, this would require two highly specific conditions to explain the observed patterns of divergence between subgenomes and between lineages: 1) each parental species would need to have contained distinct clades that could explain the between-lineage divergence, and 2) these clades would have to be equally diverged within both parental species. Overall, this scenario seems unlikely, and a shared hybridisation event predating lineage divergence provides a more probable explanation. Consequently, the hybridisation event likely occurred a considerable time ago. This also explains why the hybrid nature of *P. austrocedri* was not detected through ITS-based analyses, as rDNA arrays are expected to undergo homogenisation over time (Brasier et al. 1999; Bertier et al. 2013).

Hybridisation is increasingly being recognised as a major driver of *Phytophthora* evolution, having been documented for multiple species across several clades (Brasier et al. 1999; Bertier et al. 2013; Callaghan and Guest 2015; Van Poucke et al. 2021). A hybrid origin for *P. austrocedri* had previously been proposed based on its unusually high number of multi-allelic loci relative to other *Phytophthora* species (Van Poucke et al. 2021), and the results presented here confirm this conclusion. However, in the case of *P. austrocedri*, the parental species in the hybridisation event remain unknown. Based on the relative divergence between homoeologs, the hybridisation event could have occurred between highly divergent lineages of a single ancestral species, rather than between two different species. For example,

hybridisation has been reported between different lineages of *P. ramorum* (Hamelin et al. 2022). However, in the case of *P. austrocedri,* the parental lineages would have been sufficiently diverged to largely or entirely prevent recombination between the two subgenomes; arguably, this means the parental lineages should be considered different species.

4.4.3 Genetic clustering of isolates

The divergence between lineages is also evident in the genetic clustering of *P. austrocedri* isolates, with the vast majority of variation explained by a single PCA axis separating the two lineages (Figure 4.5A). In this analysis, the second axis of variation explained much less of the variation, and separated the ARG isolates from each other. There does not appear to be grouping by population of origin in ARG isolates, although sample size is very limited. A similar lack of clustering by population has previously been detected in other *Phytophthora* species, which is speculated as being a consequence of rapid dispersal and a high frequency of clonal reproduction (Cooke et al. 2005; Schoebel et al. 2014; Mullet et al. 2024). Interestingly, ARG isolates similarly did not cluster by ploidy, with the two closely clustering isolates representing the reference ARG isolate (fully tetraploid) and one of the near-diploid isolates. Despite limited sample size, this suggests the diploidisation may have occurred independently in the two near-diploid ARG isolates. However, a larger number of samples would be required to confirm this conclusion.

A different pattern was observed within the UK, where in most cases isolates clustered closely by population, with one exception (Figure 4.5B). There was no signal of time seen in the clustering, with isolates collected over a 10-year period still clustering very closely (Table 4.1; Figure 4.5B). Overall, this clustering pattern is consistent with reproduction occurring mostly through clonal and/or self-fertilised spores combined with limited dispersal ability, resulting in local genetic clusters that do not rapidly recombine into intermediate genotypes when a different genotype is introduced.

4.4.4 Low levels of genetic diversity but high levels of between-subgenome heterozygosity

Genome-wide genetic diversity was extremely low within both *P. austrocedri* lineages ($3.1x10^{-5}$ for UK isolates; $3.4.x10^{-5}$ for ARG isolates). Most previous studies of *Phytophthora* have assessed diversity across a limited number of genes, and typically report much higher levels of nucleotide diversity, although estimates vary: for example, 0.0001-0.002 in *P. plurivora* (Schoebel et al. 2014); 0.0004-0.0016 in *P. infestans* (Wang et al. 2019); and 0.0001-0.0046 in

P. multivora (Tsykun et al. 2022). In contrast, a recent whole-genome study of the self-fertile *P. pseudosyringae* reported even lower levels of nucleotide diversity (on average $7.3x10^{-6}$; Mullett et al. 2024). It is difficult to make direct comparisons between studies, however, as differences in methods, sample sizes and how populations are defined will strongly influence estimates. Here, nucleotide diversity was calculated within geographical lineages rather than within local populations, as sample sizes within each population were small. Thus, the true within-population diversity is likely to be even lower than reported here. Nonetheless, these results clearly demonstrate that *P. austrocedri* possesses very low levels of genetic diversity within both of its geographical lineages.

Levels of within-subgenome heterozygosity were also very low across all isolates, based on the small size or even complete absence of the monoploid (1x) peak in many of k-mer spectra (Figure 4.3). Even when a monoploid peak was detected, this may reflect the loss of single chromosome copies rather than genuine heterozygosity, since many isolates showed evidence of large-scale deletions relative to the reference genome (Figure 4.4). Indeed, this same process likely accounts for the prominent monoploid peaks observed in isolates undergoing triploidisation.

Overall, the combination of low heterozygosity and genetic diversity suggest that *P. austrocedri* has undergone repeated rounds of self-fertilisation during its evolutionary history as a homothallic invasive pathogen. Hybrid *Phytophthora* species are often reported to have difficulties producing viable oospores (Brasier et al. 2004; Man in 't Veld et al. 2012; Bertier et al. 2013), which may be particularly true for a tetraploid genome undergoing a process of triploidisation leading to aneuploidy. However, in the case of *P. austrocedri*, most of the isolates have been shown to produce oospores successfully (Greslebin et al. 2007; Henricot et al. 2017). Interestingly, the only UK isolate that does not produce oospores (BT3; Henricot et al. 2017) is one of the isolates shown in this study to be undergoing the process of triploidisation.

Despite low levels of genetic diversity and within-subgenome heterozygosity, as a hybrid tetraploid *P. austrocedri* has very high levels of between-subgenome heterozygosity. This can be observed in the isolates that appear to be undergoing diploidisation, where estimates of heterozygosity (under a diploid model) are very high (>3%; Figure S4.2B). High levels of (between-subgenome) heterozygosity resulting in heterosis (hybrid vigour) is one of the proposed advantages of allopolyploidy, and is thought to enhance a hybrid's adaptive

potential (Comai 2005). Thus, while *P. austrocedri* suffers from very low within-lineage diversity, its hybrid, polyploid genome may have compensated through the maintenance of high levels of (between-subgenome) heterozygosity.

4.4.5 Conclusion

One of the challenges faced by invasive plant pathogens is a lack of genetic diversity limiting adaptive potential to the new environment and novel hosts. This is likely to be particularly severe for self-fertile pathogens, as each round of self-fertilisation will reduce genome-wide heterozygosity by half. By bringing together divergent lineages into one genome, hybridisation instantly increases genome-wide levels of diversity and heterozygosity, potentially enhancing adaptation to novel environments and hosts. What's more, in the case of hybrid polyploids, because recombination usually occurs within rather than between subgenomes, the loss of heterozygosity associated with self-fertilisation will occur at the within-subgenome level, and heterozygosity and genetic diversity between subgenomes will be maintained. In a highly homozygous species, this strategy is almost akin to asexual reproduction, as it would maintain the same (between-subgenome) heterozygous sites over successive generations, as if the pathogen were reproducing clonally. Of course, *Phytophthora* are also able to reproduce through asexual zoospores; however, these are shorter-lived and less resilient than the sexual oospores. Thus, allotetraploidy combined with self-fertilisation may be a particularly effective strategy for an obligate plant pathogen invading new environments, effectively allowing *P. austrocedri* to maintain high levels of between-subgenome heterozygosity while still making use of longer-lasting, more resilient sexual oospores conveniently produced through self-fertilisation.

CHAPTER 5:
Comparative transcriptomic analysis of the juniper-*Phytophthora austrocedri* interaction reveals key drivers of virulence in the pathogen and resistance in the host

Abstract

Plant resistance or susceptibility to a pathogen is the outwardly observable outcome of a complex molecular battle. The molecular basis of resistance in the host and of virulence in the pathogen is often completely unknown in non-model organisms, yet such understanding can provide important insights into pathogen management, particularly in the case of invasive pathogens threatening ecologically important hosts. Here we present a transcriptomic analysis of the interaction between the invasive tree pathogen *Phytophthora austrocedri* and its host juniper. We carry out an inoculation trial using two juniper genotypes (one highly susceptible and one more resistant) and two *P. austrocedri* isolates (one more virulent and one less virulent), and generate dual RNAseq data from two timepoints. We show that the defence response in juniper is characterised by the upregulation of ethylene and associated production of secondary metabolites and pathogenesis-related proteins. Early detection of the pathogen by the host is likely to be crucial for successful resistance, with the resistant host genotype demonstrating an early response to infection compared to the susceptible genotype. At 48 hours after inoculation, the more virulent isolate had downregulated two elicitins and upregulated two protease inhibitors compared to the less virulent isolate, suggesting lower virulence may be driven by both earlier detection and a decreased ability to suppress the host response. There was also evidence that the less virulent isolate may have a shorter biotrophic phase when growing in the resistant genotype. Efficient detection of *P. austrocedri* may be driven by a transmembrane leucine-rich repeat (LRR) receptor kinase that was significantly upregulated in the resistant juniper genotype compared to the susceptible juniper genotype and the mock-inoculated control, although further studies are required to confirm the gene's involvement. This study contributes significantly to our understanding of the factors driving host resistance and pathogen virulence in a non-model, ecologically important novel pathosystem.

5.1 Introduction

Plants are subject to attack from a wide variety of pathogenic microorganisms, including bacteria, fungi and oomycetes, and have developed sophisticated defence responses in order to deal with these diverse attacks. Plant resistance or susceptibility to disease is the outwardly observed outcome of a complex battle that is taking place between host and pathogen at a molecular level. A widely accepted description of the major players on this molecular battleground is given by the zigzag model of plant-pathogen interactions (Jones and Dangl 2006; Ngou et al. 2022). According to the model, the interaction begins when the plant detects molecules that are non-self, in the form of conserved pathogen-associated molecular patterns (PAMPs). PAMPs are usually considered to be molecules necessary for pathogen growth and survival, including basic building blocks like bacterial flagellin, fungal chitin or oomycete glucans (Nürnberger and Brunner 2002; Thomma et al. 2011). As such, genes underlying PAMPs will evolve comparatively slowly, and are not easily discarded by the pathogen (Jones and Dangl 2006). The detection of PAMPs by cell-surface pattern recognition receptors elicits an immune response in the plant, involving the accumulation of toxic antimicrobial secondary metabolites and pathogenesis-related proteins, the production of reactive oxygen species (ROS), physical reinforcement of cell wall and/or programmed cell death (van Loon et al. 2006; Zipfel 2008; Nakano and Shimasaki 2024). PAMPs are thus a kind of elicitor — a general term for molecules that elicit plant defences — and the kind of immunity they trigger is termed pattern-triggered immunity.

The pathogen may, however, be able to circumvent the plant's immune reaction through secreted effector proteins, which are delivered into the apoplast (apoplastic effectors) or inside plant cells (cytoplasmic effectors) to interfere with the plant's defence response. Effector proteins are unique in that they are not otherwise required for pathogen fitness, and their sole purpose is to disrupt the plant's defence response. The only strong natural selection operating on these proteins is thus within the context of the plant-pathogen arms-race, and consequently effectors form a remarkably diverse set of proteins that show very rapid rates of evolution and extensive proliferation in pathogen genomes (Fouché et al. 2018; Sánchez-Vallet et al. 2018; Morales-Cruz et al. 2020). The last phase in the zigzag model is effector-triggered immunity, where plants recognise pathogen effector proteins by means of specific resistance genes (R genes). In contrast to the more general response involved in pattern-triggered immunity, effector-triggered immunity results in a stronger and more rapid defence response that is specific to that effector-R gene combination, and which is able to provide complete or

near-complete resistance to specific pathogen strains, generally through rapid localised programmed cell death called the hypersensitive response (Nimchuck et al. 2003).

Effector-triggered immunity does not represent an end-point in the model, however — the co-evolutionary dynamics of host-pathogen interactions will result in multiple shifts between pattern-triggered immunity and effector-triggered immunity, giving the zigzag model its name. This model of plant disease resistance is necessarily a simplification of a highly complex interaction, and some have questioned its real-world accuracy or utility (Thomma et al. 2011; Pritchard and Birch 2014), or have argued that plant immunity is better seen as a continuum, rather than a strict separation between pattern-triggered immunity and effector-triggered immunity (Thomma et al. 2011; Naveed et al. 2020). Nevertheless, the zigzag model provides a useful framework within which to explore these complex molecular interactions.

Plant defence involves a set of responses and pathways that are necessarily as diverse as the pathogens that attack them. One broad way pathogens differ is in their lifestyle as biotrophic (feed on living host cells), necrotrophic (feed on dead host cells), or hemibiotrophic (initial biotrophic phase is followed by a necrotrophic phase) (Agrios 2005). Effective defence against biotrophic pathogens typically involves the hypersensitive response, as this prevents the biotrophic pathogen from gathering the nutrients it requires from living cells (Glazebrook 2005; Mengiste and Liao 2025). The hypersensitive response is not usually an effective defence response against necrotrophic pathogens, however, and can instead promote pathogen growth and virulence by providing pathogens with more dead cells from which to gather nutrients, resulting in more severe disease (Glazebrook 2005; Mengiste 2012). Instead, defence against necrotrophic pathogens typically involves physical defences, such as cell wall reinforcement through deposition of callose or lignin, and chemical defences, such as the accumulation of toxic and enzyme-inhibiting secondary metabolites and pathogenesis-related proteins (Mengiste 2012). In hemibiotrophs, the timing of the defence response will be important, as the hypersensitive response may be effective in the early biotrophic stage of the infection but not in the subsequent necrotrophic phase.

These different defence responses depending on the type of invading pathogen are thought to be triggered by distinct phytohormone pathways, with salicylic acid typically mediating defence against biotrophs and hemibiotrophs, and jasmonic acid and ethylene generally being involved in defence against necrotrophs (Glazebrook 2005; Mengiste and Liao 2025). Moreover, these pathways are often antagonistic to each other, meaning plants may

need to prioritise one defence strategy over another (Bari and Jones 2009; Zhang et al. 2025). However, these generalisations are largely derived from eudicot model organisms (e.g., *Arabidopsis*) and, while the phytohormone pathways themselves are broadly conserved across all land plants (Wang et al. 2015; Monte 2023), the antagonism between pathways and their associations with pathogen lifestyle are not universal, particularly in the case of monocots and non-angiosperms (Thaler et al. 2012; Arnerup et al. 2013; Campos et al. 2014).

Phytophthora are an important group of oomycete filamentous pathogens that are the causal agents of many economically and ecologically devastating plant diseases, such as late potato blight caused by *P. infestans* and sudden oak death and larch death caused by *P. ramorum* (Jung et al. 2018; Brasier et al. 2022). *Phytophthora* are mostly considered to have a hemibiotrophic lifestyle (Boevink et al. 2020; Brasier et al. 2022), and are known to possess a large arsenal of apoplastic and cytoplasmic effector proteins that can inhibit host enzymes, interfere with host signalling and suppress the defence response (Naveed et al. 2020; Wang et al. 2023). RxLR effectors (named after the conserved amino-acid motif used to identify them) are a type of cytoplasmic effector protein that are particularly prevalent in *Phytophthora* genomes (Wang et al. 2023), and they can interfere with host immunity in diverse ways, including inhibition of transcription (Zhu et al. 2023; Qiu et al. 2023), suppression of the phosphorylation cascade that activates pattern-triggered immunity (Liang et al. 2021) and interference with phytohormone defence pathways (Zhao et al. 2022). However, RxLR effectors can also act as avirulence factors, causing effector-triggered immunity (Du et al. 2018). RxLR effectors are therefore key players in the plant-*Phytophthora* arms race, and show the characteristic rapid rate of evolution of effector proteins, with rapid diversification, divergence and loss of these genes being documented within and between *Phytophthora* species (Du et al. 2018; Kronmiller at al. 2023).

Much of the work on the molecular interactions between plants and pathogens has been carried out on model organisms, such as *Arabidopsis* and various crop species. While the insights gained from these studies are undeniably valuable, they are not necessarily applicable to all plants, particularly in the case of taxonomically distant species such as gymnosperms. It is therefore crucial to study other systems, particularly in the case of invasive pathogens threatening ecologically important hosts, where a mechanistic understanding of the interaction may provide key insights that can be used to inform pathogen management strategies.

Juniper (*Juniperus communis*) is a small conifer in the cypress family (Cupressaceae) with a circumboreal distribution that is currently being threatened in the UK by the invasive tree pathogen *Phytophthora austrocedri* (Green et al. 2012; Green et al. 2014). *Phytophthora austrocedri* is a hemibiotroph that causes root and stem disease in juniper, producing necrotic lesions that girdle the stem and kill the tree (Green et al. 2014; Green et al. 2020). Previous studies have shown there is considerable genetic variation in disease resistance in juniper, with some individuals apparently able to suppress infection, while most succumb to the disease very quickly (Green et al. 2020; Chapter 2 of this thesis). There is evidence for both qualitative and quantitative resistance to *P. austrocedri* in juniper (Chapter 2 of this thesis); however, the molecular basis of resistance, and whether the qualitative resistance is mediated through a classic R gene, is still unknown. There are also differences in virulence between different isolates of *P. austrocedri*, with some isolates able to cause significantly larger lesions than others within the same timeframe (Green et al. 2020; Chapter 2 of this thesis). This pathosystem therefore provides a unique opportunity to investigate the underlying molecular mechanisms of both host resistance and pathogen virulence in an ecologically important, non-model system.

One promising investigative tool for studying non-model organisms is transcriptomic analysis of the plant-pathogen interaction using dual RNAseq, which can provide an overview of the defence response in systems that have limited or no genomic resources (e.g., Carrasco et al. 2017; Dun et al. 2022; Fernandes et al. 2024). Here, we conduct a dual RNAseq inoculation trial on the juniper-*P. austrocedri* pathosystem, capturing host and pathogen transcripts from a resistant and a susceptible juniper genotype inoculated with two different isolates of *P. austrocedri* (one more virulent, one less virulent), and comparing these to a mock-inoculated control, in order to explore the molecular basis of disease resistance in juniper and of virulence in *P. austrocedri,* and to identify candidate genes underlying the divergent outcomes in this host-pathogen interaction.

5.2 Methods

5.2.1 *Phytophthora austrocedri* isolates

Two *P. austrocedri* isolates were used (Table 5.1), one highly virulent isolate and one less virulent isolate (subsequently termed 'more virulent' and 'less virulent'). Levels of virulence were based on the excised-shoot inoculation trial presented in Chapter 2 of this thesis.

Table 5.1. Details of the two *Phytophthora austrocedri* isolates used in this study. Source: Forest Research Northern Research Station, Roslin, Midlothian, Scotland

Isolate	Region isolate collected	Latitude, longitude (°) of collection site	Isolation date	Level of virulence
TDJ3	County Durham, UK	54.645, -2.169	November 2011	Less virulent
GA7	Perthshire, UK	56.337, -4.050	October 2018	More virulent

5.2.2 Juniper genotyping

Two juniper genotypes were used, with differing degrees of susceptibility to *P. austrocedri:* one more resistant and one highly susceptible (subsequently termed 'resistant' and 'susceptible'). The resistant juniper genotype consisted of multiple plants that had been grown from cuttings collected from a single healthy tree at a *P. austrocedri*-infected site in Perthshire, UK, and were thus known to be clones. This genotype has previously been shown to be highly resistant to two different isolates of *P. austrocedri* (see genotype GA5 in Green et al. 2020).

Susceptible juniper consisted of nursery-purchased plants grown from cuttings originating from a site in West Argyll, UK. Previous inoculations had shown these juniper plants to be universally highly susceptible to *P. austrocedri* (Crowson and Green, unpublished data), but it was not known if they comprised more than one genotype. Therefore, to ensure all susceptible replicates represented a single genotype, susceptible juniper individuals were genotyped using four microsatellite markers (Baker et al. 2025b). DNA was extracted from freeze-dried juniper needles using the DNeasy Plant Pro Kit (Qiagen) following the manufacturer's instructions, and PCR amplification was carried out and analysed as described in the Supplementary Methods. All nursery-grown juniper tested had the same genotype at every microsatellite marker, and were distinct at every marker from the resistant juniper. Allele frequencies at the source population were unknown, and regional allele frequencies were therefore used to calculate genotype probabilities (based on 215 juniper individuals from nine populations in Scotland; Baker et al. 2025b). The probability of a match at all four markers

between two of the susceptible juniper individuals occurring by chance was estimated to be $5.5x10^{-9}$ (see Supplementary Methods). We therefore determined that the highly susceptible juniper plants all represented a single genotype.

5.2.3 Inoculation trial

The inoculation trial involved a 3x2 factorial design: two juniper genotypes inoculated with two different *P. austrocedri* isolates, plus a mock inoculation control. Juniper plants were 40-60 cm tall and had an average stem width of 8.3 mm (±0.25 mm). Intact, potted juniper plants were inoculated following the mycelial plug method described in Green et al. (2020). Briefly, mycelial plugs (4 mm in diameter) were taken from the edge of *P. austrocedri* cultures actively growing on V8 agar. A sterile cork borer of the same diameter was used to remove a piece of bark in the middle of the stem, and the mycelial plug was placed on the exposed cambium layer. The area was covered with cotton wool moistened with sterilised distilled water, before wrapping with parafilm and tin foil. Negative controls were inoculated in the same way with plugs taken from a sterile V8 agar plate. Each plant was inoculated at three locations: at the base of the stem, and in two more locations moving up the stem, leaving a gap of approximately 6 cm between inoculation sites. There was a total of five replicates of each genotype and treatment combination (30 individuals in total), although for budgetary reasons only four replicates of each genotype and treatment combination were sequenced (see below).

Tissue was harvested for RNA extraction at two timepoints: 48 hours and one week after inoculation (or mock inoculation). As tissue harvesting required excising the main stem, the uppermost inoculation site was harvested first (48 hours) and the middle inoculation site was harvested second (one week). At 48 hours, there was no visible lesion detectable in any tree, and tissue was collected as follows: a 2 cm piece of the excised stem around the inoculation point was rapidly processed by removing the woody xylem and outer bark, and a piece of phloem/cambium 1.5 cm long and 1 cm wide was excised with the inoculation point exactly in the middle of the excised section. The sample was then rapidly cut into smaller pieces before being placed in an Eppendorf tube containing two ball bearings and flash frozen in liquid nitrogen. At one week, there was a detectable lesion in all susceptible trees and in some resistant trees. Tissue was harvested as described above, except the inoculation point was located at the lower end of the 1.5 cm excised section of phloem/cambium, to ensure the extracted area included the inoculation point, the lesion edge, and healthy tissue on the other side of the lesion edge. Samples were stored at -80°C until further processing.

At three weeks, the final inoculation point that remained near the base of the juniper plants was harvested to confirm differences in levels of susceptibility between host genotypes and differences in virulence between the two pathogen isolates. Bark was removed around the inoculation point, and the length and width of the lesion underneath was recorded. Lesion size was then approximated using the area of a rhombus (a good approximation for the shape of a typical *P. austrocedri* lesion) by multiplying lesion length by lesion width and dividing by two. To test for significant differences in lesion size between juniper genotypes and *P. austrocedri* isolates, lesion area was square-root transformed to satisfy assumptions of normality, and a linear model was fitted with *Genotype* and *Isolate* included as fixed effects.

5.2.4 RNA extractions

Collected phloem/cambium tissue was disrupted using the Tissue Lyser II (Qiagen) until samples formed a uniform fine powder. Disruption was carried out in bursts of 15 seconds, and samples were refrozen in liquid nitrogen after every three bursts to ensure samples remained completely frozen. RNA was extracted using the Monarch Total RNA Miniprep Kit (New England Biolabs) following the manufacturer's recommendations.

RNA was also extracted from cultures of both *P. austrocedri* isolates. Cultures were grown in V8 broth for one week, rinsed in sterilised distilled water, then flash frozen in liquid nitrogen and disrupted as described above. RNA was extracted using the Monarch Total RNA Miniprep Kit (New England Biolabs) following the manufacturer's recommendations.

All RNA extractions underwent quality control to ensure 260/280 nm absorbance ratios (Infinite F Nano+, Tecan), RNA concentrations (Qubit 2.0, Thermo Fisher Scientific) and RIN scores (Tapestation 2200, Agilent Technologies) were all within the recommended ranges, before normalisation and sequencing (Poly(A) RNA sequencing, 150 bp paired-end reads) on the Illumina NovaSeq 6000 platform. Four replicates of each treatment group (genotype, isolate/control and timepoint combination) and three replicates of each isolate growing in culture were sequenced, a total of 54 samples. Target sequencing depth varied depending on the sample type: 150 million reads per sample for inoculated juniper (in order to recover pathogen transcripts), 50 million reads per sample for mock-inoculated control juniper, and 25 million reads per sample for *P. austrocedri* cultures.

5.2.5 Bioinformatic analyses

Raw reads were trimmed to remove adapters and low-quality sequences using Skewer (Jiang et al. 2014). Reads were then classified as belonging to juniper, *P. austrocedri* or contamination using a k-mer-based approach implemented in kraken (Wood et al. 2019). First, the *P. austrocedri* reference genome was used to create a custom database and all reads were classified as either *P. austrocedri* or non-*P. austrocedri*. Samples originating from pure *P. austrocedri* cultures were included in the analysis to validate the approach by verifying that the vast majority of true *P. austrocedri* reads were being classified as *P. austrocedri*. Non-*P. austrocedri* reads were then classified as either contamination (e.g., symbionts) or non-contamination using a second custom kraken database that included RefSeq sequences for archaea, bacteria, fungi, protozoa and viruses. All reads that were classified as non-*P. austrocedri* and non-contamination were assumed to have originated from juniper.

Juniper reads were used to build a transcriptome *de novo,* due to the lack of genomic resources available for this species. Reads were combined from all samples to generate the transcriptome, using ~9 million paired-end reads per sample, resulting in a total of ~432 million paired-end reads across the 48 samples. The transcriptome was assembled using Trinity (Grabherr et al. 2011). Completeness of the transcriptome was assessed using BUSCO (Simão et al. 2015). Read content of the transcriptome was determined by mapping all reads back to the assembly using Bowtie (Langmead and Salzberg 2012).

The juniper transcriptome was annotated using the Trinotate pipeline (Bryant et al. 2017). An E-value cutoff of $1e^{-20}$ was used to assign functional annotation to a transcript. Despite initial filtering of reads, the assembled transcriptome included many non-plant transcripts. This is because even a very small number of reads can be assembled into a significant number of transcripts in the final transcriptome, as the assembly process aims to capture genes with very low expression levels. Therefore, to filter out non-plant transcripts the transcriptome was aligned to the protein BLAST database (nr) using DIAMOND (Buchfink et al. 2015). Any transcript with a top hit that was not classified as Viridiplantae was removed from the transcriptome.

Reads from *P. austrocedri* cultures and *P. austrocedri* reads from lesion tissue were mapped onto the *P. austrocedri* reference genome using STAR (Dobin et al. 2013). Mapping was considered successful if reads mapped uniquely or mapped to <10 loci, the default threshold for filtering out probable ribosomal RNA (rRNA), which typically maps to many loci.

Functional annotation of the *P. austrocedri* genome was carried out using Pannzer (Törönen and Holm 2022), using a Positive Predictive Value threshold of ≥0.5, and InterProScan (Jones et al. 2014) for assignation of protein domains.

To explore transcripts that may be involved in virulence, we also identified candidate effector proteins in the *P. austrocedri* genome. First, we identified all genes that contained a signal peptide using SignalP6 (Teufel et al. 2022), using a probability cutoff of 90%. These genes were classified as being part of the secretome (genes coding for proteins secreted into extracellular space). We then identified genes that were candidate RxLR effectors using the motif-based effectR package (Tabima and Grünwald 2019). We classified genes as candidate RxLR effectors if they satisfied both of these requirements: presence of a signal peptide and presence of the effector motif.

5.2.6 Differential expression analyses

Juniper transcripts were quantified using Salmon (Patro et al. 2017). *Phytophthora austrocedri* gene expression was quantified using HTSeq (Anders et al. 2015). In both cases, non-normalised gene count matrices were used as the input for gene expression analyses carried out using DESeq2 (Love et al. 2014). Genes with universally low expression (<20 counts across all samples in the case of juniper; <10 counts across all samples in the case of *P. austrocedri*) were filtered out prior to analysis. Overall patterns of gene expression were explored using principal component analyses (PCAs). We then made contrasts between specific treatment groups to identify differentially expressed genes (DEGs) between groups. DESeq2 models read counts using a negative binomial distribution, and tests whether mean expression differs significantly between experimental groups. In all cases, we used a threshold of $p<0.05$ to determine significance, based on p-values adjusted for multiple testing using the Benjamini–Hochberg false discovery rate (FDR) correction

To explore the basis of resistance in juniper, we first carried out differential expression analyses within juniper genotypes by contrasting inoculated plants with their own mock-inoculated control. Comparisons were made separately for each treatment (*P. austrocedri* isolate), and were made within rather than between timepoints. A second set of comparisons was then made between juniper genotypes by contrasting the response of resistant plants versus susceptible plants to the same treatment. Again, comparisons were made separately for each treatment (different *P. austrocedri* isolates and control), and comparisons were made within rather than between timepoints.

To explore the basis of virulence in *P. austrocedri*, we first carried out differential expression analyses between *P. austrocedri* growing *in planta* versus *P. austrocedri* growing in culture. This analysis used the susceptible genotype only, to focus on cases in which *P. austrocedri* successfully causes infection. Comparisons were made separately for each *in planta* timepoint. We then explored gene expression patterns in *P. austrocedri* when infecting a host by comparing *in planta* gene expression between isolates and between timepoints.

DEGs were explored for significantly enriched Gene Ontology (GO) terms using BiNGO (Maere et al. 2005), focussing on the Biological Process category, which describes the larger biological objective that a gene is contributing to (Ashburner et al. 2000). In the case of juniper, the background used in the analysis was the entire annotated transcriptome. In the case of *P. austrocedri*, the background used was the entire annotated genome. Significantly enriched GO terms were clustered and visualised using Enrichment Map (Isserlin et al. 2014). Gene expression patterns were visualised using pheatmap (Kolde 2025), using the default hierarchical clustering method (Euclidean distance and complete linkage).

5.3 Results

5.3.1 Confirmation of differences in susceptibility and virulence

Total lesion area differed between the two juniper genotypes and between the different treatments (Figure 5.1). Lesion size (square root of lesion area; mean = 16.2 mm) was significantly larger in individuals of the susceptible juniper genotype compared to those of the resistant juniper genotype (β=10.6, SE=1.6, t=6.7, $p < 0.001$), and significantly larger for the more virulent isolate compared to the less virulent isolate (β=11.2, SE=1.6, t=7.1, $p < 0.001$).

Additional confirmation of differences in susceptibility can be found in the percentage of total reads that were of pathogen origin recovered in the different genotypes and timepoints, with the number being similar between juniper genotypes at 48 hours but with the susceptible genotype having a considerably higher percentage of *P. austrocedri* reads after one week (Figure 5.2), suggesting the resistant genotype was better able to control the infection.

5.3.2 Classification of pathogen reads

The percentage of reads classified as originating from *P. austrocedri* in inoculated samples was generally higher in the susceptible juniper genotype than the resistant genotype, particularly at the one-week timepoint (Figure 5.2.) The percentage of reads classified as originating from

P. austrocedri in pure cultures was universally high (mean=97.3%, SE=0.1), confirming the validity of the k-mer-based method. The total number of reads successfully mapped to the *P. austrocedri* genome (average value across replicates) for all sample types are shown in Table 5.2. A substantial percentage (50-80%) of reads classified as *P. austrocedri* in inoculated samples failed to map successfully to the *P. austrocedri* genome due to mapping to too many loci (>10 loci). An inspection of these multi-mapping reads showed that they were mapping to highly repetitive regions of the *P. austrocedri* genome that contained no genes. In contrast, only 2-3% of reads in *P. austrocedri* cultures mapped to too many loci.

Table 5.2. Average number of reads per replicate successfully mapped to the *Phytophthora austrocedri* genome for the different sample types. Brackets show the percentage of the total number of reads mapped in each case.

	Inoculated juniper				***P. austrocedri* cultures**
	Susceptible genotype		**Resistant genotype**		
	48 hours	**One week**	**48 hours**	**One week**	
Control	760 (0.001%)	1,200 (0.002%)	690 (0.001%)	640 (0.001%)	
Less virulent isolate	448,000 (0.3%)	1,389,000 (0.9%)	168,000 (0.1%)	60,000 (0.04%)	25,646,000 (93.7%)
More virulent isolate	648,000 (0.4%)	3,236,000 (2%)	1,060,000 (0.7%)	1,509,000 (1%)	28,015,000 (93.4%)

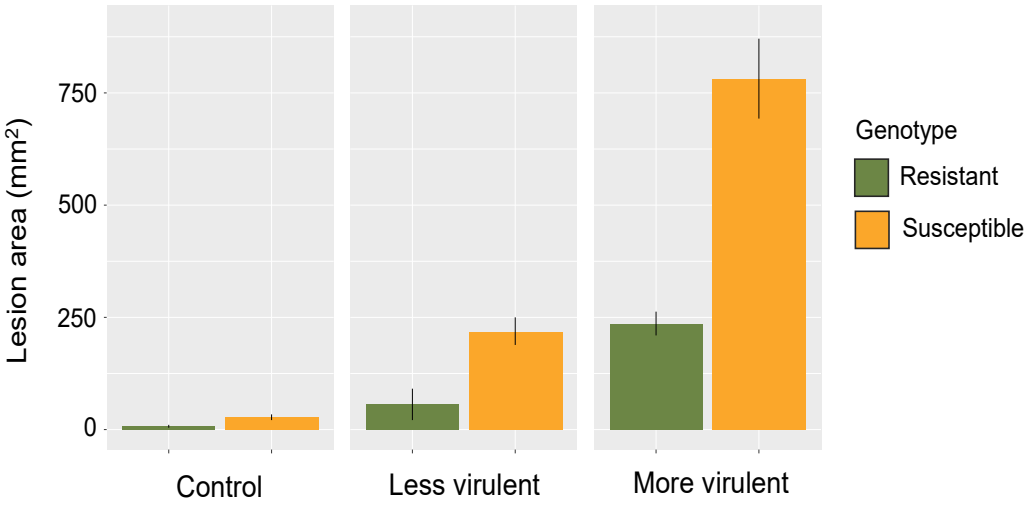

Figure 5.1. Lesion area at three weeks after inoculation for the different treatments (inoculated with a less virulent or more virulent isolate of *Phytophthora austrocedri*, or mock-inoculated control) in the two juniper genotypes (susceptible and resistant).

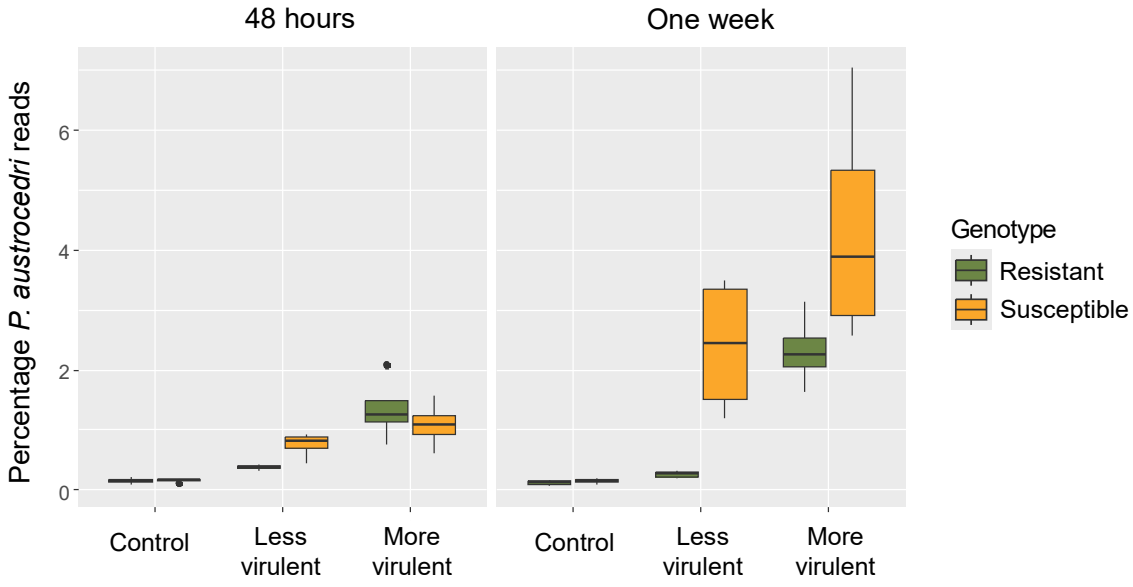

Figure 5.2. Percentage of reads classified as *Phytophthora austrocedri* in samples from different treatments and at different timepoints. There were more *P. austrocedri* reads at one week than at 48 hours, and more *P. austrocedri* reads were recovered from susceptible juniper than from resistant juniper. A negligible percentage of reads were classified as *P. austrocedri* in control samples, likely representing conserved eukaryotic sequences.

5.3.3 Juniper transcriptome assembly and annotation

After filtering non-plant transcripts, the final juniper transcriptome assembly contained 272,830 transcripts and 201,446 genes. Average contig length was 947 bp and median contig length was 516 bp. The BUSCO completeness score (Viridiplantae odb10) was 100%. Overall, 97.6% of reads aligned back to the transcriptome (prior to removing non-plant transcripts), demonstrating that most reads were successfully captured in the transcriptome. The Trinotate pipeline resulted in the successful annotation of GO terms for 76,093 genes, representing 38% of the transcriptome.

5.3.4 *Phytophthora austrocedri* annotation and identification of candidate effector proteins

The Pannzer pipeline resulted in successful annotation of GO terms for 17,864 genes (55% of genes) and the InterProScan pipeline resulted in Pfam protein domain matches for 18,463 genes (57% of genes). The secretome contained 2,260 genes, and we identified 118 candidate RxLR effector proteins that contained both a signal peptide and an effector motif.

5.3.5 Overall gene expression pattern in juniper

A PCA of gene expression counts for all juniper samples showed clear separation between the two juniper genotypes along the first axis of variation (Figure 5.3). The second axis of variation mostly separates inoculated samples at one week from all other samples, including inoculated samples at 48 hours and control samples at both timepoints. However, there were two exceptions: one control sample from each genotype is grouping with inoculated samples at one week. If this second axis of variation is driven by defence-related gene expression, this could mean two control samples were also infected with a pest or pathogen. There was no evidence of *P. austrocedri* in these control plants (no lesions at the inoculation point; negligible *P. austrocedri* transcripts in the samples; Figure 5.2), and therefore it is unlikely that the control plants were contaminated by *P. austrocedri*. However, the mock inoculation procedure did involve wounding the trees, which could have provided an entryway for a different pest or pathogen, or an opportunity for an endophyte to become an opportunistic pathogen. Alternatively, the gene expression pattern could reflect a systematic response to infection elsewhere on the plant. This result will likely decrease our power to detect defence-related gene expression at one week. Nevertheless, because this study included four replicates per treatment group, average gene expression should still, in most cases, be significantly different between groups, as only one control plant is affected in each group. Moreover, because this

clustering pattern was seen for one sample from each juniper genotype, this result should not lead to any biases in the comparison between genotype responses.

5.3.6 Differentially expressed genes in juniper

5.3.6.1 Differentially expressed genes within genotypes

When comparing gene expression within juniper genotypes, there were many more DEGs between inoculated samples and mock-inoculated controls at one week compared to 48 hours across all groups, suggesting a stronger response to the inoculation treatment at the later timepoint (Table 5.3). An exception to this is shown by the resistant genotype inoculated with the less virulent isolate, which showed similar number of DEGs at both time points – a number that represents the highest number of DEGs at 48 hours and by far the lowest number of DEGs at one week. This was in contrast to the same resistant genotype inoculated with the more virulent isolate, which had the largest number of DEGs at the one-week timepoint (Table 5.3).

A Venn diagram illustrating unique and shared DEGs across groups shows that the resistant genotype has the highest number of unique DEGs at 48 hours when inoculated with the less virulent isolate (390 genes; Figure 5.4A), and the same genotype also has the highest number of unique DEGs at one week, but in this case when inoculated with the more virulent isolate (4,400 genes; Figure 4B). At one week, there were also many DEGs shared between the susceptible genotype and the resistant genotype inoculated with the more virulent *P. austrocedri* isolate (1,670 genes), suggesting some degree of shared response to the infection between the two juniper genotypes.

5.3.6.2 Differentially expressed genes between genotypes

The number of DEGs between juniper genotypes (within treatments) was on average much higher than the number of DEGs within juniper genotypes (between treatments) (Table 5.4). This is particularly the case at the 48-hour timepoint; at the one-week timepoint, in some cases the effect of the inoculation treatment (Table 5.3) caused almost as many DEGs as the effect of juniper genotype (Table 5.4).

At 48 hours, a large number of DEGs between the genotypes were shared between all treatments, including the control (2,660 genes; Figure 5.5A), suggesting many of these genes were either constitutively differentially expressed between the two genotypes, or were differentially expressed as a response to wounding rather than as a specific response to infection by *P. austrocedri*. However, the group inoculated with the less virulent *P. austrocedri*

isolate had almost twice as many unique DEGs between the susceptible and resistant genotypes compared to the control group (1,950 vs 1,070 genes), suggesting some specific pathogen-related expression is also occurring. At one week, the largest number of unique DEGs between the two genotypes was in the group inoculated with the more virulent *P. austrocedri* isolate (3,200 genes; Figure 5.5B).

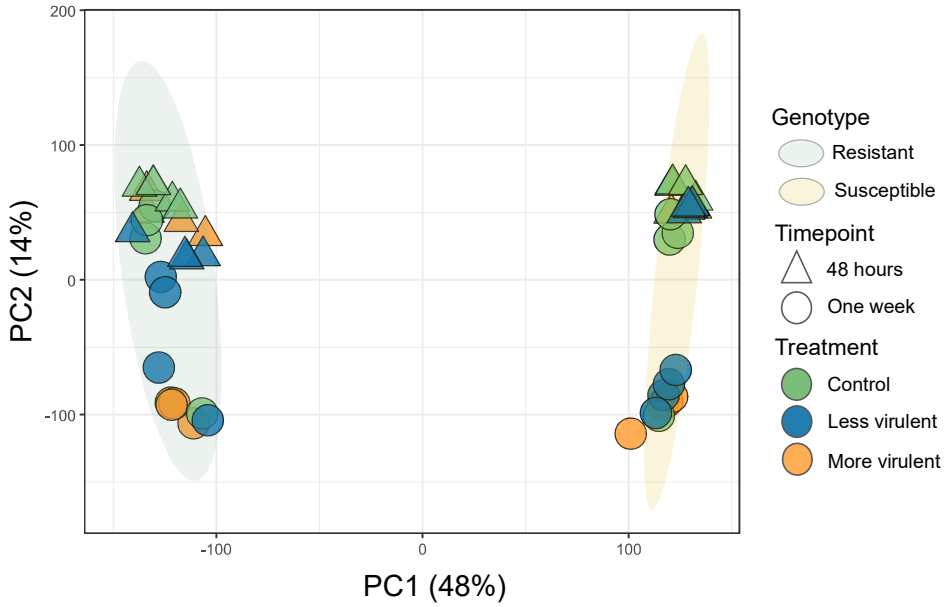

Figure 5.3. Principal component analysis (PCA) of gene expression patterns in juniper inoculated with *Phytophthora austrocedri* or mock-inoculated as a control. Gene expression data underwent variance stabilising transformation prior to the analysis. There is a clear separation of the two juniper genotypes (resistant vs. susceptible) on the first axis of variation. The second axis of variation seems to be driven by treatment and timepoint, with most inoculated samples at one week clustering away from control samples and inoculated samples at 48 hours. However, one control sample for each genotype is clustering with inoculated samples.

Table 5.3. Number of differentially expressed genes within juniper genotypes when comparing plants inoculated with two different isolates of *Phytophthora austrocedri* (less virulent and more virulent) versus a mock-inoculated control at two timepoints. Number of genes upregulated in treated group versus control are shown in orange; number of genes downregulated in treated group versus control are shown in blue; total number of differentially expressed genes are shown in black.

	Susceptible genotype		Resistant genotype	
	Less virulent	More virulent	Less virulent	More virulent
48 hours	548	465	733	416
	(185, 363)	(239, 226)	(307, 426)	(170, 246)
One week	5039	5330	750	7508
	(1644, 3395)	(1724, 3606)	(236, 514)	(2619, 4889)

Table 5.4. Number of differentially expressed genes between resistant and susceptible juniper genotypes within each treatment (inoculated with two different isolates of *Phytophthora austrocedri* or mock-inoculated control) at two timepoints. Number of genes upregulated in the resistant genotype compared to the susceptible genotype are shown in orange; number of genes downregulated in the resistant genotype compared to the susceptible genotype are shown in blue; total number of differentially expressed genes are shown in black.

	Control	Less virulent	More virulent
48 hours	5033	5898	5097
	(2880, 2153)	(3166, 2732)	(2872, 2225)
One week	6373	6251	7588
	(3793, 2580)	(3919, 2332)	(4667, 2921)

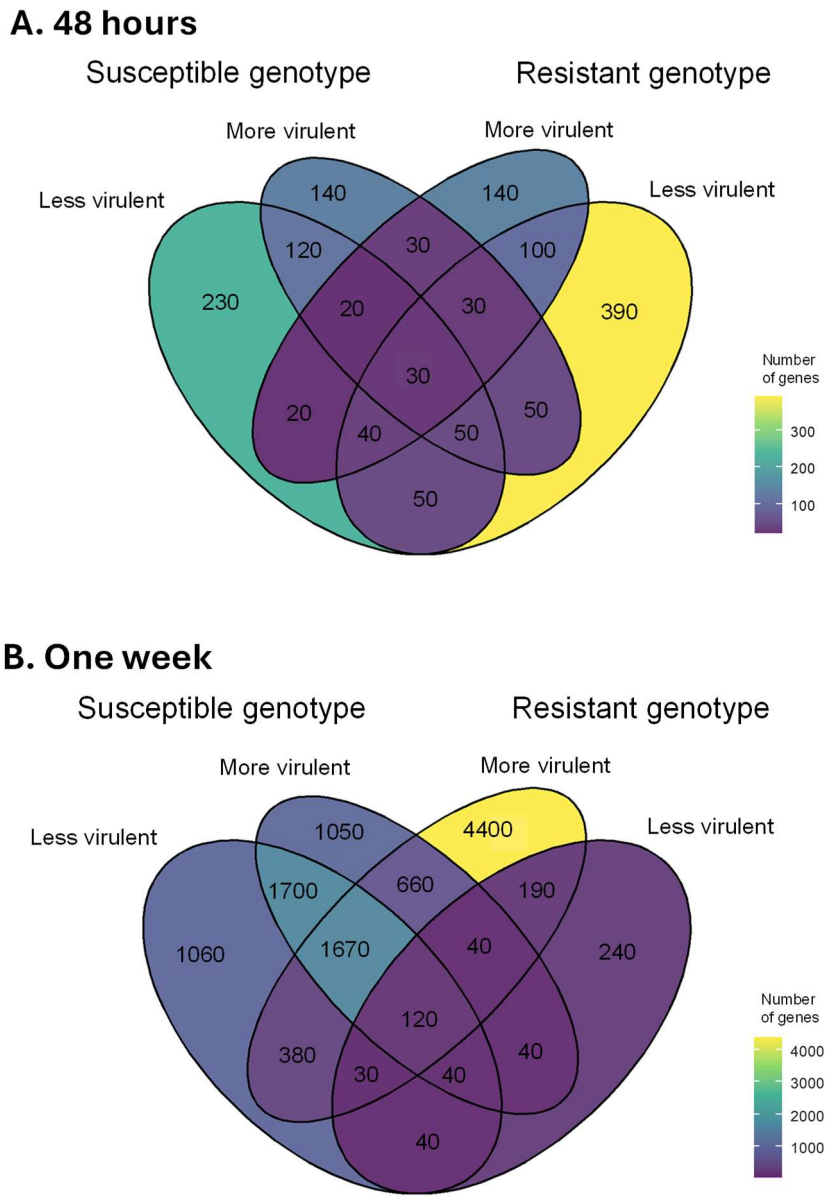

Figure 5.4. Venn diagrams showing the overlap of differentially expressed genes (DEGs) when contrasting juniper genotypes (resistant and susceptible) inoculated with *Phytophthora austrocedri* isolates (more virulent and less virulent) compared to a mock-inoculated control. Comparisons were made within juniper genotype and within timepoints. The resistant juniper genotype had the largest number of unique DEGs at both timepoints: when infected with the less virulent isolate at 48 hours (390 genes) and when infected with the more virulent isolate at one week (4,400 genes). At one week, there was also a large number of DEGs (1,670 genes) shared between the two juniper genotypes when infected with the more virulent isolate (resistant genotype) and when infected with both isolates (susceptible genotype). Numbers have been rounded to facilitate interpretation.

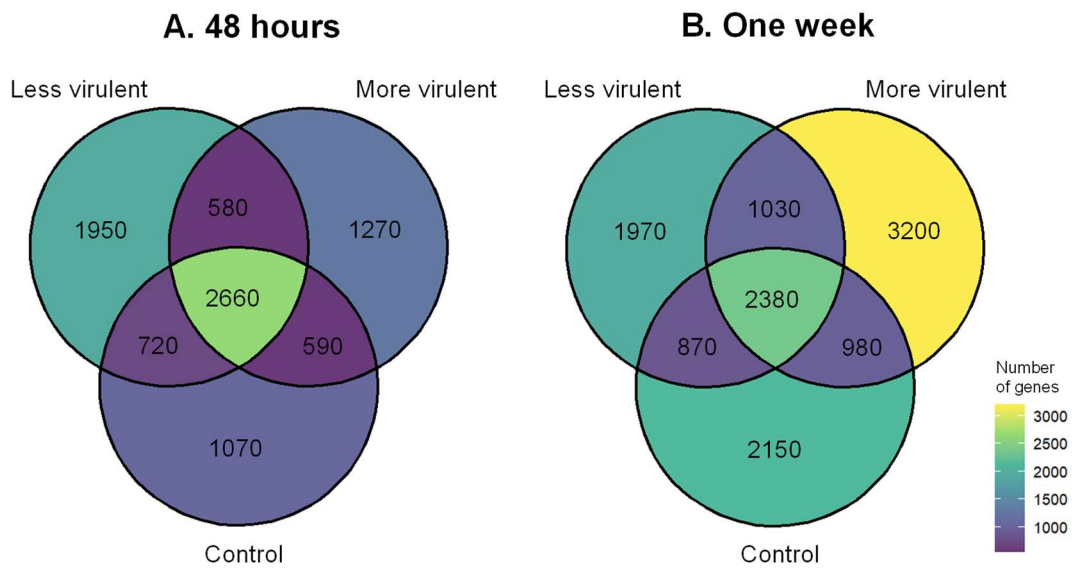

Figure 5.5. Venn diagrams showing the overlap of differentially expressed genes when contrasting resistant versus susceptible juniper genotypes inoculated with *Phytophthora austrocedri* isolates (more virulent and less virulent) or mock-inoculated controls. Comparisons were made among juniper genotypes and within treatments and timepoints. At 48 hours the largest group of DEGs between resistant and susceptible juniper (2,660 genes) was shared across all treatments, including the control. At one week, the largest group of DEGs (3,200 genes) was unique to juniper inoculated with the more virulent *P. austrocedri* isolate. Numbers have been rounded to facilitate interpretation.

5.3.7 Gene Ontology enrichment of differentially expressed genes in juniper

5.3.7.1 Gene Ontology enrichment within juniper genotypes

Full lists of significantly enriched GO terms (Biological Process) in upregulated and downregulated genes for each comparison (inoculated compared to mock-inoculated control within juniper genotype) are shown in Tables S5.1-S5.8. The most significantly enriched GO terms for each treatment group for upregulated genes (inoculated vs. control) are shown in Table 5.5 and Table 5.6 for the 48-hour timepoint and Table 5.7 and Table 5.8 for the one-week timepoint. Clusters of all significantly enriched GO terms for both upregulated and downregulated genes are shown in Figure 5.6 (48 hours) and Figure 5.7 (one week).

At 48 hours, the susceptible juniper genotype had no defence-related enriched GO terms (Table 5.5), with the only significantly enriched GO clusters corresponding to *Translation* (in both upregulated and downregulated genes) and *Photosynthesis* (downregulated genes)

(Figure 5.6). This was in contrast to the pattern shown by the resistant genotype, which showed signs of defence-related gene expression. When inoculated with the more virulent *P. austrocedri* isolate, the resistant genotype had significantly upregulated genes involved in *Ethylene biosynthesis* and *Alkene biosynthesis* (Figure 5.6; Table 5.6). Interestingly, the resistant genotype had a stronger reaction when inoculated with the less virulent isolate, with many more significantly enriched GO terms (Figure 5.6), which seem to be related to processes further along in the defence response, including *Response to ethylene*, *Defence response*, and *Secondary metabolite biosynthesis* (Table 5.6; Figure 5.6). In both cases, significantly downregulated genes were associated with *Translation* and *Photosynthesis*, as seen in the susceptible genotype (Figure 5.6).

By the one-week timepoint, the susceptible genotype had multiple defence-related GO terms present in its upregulated genes, including *Lignan biosynthesis*, *Flavonoid biosynthesis* and *Secondary metabolite biosynthesis* (Table 5.7; Figure 5.7). Interestingly, however, there are many more significant GO terms associated with downregulated genes, which clustered broadly into a group characterised by the GO term *Response to stimulus*, and which included defence-related GO terms such as *Response to other organism, Defence response, Innate immune response,* and *Hormone-mediated signalling pathway*, among many others (Table S5.5 and Table S5.6).

When inoculated with the more virulent isolate, the resistant genotype had more significantly enriched GO terms at the one-week timepoint compared to the susceptible genotype, particularly in upregulated genes (Figure 5.7). Upregulated genes included GO terms such as *Defence response*, *Secondary metabolite biosynthesis*, *Response to arachinodate* and *Killing of cells of another organism*, among many others (Table 5.8; Table S5.8). As with the susceptible genotype, there were also many defence-related GO terms enriched in downregulated genes (Figure 5.7; Table S5.8), including *Defence response*, *Response to other organism* and *Innate immune response*, among others.

The pattern shown by the resistant genotype inoculated with the less virulent isolate is distinct from the patterns observed in the other treatment groups. The number of enriched GO terms was lower in both upregulated and downregulated genes, and the GO terms themselves were also different in many cases (Table 5.8; Figure 5.7). In upregulated genes, enriched GO terms included *Cell wall macromolecule catabolism, Chitin catabolism*, *Killing of cells of another organism* and *Disruption of anatomical structure in another organism* (Table

5.8; Table S5.7). Enriched GO terms in downregulated genes included *Diterpenoid biosynthesis* and *Phenylpropanoid metabolism* (Figure 5.7; Table S5.7).

5.3.7.2 Gene Ontology enrichment between juniper genotypes

Full lists of GO terms (Biological Process) associated with upregulated and downregulated genes for each comparison (resistant genotype compared to susceptible genotype within each treatment) are shown in Tables S5.9-S5.14. There were many defence-related significantly enriched GO terms for both upregulated and downregulated genes across all treatment groups, including the mock-inoculated control; in fact, in most cases the most significantly enriched GO term across all treatment groups was *Defence response*.

At 48 hours, between-genotype comparisons included unique enriched GO terms that were not identified in any of the within-genotype comparisons at this early timepoint, including *Cell wall macromolecule catabolism, Killing of cells of another organism* and *Disruption of anatomical structure in another organism* upregulated in the resistant genotype compared to the susceptible genotype; *Response to salicylic acid, Regulation of jasmonic acid mediated signalling pathway* and *Response to oomycetes* downregulated in the resistant genotype compared to the susceptible genotype; and *Plant-type hypersensitive response, Regulation of programmed cell death* and *Innate immune response* in both upregulated and downregulated genes. At one week, there were fewer GO terms that were unique to between-genotype comparisons, but these included *Indole alkaloid biosynthesis* and *Thiazole biosynthesis* upregulated in the resistant genotype compared to the susceptible genotype, and *Sesquiterpenoid biosynthesis* and *Olefinic compound biosynthesis* downregulated in the resistant genotype compared to the susceptible genotype. Many of these GO terms were found when comparing mock-inoculated control plants in addition to when comparing plants inoculated with *P. austrocedri*. Overall, these results suggest there are broad differences in the defence response of the two genotypes, which includes their response to wounding and/or endosymbionts in addition to their response to infection by *P. austrocedri*.

Table 5.5. All significantly enriched GO terms (Biological Process) for upregulated genes in the susceptible juniper genotype at 48 hours post-inoculation. Listed p-values have been corrected for FDR.

ALL ENRICHED GO TERMS (BP) FOR UPREGULATED GENES IN SUSCEPTIBLE GENOTYPE AT 48 HOURS					
LESS VIRULENT ISOLATE			MORE VIRULENT ISOLATE		
GO ID	GO description	p-value	GO ID	GO description	p-value
6412	translation	2.00E-02	6412	translation	3.02E-06
2181	cytoplasmic translation	2.00E-02	2181	cytoplasmic translation	2.68E-04
9772	photosynthetic electron transport in photosystem II	2.00E-02	10467	gene expression	1.78E-02
			9059	macromolecule biosynthetic process	2.65E-02
			63	maturation of LSU-rRNA from tricistronic rRNA transcript	3.15E-02

Table 5.6. Top 10 most significantly enriched GO terms (Biological Process) for upregulated genes in the resistant juniper genotype at 48 hours post-inoculation. Listed p-values have been corrected for FDR. GO terms that have a connection with plant defence have been highlighted in yellow.

TOP 10 ENRICHED GO TERMS FOR UPREGULATED GENES IN RESISTANT GENOTYPE AT 48 HOURS					
LESS VIRULENT ISOLATE			MORE VIRULENT ISOLATE		
GO ID	GO description	p-value	GO ID	GO description	p-value
9723	response to ethylene	2.20E-18	0006412	translation	2.73E-03
9873	ethylene-activated signalling pathway	9.20E-17	0043449	ethylene biosynthetic process	2.73E-03
71369	cellular response to ethylene stimulus	1.12E-16	43450	alkene biosynthetic process	2.73E-03
160	phosphorelay signal transduction system	1.99E-15	9692	ethylene metabolic process	2.73E-03
9719	response to endogenous stimulus	6.17E-13	9693	alkene metabolic process	2.73E-03
9725	response to hormone	2.86E-12	1900673	olefin metabolic process	2.73E-03
9755	hormone-mediated signalling pathway	2.21E-11	1900674	olefin biosynthetic process	2.73E-03
71495	cellular response to endogenous stimulus	2.23E-11	9835	fruit ripening	3.04E-03
42221	response to chemical	4.32E-11	120251	hydrocarbon biosynthetic process	2.98E-02
44550	secondary metabolite biosynthetic process	7.64E-11	120255	olefinic compound biosynthetic process	2.98E-02

Table 5.7. Top 20 most significantly enriched GO terms (Biological Process) for upregulated genes in the susceptible juniper genotype at one week post-inoculation. Listed p-values have been corrected for FDR. GO terms that have a connection with plant defence have been highlighted in yellow.

TOP 20 ENRICHED GO TERMS FOR UPREGULATED GENES IN SUSCEPTIBLE GENOTYPE AT ONE WEEK					
LESS VIRULENT ISOLATE			MORE VIRULENT ISOLATE		
GO ID	**GO description**	**p-value**	**GO ID**	**GO description**	**p-value**
6412	translation	9.67E-22	6412	translation	2.73E-16
9451	RNA modification	2.77E-21	9813	flavonoid biosynthetic process	4.06E-11
10467	gene expression	3.75E-12	9812	flavonoid metabolic process	1.02E-09
16556	mRNA modification	3.99E-12	9699	phenylpropanoid biosynthetic process	2.65E-08
9059	macromolecule biosynthetic process	5.94E-11	44550	secondary metabolite biosynthetic process	2.89E-08
959	mitochondrial RNA metabolic process	2.61E-08	6694	steroid biosynthetic process	2.48E-07
80156	mitochondrial mRNA modification	4.29E-08	9698	phenylpropanoid metabolic process	8.36E-07
1900864	mitochondrial RNA modification	1.13E-07	19748	secondary metabolic process	1.22E-06
9806	lignan metabolic process	3.51E-05	8202	steroid metabolic process	4.86E-06
9807	lignan biosynthetic process	3.51E-05	9806	lignan metabolic process	3.97E-05
9699	phenylpropanoid biosynthetic process	6.36E-05	9807	lignan biosynthetic process	3.97E-05
16070	RNA metabolic process	2.70E-04	9451	RNA modification	3.97E-05
9058	biosynthetic process	2.70E-04	9058	biosynthetic process	1.02E-04
19748	secondary metabolic process	2.96E-04	19287	isopentenyl diphosphate biosyntheis	2.32E-03
16553	base conversion or substitution editing	2.96E-04	10467	gene expression	2.32E-03
16554	cytidine to uridine editing	2.96E-04	42274	ribosomal small subunit biogenesis	2.49E-03
44550	secondary metabolite biosynthetic process	2.96E-04	9059	macromolecule biosynthetic process	3.31E-03
963	mitochondrial RNA processing	8.00E-04	16126	sterol biosynthetic process	1.26E-02
43170	macromolecule metabolic process	1.37E-03	30490	maturation of SSU-rRNA	1.44E-02
9698	phenylpropanoid metabolic process	1.38E-03	10023	proanthocyanidin biosynthetic process	1.63E-02

Table 5.8. Top 20 most significantly enriched GO terms (Biological Process) for upregulated genes in the resistant juniper genotype at one week post-inoculation. Listed p-values have been corrected for FDR. GO terms that have a connection with plant defence have been highlighted in yellow.

TOP 20 ENRICHED GO TERMS FOR UPREGULATED GENES IN RESISTANT GENOTYPE AT ONE WEEK					
LESS VIRULENT ISOLATE			MORE VIRULENT ISOLATE		
GO ID	**GO description**	**p-value**	**GO ID**	**GO description**	**p-value**
16998	cell wall macromolecule catabolic process	8.7059E-19	6952	defence response	6.78E-13
6032	chitin catabolic process	8.7059E-19	50896	response to stimulus	1.48E-09
1901072	glucosamine-containing compound catabolic process	8.7059E-19	6950	response to stress	2.16E-08
46348	amino sugar catabolic process	8.7059E-19	16137	glycoside metabolic process	6.30E-06
6030	chitin metabolic process	8.7059E-19	42221	response to chemical	1.82E-05
6026	aminoglycan catabolic process	1.8726E-18	44550	secondary metabolite biosynthetic process	3.76E-05
1901071	glucosamine-containing compound metabolic process	5.8474E-18	9699	phenylpropanoid biosynthetic process	3.76E-05
6022	aminoglycan metabolic process	3.0635E-16	70542	response to fatty acid	4.04E-05
6040	amino sugar metabolic process	1.6081E-15	1904550	response to arachidonate	6.90E-05
44036	cell wall macromolecule metabolic process	9.3355E-14	2000032	regulation of secondary shoot formation	6.90E-05
272	polysaccharide catabolic process	1.8615E-13	60688	regulation of morphogenesis of a branching structure	6.90E-05
16052	carbohydrate catabolic process	4.8753E-13	18158	protein oxidation	6.90E-05
1901136	carbohydrate derivative catabolic process	4.6365E-11	18171	peptidyl-cysteine oxidation	6.90E-05
5976	polysaccharide metabolic process	9.4417E-10	22603	regulation of anatomical structure morphogenesis	1.22E-04
5975	carbohydrate metabolic process	6.7626E-9	16138	glycoside biosynthetic process	1.57E-04
141060	disruption of anatomical structure in another organism	1.2681E-7	1905428	regulation of plant organ formation	1.98E-04
141061	disruption of cell in another organism	1.2681E-7	8299	isoprenoid biosynthetic process	2.14E-04
31640	killing of cells of another organism	1.2681E-7	70483	detection of hypoxia	2.71E-04
71554	cell wall organization or biogenesis	2.1865E-7	1901657	glycosyl compound metabolic process	2.71E-04
1906	cell killing	2.5553E-7	9806	lignan metabolic process	3.53E-04

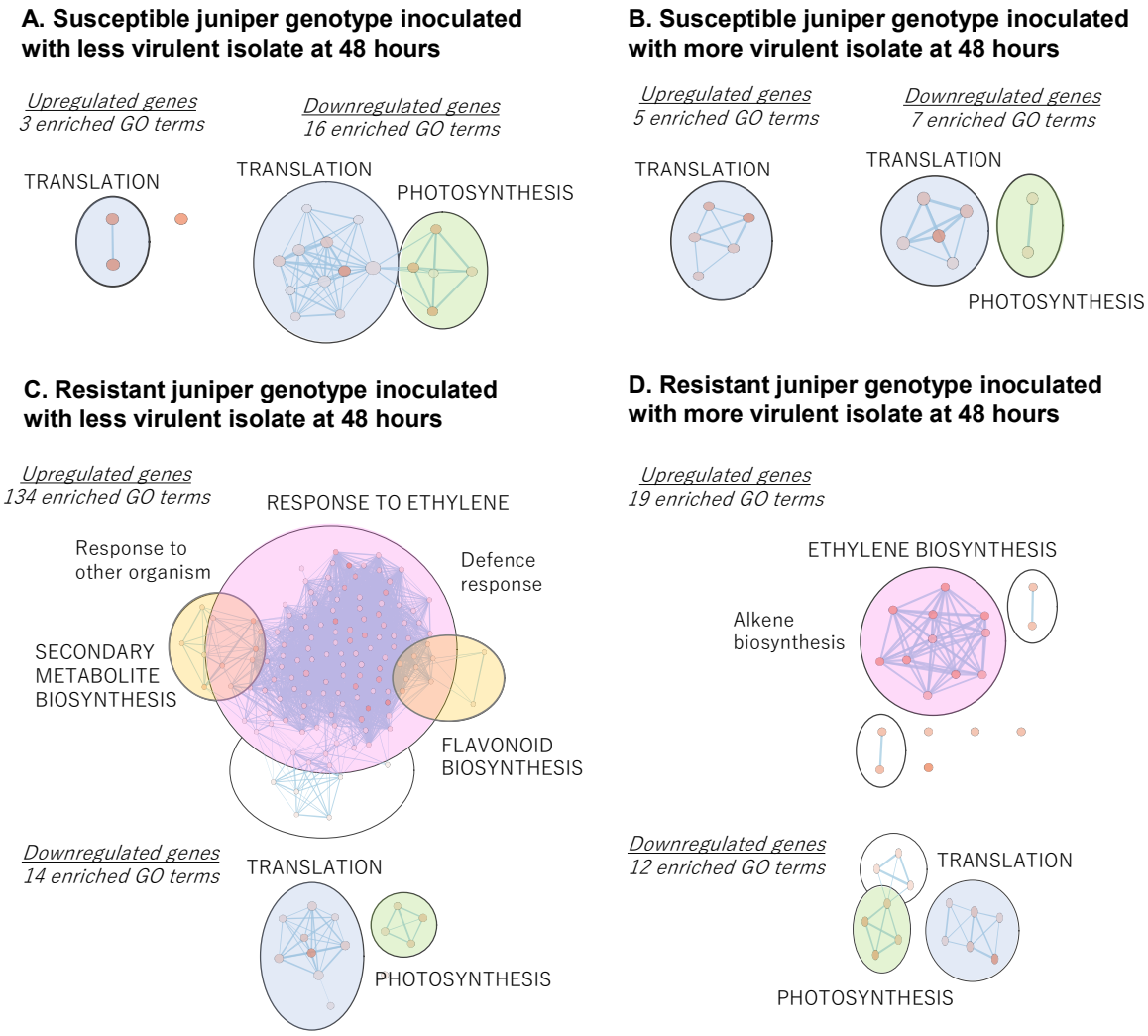

Figure 5.6. Clusters of significantly enriched GO terms (Biological Process) in upregulated and downregulated genes in juniper inoculated with *Phytophthora austrocedri* compared to a mock inoculated control at 48 hours after inoculation. Each enriched GO term is indicated by an orange dot, and related GO terms are connected by lines. Clusters of interest have been coloured to indicate similarity. The most statistically significant GO terms for each cluster of interest are indicated in capital letters. In some cases, other relevant GO terms within the cluster are noted in lower case. There are no defence-related enriched GO terms in the susceptible genotype. The resistant genotype does have defence-related enriched GO terms, and has a greater number when inoculated with the less virulent isolate.

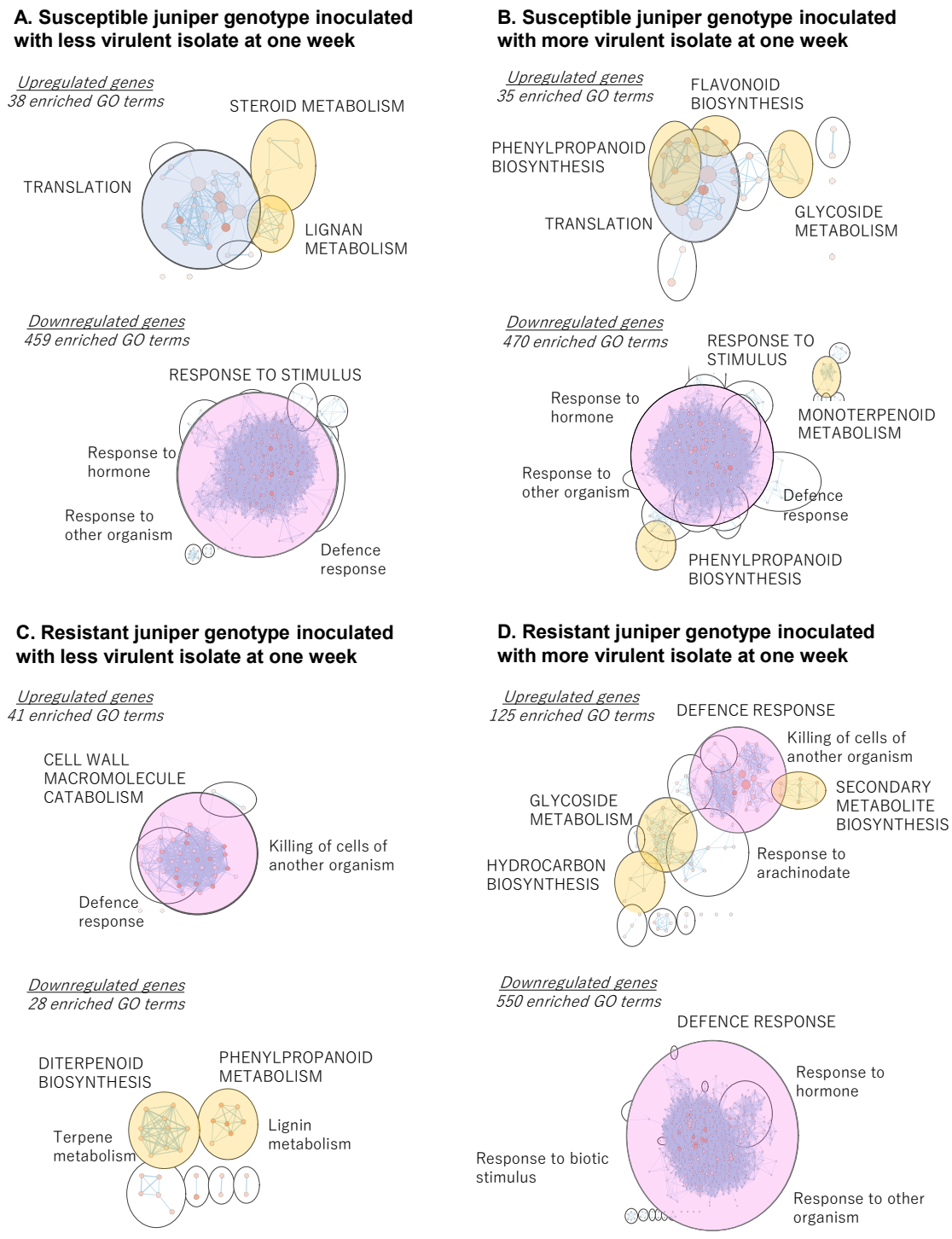

Figure 5.7. Clusters of significantly enriched GO terms (Biological Process) in upregulated and downregulated genes in juniper inoculated with *Phytophthora austrocedri* compared to a mock inoculated control at one week after inoculation. Each enriched GO term is indicated by an orange dot, and related GO terms are connected by lines. Clusters of interest have been coloured to indicate similarity. The most statistically significant GO terms for each cluster of interest are indicated in capital letters. Other relevant GO terms within the cluster are noted in lower case. The susceptible juniper genotype has some defence-related GO terms in upregulated genes in inoculated trees compared to the control, but have many more defence-related GO terms in downregulated genes. A similar pattern is observed in the resistant genotype inoculated with the more virulent isolate, although with more defence-related GO terms in upregulated genes. The resistant genotype inoculated with the less virulent isolate shows a distinct pattern, with fewer defence-related GO terms in downregulated genes, and different GO terms in upregulated genes.

5.3.8 Identifying candidate genes important in juniper defence

The results presented above demonstrate there are many hundreds of genes involved in the defence response in juniper. We therefore attempted to narrow down these genes to identify only those that are likely to be most important in successfully supressing infection by *P. austrocedri* in particular. For this, we were particularly interested in the response of the resistant genotype to the less virulent isolate, as this group showed distinct patterns at both 48 hours (Figure 5.6) and one week (Figure 5.7) that suggested successful suppression of the infection. We took two approaches to identifying genes likely to be of particular importance.

First, we explored whether defence-related genes upregulated early in the resistant genotype (when inoculated with the less virulent isolate) were unique to this genotype/isolate combination, or whether they were also subsequently upregulated in other groups. Figure 5.8 shows expression levels of these genes at 48 hours and at one week for each treatment group relative to the average expression across all samples at 48 hours. Many genes upregulated early in the group of interest showed higher expression at one week in inoculated samples of both genotypes, suggesting they were not unique to the group of interest. In fact, some of these genes showed lower expression in the group of interest at the one-week timepoint compared to the other treatment combinations. In the case of these genes, it may be the timing of expression that is important, with earlier activation allowing suppression of the pathogen. However, there were also some genes that are uniquely highly expressed in the resistant genotype (Figure 5.8), which could also be important determinants of susceptibility. One gene worth noting is *Mitogen-activated protein kinase kinase 5*, which is likely involved in the activation of the immune response and is uniquely highly expressed in the resistant genotype.

The second approach to identify candidate genes underlying successful defence against *P. austrocedri* was to focus on the overlap between genes significantly upregulated in two different comparisons: 1) inoculated (less virulent isolate) vs control in resistant genotype at 48 hours, and 2) resistant vs susceptible (both inoculated with the less virulent isolate) at 48 hours. The overlap in upregulated genes resulted in 51 genes that had an annotation with a UniProt database entry, and 29 of these had functions that related to plant defence. These included several genes involved in the ethylene-activated signalling pathway, the jasmonic acid-activated signalling pathway, and genes involved in secondary metabolite biosynthesis, which highlight the same defence processes previously identified (Table 5.9). There were also

some pathogenesis-related proteins, such as a proteinase and genes involved in generating ROS. The same *Mitogen-activated protein kinase kinase 5* as seen above was also identified as significant. Finally, one gene particularly worth noting is *Probable LRR receptor-like serine/threonine-protein kinase*, a leucine-rich receptor-like kinase which could be involved in the recognition of pathogen elicitors such as PAMPs. This gene showed higher expression in the resistant genotype compared to the susceptible genotype, particularly in the case of the less virulent isolate at 48 hours and in the case of the more virulent isolate at one week (Figure 5.9).

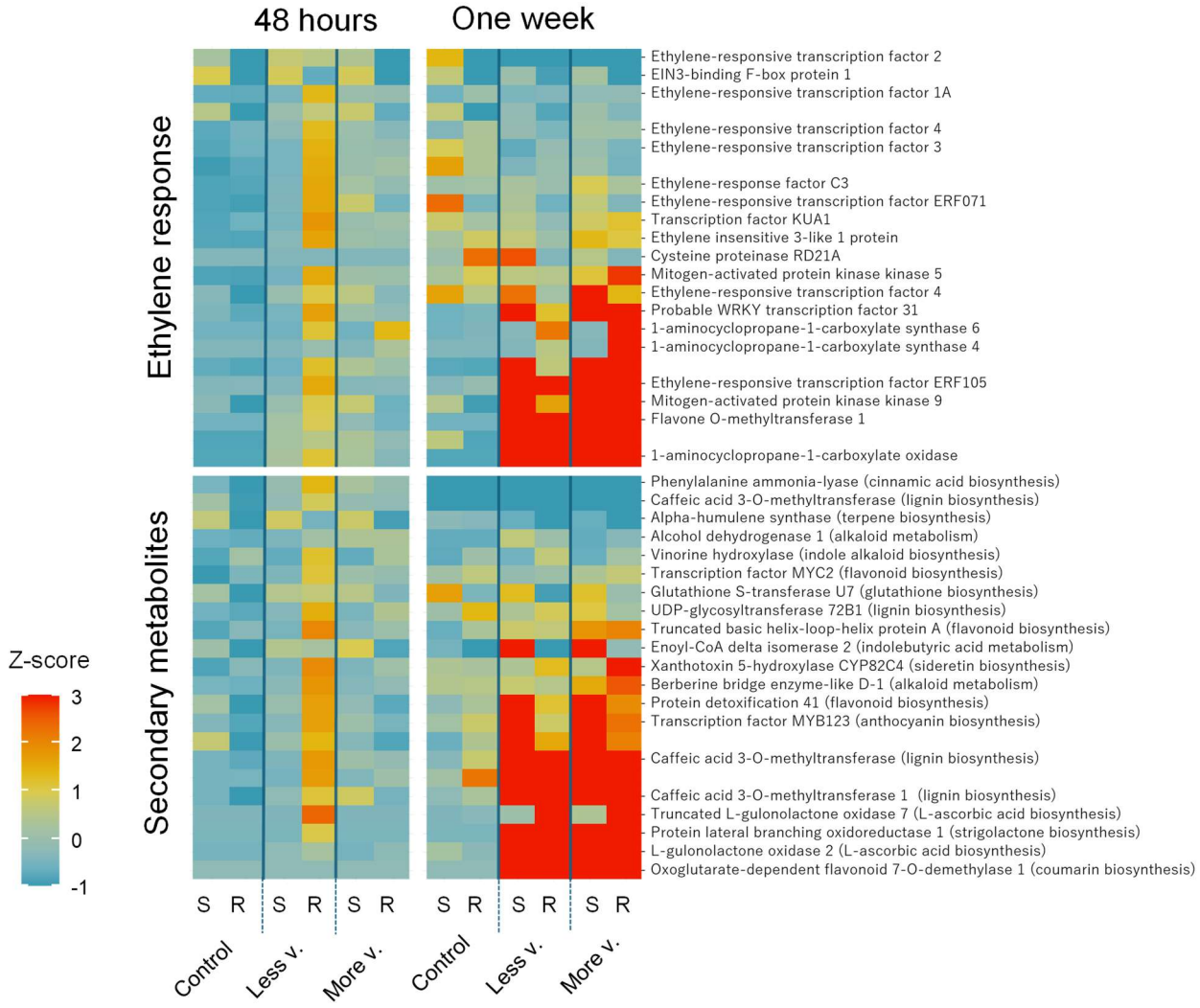

Figure 5.8. Heatmap of gene expression of defence-related genes that were significantly upregulated in the resistant genotype inoculated with the less virulent *Phytophthora austrocedri* isolate compared to a mock-inoculated control at 48 hours. R: Resistant genotype; S: Susceptible genotype; Less v.: Less virulent isolate; More v.: More virulent isolate. Genes have been separated into two broad categories depending on function: ethylene response and secondary metabolite biosynthesis. In cases where gene function matched both these categories, they were put in the ethylene response group. Gene expression Z-score was calculated relative to average gene expression across samples at 48 hours. Many of the genes upregulated in the group of interest (resistant genotype inoculated with the less virulent isolate) at 48 hours showed higher expression at one week in the other groups, suggesting the timing of gene expression is important.

Table 5.9. Annotation of genes that are candidates for being most important in the successful suppression of infection by *Phytophthora austrocedri*. Annotation is based on homology to the listed UniProt entry. ROS: reactive oxygen species.

Group	Protein name	UniProt entry	Possible role in defence response
Abscisic acid	Mitogen-activated protein kinase kinase kinase 17	M3K17_ARATH	Abscisic acid-activated signalling pathway
Abscisic acid	NDR1/HIN1-like protein 6	NHL6_ARATH	Abscisic acid-activated signalling pathway
Ethylene	1-aminocyclopropane-1-carboxylate synthase 4	1A14_SOLLC	Ethylene biosynthesis
Ethylene	1-aminocyclopropane-1-carboxylate synthase 6	1A16_ARATH	Ethylene biosynthesis
Ethylene	Ethylene insensitive 3-like 1 protein	EIL1_ARATH	Ethylene-activated signalling pathway
Ethylene	Ethylene-responsive transcription factor 1A	EF100_ARATH	Ethylene-activated signalling pathway
Ethylene	Ethylene-responsive transcription factor 3	ERF82_ARATH	Ethylene-activated signalling pathway
Ethylene	Ethylene-responsive transcription factor 4	ERF78_ARATH	Ethylene-activated signalling pathway
Ethylene	Ethylene-responsive transcription factor ERF071	ERF71_ARATH	Ethylene-activated signalling pathway
Ethylene	Ethylene-responsive transcription factor ERF105	EF105_ARATH	Ethylene-activated signalling pathway
Ethylene	Transcription factor KUA1	KUA1_ARATH	Ethylene-activated signalling pathway
Jasmonic acid	Transcription factor MYC2	MYC2_ARATH	Jasmonic acid-activated signalling pathway
Jasmonic acid	Transcription factor MYC2	MYC2_SOLLC	Jasmonic acid-activated signalling pathway
Other defence response	Aldehyde oxidase GLOX1	GLOX1_ARATH	Generation of ROS
Other defence response	Cysteine proteinase RD21A	RD21A_ARATH	Role in plant immunity
Other defence response	Lipoxygenase 4	LOX4_ARATH	Lipid oxidation
Other defence response	Mitogen-activated protein kinase kinase 5	M2K5_ARATH	Activation of immune response
Other defence response	Pathogenesis-related thaumatin-like protein 3.8	CRJ38_CRYJA	Cell membrane disruption
Other defence response	Peroxidase 5	PER5_VITVI	Cell wall strengthening; generation of ROS
Other defence response	Probable LRR receptor-like serine/threonine-protein kinase At1g53420	Y1534_ARATH	Potential cell-surface pattern recognition receptor
Other defence response	Wound-induced protein WIN2	WIN2_SOLTU	Chitin binding
Secondary metabolites	Caffeic acid 3-O-methyltransferase	COMT1_AMMMJ	Lignin biosynthesis
Secondary metabolites	UDP-glycosyltransferase 72B	U72B1_ARATH	Lignin biosynthesis
Secondary metabolites	Linamarin synthase 1	UGTK4_MANES	Linamarin synthase activity
Secondary metabolites	Oxoglutarate-dependent flavonoid 7-O-demethylase 1	F7ODM_OCIBA	Coumarin biosynthesis
Secondary metabolites	Truncated basic helix-loop-helix protein A	BHLHM_PEA	Flavonoid biosynthesis
Secondary metabolites	Vinorine hydroxylase	VINHY_RAUSE	Alkaloid biosynthesis
Secondary metabolites	Xanthotoxin 5-hydroxylase CYP82C4	C82C4_ARATH	Phenylpropanoid metabolism

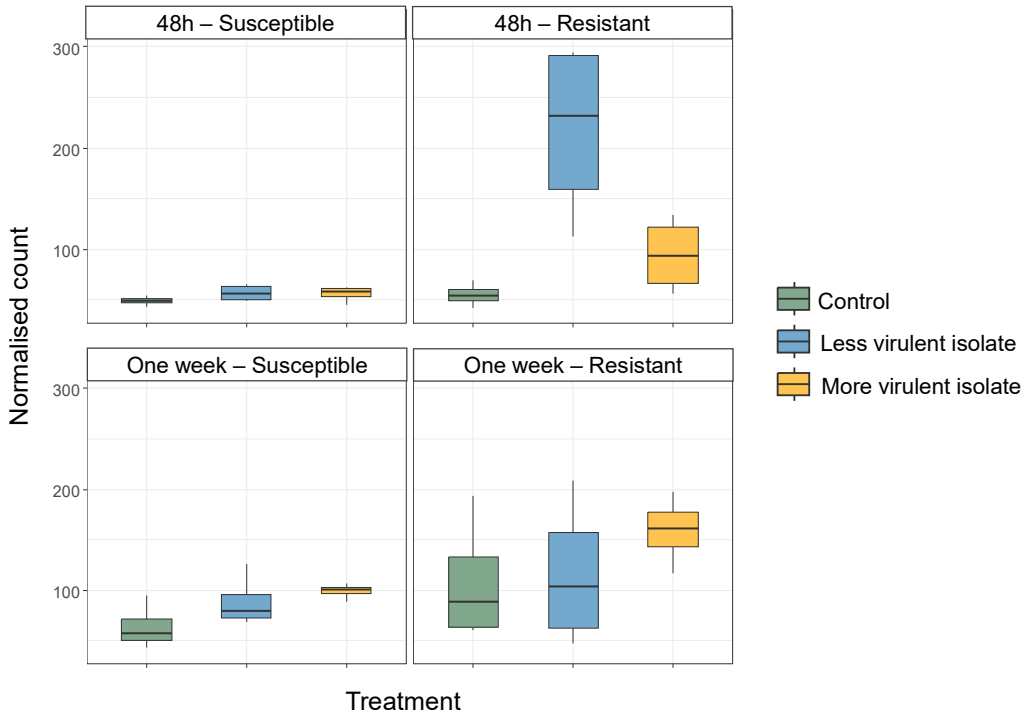

Figure 5.9. Normalised count of gene expression of a probable LRR receptor-like serine/threonine-protein kinase in the different genotypes, treatments and timepoints.

5.3.9 Overall gene expression in *Phytophthora austrocedri*

A PCA of gene expression counts across all *P. austrocedri* samples showed good separation of treatments, with the first axis of variation separating cultures from *in planta* samples, and the second axis of variation separating the two *in planta* timepoints and the two isolates (Figure 5.10). A second PCA focusing on just *in planta* gene expression separated samples based on timepoint along the first axis of variation and based on isolate along the second axis of variation (Figure 5.11).

5.3.10 Differentially expressed genes in *Phytophthora austrocedri*

An initial exploratory analysis of all *in planta* samples demonstrated there was very low power to detect DEGs in the case of the less virulent isolate in the resistant genotype at one week, due to the low number of reads in this group (Table 5.2). This treatment group was therefore removed from subsequent analyses, as low power in this case would bias the results, with only very highly expressed genes having the potential to be classified as being differentially expressed.

Table 5.10 shows the number of DEGs within and between the two *P. austrocedri* isolates under different conditions. Within isolates, there were many DEGs between samples growing in culture versus *in planta* at both timepoints. There were also many DEGs between the two timepoints *in planta*, although the number of DEGs was much lower in the case of the less virulent isolate in the resistant genotype. Note that this effect was not driven by low power caused by a smaller number of reads, as the susceptible genotype was used for the one-week timepoint (the less virulent isolate in the resistant genotype at one week had been discarded from the analysis; see above).

When comparing between *P. austrocedri* isolates, there were many DEGs for samples growing in culture (Table 5.10). However, it is worth noting that this may in part be driven by the higher power to detect DEGs when analysing cultures, due to the much greater number of reads. When *in planta*, there were many more DEGs between the two isolates when they were growing in the resistant genotype than when they were growing in the susceptible genotype (Table 5.10).

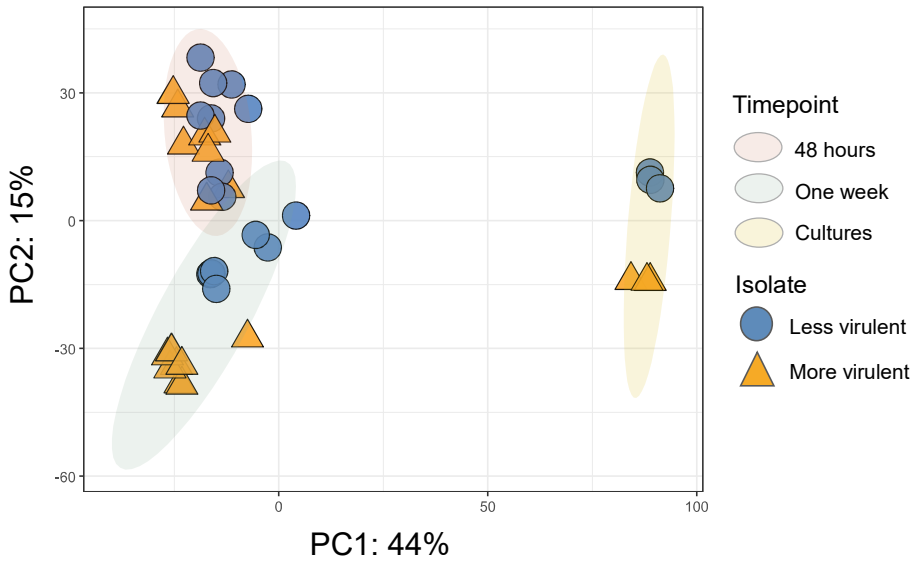

Figure 5.10. Principal component analysis of gene expression patterns in *Phytophthora austrocedri* in cultures and *in planta* at two timepoints. Gene expression data underwent regularised log transformation prior to the analysis. The first axis of variation separates cultures from *in planta* samples; the second axis of variation separates samples based on timepoint and isolate.

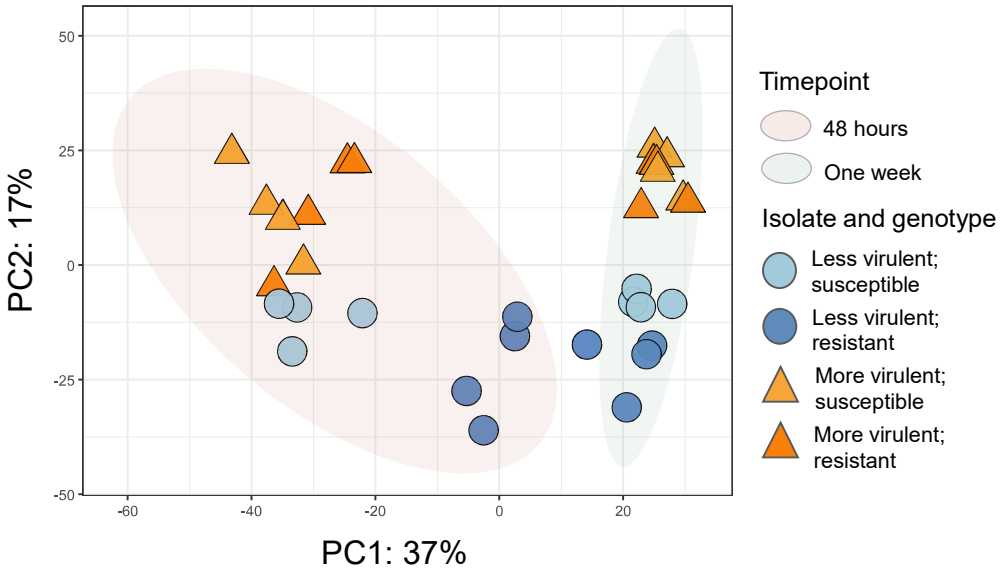

Figure 5.11. Principal component analysis of gene expression patterns in *Phytophthora austrocedri in planta* at two timepoints. Gene expression data underwent regularised log transformation prior to the analysis. The first axis of variation separates samples based on timepoint; the second axis of variation separates the two isolates.

Table 5.10. Differentially expressed genes within and between *Phytophthora austrocedri* isolates and conditions. Number of genes upregulated are shown in orange; number of genes downregulated are shown in blue; total number of differentially expressed genes are shown in black. In the comparison between isolates upregulated genes refer to genes upregulated in the more virulent isolate compared to the less virulent isolate. Comparisons of *in planta* vs cultures were made using the susceptible host genotype only. *Note: comparison between timepoints for the less virulent isolate used the susceptible genotype at the one-week timepoint for comparisons to the resistant genotype at 48 hours, due to an insufficient number of reads in the case of the less virulent isolate at one week in the resistant genotype.

WITHIN ISOLATES		
	Less virulent isolate	**More virulent isolate**
48 hours *in planta* vs culture	7,681	7,437
	(2,520; 5,161)	(2,576; 4,861)
One week *in planta* vs culture	4,611	4,368
	(2,107; 2,504)	(2,245; 2,123)
One week *in planta* vs 48 hours *in planta* (susceptible genotype)	2,275	2,760
	(1,366; 909)	(1,710; 1,050)
One week *in planta* vs 48 hours *in planta* (resistant genotype*)	216*	2,626
	(220; 194)	(1,746; 880)
BETWEEN ISOLATES		
In culture	4,865	
	(2,887; 1,978)	
48 hours *in planta* (susceptible genotype)	262	
	(116, 146)	
48 hours *in planta* (resistant genotype)	1,712	
	(757; 955)	
One week *in planta* (susceptible genotype)	144	
	(69, 75)	

5.3.11 Candidate drivers of pathogenicity in *Phytophthora austrocedri*

To explore genes that may underlie *P. austrocedri*'s ability to infect juniper, we compared patterns of gene expression *in planta* versus in culture. This analysis was carried out using the susceptible genotype only, to focus on cases where *P. austrocedri* was able to successfully cause infection. Figure 5.12 shows a Venn diagram of unique and shared genes upregulated *in planta* compared to in culture for the two isolates at both timepoints. The largest group of upregulated genes (860 genes) was shared between the two isolates at 48 hours, and the second largest group was shared genes at one week (650 genes). There were also 540 genes upregulated in all *in planta* samples compared to culture samples. Overall, this suggests a large shared basis of virulence between the two isolates. However, there were also many genes unique to each isolate at each timepoint (Figure 5.12).

To explore gene function, we carried out a GO enrichment analysis of genes that were significantly upregulated *in planta* compared to in culture. Full lists of GO terms (Biological Process) are shown in Table S5.15 and Table S5.16. At 48 hours, the most significantly enriched GO terms in upregulated genes were dominated by processes related to core gene expression and protein synthesis, including *Ribosome biogenesis, RNA processing* and *Cellular component biogenesis*. At one week, the most significantly enriched GO terms in upregulated genes related to catabolic processes, including *Organic acid catabolism, Lipid catabolism* and *Carbohydrate catabolism*. Both timepoints also contained significantly enriched GO terms related to plant cell wall degradation (e.g., *Pectin catabolism* and *Cellulose catabolism*) and oxidative stress (e.g., *Response to reactive oxygen species* and *Reactive oxygen species metabolism*); however, the latter were more prominent at the one-week timepoint.

Out of the 118 candidate RxLR effector proteins identified, 54 were differentially expressed between samples growing *in planta* versus in culture, 46 of which were significantly upregulated *in planta*. Of candidate RxLR effectors upregulated *in planta*, 29 were significantly upregulated in both isolates and at both timepoints, suggesting these may be essential for *P. austrocedri* pathogenicity in juniper. Effectors with differential expression between samples growing in culture versus *in planta* showed an expression pattern that was broadly shared by both isolates (Figure 5.13), suggesting a likely role of these genes in successful growth *in planta*. However, when *in planta* each isolate and timepoint was also associated with uniquely elevated expression of some gene clusters.

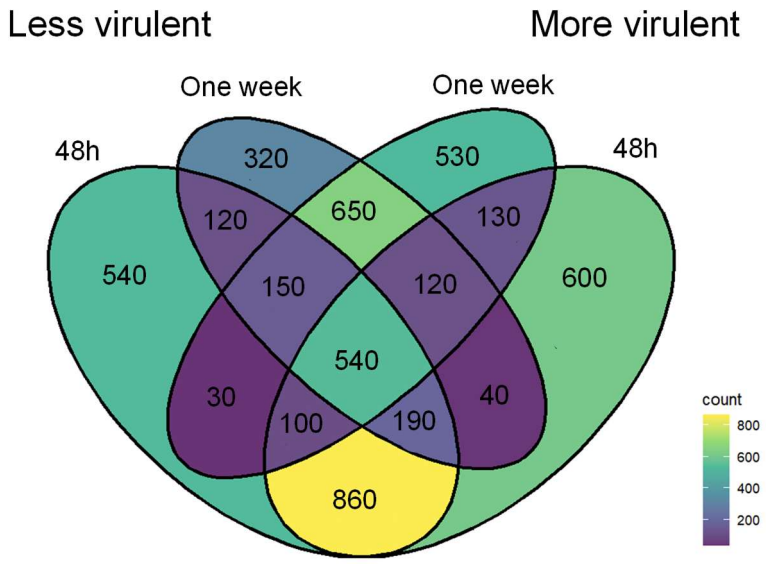

Figure 5.12. Venn diagram showing the overlap of upregulated genes between *in planta* samples compared to cultures at two timepoints for the two *Phytophthora austrocedri* isolates (more virulent and less virulent). This analysis used the susceptible host genotype only. Numbers have been rounded to facilitate interpretation.

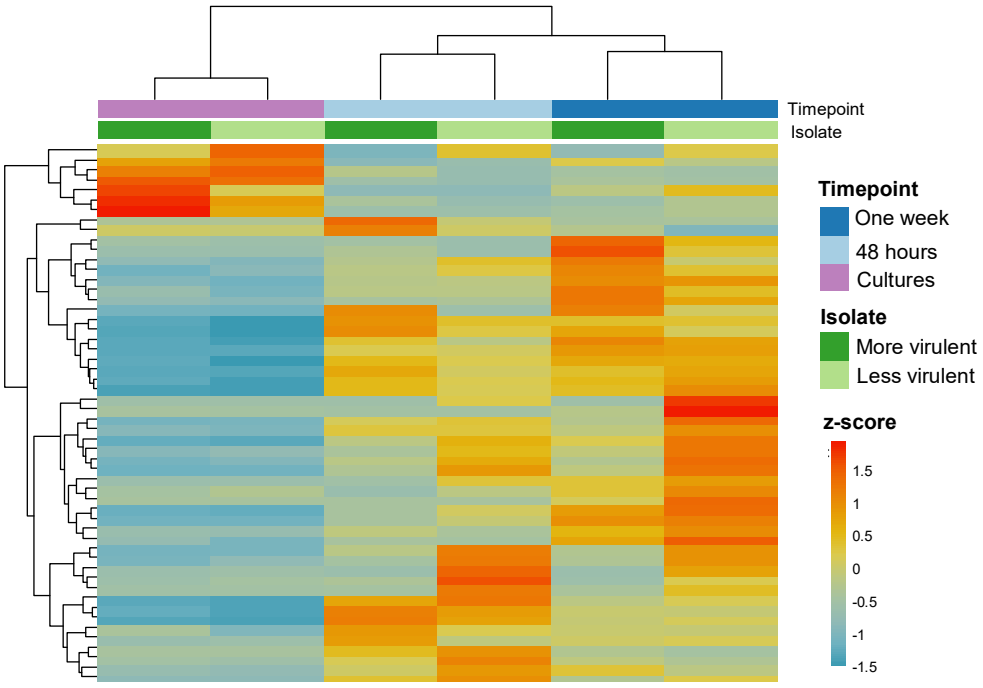

Figure 5.13. Heatmap showing expression patterns of candidate RxLR effectors proteins that were differentially expressed between *Phytophthora austrocedri* isolates growing in culture versus growing *in planta*. The differential expression analysis was carried out separately for each isolate, but the gene expression pattern *in planta* vs in culture is broadly shared by both isolates.

5.3.12 Effect of timepoint on *Phytophthora austrocedri* gene expression

To explore differences in gene expression between timepoints, and investigate whether they may represent different phases in the *Phytophthora* lifecycle (biotrophic versus necrotrophic), we explored expression patterns for all DEGs between the two timepoints. Because the less virulent isolate in the resistant genotype represented an outlier that may share more similarities with one-week samples than other 48-hour samples (Table 5.10), this sample was initially excluded from the analysis to identify DEGs between timepoints, but was subsequently included in the clustering analysis to determine which timepoint the sample would cluster with. Overall, there were 7,285 DEGs between timepoints, 5,124 upregulated at one week and 2,161 downregulated at one week compared to the 48-hour timepoint. The expression patterns of these DEGs showed three large clusters, with Cluster 1 showing high expression at 48 hours (except for in the case of the less virulent isolate in the resistant genotype), Cluster 2 showing high expression at one week, and Cluster 3 showing high expression at one week and in the less virulent isolate in the resistant genotype at 48 hours (Figure 5.14A). A GO enrichment analysis of these clusters showed that Cluster 1 related to growth and protein formation, including GO terms such as *Ribosome biogenesis*, *Cellular component biogenesis* and *Macromolecule biosynthesis*, while Cluster 2 and Cluster 3 were dominated by GO terms such as *Catabolic process*, *Autophagy* and *Peroxisome organisation* (Table S5.17; Figure 5.14B).

We then explored expression patterns of several groups of important secreted proteins for which we had *a priori* expectations of different expression patterns depending on the lifecycle stage, based on the results presented by Zuluaga et al. (2016). These included Kazal-type protease inhibitors and elicitins (likely to be associated with biotrophy), ROS-associated enzymes (likely to have distinct gene expression patterns according to lifecycle stage), and necrosis-inducing proteins and cell-wall degrading enzymes (likely to be associated with necrotrophy) (Figure 5.15). In most cases, the two timepoints showed distinct gene expression patterns for all functional groups, although the less virulent isolate in the resistant genotype at 48 hours was often an outlier. Compared to the 48-hour timepoint, the one-week timepoint had lower expression of Kazal-type protease inhibitors and higher expression of necrosis-inducing proteins, particularly in the case of the more virulent isolate (Figure 5.15). Both timepoints had similar overall expression levels of elicitins and ROS-associated enzymes, although different genes were involved at each timepoint. The 48-hour timepoint had higher expression of enzymes targeting pectin, but overall similar levels of enzymes targeting

cellulose and xylan. However, the 48-hour timepoint had very low expression levels of enzymes targeting cutin (Figure 5.15).

5.3.13 Candidate drivers of variation in virulence between *Phytophthora austrocedri* isolates

To explore genes underlying differences in virulence between the two isolates, we analysed differences in expression patterns between isolates growing *in planta*. Of the 118 candidate RxLR effector proteins, 83 had detectable expression *in planta*. Expression patterns clustered by isolate, although there was also an effect of timepoint (Figure 5.16). Effectors were divided into six groups based on their expression pattern, and some of these clusters were unique to particular treatment groups. For example, Cluster 2 was uniquely highly expressed by the less virulent isolate in the susceptible genotype at 48 hours, Cluster 4 was uniquely highly expressed by the less virulent isolate in the susceptible genotype at one week, and Cluster 5 was uniquely highly expressed by the more virulent isolate in the resistant genotype at one week.

To explore other types of genes that may be driving differences in virulence, we explored significantly upregulated and downregulated genes between isolates across host genotypes but within timepoints, focusing on the secretome. There were 68 secretome DEGs that could be assigned a protein domain annotation at 48 hours (Table 5.11), compared to just nine at the one-week timepoint (Table 5.12). At 48 hours, the top 10 genes downregulated in the more virulent isolate compared to the less virulent isolate included three candidate RxLR effectors and two elicitins. The top 10 genes upregulated in the more virulent isolate contained one RxLR effector, one cysteine-rich secretory protein, and two Kazal-type protease inhibitors (Table 5.11). There were fewer DEGs at the one-week timepoint, and most were shared with the 48-hour timepoint (Table 5.12).

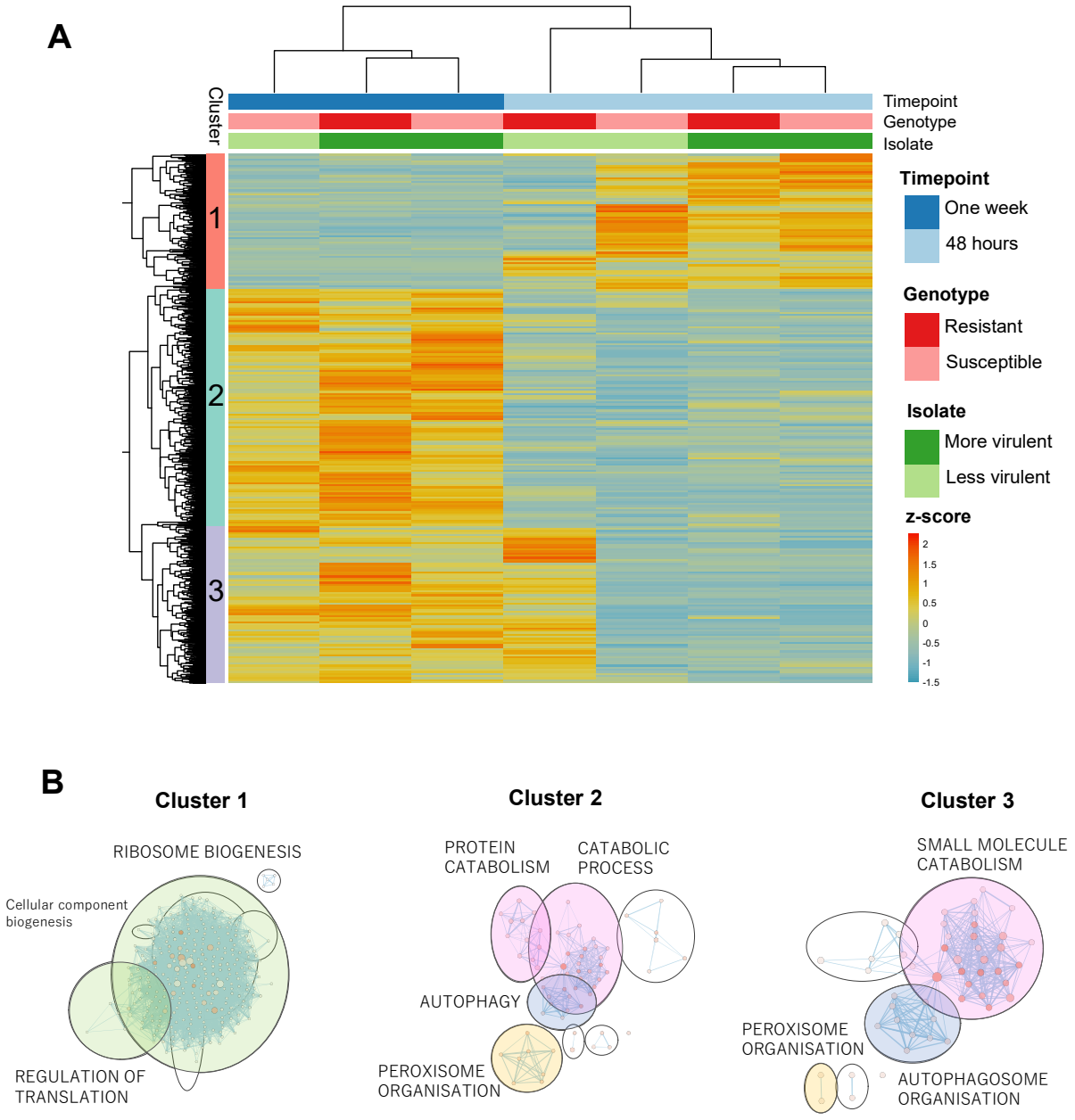

Figure 5.14. A: Heatmap showing expression patterns of DEGs between the timepoints. The less virulent *Phytophthora austrocedri* isolate in the resistant juniper genotype was excluded from the calculation of DEGs but then included in the clustering to assess which timepoint it would cluster with. Genes were grouped into three clusters using the elbow method. B: Gene ontology enrichment of the three clusters identified in A. Clusters have been colour-coded to indicate similarity.

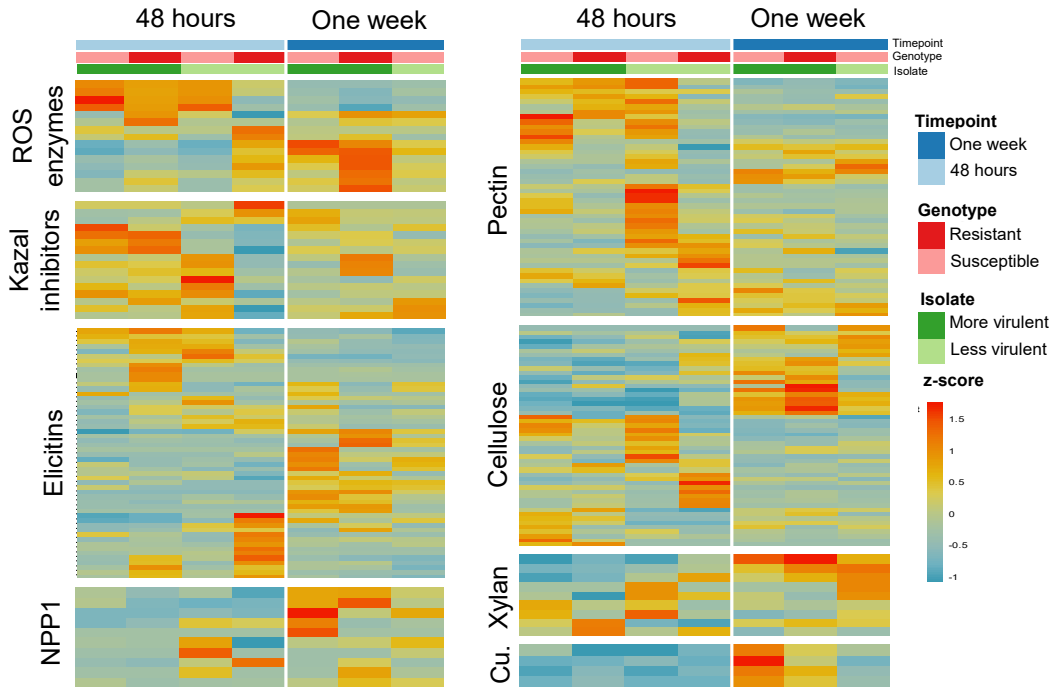

Figure 5.15. Heatmap showing gene expression patterns for categories of proteins likely to be markers of different lifecycle stages (biotrophy vs. necrotrophy). ROS enzymes: Catalase, Copper/zinc superoxide dismutase and Peroxiredoxin. Kazal inhibitors: Kazal-type serine protease inhibitors. NPP1: Necrosis inducing protein. Plant cell-wall degrading activity was classified based on specific enzymes and GO terms. Pectin: *Pectin catabolic process* and *Pectinesterase activity*. Cellulose: *Cellulose catabolic process, Cellulase activity*, and *Cellulose binding*. Xylan: *Xylan catabolic process* and *endo-1,4-beta-xylanase activity*. Cutin: *Cutin hydrolase activity*.

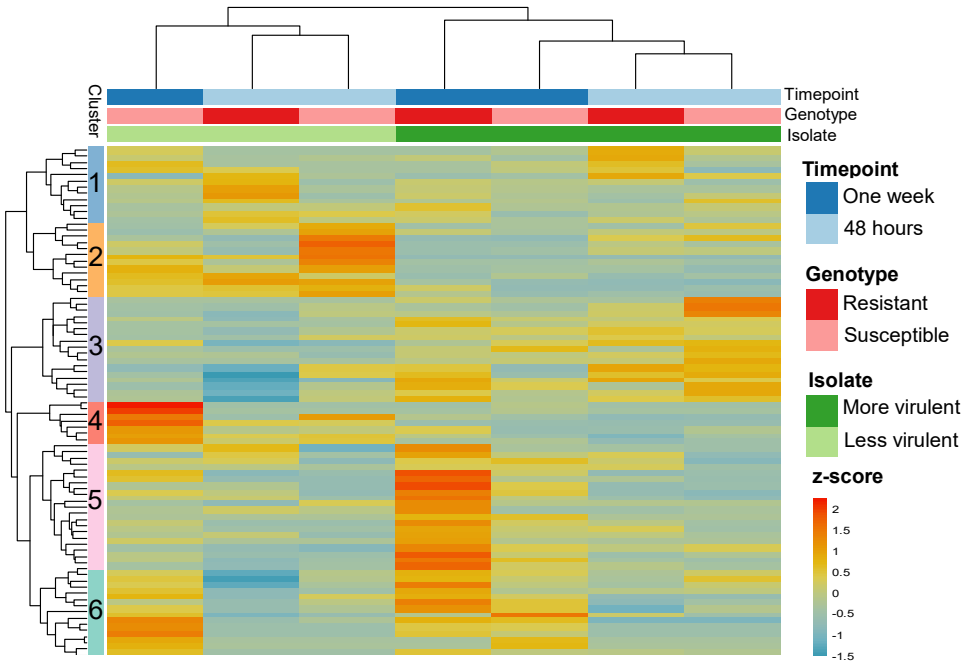

Figure 5.16. Heatmap showing expression patterns of all candidate RxLR effector proteins that had detectable expression *in planta*. Effectors were grouped into six clusters using the elbow method to determine the optimal number of clusters.

Table 5.11. Proposed function based on Interpro protein domains for the top 10 most significantly upregulated and downregulated genes (secretome only) in the more virulent isolate compared to the less virulent isolate of *Phytophthora austrocedri* at 48 hours post-inoculation. All proposed RxLR effector proteins had both the RxLR motif and presence of a signal peptide. *Also upregulated/downregulated at one week.

Domain name	Proposed function	Mean; Log_2-fold change; adjusted p-value	Interpro number
UPREGULATED			
Aldose 1-epimerase*	Carbohydrate metabolism	100; 2.0; $3.0e^{-11}$	IPR008183
Temptin C-terminal*	Unknown	21; 6.1; $6.8e^{-11}$	IPR057626
Kazal-type serine protease inhibitor domain	Serine protease inhibitor	108; 2.2; $1.2e^{-8}$	IPR002350
Kazal-type serine protease inhibitor domain	Serine protease inhibitor	34; 1.8; $4.1e^{-6}$	IPR002350
Cysteine-rich secretory protein family*	Known virulence factors and elicitors	6.3; 4.7; $2.4e^{-5}$	IPR014044
Hsp70 protein	Protein folding	308; 0.88; $5.5e^{-5}$	IPR013126
Protein phosphatase 2C	Protein dephosphorylation	42; 1.5; $1.2e^{-4}$	IPR001932
RxLR phytopathogen effector protein	Known *Phytophthora* effector proteins	71; 1.7; $1.4e^{-4}$	IPR031825
Cytochrome C1 family	Proton transmembrane transport	248; 0.7; $4.0e^{-4}$	IPR002326
Pectate lyase	Enzymatic break-down of plant tissues	211; 1.2; 0.0027	IPR002022
DOWNREGULATED			
RxLR phytopathogen effector protein; WYL domain	Known *Phytophthora* effector proteins	126; -6.7; $4.9e^{-12}$	IPR040691
Elicitin	Known *Phytophthora* elicitor	46; -5.1; $1.6e^{-11}$	IPR002200
Elicitin	Known *Phytophthora* elicitor	193; -3.0 $9.4e^{-11}$	IPR002200
RxLR phytopathogen effector protein	Known *Phytophthora* effector proteins	11; -6.5; $2.2e^{-8}$	IPR031825
Lipase-like, C-terminal domain	Lipid metabolism	72; -2.2; $5.3e^{-5}$	IPR056304
E1-E2 ATPase	Transmembrane transport	41; -1.6; $4.9e^{-4}$	IPR027256
Apoptosis-inducing factor, mitochondrion-associated, C-term*	Involved in inducing programmed cell death	47; -1.2; $5.2e^{-4}$	IPR029324
DnaJ domain	Protein organisation and folding	5.9; -4.0; $5.3e^{-4}$	IPR001623
RxLR phytopathogen effector protein	Known *Phytophthora* effector proteins	74; -1.4; $5.9e^{-4}$	IPR031825
Glycosyl hydrolase family 1	Carbohydrate metabolism	51; -3.7; $8.1e^{-4}$	IPR001360

Table 5.12. Proposed function based on Interpro protein domains for all upregulated and downregulated genes (secretome only) in the more virulent isolate compared to the less virulent isolate of *Phytophthora austrocedri* at one week post-inoculation. All proposed RxLR effector proteins had both the RxLR motif and presence of a signal peptide. *Also upregulated/downregulated at 48 hours.

Domain name	Proposed function	Mean; Log_2-fold change; adjusted p-value	Interpro number
UPREGULATED			
Temptin C-terminal*	Unknown	21; 8.4; $1.2e^{-10}$	IPR057626
Aldose 1-epimerase*	Carbohydrate metabolism	101; 2.0; $1.8e^{-10}$	IPR008183
Cysteine-rich secretory protein family*	Known virulence factors and elicitors	6; 6.1; $7.7e^{-5}$	IPR014044
Alpha/beta hydrolase family	Hydrolytic enzyme	2; 5.6; 0.02	IPR000073
Putative auto-transporter adhesin	Unknown	2; 6.2; 0.03	IPR021255
DOWNREGULATED			
RxLR phytopathogen effector protein*	Known *Phytophthora* effector proteins	11; -6.5; $1.5e^{-9}$	IPR031825
RxLR phytopathogen effector protein; WYL domain*	Known *Phytophthora* effector proteins	126; -6.5; $2.5e^{-8}$	IPR040691
Sodium/hydrogen exchanger, transmembrane	Transmembrane transport of protons and sodium ions	79; -2; 0.0067	IPR006153
Aldose 1-epimerase	Carbohydrate metabolism	47; -1.4; 0.017	IPR008183
RxLR phytopathogen effector protein*	Known *Phytophthora* effector proteins	339; -1.0; 0.017	IPR031825
Apoptosis-inducing factor, mitochondrion-associated, C-term*	Involved in inducing programmed cell death	47; -1.0; 0.026	IPR029324

5.4 Discussion

5.4.1 Overview of the defence response in resistant juniper

The response to inoculation by *P. austrocedri* in resistant juniper at 48 hours was characterised by an upregulation of genes associated with ethylene signalling, secondary metabolite biosynthesis, and the production of pathogenesis-related proteins (Figure 5.6; Table 5.9). Based on gene expression patterns one week post-inoculation, resistant juniper appeared to have successfully suppressed infection by the less virulent isolate, although there was still some defence-related gene expression related to cell-killing processes (Figure 5.7). Conversely, when inoculated with the more virulent isolate, there were a very large number of upregulated genes at the one-week timepoint related to the defence response, including secondary metabolite biosynthesis as well as cell killing, suggesting the infection had not been successfully suppressed in that case.

Ethylene is a major regulator of plant immunity, with well-established roles in defence signalling across many plant hosts, including conifers (Hudgins and Franceschi 2004; Broekaert et al. 2006; Broekgaarden et al. 2015). A key ethylene-mediated defence output is the induction of secondary metabolites (Hudgins and Franceschi 2004; Hudgins et al. 2006). These compounds are an important defence mechanism in plants, acting as inducible chemical defences that have a toxic antimicrobial effect, inhibit pathogen growth, or form physical barriers that prevent pathogen spread (Franceschi et al. 2005; Eyles et al. 2010). Here, juniper showed evidence of biosynthesis of multiple compounds in the phenylpropanoid pathway (including lignan, flavonoids, coumarin and lignin) and several different terpenoids, including monoterpenes and diterpenes.

Ethylene also triggers the synthesis of pathogenesis-related proteins (Broekaert et al. 2006), a diverse group of defence-related proteins that accumulate in plants as a response to pathogen attack or wounding (van Loon et al. 2006; Jain and Khurana 2018). These proteins include chitinases, glucanases, peroxidases and antimicrobial peptides, and are typically secreted into the apoplast where they can directly damage invading pathogens (van Loon et al. 2006). Several pathogenesis-related proteins were identified as likely to be important in the successful defence response in resistant juniper (Table 5.9), including homologs of *Pathogenesis-related thaumatin-like protein 3.8*, *Peroxidase 5* and *Cysteine proteinase RD21A,* the last of which has been shown to be essential for resistance against a necrotrophic pathogen in *Arabidopsis thaliana* (Shindo et al. 2012).

The ethylene/jasmonic acid pathway is classically associated with defence against necrotrophic pathogens, while defence against biotrophic and hemibiotrophic pathogens is usually mediated through the salicylic acid pathway (Bari and Jones 2009; Mengiste and Liao 2025). This generalisation does not always hold true, however, and there are multiple examples of salicylic acid, jasmonic acid and ethylene all playing essential roles in defence against various *Phytophthora* species (Sugano et al. 2013; van den Berg et al. 2018; Fan et al. 2022; Obel et al. 2025). Furthermore, although salicylic acid and jasmonic acid/ethylene signalling are often described as antagonistic (Bari and Jones 2009; Robert-Seilaniantz et al. 2011; Broekgaarden et al. 2015), meaning plants may have to prioritise one pathway over the other, this antagonistic relationship may be absent in gymnosperms (Arnerup et al. 2013). In the present study, there was little evidence of salicylic acid playing a major role, with the defence response to *P. austrocedri* in the resistant juniper genotype apparently mediated through ethylene, at least at the timepoints sampled.

One possibility is that by the first timepoint of 48 hours, *P. austrocedri* had already transitioned into the necrotrophic phase of its lifecycle, meaning any defence response associated with the biotrophic phase may have been missed. The duration of the biotrophic phase in *Phytophthora* varies considerably depending on both host and pathogen species, from less than 24 hours to several days (Jupe et al. 2013; van den Berg et al. 2018; Zuluaga et al. 2016; Fernandes et al. 2024). In this case, the lack of visible lesions at 48 hours combined with pathogen gene expression profiles at the two timepoints suggest *P. austrocedri* may have been in the process of transitioning to the necrotrophic phase by 48 hours (see detailed discussion below). Thus, a greater involvement of salicylic acid at the early stages of infection cannot be ruled out. For example, in avocado infected with *P. cinnamomi,* salicylic acid was upregulated at just 6 hours post-inoculation, and tapered off by 18 hours, after which jasmonic acid-mediated defences predominated (van den Berg et al. 2018). Any similar rapid, transient responses would have been missed in the current study. Finally, it is also possible that salicylic acid may be equally induced by wounding alone. In that case, its contribution to pathogen-specific defence would remain undetected here, as all differential expression was quantified relative to a wounded control.

In a previous study on this pathosystem, the resistant juniper genotype was able to fully control infection by even the more virulent isolate of *P. austrocedri* (Green et al. 2020). Here, the resistant genotype was not able to suppress infection by the more virulent isolate, at least

within the timeframe of the study, as many pathogen transcripts were recovered at one week (demonstrating the infection was still active) and clear lesions were visible at the three-week timepoint (Figure 5.1). This discrepancy may be attributable to the inoculation process used in this study, where each plant was inoculated in three locations along the stem, meaning each plant received a very strong pathogen load. Moreover, the sequential harvesting of inoculation points would have imposed additional stress on the plants, and could have provided an entryway for opportunistic pathogens. Resistance and susceptibility in plants is known to be affected by drought and other stressors (Desprez-Loustau et al. 2006; Bostock et al. 2014), which may explain why in this study the resistant genotype only successfully controlled the infection in the case of the less virulent *P. austrocedri* isolate.

5.4.2 Contrasting the defence response in resistant versus susceptible juniper

A striking difference between the two genotypes was the timing of their defence response. The resistant genotype responded more rapidly to inoculation than the susceptible genotype, activating the ethylene signalling pathway before the susceptible genotype showed any sign of having detected an infection (Figure 5.6). Furthermore, many of the genes upregulated early (48-hour timepoint) in the resistant genotype were subsequently expressed at high levels in the susceptible genotype (Figure 5.8), again suggesting that the timing of defence activation may determine the eventual outcome. Rapid expression of defence genes in response to pathogen infection has previously been associated with enhanced resistance (Glazebrook 2005; Bari and Jones 2009), and the results presented here suggest that an early activation of the defence response is likely critical for effective resistance to *P. austrocedri*.

One way to achieve a rapid response to infection is through efficient pathogen detection. Plants recognise pathogens through transmembrane proteins that recognise PAMPs, or through intracellular receptors that recognise effectors (Jones and Dangl 2006). One of the candidate genes identified as likely important in successful suppression of the infection in this case was a probable LRR receptor-like serine/threonine-protein kinase, a transmembrane protein which could be involved in the recognition of *P. austrocedri* as a pattern-recognition receptor (Table 5.9; Figure 5.9). Although not generally considered classic R genes, pattern-recognition receptors are nevertheless important triggers of immunity, and have been shown to be important in determining levels of resistance to *Phytophthora* (e.g., Albert et al. 2015; Du et al. 2015; Wang et al. 2018; Kato et al. 2022) and to many other pathogens (Ngou et al. 2022).

Thus, this receptor could be a crucial determinant of resistance to *P. austrocedri* in juniper. However, further studies would be needed to validate this result.

Early detection was not the only difference between the two genotypes in their response to *P. austrocedri*. At one week post-inoculation, the resistant genotype maintained a stronger defence response to the more virulent isolate, despite not having successfully suppressed the infection (Figure 5.7). In contrast, the susceptible genotype showed a markedly attenuated response, with fewer upregulated genes and fewer defence-related GO terms. Possibly the more efficient detection of *P. austrocedri* in the resistant genotype continues to stimulate a stronger defence response over time.

Finally, there were many defence-related GO terms enriched in all comparisons between resistant and susceptible genotypes, including comparisons between mock-inoculated controls. This shows that there are fundamental differences in how the two genotypes respond to wounding (and/or opportunistic pathogens), as well as in how they respond to infection with *P. austrocedri* in particular. The susceptible genotype could generally be more susceptible to all pathogens, as fitness costs associated with investment in resistance in the absence of pathogens should select for different optimal levels of investment depending on local conditions (Purrington 2000; Cipollini et al. 2014). However, the presence of defence-related GO terms among both upregulated and downregulated genes between the two genotypes suggests a more qualitative difference in the defence response. For example, several GO terms related to salicylic acid were enriched in genes downregulated in the resistant genotype compared to the susceptible genotype at 48 hours. Thus, it is also possible that the susceptible genotype, whilst vulnerable to *P. austrocedri*, may have effective resistance mechanisms to other pests or pathogens.

5.4.3 Overview of pathogenicity and virulence in *Phytophthora austrocedri*

The number of candidate RxLR effector proteins identified in the *P. austrocedri* genome (118 in total) was modest compared with reports from other *Phytophthora* species, which typically reach multiple hundreds (e.g., Haas et al. 2009; Morales-Cruz et al. 2020; Lee et al. 2021). Expression patterns of these effectors differed markedly between *in planta* samples and cultures, and these differences were largely shared between the two *P. austrocedri* isolates and timepoints, underlining the importance of these proteins for *in planta* growth (Figure 5.13). Other genes upregulated *in planta* compared to in culture at both timepoints included plant

cell wall degrading enzymes, which play a key role in pathogenicity during necrotrophy (Mengiste 2012), and genes involved in responding to oxidative stress, likely due to the accumulation of ROS as part of the plant's defence response.

An interesting insight into *P. austrocedri*'s ability to cause disease comes from the evidence for suppression of defence-related response pathways in the host, as many enriched GO terms in downregulated genes in inoculated juniper samples were related to the defence response (Figure 5.7). The effect was greater in the susceptible genotype compared to the resistant genotype, suggesting the resistant genotype can mitigate this effect to some extent. Pathogen effector proteins are known to disrupt the host's defence response by interfering with signalling, inhibiting enzymes, manipulating key immune regulators, or otherwise disrupting diverse plant cell processes (Naveed et al. 2020; Wang et al. 2023). For example, in *P. sojae* an RxLR effector binds an enzyme involved in ethylene signalling and attenuates host defence (Yang et al. 2019). Pathogens can also suppress the host's immune response through RNA silencing, using small RNAs derived from transposable elements (Weiberg et al. 2013). Interestingly, in this study 50-80% of all *P. austrocedri* reads captured from *in planta* samples mapped to repetitive genomic regions, compared to only 2-3% of reads from cultures. Thus, *P. austrocedri* is probably using effector proteins, and possibly using transposable element-derived RNA, to suppress juniper's defence response very effectively, particularly in the case of the susceptible genotype.

The two timepoints captured in this study showed distinct gene expression patterns (Figure 5.14), which may be indicative of different lifecycle stages in the pathogen (biotrophy versus necrotrophy). At the 48-hour timepoint, *P. austrocedri* showed elevated expression of genes involved in protein biosynthesis, which has previously been associated with early infection stages (Ah-Fong et al. 2017) and may therefore relate to biotrophy. Conversely, upregulated genes at the one-week timepoint related to catabolism, autophagy and oxidative stress, which are more likely to relate to necrotrophy. When focusing on specific protein classes expressed *in planta* (Figure 5.15), the 48-hour timepoint was more associated with Kazal-type protease inhibitors, which have previously been associated with biotrophy (Zuluaga et al. 2016), while the one-week timepoint was more associated with necrosis-inducing proteins, which would be expected to be upregulated during the necrotrophic phase of the lifecycle (Zuluaga et al. 2016; Midgley et al. 2022).

However, both timepoints showed evidence of cell-wall degrading enzymes, despite these being associated with the necrotrophic phase (Zuluaga et al. 2016). The 48-hour timepoint had higher expression of enzymes targeting pectin, while enzymes targeting cellulose and xylan were expressed at similar levels at both timepoints (Figure 5.15). A similar earlier peak in expression of pectinases was reported in *P. parasitica* infecting lupin (Blackman et al. 2015), suggesting there may be an ordered sequence of events during the degradation of the complex carbohydrates that make up plant cell walls. Taken together, these findings indicate that the 48-hour timepoint likely reflects an intermediate stage in which *P. austrocedri* is in the process of transitioning from biotrophy to necrotrophy.

5.4.4 Key differences between the more virulent and the less virulent *Phytophthora austrocedri* isolate

The difference in virulence between the two *P. austrocedri* isolates appears to be driven by the more rapid defence response triggered by the less virulent isolate compared to the more virulent isolate (Figure 5.6). One explanation for this is that the less virulent isolate is detected earlier and more effectively than the more virulent isolate. This would suggest that the less virulent isolate is producing elicitors or effectors that are triggering the immune response, and that are not produced or produced at lower levels in the more virulent isolate. Alternatively, the more virulent isolate may be better able to suppress the defence response in juniper. In this case, the more virulent isolate would be secreting effector proteins that are not produced or produced at lower levels in the less virulent isolate.

Supporting the former explanation, there were three RxLR proteins and two elicitins significantly downregulated in the more virulent isolate compared to the less virulent isolate at 48 hours (Table 5.11). Elicitins are *Phytophthora*-specific proteins that are known to act as defence elicitors (Derevnina et al. 2016). These elicitins could, therefore, be triggering the earlier immune activation by the less virulent isolate. On the other hand, genes upregulated in the more virulent isolate included one RxLR effector protein, a cysteine-rich secretory protein (known virulence factors; Chen et al. 2016; Lin et al. 2020), and two Kazal-type protease inhibitors. Kazal inhibitors have been detected in other *Phytophthora* species (Tian et al. 2004; Zuluaga et al. 2016), and are thought to disrupt proteases, which are key components of the plant defence response (Boevink et al. 2020). For example, in *P. infestans*, Kazal-type protease inhibitors target pathogenesis-related proteases in tomato (Tian et al. 2004; Tian et al. 2005). Together, these patterns suggest that both mechanisms may be operating simultaneously,

meaning the less virulent isolate is more easily detected and the more virulent isolate is better able to interfere with the host's defence response.

Another interesting difference between the isolates concerns the possible earlier transition out of biotrophy in the case of the less virulent isolate in the resistant genotype, based on this group's distinct gene expression pattern at 48 hours that appeared to be halfway between the other treatment groups at 48 hours and all treatment groups at one week (Table 5.10; Figure 5.14). This seems to mostly be a host genotype-dependent effect, with little evidence of a similar early transition in the susceptible genotype. Thus, it could be that earlier detection of the pathogen in the resistant juniper genotype is driving a more rapid transition out of the biotrophic phase. On the other hand, the less virulent isolate did have higher expression of necrosis-inducing proteins at 48 hours compared to the more virulent isolate in both genotypes (Figure 5.15), which may indicate a more general difference in the length of the biotrophic phase between the two isolates. In *P. infestans*, isolates specialised on tomato have a longer biotrophic phase on their preferred host (Smart et al. 2003), and an extended biotrophic phase has also been correlated with greater virulence in potato (Cooke et al. 2012). Thus, it could be that the ability to evade detection and suppress the host defence response long enough to have a more prolonged biotrophic phase may be an important determinant of virulence in *P. austrocedri* as well as other *Phytophthora* species.

5.4.5 Conclusion: is resistance to *Phytophthora austrocedri* in juniper governed by an R gene?

Based on the results of this study, resistance to *P. austrocedri* in juniper arises when there is rapid detection of the pathogen followed by a strong sustained defence response mediated through the jasmonic acid/ethylene pathway, resulting in the upregulation of secondary metabolites and pathogenesis-related proteins. Rapid detection of the pathogen appears to be affected by both pathogen properties (likely the expression of certain effector proteins and/or elicitins) as well as host properties (possibly the presence of a particular LRR receptor-like kinase), resulting in a genotype-by-genotype interaction that determines the eventual outcome (resistance or susceptibility). We cannot rule out an earlier response to the biotrophic phase of the pathogen's lifecycle mediated through salicylic acid, if this occurred prior to the 48-hour timepoint; however, if present, this response would not have effectively suppressed the pathogen, as even the less virulent isolate appeared to transition to necrotrophy and caused a strong ethylene-mediated response in the resistant host.

Previous work has demonstrated both quantitative and qualitative resistance to *P. austrocedri* in juniper (Green et al. 2020; Chapter 2 of this thesis), suggesting that qualitative resistance in juniper could be mediated by an R gene. By the strictest definition, R gene-based resistance would involve intracellular detection of pathogen effectors followed by rapid onset of programmed cell death, effectively targeting the biotrophic phase of the pathogen's lifecycle and causing an incompatible reaction (Nimchuck et al. 2003). The results presented here are more supportive of qualitative resistance in juniper being driven by a threshold effect, where given the right combination of pathogen genotype and host genotype, the defence response is initiated early enough and is strong enough to effectively suppress the pathogen, despite entering the necrotrophic phase of its lifecycle. In this case, it would suggest resistance is driven by a particularly strong response to PAMPs (pattern-driven immunity), rather than by a specific effector-R gene combination. The identification of a probable transmembrane LRR receptor-like kinase among upregulated genes in the resistant genotype provides further support to this conclusion.

However, not all authors use this strict definition of an R gene. Transmembrane pattern-recognition receptors are sometimes considered to be a subclass of R gene (Agrios 2005; Kourelis and van der Hoorn 2018; Zhang et al. 2022), and some have argued that resistance is better seen as a continuum between pattern-triggered immunity and effector-triggered immunity (Thomma et al. 2011; Naveed et al. 2020). Moreover, it is certainly the case that genes other than classic intracellular R genes can have very large phenotypic effects on levels of resistance. Thus, regardless of the exact definition used, this study has identified candidate genes on both sides of the host-pathogen interaction that should be pursued as key drivers of virulence in the pathogen and of resistance in the plant host. These loci represent promising targets for functional validation, and may ultimately contribute to the development of more informed pathogen management strategies by identifying host genes that could be prioritised in breeding programmes and pathogen genes that could be monitored as markers of virulence.

CHAPTER 6:
Discussion

In this thesis, I used diverse methods to investigate the ecological genetics of the invasive tree pathogen *Phytophthora austrocedri* and its host juniper. Below, I synthesise the key findings from the preceding chapters and discuss their implications within the broader context of the evolutionary dynamics that shape plant-pathogen interactions.

6.1 Qualitative resistance as a threshold effect and implications for durability

The work presented here has substantially advanced our understanding of resistance to *P. austrocedri* in juniper, and we can now begin to build a conceptual model of the underlying processes. Firstly, in Chapter 2, I demonstrated that juniper populations harbour heritable genetic variation in disease resistance, and exhibit both quantitative and qualitative phenotypic variation in resistance, with some individuals showing complete absence of lesion development following inoculation. However, this analysis could not reveal the genetic basis of qualitative resistance, which could be driven by the effect of a major gene or by a threshold effect involving the cumulative action of many genes.

In Chapter 5, I identified a candidate gene potentially underpinning resistance in a resistant juniper genotype: an LRR receptor-like kinase that is likely functioning as a pattern-recognition receptor. According to current models of plant immunity, such receptors activate mitogen-activated protein kinase signalling cascades, which in turn trigger downstream defence responses to suppress infection. As a transmembrane receptor, this pattern-recognition receptor is expected to recognise conserved pathogen-associated molecular patterns (PAMPs) rather than specific pathogen effector proteins. Thus, while this gene may play an important role in resistance and could have a major effect, it does not represent a classic intracellular R gene.

Both effector-triggered immunity mediated by intracellular R genes and pattern-triggered immunity mediated by transmembrane receptors can produce qualitative (complete) resistance, and the distinction between them is increasingly seen as a continuum (Thomma et al. 2011; Naveed et al. 2020). However, although both types of immunity share many of the same signalling pathways, pattern-triggered immunity is generally a slower, more transient,

and less robust response compared to effector-triggered immunity. This difference might be particularly relevant in interactions with hemibiotrophic pathogens like *Phytophthora*, where R-gene resistance should effectively target the biotrophic phase of the lifecycle and prevent the transition to necrotrophy. For example, R-gene resistance to *P. infestans* can confine the pathogen so rapidly that it results in the death of just a few host cells (Vleeshouwers et al. 2000). In contrast, in Chapter 5, there was evidence of a transition to necrotrophy in both resistant and susceptible juniper genotypes. This is an important distinction, because once the pathogen enters the necrotrophic phase, programmed cell death is likely to be ineffective (Mengiste 2012) and the infection may become harder to control.

In Chapter 5, the resistant genotype did not display complete resistance to the more virulent pathogen isolate, despite this same genotype previously showing complete resistance to the same isolate (Green et al. 2020). I believe the discrepancy is likely due to differences in the inoculation procedure. Instead of inoculating each plant in one location at the stem base, in Chapter 5 each plant received three inoculations along the stem, which were harvested sequentially, likely imposing cumulative stress on the plants, including drought stress. Thus, resistance to *P. austrocedri* in juniper appears to be influenced to some extent by abiotic stress and/or pathogen load. Although R-gene immunity can also be impacted by environmental stressors (Velásquez et al. 2018), pattern-triggered immunity is generally considered to be less robust to perturbation (Tsuda and Katagiri 2010), and is therefore likely to be more sensitive to environmental variability. The extent to which natural environmental variation would affect resistance to *P. austrocedri* in juniper remains unknown, but could have a significant impact on the estimates of heritability reported in Chapter 2.

Chapter 2 demonstrated there was a significant genotype-by-genotype (GxG) interaction between juniper and *P. austrocedri*. Interestingly, isolates that were less virulent on average sometimes caused the largest lesions on more susceptible genotypes. This reversal of virulence levels was not observed in Chapter 5, where the more virulent isolate consistently produced larger lesions on both host genotypes. However, a GxG interaction was still observed, as the resistant genotype was able to suppress infection in the case of the less virulent isolate, but not in the case of the more virulent isolate. GxG interactions are expected if resistance is mediated by an R gene (gene-for-gene model; Flor 1971), but have also been observed in partial or quantitative resistance (Darvishzadeh et al. 2007; Capador-Barreto et al. 2025). In this case, based on the results of Chapter 5, the GxG interaction may depend on the presence of a

specific pattern-recognition receptor in the host and on the timing or levels of expression of elicitors in the pathogen.

Overall, the combined results from Chapter 2 and Chapter 5 suggest that qualitative resistance to *P. austrocedri* in juniper arises from a threshold effect, in which multiple host and pathogen factors collectively contribute to a defence response that, in some cases, reaches a critical threshold of timing and intensity sufficient to control the infection and result in complete resistance (Figure 6.1). This interpretation aligns with the view that the distinction between qualitative and quantitative resistance represents a continuum rather than a strict dichotomy, as the mechanisms underlying both types of resistance can be largely shared. Importantly, a threshold effect does not preclude the involvement of major-effect genes that are essential for resistance. For example, the specific pattern-recognition receptor identified in Chapter 5 may be necessary, but not on its own sufficient, to confer complete resistance.

The term "threshold effect" is not widely used in plant resistance literature, outside of the specific context of quantitative genetics, where a threshold model underlies the classical mathematical basis for estimating the heritability of qualitative traits (Falconer and Mackay 1996). Nevertheless, numerous studies have shown how variation in factors such as pathogen load, receptor sensitivity, environmental conditions, or number of defence-associated quantitative trait loci determine the severity of disease and overall outcome of infection (e.g., Landa et al. 2001; Bostock et al. 2014; Fukuoka et al. 2015; Chatterton et al. 2023; Hudson et al. 2024). Thus, the proposed threshold model of resistance (Figure 6.1) represents a conceptual synthesis of these well-established functional observations, providing a framework for understanding how multiple interacting quantitative factors can give rise to apparently qualitative outcomes.

The next critical question concerns the long-term evolutionary trajectory of the interaction. Within the co-evolutionary arms race between plant and pathogen described by the zig-zag model of plant immunity (Jones and Dangl 2006), the juniper-*P. austrocedri* pathosystem appears to be in the first "zag" stage (Figure 6.2): there is pattern-triggered immunity that, in some host genotypes, can confer complete resistance, but which may be partially suppressed by certain pathogen isolates with more effective effector protein repertoires. Continued pathogen adaptation could further enhance its ability to suppress host defences; conversely, juniper populations may harbour standing genetic variation that could give rise to R-gene-mediated resistance in response to selection imposed by *P. austrocedri*.

The long-term outcome of this interaction will thus depend on the evolutionary potential of both host and pathogen (Figure 6.2). By making use of our understanding of the eco-evolutionary factors at play, we can aim to enhance the evolutionary potential of juniper while limiting that of *P. austrocedri* (Figure 6.2), improving the likelihood that the juniper-*P. austrocedri* interaction can develop into a dynamically stable co-evolutionary relationship akin to those observed in long-term native plant-pathogen associations.

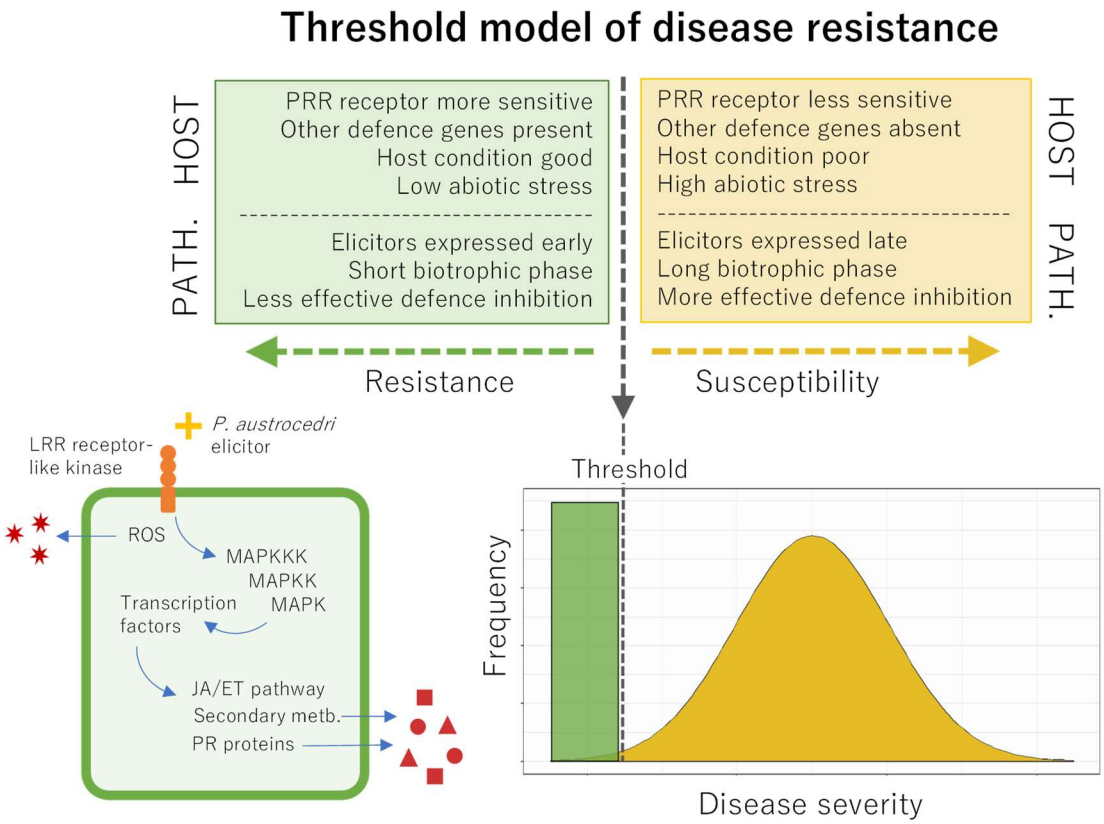

Figure 6.1. Visual representation of a threshold model of disease resistance, where multiple factors on both side of the host-pathogen interaction combine to determine the outcome of infection. When there are sufficient factors favouring resistance over susceptibility, a threshold is reached allowing complete (qualitative) resistance. Below on the left: visual representation of the molecular basis of resistance to *Phytophthora austrocedri* in juniper. A pattern-recognition receptor may play an important role, but is not sufficient to always provide qualitative resistance without the involvement of other factors. PRR: pattern-recognition receptor. LRR: leucine-rich repeat. ROS: reactive oxygen species. MAPK: mitogen-activated protein kinase. JA: jasmonic acid. ET: ethylene. PR: pathogenesis-related.

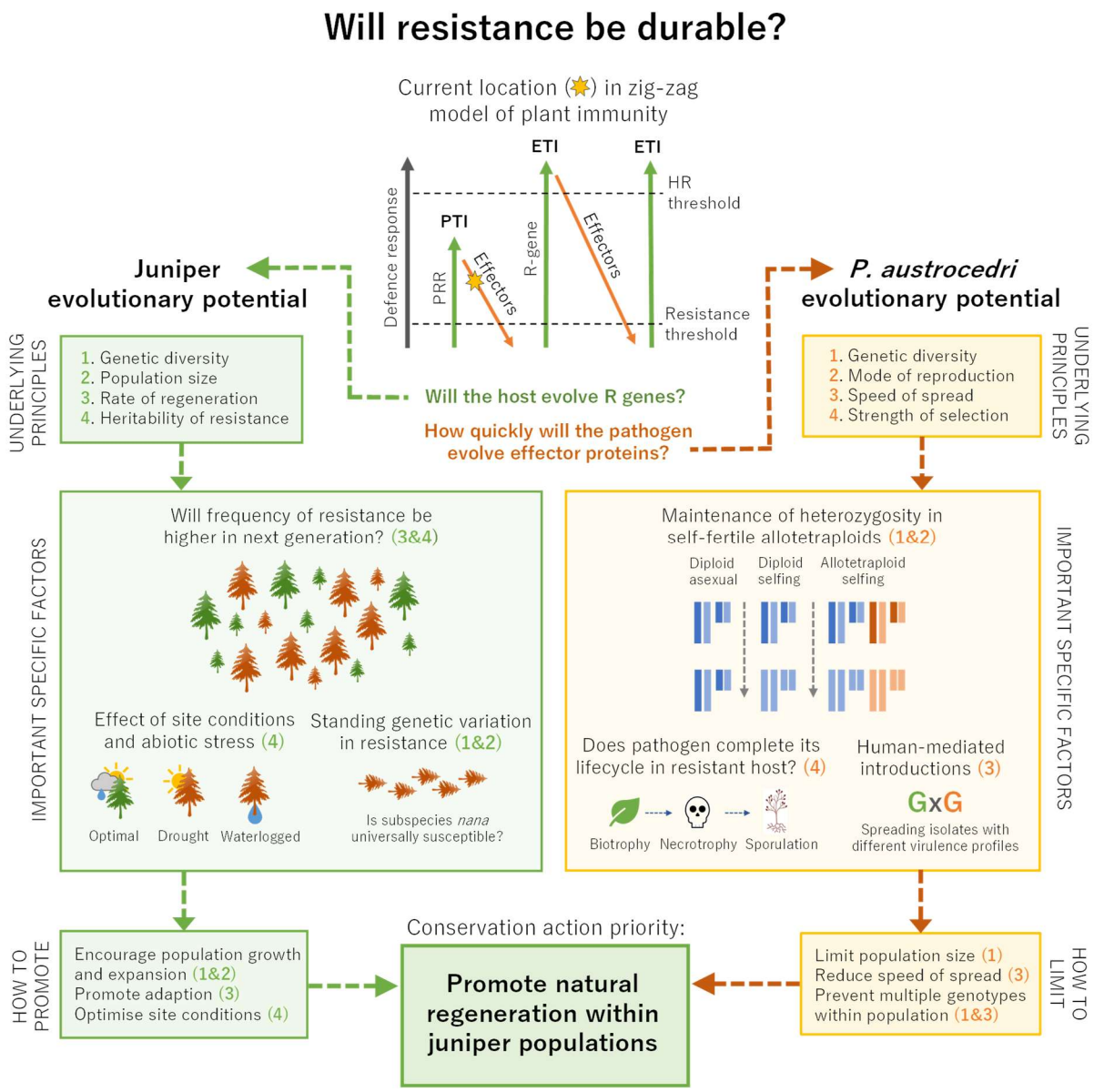

Figure 6.2. A visual depiction of where the juniper-*Phytophthora austrocedri* pathosystem is currently positioned in the zig-zag model of plant immunity, and a summary of the factors influencing the evolutionary potential of host and pathogen that may determine the eventual outcome of this interaction. Top boxes: fundamental factors governing evolutionary potential. Middle boxes: Some specific examples of these factors in the juniper-*P. austrocedri* pathosystem. Lower boxes: how to promote or limit evolutionary potential based on these principles. PRR: pattern-recognition receptor. PTI: pattern-triggered immunity, mediated through a PRR. ETI: effector-triggered immunity, mediated through an R gene. HR: hypersensitive response.

6.2 Allopolyploidy as a long-term strategy for invasive *Phytophthora*

In Chapter 3 and Chapter 4, I explored the genomics of *P. austrocedri*, demonstrating that it is a hybrid tetraploid that forms two genetically diverged lineages. Both polyploidy and hybridisation are increasingly recognised to play an important role in *Phytophthora* evolution (Bertier et al. 2013; Van Poucke et al. 2021), and many studies emphasise the dynamic, unstable nature of these genomes. Consistent with this, in Chapter 4 I found evidence of diploidisation and triploidisation occurring in some *P. austrocedri* isolates. However, I also showed that the hybridisation event very likely predates the divergence between the two geographical lineages.

A rough, back-of-the-envelope calculation based on the estimated average substitution rate for mitochondrial DNA for *P. infestans* (2.4×10^{-6} substitutions per site per year) suggests that the two *P. austrocedri* lineages diverged ~4,800 years ago, based on the ~2.3% divergence between mitogenomes. Although this estimate carries substantial uncertainty – both from molecular clock calibration error, as well as from the possibility that the two lineages inherited different mitochondrial haplotypes following hybridisation (e.g., Donahoo and Lamour 2008) – evidence from the nuclear genome supports the idea that the lineages are significantly diverged, and considerable time must therefore have elapsed since the split. Because most *P. austrocedri* isolates remain fully tetraploid, this implies that hybrid tetraploidy can be stably maintained in *Phytophthora* over thousands of years.

In Chapter 4, I proposed that allopolyploidy may represent a particularly advantageous strategy for invasive *Phytophthora*. Hybridisation brings together divergent lineages into a single genome, increasing genetic diversity and potentially expanding the repertoire of effector proteins. Subsequently, repeated rounds of self-fertilisation would reduce within-subgenome heterozygosity to very low levels, but between-subgenome heterozygosity could be maintained (assuming pairing of homologous chromosomes occurs within, rather than between, subgenomes). The long-term result would become similar to clonal reproduction (Figure 6.2): once within-subgenome heterozygosity has been reduced to negligible levels, recombination becomes ineffective, and lineages would replicate genetically identical copies of themselves, maintaining the same levels of heterozygosity. Thus, this strategy does not provide the benefits of sexual reproduction (such as the creation of novel allele combinations or enhanced efficacy of selection), but does preserve the between-subgenome diversity and

adaptive potential captured in the hybrid genome. For *Phytophthora* species, this strategy carries the added advantage of achieving this outcome while making use of longer-lived, resilient oospores. By allowing higher levels of genetic diversity to be captured in resilient, sexual oospores, allotetraploidy could therefore be a force driving increased invasiveness in *Phytophthora* species.

6.3 Population structure of *Phytophthora austrocedri* in the UK

The analysis of *P. austrocedri* genetic diversity and population structure within the UK was constrained in this thesis by the limited sample size of *P. austrocedri* isolates, a reflection of the difficulty of isolating this pathogen from the field. Nevertheless, Chapter 4 does provide some insight into *P. austrocedri*'s population history in the UK that can be used to understand how best to manage pathogen impact.

In particular, there are two aspects to the genetic clustering of UK isolates that have important management implications. First, most UK isolates showed strong genetic clustering by population of origin. This is not always the case for *Phytophthora* species, where clonal reproduction can lead to the emergence of distinct genotypes that do not always reflect geographical patterns (e.g., Schoebel et al. 2014; Mullet et al. 2024). In fact, *P. austrocedri* isolates from Argentina showed no clustering by population of origin. Second, there was no signal of time in the genetic clustering, as isolates were collected over a ten-year period yet remained closely grouped by population of origin. Together, these results suggest that *P. austrocedri* is not spreading rapidly between UK populations. This is consistent with its biology as a soil- and water-borne pathogen, which will limit its dispersal ability compared to aerially dispersing pathogens.

One mechanism by which *P. austrocedri* may be introduced into new populations is through the movement of nursery-grown plants, which is a known phytosanitary risk (Prigigallo et al. 2015; Green et al. 2025). Indeed, previous work has associated the presence of *P. austrocedri* in UK juniper populations with the extent of local planting activity (Donald et al. 2021). This may explain the single observed exception to the population-based clustering, where an isolate from Durham grouped genetically with Grampian isolates. The population of origin in Durham is a site that has undergone extensive juniper planting as part of restoration efforts, which could plausibly have facilitated the introduction of multiple pathogen genotypes. Although direct movement of inoculum between the two populations cannot be ruled out, the large geographical separation between them, lack of evidence for other long-

distance dispersal events and the high level of planting activity at the Durham site all support the interpretation that this represents a planting-mediated introduction.

6.4 Management recommendations for the conservation of juniper

Overall, the findings presented in this thesis demonstrate that although UK juniper populations are vulnerable and require active conservation, there is still cause for optimism. Juniper has substantial genetic variation in resistance to *P. austrocedri*, and resistance is present in most populations sampled. Moreover, evidence of natural selection acting in populations exposed to *P. austrocedri* suggests that resistance observed under controlled inoculation experiments can be translated into genuine adaptive responses in the field. The key to effective juniper conservation will be to apply insights from the evolutionary-ecology of host-pathogen interactions to enhance the evolutionary potential of juniper while constraining that of the pathogen (Figure 6.2). To achieve this, I propose the following management recommendations:

1) Encourage natural regeneration within juniper populations

Genetic variation in resistance to *P. austrocedri* provides the raw material for adaptation. However, many juniper populations in the UK exhibit very low rates of natural regeneration (Thomas et al. 2007; Broome et al. 2017). This is a major cause for concern, as an adaptive response depends on the establishment of young juniper seedlings representing the next generation.

Juniper is a pioneer species, requiring disturbed, open ground for seed germination and establishment. Disturbance to create bare ground must, however, be followed by a prolonged period of low disturbance to allow seedlings to establish (Plantlife 2011). A review of management interventions in north-western Europe concluded that low-impact ground disturbance (e.g., scarification or turf stripping) promoted juniper regeneration, competition and shading from surrounding vegetation limited seedling emergence, and the effect of grazing was variable (Broome et al. 2017). Unfortunately, a study documenting attempts to implement these strategies in the UK yielded largely negative results, and suggested the effectiveness of management strategies would depend strongly on local site conditions (Broome et al. 2017). However, a trial using scrapes sown with locally collected juniper seeds in southern England has yielded some positive results (Reading & District Natural History Society 2023). Continuing to develop and implement effective strategies to enhance natural

regeneration in juniper, tailored to local site conditions, should be considered a top priority to conserve UK juniper.

2) Avoid supplemental planting

Despite the appeal of using resistant juniper genotypes for restocking, supplemental planting poses significant phytosanitary risks. This remains true even in populations already exposed to the pathogen, as the significant genotype-by-genotype interaction between *P. austrocedri* and juniper means that the introduction of a different pathogen genotype could alter local disease dynamics and erode existing resistance.

Plant nurseries are known to pose a major phytosanitary risk (Prigigallo et al. 2015; Green et al. 2025), and any situation that involves moving plants from one location to another carries the risk of moving pathogens at the same time. This mode of introduction is particularly relevant in the case of pathogens like *P. austrocedri*, which are soil and water-borne, and therefore have limited innate dispersal ability. Overall, the risk of introducing and spreading the pathogen outweighs the benefit of supplemental planting. Conservation efforts should therefore prioritise *in situ* regeneration and containment, rather than translocation or planting.

3) Continue to emphasise phytosanitary risk

Preventing further spread of *P. austrocedri* remains critical, even in regions where the pathogen is already present, because pathogen genotypes differ in their virulence profiles. Communication and outreach should continue to emphasise best-practice hygiene measures to limit soil and water movement between sites. A particularly important case is the subspecies *J. communis* ssp. *nana* on the Isle of Arran, which showed uniform high susceptibility to *P. austrocedri*. Currently, there is no evidence of *P. austrocedri* presence on the island, and protecting this pathogen-free status should be a local management priority, supported by targeted awareness campaigns and restrictions on the movement of nursery material.

4) Consider site conditions influencing host health and pathogen load

Even when resistance is present, its effectiveness may be impacted by environmental conditions (e.g., abiotic stress) and pathogen load. *Phytophthora austrocedri* has been shown to be more likely to infect juniper in wetter microsites (Donald et al. 2020), where high soil moisture favours pathogen survival and zoospore dispersal. Management and regeneration efforts should therefore prioritise drier microsites and areas offering optimal conditions for

juniper growth, helping to minimise environmental stress and limit pathogen load. Creating environments that support host vigour while reducing pathogen activity is essential to ensure that any genetic resistance present in juniper populations is effectively expressed and delivers meaningful protection in the field.

6.5 Limitations and future work

There are several important outstanding questions arising from the findings presented in this thesis. In Chapter 2, I showed that juniper populations already exposed to *P. austrocedri* had a higher frequency of resistant individuals, suggesting natural selection is acting on resistance traits. However, this alone does not demonstrate that adaptation is occurring, which would require evidence of a shift in allele frequencies across generations due to differential reproductive success. A logical next step would therefore be to assess the frequency of disease resistance in young juniper in exposed populations, and compare frequencies across age cohorts. Any age-associated increase in frequency of resistance could, however, also reflect higher mortality among susceptible seedlings. It could be possible to incorporate information on potential fecundity (e.g., seed cone count) to strengthen evidence for differential reproductive success (see Semizer-Cuming et al. 2019), but realised fecundity would be difficult to measure without also including the effect of selection in exposed sites. Ultimately, demonstrating true adaptation is inherently challenging in long-lived species such as trees. However, even finding evidence that young, regenerating juniper exhibit higher frequencies of resistance would be a valuable and encouraging finding.

Another major avenue for future work concerns the candidate pattern-recognition receptor identified in Chapter 5 as potentially being important for disease resistance in juniper. Validating the role of this gene across a broader set of host genotypes is essential, as the analysis presented in this thesis was based on only one resistant and one susceptible genotype. Developing a qPCR-based assay to quantify gene expression during infection would allow a targeted screening trial to determine whether this particular pattern-recognition receptor is necessary and/or sufficient for effective defence against *P. austrocedri*.

Chapter 3 and Chapter 4 established that *P. austrocedri* is a hybrid tetraploid, with evidence of large-scale deletions and duplications and overall low levels of genetic diversity. However, the relationship between these genomic features and the functional characterisation of gene content remains unexplored. Future work should therefore integrate knowledge of genome structure, ploidy and diversity with insights gained from Chapter 5 on virulence-

associated genes. A comparative approach could also be used to examine the extent to which effector gene content varies among isolates, adding to our understanding of the likely drivers of variation in virulence identified in Chapter 5. Lastly, assessing whether one subgenome shows consistently higher gene expression (indicative of subgenome dominance; Bird et al. 2018) would also shed light on the evolutionary dynamics of *P. austrocedri*'s hybrid genome.

Finally, the observation in Chapter 5 that a longer biotrophic phase may be associated with increased virulence merits further investigation. Microscopy-based analyses could enable direct comparisons of the duration of the biotrophic phase among isolates with differing levels of virulence, and between resistant and susceptible host genotypes. Determining whether more resistant hosts trigger an earlier transition to necrotrophy would provide valuable insight into how host resistance shapes pathogen infection strategy, and could contribute to a general understanding of important drivers of virulence in *Phytophthora*.

6.6 Conclusion

In summary, this thesis highlights the value of taking an integrated approach to understanding novel plant-pathogen interactions. I have substantially advanced our understanding of the juniper-*P. austrocedri* pathosystem, providing a foundation for evidence-based conservation of juniper. More broadly, by combining insights gained from quantitative genetic analysis of the host, genomic analysis of the pathogen, and molecular analysis of their interaction, I have provided a unique perspective on the evolutionary forces shaping disease resistance in novel hosts and virulence in invasive pathogens. I hope this work will encourage future research to adopt a similarly integrated approach, advancing our understanding of emerging pathosystems and strengthening our capacity to mitigate their substantial economic and ecological impacts.

References

Agrios, G.N., 2005. Plant Pathology, 5th ed. Elsevier Academic Press, London.

Ah-Fong, A.M.V., Shrivastava, J., and Judelson, H.S., 2017. Lifestyle, gene gain and loss, and transcriptional remodeling cause divergence in the transcriptomes of Phytophthora infestans and Pythium ultimum during potato tuber colonization. *BMC Genomics* 18, 764. https://doi.org/10.1186/s12864-017-4151-2

Albert, I. et al., 2015. An RLP23–SOBIR1–BAK1 complex mediates NLP-triggered immunity. *Nature Plants* 1, 15140. https://doi.org/10.1038/nplants.2015.140

Al-Qurainy, F. et al., 2021. Estimation of Genome Size in the Endemic Species Reseda pentagyna and the Locally Rare Species Reseda lutea Using comparative Analyses of Flow Cytometry and K-Mer Approaches. *Plants* 10, 1362. https://doi.org/10.3390/plants10071362

Anders, S., Pyl, P.T., and Huber, W., 2015. HTSeq—a Python framework to work with high-throughput sequencing data. *Bioinformatics* 31, 166–169 https://doi.org/10.1093/bioinformatics/btu638

Arnerup, J. et al., 2013. The primary module in Norway spruce defence signalling against H. annosum s.l. seems to be jasmonate-mediated signalling without antagonism of salicylate-mediated signalling. *Planta* 237, 1037–1045. https://doi.org/10.1007/s00425-012-1822-8

Ashburner, M. et al., 2000. Gene Ontology: tool for the unification of biology. *Nat Genet* 25, 25–29. https://doi.org/10.1038/75556

Ayala-Usma, D.A. et al., 2021. A whole genome duplication drives the genome evolution of Phytophthora betacei, a closely related species to Phytophthora infestans. *BMC Genomics* 22. https://doi.org/10.1186/s12864-021-08079-y

Babadoost, M., and Pavon, C., 2013. Survival of Oospores of *Phytophthora capsici* in Soil. *Plant Disease* 97, 1478–1483. https://doi.org/10.1094/PDIS-12-12-1123-RE

Baker, J. et al., 2025a. Local Genetic Adaptations Among Remnant Populations of British Common Juniper, JUNIPERUS COMMUNIS, Indicated by a Common Garden Trial. *Ecology and Evolution* 15, e71049. https://doi.org/10.1002/ece3.71049

Baker, J. et al., 2025b. Evidence of Genetic Isolation and Differentiation Among Historically Fragmented British Populations of Common Juniper, *Juniperus communis* L. *Ecology and Evolution* 15. https://doi.org/10.1002/ece3.71818

Banks, N.C. et al., 2015. The role of global trade and transport network topology in the human-mediated dispersal of alien species. *Ecol Lett* 18, 188–199. https://doi.org/10.1111/ele.12397

Bari, R., and Jones, J.D.G., 2009. Role of plant hormones in plant defence responses. *Plant Mol Biol* 69, 473–488. https://doi.org/10.1007/s11103-008-9435-0

Bates, D. et al., 2015. Fitting Linear Mixed-Effects Models Using lme4. *J. Stat. Soft.* 67. https://doi.org/10.18637/jss.v067.i01

Beakes, G.W., Glockling, S.L., and Sekimoto, S., 2012. The evolutionary phylogeny of the oomycete "fungi." *Protoplasma* 249, 3–19. https://doi.org/10.1007/s00709-011-0269-2

Bebber, D.P., Ramotowski, M.A.T., and Gurr, S.J., 2013. Crop pests and pathogens move polewards in a warming world. *Nature Clim Change* 3, 985–988. https://doi.org/10.1038/nclimate1990

Bertier, L. et al., 2013. Host Adaptation and Speciation through Hybridization and Polyploidy in *Phytophthora*. *PLoS ONE* 8, e85385. https://doi.org/10.1371/journal.pone.0085385

Birchler, J.A., Yao, H., and Chudalayandi, S., 2006. Unraveling the genetic basis of hybrid vigor. *Proc. Natl. Acad. Sci. U.S.A.* 103, 12957–12958. https://doi.org/10.1073/pnas.0605627103

Bird, K.A. et al., 2018. The causes and consequences of subgenome dominance in hybrids and recent polyploids. *New Phytologist* 220, 87–93. https://doi.org/10.1111/nph.15256

Blackman, L.M. et al., 2015. RNA-Seq Analysis of the Expression of Genes Encoding Cell Wall Degrading Enzymes during Infection of Lupin (Lupinus angustifolius) by Phytophthora parasitica. *PLoS ONE* 10, e0136899. https://doi.org/10.1371/journal.pone.0136899

Boevink, P.C. et al., 2020. Devastating intimacy: the cell biology of plant– *Phytophthora* interactions. *New Phytol* 228, 445–458. https://doi.org/10.1111/nph.16650

Bostock, R.M., Pye, M.F., and Roubtsova, T.V., 2014. Predisposition in Plant Disease: Exploiting the Nexus in Abiotic and Biotic Stress Perception and Response. *Annu. Rev. Phytopathol.* 52, 517–549. https://doi.org/10.1146/annurev-phyto-081211-172902

Brasier, C. et al., 2022. Phytophthora: an ancient, historic, biologically and structurally cohesive and evolutionarily successful generic concept in need of preservation. *IMA Fungus* 13, 12. https://doi.org/10.1186/s43008-022-00097-z

Brasier, C., and Webber, J., 2010. Sudden larch death. *Nature* 466, 824–825. https://doi.org/10.1038/466824a

Brasier, C.M. et al., 2005. Phytophthora kernoviae sp. nov., an invasive pathogen causing bleeding stem lesions on forest trees and foliar necrosis of ornamentals in the UK. *Mycological Research* 109, 853–859. https://doi.org/10.1017/S0953756205003357

Brasier, C.M. et al., 2004. Phytophthora alni sp. nov. and its variants: designation of emerging heteroploid hybrid pathogens spreading on Alnus trees. *Mycological Research* 108, 1172–1184. https://doi.org/10.1017/S0953756204001005

Brasier, C.M., Cooke, D.E.L., and Duncan, J.M., 1999. Origin of a new *Phytophthora* pathogen through interspecific hybridization. *Proc. Natl. Acad. Sci. U.S.A.* 96, 5878–5883. https://doi.org/10.1073/pnas.96.10.5878

BRIG, 2007. Report on the Species and Habitat Review 2007 172.

Briggs, H., 2019. "Forgotten" elm tree set to make a comeback. *BBC News*. Available at: https://www.bbc.co.uk/news/science-environment-50519036

Broekaert, W.F. et al., 2006. The Role of Ethylene in Host-Pathogen Interactions. *Annu. Rev. Phytopathol.* 44, 393–416. https://doi.org/10.1146/annurev.phyto.44.070505.143440

Broekgaarden, C. et al., 2015. Ethylene: traffic controller on hormonal crossroads to defense. *Plant Physiol.* pp.01020.2015. https://doi.org/10.1104/pp.15.01020

Broome, A. et al., 2017. Promoting natural regeneration for the restoration of *Juniperus communis:* a synthesis of knowledge and evidence for conservation practitioners. *Appl Veg Sci* 20, 397–409. https://doi.org/10.1111/avsc.12303

Brown, J.K.M., 2015. Durable Resistance of Crops to Disease: A Darwinian Perspective. *Annu. Rev. Phytopathol.* 53, 513–539. https://doi.org/10.1146/annurev-phyto-102313-045914

Brown, J.K.M., and Tellier, A., 2011. Plant-Parasite Coevolution: Bridging the Gap between Genetics and Ecology. *Annu. Rev. Phytopathol.* 49, 345–367. https://doi.org/10.1146/annurev-phyto-072910-095301

Bryant, D., and Huson, D.H., 2023. NeighborNet: improved algorithms and implementation. *Front. Bioinform.* 3, 1178600. https://doi.org/10.3389/fbinf.2023.1178600

Bryant, D.M. et al., 2017. A Tissue-Mapped Axolotl De Novo Transcriptome Enables Identification of Limb Regeneration Factors. *Cell Reports* 18, 762–776. https://doi.org/10.1016/j.celrep.2016.12.063

Buchfink, B., Xie, C., and Huson, D.H., 2015. Fast and sensitive protein alignment using DIAMOND. *Nat Methods* 12, 59–60. https://doi.org/10.1038/nmeth.3176

Budde, K.B. et al., 2016. The Natural Evolutionary Potential of Tree Populations to Cope with Newly Introduced Pests and Pathogens—Lessons Learned From Forest Health Catastrophes in Recent Decades. *Curr Forestry Rep* 2, 18–29. https://doi.org/10.1007/s40725-016-0029-9

Burdon, J.J., and Laine, A.-L., 2019. Evolutionary Dynamics of Plant-Pathogen Interactions, 1st ed. Cambridge University Press. https://doi.org/10.1017/9781108625517

Burdon, J.J., and Thrall, P.H., 2009. Coevolution of Plants and Their Pathogens in Natural Habitats. *Science* 324, 755–756. https://doi.org/10.1126/science.1171663

Burki, F., 2014. The Eukaryotic Tree of Life from a Global Phylogenomic Perspective. *Cold Spring Harbor Perspectives in Biology* 6, a016147–a016147. https://doi.org/10.1101/cshperspect.a016147

Busch, J.W., Neiman, M., and Koslow, J.M., 2004. Evidence for Maintenance of Sex by Pathogens in Plants. *Evolution* 58, 2584–2590. https://doi.org/10.1111/j.0014-3820.2004.tb00886.x

Cabanettes, F., and Klopp, C., 2018. D-GENIES: dot plot large genomes in an interactive, efficient and simple way. *PeerJ* 6, e4958. https://doi.org/10.7717/peerj.4958

Callaghan, S., and Guest, D., 2015. Globalisation, the founder effect, hybrid Phytophthora species and rapid evolution: new headaches for biosecurity. *Australasian Plant Pathol.* 44, 255–262. https://doi.org/10.1007/s13313-015-0348-5

Campos, M.L., Kang, J.-H., and Howe, G.A., 2014. Jasmonate-Triggered Plant Immunity. *J Chem Ecol* 40, 657–675. https://doi.org/10.1007/s10886-014-0468-3

Capador, H. et al., 2020. Genetic evidence for sexual reproduction and multiple infections of Norway spruce cones by the rust fungus *Thekopsora areolata*. *Ecol Evol* 10, 7389–7403. https://doi.org/10.1002/ece3.6466

Capador-Barreto, H.D. et al., 2025. Genotype-by-genotype interactions reveal transcription patterns underlying resistance responses in Norway spruce to Heterobasidion annosum s.s. *BMC Plant Biol* 25, 1326. https://doi.org/10.1186/s12870-025-07438-1

Carlson, S.M., Cunningham, C.J., and Westley, P.A.H., 2014. Evolutionary rescue in a changing world. *Trends in Ecology & Evolution* 29, 521–530. https://doi.org/10.1016/j.tree.2014.06.005

Carrasco, A. et al., 2017. Expression profiling in Pinus radiata infected with Fusarium circinatum. *Tree Genetics & Genomes* 13, 46. https://doi.org/10.1007/s11295-017-1125-0

Carrington, D., 2025. 'New hope': ash trees rapidly evolving resistance to dieback, study reveals. *The Guardian*. Available at: https://www.theguardian.com/environment/2025/jun/26/ash-trees-evolve-resistance-dieback-study

Cavers, S., and Cottrell, J.E., 2015. The basis of resilience in forest tree species and its use in adaptive forest management in Britain. *Forestry* 88, 13–26. https://doi.org/10.1093/forestry/cpu027

Challis, R. et al., 2020. BlobToolKit – Interactive Quality Assessment of Genome Assemblies. *G3 Genes|Genomes|Genetics* 10, 1361–1374. https://doi.org/10.1534/g3.119.400908

Chapman, D. et al., 2017. Global trade networks determine the distribution of invasive non-native species. *Global Ecol Biogeogr* 26, 907–917. https://doi.org/10.1111/geb.12599

Charlesworth, B., and Charlesworth, D., 2010. Elements of Evolutionary Genetics. Roberts and Company Publishers, Greenwood Village, Colorado.

Charron, G. et al., 2019. Spontaneous whole-genome duplication restores fertility in interspecific hybrids. *Nat Commun* 10, 4126. https://doi.org/10.1038/s41467-019-12041-8

Chatterton, S. et al., 2023. Inoculum dose–disease response relationships for the pea root rot pathogen, Aphanomyces euteiches, are dependent on soil type and other pathogens. *Front. Plant Sci.* 14, 1115420. https://doi.org/10.3389/fpls.2023.1115420

Chaudhry, S., and Sidhu, G.P.S., 2021. Climate change regulated abiotic stress mechanisms in plants: a comprehensive review. *Plant Cell Rep*. https://doi.org/10.1007/s00299-021-02759-5

Chen, X. et al., 2016. SCR 96, a small cysteine-rich secretory protein of *P hytophthora cactorum* , can trigger cell death in the Solanaceae and is important for pathogenicity and oxidative stress tolerance. *Molecular Plant Pathology* 17, 577–587. https://doi.org/10.1111/mpp.12303

Cheng, H. et al., 2021. Haplotype-resolved de novo assembly using phased assembly graphs with hifiasm. *Nat Methods* 18, 170–175. https://doi.org/10.1038/s41592-020-01056-5

Cipollini, D., Walters, D., and Voelckel, C., 2014. Costs of Resistance in Plants: From Theory to Evidenc. *Annual Plant Reviews Online*. 47, 263–307. https://doi.org/10.1002/9781119312994.apr0512

Comai, L., 2005. The advantages and disadvantages of being polyploid. *Nat Rev Genet* 6, 836–846. https://doi.org/10.1038/nrg1711

Cooke, D.E.L. et al., 2012. Genome Analyses of an Aggressive and Invasive Lineage of the Irish Potato Famine Pathogen. *PLoS Pathog* 8, e1002940. https://doi.org/10.1371/journal.ppat.1002940

Cooke, D.E.L., et al., 2005. Genetic diversity of European populations of the oak fine-root pathogen *Phytophthora quercina*. *Forest Pathology* 35, 57–70.

Cox, M.P. et al., 2022. Chromosome-level assembly of the Phytophthora agathidicida genome reveals adaptation in effector gene families. *Front. Microbiol.* 13, 1038444. https://doi.org/10.3389/fmicb.2022.1038444

Dai, S. et al., 2022. Genome Size Variation and Evolution Driven by Transposable Elements in the Genus Oryza. *Front. Plant Sci.* 13, 921937. https://doi.org/10.3389/fpls.2022.921937

Dale, A.L. et al., 2019. Mitotic Recombination and Rapid Genome Evolution in the Invasive Forest Pathogen *Phytophthora ramorum*. *mBio* 10, e02452-18. https://doi.org/10.1128/mBio.02452-18

D'Amato, A.W. et al., 2023. Species Preservation in the Face of Novel Threats: Cultural, Ecological, and Operational Considerations for Preserving Tree Species in the Context of Non-Indigenous Insects and Pathogens. *Journal of Forestry* 121, 470–479. https://doi.org/10.1093/jofore/fvad024

Danecek, P. et al., 2021. Twelve years of SAMtools and BCFtools. *GigaScience* 10, giab008. https://doi.org/10.1093/gigascience/giab008

Danecek, P. et al., 2011. The variant call format and VCFtools. *Bioinformatics* 27, 2156–2158. https://doi.org/10.1093/bioinformatics/btr330

Darvishzadeh, et al., 2007. Genotype-isolate interaction for resistance to black stem in sunflower (Helianthus annuus). *Plant Pathology* 56, 654–660.

De La Mata, R. et al., 2024. Genetic variation in susceptibility of *Phytophthora cinnamomi* -infected holm oak in the absence or presence of severe drought. *Forestry: An International Journal of Forest Research* cpae045. https://doi.org/10.1093/forestry/cpae045

De La Torre, A.R. et al., 2014. Insights into Conifer Giga-Genomes. *Plant Physiol.* 166, 1724–1732. https://doi.org/10.1104/pp.114.248708

De Villemereuil, P. et al., 2016. General Methods for Evolutionary Quantitative Genetic Inference from Generalized Mixed Models. *Genetics* 204, 1281–1294. https://doi.org/10.1534/genetics.115.186536

Delph, L.F., and Kelly, J.K., 2014. On the importance of balancing selection in plants. *New Phytol* 201, 45–56. https://doi.org/10.1111/nph.12441

Derevnina, L. et al., 2016. Nine things to know about elicitins. *New Phytologist* 212, 888–895. https://doi.org/10.1111/nph.14137

Desprez-Loustau, M.-L. et al., 2016. An evolutionary ecology perspective to address forest pathology challenges of today and tomorrow. *Annals of Forest Science* 73, 45–67. https://doi.org/10.1007/s13595-015-0487-4

Desprez-Loustau, M.-L. et al., 2006. Interactive effects of drought and pathogens in forest trees. *Ann. For. Sci.* 63, 597–612. https://doi.org/10.1051/forest:2006040

Dobin, A. et al., 2013. STAR: ultrafast universal RNA-seq aligner. *Bioinformatics* 29, 15–21. https://doi.org/10.1093/bioinformatics/bts635

Dodds, P.N., 2023. From Gene-for-Gene to Resistosomes: Flor's Enduring Legacy. *MPMI* 36, 461–467. https://doi.org/10.1094/MPMI-06-23-0081-HH

Doležel, J., Greilhuber, J., and Suda, J., 2007. Estimation of nuclear DNA content in plants using flow cytometry. *Nat Protoc* 2, 2233–2244. https://doi.org/10.1038/nprot.2007.310

Donahoo, R.S., and Lamour, K.H., 2008. Interspecific hybridization and apomixis between *Phytophthora capsici* and *Phytophthora tropicalis*. *Mycologia* 100, 911–920.

https://doi.org/10.3852/08-028
Donald, F. et al., 2020. Small scale variability in soil moisture drives infection of vulnerable juniper populations by invasive forest pathogen. *Forest Ecology and Management* 473, 118324. https://doi.org/10.1016/j.foreco.2020.118324
Donald, F., Purse, B.V., and Green, S., 2021. Investigating the Role of Restoration Plantings in Introducing Disease—A Case Study Using Phytophthora. *Forests* 12, 764. https://doi.org/10.3390/f12060764
Downey, H., et al., 2025. State of the UK's Woods and Trees 2025.
Drenth, A., Janssen, E.M., and Govers, F., 1995. Formation and survival of oospores of *Phytophthora infestans* under natural conditions. *Plant Pathology* 44, 86–94. https://doi.org/10.1111/j.1365-3059.1995.tb02719.x
Du, J. et al., 2015. Elicitin recognition confers enhanced resistance to Phytophthora infestans in potato. *Nature Plants* 1, 15034. https://doi.org/10.1038/nplants.2015.34
Du, Y. et al., 2018. RXLR effector diversity in *Phytophthora infestans* isolates determines recognition by potato resistance proteins; the case study AVR1 and R1. *Studies in Mycology* 89, 85–93. https://doi.org/10.1016/j.simyco.2018.01.003
Dudney, J. et al., 2021. Nonlinear shifts in infectious rust disease due to climate change. *Nat Commun* 12, 5102. https://doi.org/10.1038/s41467-021-25182-6
Dun, H.F. et al., 2022. Comparative transcriptomic responses of European and Japanese larches to infection by Phytophthora ramorum. *BMC Plant Biol* 22, 480. https://doi.org/10.1186/s12870-022-03806-3
Ennos, R.A., 2015. Resilience of forests to pathogens: an evolutionary ecology perspective. *Forestry* 88, 41–52. https://doi.org/10.1093/forestry/cpu048
Érsek, T., English, J.T., and Schoelz, J.E., 1995. Creation of species hybrids of *Phytophthora* with modified host ranges by zoospore fusion 85, 1343–1347.
Erwin, D. C. and Ribeiro, O. K., 1996. *Phytophthora* diseases worldwide. The American Phytopathological Society, St Paul, Minnesota.
Eschen, R. et al., 2023. An updated assessment of the direct costs of invasive non-native species to the United Kingdom. *Biol Invasions* 25, 3265–3276. https://doi.org/10.1007/s10530-023-03107-2
Everhart, S., Gambhir, N., and Stam, R., 2021. Population Genomics of Filamentous Plant Pathogens—A Brief Overview of Research Questions, Approaches, and Pitfalls. *Phytopathology®* 111, 12–22. https://doi.org/10.1094/PHYTO-11-20-0527-FI
Eyles, A. et al., 2010. Induced resistance to pests and pathogens in trees. *New Phytologist* 185, 893–908. https://doi.org/10.1111/j.1469-8137.2009.03127.x
Falconer, D.S., and Mackay, T.F.C., 1996. Introduction to Quantitative Genetics, 4th ed. Pearson Education Limited, Harlow.
Falk, A. et al., 1999. *EDS1*, an essential component of *R* gene-mediated disease resistance in *Arabidopsis* has homology to eukaryotic lipases. *Proc. Natl. Acad. Sci. U.S.A.* 96, 3292–3297. https://doi.org/10.1073/pnas.96.6.3292

Fan, R. et al., 2022. Comparative Transcriptome and Metabolome Analysis of Resistant and Susceptible Piper Species Upon Infection by the Oomycete Phytophthora Capsici. *Front. Plant Sci.* 13, 864927. https://doi.org/10.3389/fpls.2022.864927

Fernandes, P. et al., 2024. Dual transcriptomic analysis reveals early induced Castanea defense-related genes and Phytophthora cinnamomi effectors. *Front. Plant Sci.* 15, 1439380. https://doi.org/10.3389/fpls.2024.1439380

Flier, W.G., Van Den Bosch, G.B.M., and Turkensteen, L.J., 2003. Stability of partial resistance in potato cultivars exposed to aggressive strains of *Phytophthora infestans*. *Plant Pathology* 52, 326–337. https://doi.org/10.1046/j.1365-3059.2003.00862.x

Flor, H.H., 1971. Current status of the gene-for-gene concept. *Annual Review of Phytopathology* 9, 275–296.

Flynn, J.M. et al., 2020. RepeatModeler2 for automated genomic discovery of transposable element families. *Proc. Natl. Acad. Sci. U.S.A.* 117, 9451–9457. https://doi.org/10.1073/pnas.1921046117

Fouché, S., Plissonneau, C., and Croll, D., 2018. The birth and death of effectors in rapidly evolving filamentous pathogen genomes. *Current Opinion in Microbiology* 46, 34–42. https://doi.org/10.1016/j.mib.2018.01.020

Frampton, J., Pettersson, M., and Braham, A., 2018. Genetic Variation for Resistance to Phytophthora Root Rot in Eastern White Pine Seedlings. *Forests* 9, 161. https://doi.org/10.3390/f9040161

Franceschi, V.R. et al., 2005. Anatomical and chemical defenses of conifer bark against bark beetles and other pests. *New Phytologist* 167, 353–376. https://doi.org/10.1111/j.1469-8137.2005.01436.x

Fry, W.E. et al., 1992. Population Genetics and Intercontinental Migrations of Phytophthora Infestans. *Annu. Rev. Phytopathol.* 30, 107–130. https://doi.org/10.1146/annurev.py.30.090192.000543

Fukuoka, S. et al., 2015. Gene pyramiding enhances durable blast disease resistance in rice. *Sci Rep* 5, 7773. https://doi.org/10.1038/srep07773

Gabriel, L. et al., 2024. BRAKER3: Fully automated genome annotation using RNA-seq and protein evidence with GeneMark-ETP, AUGUSTUS and TSEBRA. *Genome Res.* 34, 769-777. https://doi.org/10.1101/gr.278090.123

Garbelotto, M., and Gonthier, P., 2022. Ecological, evolutionary, and societal impacts of invasions by emergent forest pathogens. *Forest Microbiology* 2, 107–130. https://doi.org/10.1016/b978-0-323-85042-1.00040-9

Gilbert, G.S., 2002. Evolutionary Ecology of Plant Diseases in Natural Ecosystems. *Annu. Rev. Phytopathol.* 40, 13–43. https://doi.org/10.1146/annurev.phyto.40.021202.110417

Glazebrook, J., 2005. Contrasting Mechanisms of Defense Against Biotrophic and Necrotrophic Pathogens. *Annu. Rev. Phytopathol.* 43, 205–227. https://doi.org/10.1146/annurev.phyto.43.040204.135923

Glover, N.M., Redestig, H., and Dessimoz, C., 2016. Homoeologs: What Are They and How Do We Infer Them? *Trends in Plant Science* 21, 609–621. https://doi.org/10.1016/j.tplants.2016.02.005

Gómez-Gómez, L., and Boller, T., 2000. FLS2: An LRR Receptor–like Kinase Involved in the Perception of the Bacterial Elicitor Flagellin in Arabidopsis. *Molecular Cell*.

Goodwin, S.B., 1997. The Population Genetics of *Phytophthora*. *Phytopathology®* 87, 462–473. https://doi.org/10.1094/PHYTO.1997.87.4.462

Goss, E.M. et al., 2011. The Plant Pathogen Phytophthora andina Emerged via Hybridization of an Unknown Phytophthora Species and the Irish Potato Famine Pathogen, P. infestans. *PLoS ONE* 6, e24543. https://doi.org/10.1371/journal.pone.0024543

Grabherr, M.G. et al., 2011. Full-length transcriptome assembly from RNA-Seq data without a reference genome. *Nat Biotechnol* 29, 644–652. https://doi.org/10.1038/nbt.1883

Graham, N.J. et al., 2018. Assessing the genetic variation of tolerance to red needle cast in a Pinus radiata breeding population. *Tree Genetics & Genomes* 14, 55. https://doi.org/10.1007/s11295-018-1266-9

Green, S. et al., 2020. Evidence for natural resistance in *Juniperus communis* to *Phytophthora austrocedri*. *J Plant Pathol* 103, 55–59. https://doi.org/10.1007/s42161-020-00693-1

Green, S. et al., 2016. First report of *Phytophthora austrocedri* infecting Nootka cypress in Britain. *New Disease Reports* 33, 21–21. https://doi.org/10.5197/j.2044-0588.2016.033.021

Green, S. et al., 2014. *Phytophthora austrocedrae* emerges as a serious threat to juniper (*Juniperus communis*) in Britain. *Plant Pathol* 64, 456–466. https://doi.org/10.1111/ppa.12253

Green, S. et al., 2012. Dieback and mortality of *Juniperus communis* in Britain associated with *Phytophthora austrocedrae*. *New Disease Reports* 26, 2–2. https://doi.org/10.5197/j.2044-0588.2012.026.002

Green, S. et al., 2025. The prevalence of Phytophthora in British plant nurseries; high-risk hosts and substrates and opportunities to implement best practice. *Plant Pathol* 74, 696–717. https://doi.org/DOI: 10.1111/ppa.14044

Greslebin, A.G., and Hansen, E.M., 2010. Pathogenicity of *Phytophthora austrocedrae* on *Austrocedrus chilensis* and its relation with mal del ciprés in Patagonia. *Plant Pathology* 59, 604–612. https://doi.org/10.1111/j.1365-3059.2010.02258.x

Greslebin, A.G., Hansen, E.M., and Sutton, W., 2007. Phytophthora austrocedrae sp. nov., a new species associated with Austrocedrus chilensis mortality in Patagonia (Argentina). *Mycological Research* 111, 308–316. https://doi.org/10.1016/j.mycres.2007.01.008

Guan, D. et al., 2020. Identifying and removing haplotypic duplication in primary genome assemblies. *Bioinformatics* 36, 2896–2898. https://doi.org/10.1093/bioinformatics/btaa025

Guo, L.T. et al., 2015. Flow cytometry and K-mer analysis estimates of the genome sizes of Bemisia tabaci B and Q (Hemiptera: Aleyrodidae). *Front. Physiol.* 6. https://doi.org/10.3389/fphys.2015.00144

Haas, B.J. et al., 2009. Genome sequence and analysis of the Irish potato famine pathogen Phytophthora infestans. *Nature* 461, 393–398. https://doi.org/10.1038/nature08358

Hadfield, J., 2019. MCMCglmm Course Notes.
Hadfield, J., 2010. MCMC Methods for Multi-Response Generalized Linear Mixed Models: The MCMCglmm R Package. *J. Stat. Soft.* 33. https://doi.org/10.18637/jss.v033.i02
Hall, J.E., Kirby, K.J., and Whitbread, A.M., 2004. National vegetation classification: field guide to woodland, Rev. pr. ed. Joint Nature Conservation Committee, Peterborough.
Hamelin, R.C. et al., 2022. Genomic biosurveillance detects a sexual hybrid in the sudden oak death pathogen. *Commun Biol* 5, 477. https://doi.org/10.1038/s42003-022-03394-w
Hansen, E.M., 2015. *Phytophthora* Species Emerging as Pathogens of Forest Trees. *Curr Forestry Rep* 1, 16–24. https://doi.org/10.1007/s40725-015-0007-7
Hansen, E.M., and Goheen, E.M., 2000. *Phellinus Weirii* and Other Native Root Pathogens as Determinants of Forest Structure and Process in Western North America. *Annu. Rev. Phytopathol.* 38, 515–539. https://doi.org/10.1146/annurev.phyto.38.1.515
Hardham, A.R., and Blackman, L.M., 2018. Phytophthora cinnamomi. *Molecular Plant Pathology* 19, 260–285. https://doi.org/10.1111/mpp.12568
Harry, E., 2021. PretextView. https://github.com/wtsi-hpag/PretextView
Harwood, T.D. et al., 2011. Dutch elm disease revisited: past, present and future management in Great Britain. *Plant Pathology* 60, 545–555. https://doi.org/10.1111/j.1365-3059.2010.02391.x
He, L. et al., 2018. Chromosome painting in meiosis reveals pairing of specific chromosomes in polyploid Solanum species. *Chromosoma* 127, 505–513. https://doi.org/10.1007/s00412-018-0682-9
Henricot, B. et al., 2017. Morphological and Genetic Analyses of the Invasive Forest Pathogen *Phytophthora austrocedri* Reveal that Two Clonal Lineages Colonized Britain and Argentina from a Common Ancestral Population. *Phytopathology®* 107, 1532–1540. https://doi.org/10.1094/PHYTO-03-17-0126-R
Hesse, U., 2023. K-Mer-Based Genome Size Estimation in Theory and Practice, in: *Plant Cytogenetics and Cytogenomics: Methods and Protocols*.
Hill, L. et al., 2019. The £15 billion cost of ash dieback in Britain. *Current Biology* 29, R315–R316. https://doi.org/10.1016/j.cub.2019.03.033
Hill, W.G., and Robertson, A., 1966. The effect of linkage on limits to artificial selection. *Genet. Res. Camb.* 89, 311–336. https://doi.org/10.1017/S001667230800949X
Hudgins, J.W. et al., 2006. Ethylene in induced conifer defense: cDNA cloning, protein expression, and cellular and subcellular localization of 1-aminocyclopropane-1-carboxylate oxidase in resin duct and phenolic parenchyma cells. *Planta* 224, 865–877. https://doi.org/10.1007/s00425-006-0274-4
Hudgins, J.W., and Franceschi, V.R., 2004. Methyl Jasmonate-Induced Ethylene Production Is Responsible for Conifer Phloem Defense Responses and Reprogramming of Stem Cambial Zone for Traumatic Resin Duct Formation. *Plant Physiology* 135, 2134–2149. https://doi.org/10.1104/pp.103.037929

Hudson, A. et al., 2024. Natural variation in the pattern-triggered immunity response in plants: Investigations, implications and applications. *Molecular Plant Pathology* 25, e13445. https://doi.org/10.1111/mpp.13445

Huson, D.H., and Bryant, D., 2024. The SplitsTree App: interactive analysis and visualization using phylogenetic trees and networks. *Nat Methods* 21, 1773–1774. https://doi.org/10.1038/s41592-024-02406-3

Isserlin, R. et al., 2014. Enrichment Map – a Cytoscape app to visualize and explore OMICs pathway enrichment results. *F1000Res* 3, 141. https://doi.org/10.12688/f1000research.4536.1

Jain, D., and Khurana, J.P., 2018. Role of Pathogenesis-Related (PR) Proteins in Plant Defense Mechanism, in: Singh, A., and Singh, I.K. (Eds.), *Molecular Aspects of Plant-Pathogen Interaction*. Springer Singapore, Singapore, pp. 265–281. https://doi.org/10.1007/978-981-10-7371-7_12

Jeger, M.J. et al., 2014. Effects of plant pathogens on population dynamics and community composition in grassland ecosystems: two case studies. *Eur J Plant Pathol* 138, 513–527. https://doi.org/10.1007/s10658-013-0325-1

Jiang, H. et al., 2014. Skewer: a fast and accurate adapter trimmer for next-generation sequencing paired-end reads. *BMC Bioinformatics* 15, 182. https://doi.org/10.1186/1471-2105-15-182

Johnson, O. and More, David, 2015. British Tree Guide. Harper Collins Publishers.

Jombart, T., 2008. *adegenet* : a R package for the multivariate analysis of genetic markers. *Bioinformatics* 24, 1403–1405. https://doi.org/10.1093/bioinformatics/btn129

Jones, D.R., and Baker, R.H.A., 2007. Introductions of non-native plant pathogens into Great Britain, 1970-2004. *Plant Pathology* 56, 891–910. https://doi.org/10.1111/j.1365-3059.2007.01619.x

Jones, J.D.G., and Dangl, J.L., 2006. The plant immune system. *Nature* 444, 323–329. https://doi.org/10.1038/nature05286

Jones, P. et al., 2014. InterProScan 5: genome-scale protein function classification. *Bioinformatics* 30, 1236–1240. https://doi.org/10.1093/bioinformatics/btu031

Judelson, H.S., 2009. Sexual Reproduction in Oomycetes: Biology, Diversity, and Contributions to Fitness, in: Lamour, K., and Kamoun, S. (Eds.), *Oomycete Genetics and Genomics*. Wiley, pp. 121–138. https://doi.org/10.1002/9780470475898.ch6

Jung, T. et al., 2021. The Destructive Tree Pathogen Phytophthora ramorum Originates from the Laurosilva Forests of East Asia. *JoF* 7, 226. https://doi.org/10.3390/jof7030226

Jung, T. et al., 2018. Canker and decline diseases caused by soil- and airborne *Phytophthora* species in forests and woodlands. *persoonia* 40, 182–220. https://doi.org/10.3767/persoonia.2018.40.08

Jung, T. et al., 2017. Six new *Phytophthora* species from ITS Clade 7a including two sexually functional heterothallic hybrid species detected in natural ecosystems in Taiwan. *persoonia* 38, 100–135. https://doi.org/10.3767/003158517X693615

Jupe, J. et al., 2013. Phytophthora capsici-tomato interaction features dramatic shifts in gene expression associated with a hemi-biotrophic lifestyle. *Genome Biol* 14, R63. https://doi.org/10.1186/gb-2013-14-6-r63

Kamoun, S., Huitema, E., and Vleeshouwers, V.G.A.A., 1999. Resistance to oomycetes: a general role for the hypersensitive response? *Trends in Plant Science* 4, 196–200.

Karlicki, M., Antonowicz, S., and Karnkowska, A., 2022. Tiara: deep learning-based classification system for eukaryotic sequences. *Bioinformatics* 38, 344–350. https://doi.org/10.1093/bioinformatics/btab672

Kato, H. et al., 2022. Recognition of pathogen-derived sphingolipids in *Arabidopsis*. *Science* 376, 857–860. https://doi.org/10.1126/science.abn0650

Katoh, K., and Standley, D.M., 2013. MAFFT Multiple Sequence Alignment Software Version 7: Improvements in Performance and Usability. *Molecular Biology and Evolution* 30, 772–780. https://doi.org/10.1093/molbev/mst010

Keightley, P.D., and Otto, S.P., 2006. Interference among deleterious mutations favours sex and recombination in finite populations. *Nature* 443, 89–92. https://doi.org/10.1038/nature05049

Kenis, M. et al., 2017. Impact of Non-native Invertebrates and Pathogens on Market Forest Tree Resources, in: *Impact of Biological Invasions on Ecosystem Services*. Springer International Publishing, Cham, pp. 103–117. https://doi.org/10.1007/978-3-319-45121-3_7

Kinloch, B.B., 2003. White Pine Blister Rust in North America: Past and Prognosis. *Phytopathology®* 93, 1044–1047. https://doi.org/10.1094/PHYTO.2003.93.8.1044

Kinver, M., 2020. National Trust suffers "worst year" for ash dieback. *BBC News*. Available at: https://www.bbc.co.uk/news/science-environment-54373214

Kipp, C., 2024. New Phytophthora pathogen — not P. ramorum — found on two nurseries. *Digger*.

Kokot, M., Długosz, M., and Deorowicz, S., 2017. KMC 3: counting and manipulating *k* -mer statistics. *Bioinformatics* 33, 2759–2761. https://doi.org/10.1093/bioinformatics/btx304

Kolde, R., 2025. pheatmap: Pretty Heatmaps. R package version 1.0.13, https://github.com/raivokolde/pheatmap.

Korunes, K.L., and Samuk, K., 2021. PIXY : Unbiased estimation of nucleotide diversity and divergence in the presence of missing data. *Molecular Ecology Resources* 21, 1359–1368. https://doi.org/10.1111/1755-0998.13326

Kourelis, J., and Van Der Hoorn, R.A.L., 2018. Defended to the Nines: 25 Years of Resistance Gene Cloning Identifies Nine Mechanisms for R Protein Function. *Plant Cell* 30, 285–299. https://doi.org/10.1105/tpc.17.00579

Kozlov, A.M. et al., 2019. RAxML-NG: a fast, scalable and user-friendly tool for maximum likelihood phylogenetic inference. *Bioinformatics* 35, 4453–4455. https://doi.org/10.1093/bioinformatics/btz305

Kremer, A., Chen, J., and Lascoux, M., 2025. 'Chimes of resilience': what makes forest trees genetically resilient? *New Phytologist* 246, 1934–1951. https://doi.org/10.1111/nph.70108

Kronmiller, B.A. et al., 2023. Comparative Genomic Analysis of 31 *Phytophthora* Genomes Reveals Genome Plasticity and Horizontal Gene Transfer. *MPMI* 36, 26–46.

https://doi.org/10.1094/MPMI-06-22-0133-R
Langmead, B., and Salzberg, S.L., 2012. Fast gapped-read alignment with Bowtie 2. *Nat Methods* 9, 357–359. https://doi.org/10.1038/nmeth.1923
Landa, B.B. et al., 2001. Influence of Temperature and Inoculum Density of *Fusarium oxysporum* f. sp. *ciceris* on Suppression of Fusarium Wilt of Chickpea by Rhizosphere Bacteria. *Phytopathology* 91, 807–816. https://doi.org/10.1094/PHYTO.2001.91.8.807
Lee, J.-H. et al., 2021. Comparative Genomic Analysis Reveals Genetic Variation and Adaptive Evolution in the Pathogenicity-Related Genes of Phytophthora capsici. *Front. Microbiol.* 12, 694136. https://doi.org/10.3389/fmicb.2021.694136
Levin, D.A., 1975. Pest Pressure and Recombination Systems in Plants. *The American Naturalist* 109, 437–451. https://doi.org/10.1086/283012
Li, H. et al., 2009. The Sequence Alignment/Map format and SAMtools. *Bioinformatics* 25, 2078–2079. https://doi.org/10.1093/bioinformatics/btp352
Li, H., and Durbin, R., 2009. Fast and accurate short read alignment with Burrows–Wheeler transform. *Bioinformatics* 25, 1754–1760. https://doi.org/10.1093/bioinformatics/btp324
Li, Y. et al., 2017. Changing Ploidy as a Strategy: The Irish Potato Famine Pathogen Shifts Ploidy in Relation to Its Sexuality. *MPMI* 30, 45–52. https://doi.org/10.1094/MPMI-08-16-0156-R
Liang, X. et al., 2021. A *Phytophthora capsici* RXLR effector targets and inhibits the central immune kinases to suppress plant immunity. *New Phytologist* 232, 264–278. https://doi.org/10.1111/nph.17573
Liebhold, A.M. et al., 2012. Live plant imports: the major pathway for forest insect and pathogen invasions of the US. *Frontiers in Ecol & Environ* 10, 135–143. https://doi.org/10.1890/110198
Lin, X. et al., 2020. Divergent Evolution of PcF/SCR74 Effectors in Oomycetes Is Associated with Distinct Recognition Patterns in Solanaceous Plants. *mBio* 11, e00947-20. https://doi.org/10.1128/mBio.00947-20
Loureiro, J. et al., 2023. The Use of Flow Cytometry for Estimating Genome Sizes and DNA Ploidy Levels in Plants, in: *Plant Cytogenetics and Cytogenomics: Methods and Protocols*.
Love, M.I., Huber, W., and Anders, S., 2014. Moderated estimation of fold change and dispersion for RNA-seq data with DESeq2. *Genome Biol* 15, 550. https://doi.org/10.1186/s13059-014-0550-8
Lovett, G.M. et al., 2016. Nonnative forest insects and pathogens in the United States: Impacts and policy options. *Ecological Applications* 26, 1437–1455. https://doi.org/10.1890/15-1176
Lüdecke, D., Waggoner, P., and Makowski, D., 2019. insight: A Unified Interface to Access Information from Model Objects in R. *JOSS* 4, 1412. https://doi.org/10.21105/joss.01412
Maere, S., Heymans, K., and Kuiper, M., 2005. BiNGO: a Cytoscape plugin to assess overrepresentation of Gene Ontology categories in Biological Networks. *Bioinformatics* 21, 3448–3449. https://doi.org/10.1093/bioinformatics/bti551
Mahdikhani M., Matinfar M., and Aghaalikhani A., 2017. First report of *Phytophthora austrocedri* causing phloem lesions and bronzing on *Cupressus sempervirens* in northern Iran. *New Disease Reports* 36, 10–10. https://doi.org/10.5197/j.2044-0588.2017.036.010

Man In 'T Veld, W.A., De Cock, A.W.A.M., and Summerbell, R.C., 2007. Natural hybrids of resident and introduced Phytophthora species proliferating on multiple new hosts. *Eur J Plant Pathol* 117, 25–33. https://doi.org/10.1007/s10658-006-9065-9

Martens, C., and Van de Peer, Y., 2010. The hidden duplication past of the plant pathogen Phytophthora and its consequences for infection.

Martin, M., 2011. Cutadapt removes adapter sequences from high-throughput sequencing reads. *EMBnet.journal* 17, 10–12. https://doi.org/10.14806/ej.17.1.200

McDonald, B.A., and Linde, C., 2002. The population genetics of plant pathogens and breeding strategies for durable resistance. *Euphytica* 124, 163–180.

Meffert, L.M., 2006. Population Bottlenecks and Founder Effects, in: Fox, C.W., and Wolf, J.B. (Eds.), *Evolutionary Genetics Concepts and Case Studies*. Oxford University PressNew York, NY, pp. 414–425. https://doi.org/10.1093/oso/9780195168174.003.0027

Mengiste, T., 2012. Plant Immunity to Necrotrophs. *Annu. Rev. Phytopathol.* 50, 267–294. https://doi.org/10.1146/annurev-phyto-081211-172955

Mengiste, T., and Liao, C.-J., 2025. Contrasting Mechanisms of Defense Against Biotrophic and Necrotrophic Pathogens, 20 Years Later: What Has Changed? *Annual Review of Phytopathology* 63, 279–308. https://doi.org/10.1146/annurev-phyto-121823031139

Metheringham, C.L. et al., 2025. Rapid polygenic adaptation in a wild population of ash trees under a novel fungal epidemic. *Science* 388, 1422–1425 https://doi.org/10.1101/2022.08.01.502033

Midgley, K.A., Van Den Berg, N., and Swart, V., 2022. Unraveling Plant Cell Death during Phytophthora Infection. *Microorganisms* 10, 1139. https://doi.org/10.3390/microorganisms10061139

Mode, C., 1958. A Mathematical Model for the Co-Evolution of Obligate Parasites and Their Hosts. *Evolution* 12, 158–165.

Monte, I., 2023. Jasmonates and salicylic acid: Evolution of defense hormones in land plants. *Current Opinion in Plant Biology* 76, 102470. https://doi.org/10.1016/j.pbi.2023.102470

Morales-Cruz, A. et al., 2020. Independent Whole-Genome Duplications Define the Architecture of the Genomes of the Devastating West African Cacao Black Pod Pathogen *Phytophthora megakarya* and Its Close Relative *Phytophthora palmivora*. *G3 Genes|Genomes|Genetics* 10, 2241–2255. https://doi.org/10.1534/g3.120.401014

Mordecai, E.A., 2011. Pathogen impacts on plant communities: unifying theory, concepts, and empirical work. *Ecological Monographs* 81, 429–441. https://doi.org/10.1890/10-2241.1

Mulholland, V. et al., 2013. Development of a quantitative real-time PCR assay for the detection of *Phytophthora austrocedrae*, an emerging pathogen in Britain. *For. Path.* 43, 513–517. https://doi.org/10.1111/efp.12058

Mullett, M.S., et al., 2024. Phylogeography, origin and population structure of the selffertile emerging plant pathogen Phytophthora pseudosyringae. *Molecular Plant Pathology* 25, e13450. https://doi.org/10.1111/mpp.13450

Nakano, R.T., and Shimasaki, T., 2024. Long-Term Consequences of PTI Activation and Its Manipulation by Root-Associated Microbiota. *Plant And Cell Physiology* 65, 681–693. https://doi.org/10.1093/pcp/pcae033

Naveed, Z.A. et al., 2020. The PTI to ETI Continuum in Phytophthora-Plant Interactions. *Front. Plant Sci.* 11, 593905. https://doi.org/10.3389/fpls.2020.593905

Ngou, B.P.M., Ding, P., and Jones, J.D.G., 2022. Thirty years of resistance: Zig-zag through the plant immune system. *The Plant Cell* 34, 1447–1478. https://doi.org/10.1093/plcell/koac041

Nicholas, F.W., Arnott, E.R., and McGreevy, P.D., 2016. Hybrid vigour in dogs? *The Veterinary Journal* 214, 77–83. https://doi.org/10.1016/j.tvjl.2016.05.013

Nimchuk, Z. et al., 2003. Recognition and Response in the Plant Immune System. *Annu. Rev. Genet.* 37, 579–609. https://doi.org/10.1146/annurev.genet.37.110801.142628

Nürnberger, T., and Brunner, F., 2002. Innate immunity in plants and animals: emerging parallels between the recognition of general elicitors and pathogen-associated molecular patterns. *Current Opinion in Plant Biology* 5, 318–324. https://doi.org/10.1016/S1369-5266(02)00265-0

Obel, H.O. et al., 2025. Transcriptomic Analysis of Resistant and Susceptible Eggplant Genotypes (Solanum melongena L.) Provides Insights into Phytophthora capsici Infection Defense Mechanisms. *Horticulturae* 11, 1026. https://doi.org/10.3390/horticulturae11091026

Oerke, E.-C., 2006. Crop losses to pests. *J. Agric. Sci.* 144, 31–43. https://doi.org/10.1017/s0021859605005708

Parke, J.L. et al., 2014. *Phytophthora* Community Structure Analyses in Oregon Nurseries Inform Systems Approaches to Disease Management. *Phytopathology®* 104, 1052–1062. https://doi.org/10.1094/PHYTO-01-14-0014-R

Parker, I.M., and Gilbert, G.S., 2004. The Evolutionary Ecology of Novel Plant-Pathogen Interactions. *Annu. Rev. Ecol. Evol. Syst.* 35, 675–700. https://doi.org/10.1146/annurev.ecolsys.34.011802.132339

Patro, R. et al., 2017. Salmon provides fast and bias-aware quantification of transcript expression. *Nat Methods* 14, 417–419. https://doi.org/10.1038/nmeth.4197

Pecl, G.T. et al., 2017. Biodiversity redistribution under climate change: Impacts on ecosystems and human well-being. *Science* 355, eaai9214. https://doi.org/10.1126/science.aai9214

Pennisi, E., 2010. Armed and Dangerous. *Science* 327.

Petit, R.J., and Hampe, A., 2006. Some Evolutionary Consequences of Being a Tree. *Annu. Rev. Ecol. Evol. Syst.* 37, 187–214. https://doi.org/10.1146/annurev.ecolsys.37.091305.110215

Pimentel, D., Zuniga, R., and Morrison, D., 2005. Update on the environmental and economic costs associated with alien-invasive species in the United States. *Ecological Economics* 52, 273–288. https://doi.org/10.1016/j.ecolecon.2004.10.002

Plantlife, 2011. Breaking new ground for juniper: A management handbook for lowland England.

Poland, J.A. et al., 2009. Shades of gray: the world of quantitative disease resistance. *Trends in Plant Science* 14, 21–29. https://doi.org/10.1016/j.tplants.2008.10.006

Prigigallo, M.I. et al., 2015. Molecular analysis of *Phytophthora* diversity in nursery-grown ornamental and fruit plants. *Plant Pathology* 64, 1308–1319.

https://doi.org/10.1111/ppa.12362
Pritchard, L., and Birch, P.R.J., 2014. The zigzag model of plant–microbe interactions: is it time to move on? *Molecular Plant Pathology* 15, 865–870. https://doi.org/10.1111/mpp.12210
Puertolas, A. et al., 2021. Application of Real-Time PCR for the Detection and Quantification of Oomycetes in Ornamental Nursery Stock. *JoF* 7, 87. https://doi.org/10.3390/jof7020087
Purrington, C.B., 2000. Costs of resistance. *Current Opinion in Plant Biology* 3, 305–308. https://doi.org/10.1016/S1369-5266(00)00085-6
Qiu, X. et al., 2023. The *Phytophthora sojae* nuclear effector PsAvh110 targets a host transcriptional complex to modulate plant immunity. *The Plant Cell* 35, 574–597. https://doi.org/10.1093/plcell/koac300
Ramírez, F. et al., 2014. deepTools: a flexible platform for exploring deep-sequencing data. *Nucleic Acids Research* 42, W187–W191. https://doi.org/10.1093/nar/gku365
Ramsey, J., 2011. Polyploidy and ecological adaptation in wild yarrow. *Proc. Natl. Acad. Sci. U.S.A.* 108, 7096–7101. https://doi.org/10.1073/pnas.1016631108
Ranallo-Benavidez, T.R., Jaron, K.S., and Schatz, M.C., 2020. GenomeScope 2.0 and Smudgeplot for reference-free profiling of polyploid genomes. *Nat Commun* 11, 1432. https://doi.org/10.1038/s41467-020-14998-3
Reading & District Natural History Society, 2023. The Reading Naturalist 75.
Redondo, M.A., Stenlid, J., and Oliva, J., 2020. Genetic Variation Explains Changes in Susceptibility in a Naïve Host Against an Invasive Forest Pathogen: The Case of Alder and the *Phytophthora alni* Complex. *Phytopathology®* 110, 517–525. https://doi.org/10.1094/PHYTO-07-19-0272-R
Riddell, C.E. et al., 2020. Detection and spread of *Phytophthora austrocedri* within infected *Juniperus communis* woodland and diversity of co-associated Phytophthoras as revealed by metabarcoding. *For. Path.* 50, e12602. https://doi.org/10.1111/efp.12602
Rigling, D., and Prospero, S., 2018. *Cryphonectria parasitica*, the causal agent of chestnut blight: invasion history, population biology and disease control. *Molecular Plant Pathology* 19, 7–20. https://doi.org/10.1111/mpp.12542
Ristaino, J.B. et al., 2021. The persistent threat of emerging plant disease pandemics to global food security. *Proc. Natl. Acad. Sci. U.S.A.* 118, e2022239118. https://doi.org/10.1073/pnas.2022239118
Ristaino, J.B., 2002. Tracking historic migrations of the Irish potato famine pathogen, *Phytophthora infestans*. *Microbes and Infection* 4, 1369–1377. https://doi.org/10.1016/S1286-4579(02)00010-2
Rizzo, D.M., Garbelotto, M., and Hansen, E.M., 2005. Phytophthora ramorum: Integrative Research and Management of an Emerging Pathogen in California and Oregon Forests. *Annu. Rev. Phytopathol.* 43, 309–335. https://doi.org/10.1146/annurev.phyto.42.040803.140418
Robert-Seilaniantz, A., Grant, M., and Jones, J.D.G., 2011. Hormone Crosstalk in Plant Disease and Defense: More Than Just JASMONATE-SALICYLATE Antagonism. *Annu. Rev. Phytopathol.* 49, 317–343. https://doi.org/10.1146/annurev-phyto-073009-114447

Robinson, O., Dylus, D., and Dessimoz, C., 2016. *Phylo.io* : Interactive Viewing and Comparison of Large Phylogenetic Trees on the Web. *Mol Biol Evol* 33, 2163–2166. https://doi.org/10.1093/molbev/msw080

Roff, D.A., 1997. Evolutionary Quantitative Genetics. Springer New York, New York.

Sánchez-Vallet, A. et al., 2018. The Genome Biology of Effector Gene Evolution in Filamentous Plant Pathogens. *Annu. Rev. Phytopathol.* 56, 21–40. https://doi.org/10.1146/annurev-phyto-080516-035303

Sansome, E., 1977. Polyploidy and Induced Gametangial Formation in British Isolates of Phytophthora infestans. *Journal of General Microbiology* 99, 311–316. https://doi.org/10.1099/00221287-99-2-311

Sansome, E., Brasier, C.M., and Hamm, P.B., 1991. Phytophthora meadii may be a species hybrid. *Mycological Research* 95, 273–277. https://doi.org/10.1016/S0953-7562(09)81232-X

Santini, A. et al., 2013. Biogeographical patterns and determinants of invasion by forest pathogens in Europe. *New Phytologist* 197, 238–250. https://doi.org/10.1111/j.1469-8137.2012.04364.x

Schwessinger, B., and Rathjen, J.P., 2017. Extraction of High Molecular Weight DNA from Fungal Rust Spores for Long Read Sequencing, in: *Wheat Rust Diseases: Methods and Protocols*. https://doi.org/10.1007/978-1-4939-7249-4_5

Schoebel, C.N. et al., 2014. Population History and Pathways of Spread of the Plant Pathogen Phytophthora plurivora. *PLoS ONE* 9, e85368. https://doi.org/10.1371/journal.pone.0085368

Searle, C.L., and Christie, M.R., 2021. Evolutionary rescue in host-pathogen systems*. *Evolution* 75, 2948–2958. https://doi.org/10.1111/evo.14269

Semizer-Cuming, D. et al., 2021. Gene flow and reproductive success in ash (Fraxinus excelsior L.) in the face of ash dieback: restoration and conservation. *Annals of Forest Science* 78, 14. https://doi.org/10.1007/s13595-020-01025-0

Semizer-Cuming, D. et al., 2019. Negative correlation between ash dieback susceptibility and reproductive success: good news for European ash forests. *Annals of Forest Science* 76, 16. https://doi.org/10.1007/s13595-019-0799-x

Shindo, T. et al., 2012. A Role in Immunity for Arabidopsis Cysteine Protease RD21, the Ortholog of the Tomato Immune Protease C14. *PLoS ONE* 7, e29317. https://doi.org/10.1371/journal.pone.0029317

Simão, F.A. et al., 2015. BUSCO: assessing genome assembly and annotation completeness with single-copy orthologs. *Bioinformatics* 31, 3210–3212. https://doi.org/10.1093/bioinformatics/btv351

Smart, C.D. et al., 2003. Partial Resistance of Tomato to *Phytophthora infestans* Is Not Dependent upon Ethylene, Jasmonic Acid, or Salicylic Acid Signaling Pathways. *MPMI* 16, 141–148. https://doi.org/10.1094/MPMI.2003.16.2.141

Smit, A., Hubley, R., and Green, P., 2015. RepeatMasker Open-4.0. http://www.repeatmasker.org

Smith, T.W., Kron, P., and Martin, S.L., 2018. flowPloidy: An R package for genome size and ploidy assessment of flow cytometry data. *Appl Plant Sci* 6, e01164. https://doi.org/10.1002/aps3.1164

Sniezko, R. et al., 2014. Genetic Resistance to Fusiform Rust in Southern Pines and White Pine Blister Rust in White Pines—A Contrasting Tale of Two Rust Pathosystems—Current Status and Future Prospects. *Forests* 5, 2050–2083. https://doi.org/10.3390/f5092050

Sniezko, R.A. et al., 2020. Genetic resistance to *Phytophthora lateralis* in Port-Orford-cedar (*Chamaecyparis lawsoniana*) – Basic building blocks for a resistance program. *Plants People Planet* 2, 69–83. https://doi.org/10.1002/ppp3.10081

Sniezko, R.A., and Dana Nelson, C., 2022. Resistance breeding against tree pathogens, in: *Forest Microbiology*. Elsevier, pp. 159–175. https://doi.org/10.1016/B978-0-323-85042-1.00007-0

Sniezko, R.A., Johnson, J.S., and Savin, D.P., 2019. Assessing the durability, stability, and usability of genetic resistance to a non-native fungal pathogen in two pine species.

Sniezko, R.A., and Liu, J.-J., 2023. Prospects for developing durable resistance in populations of forest trees. *New Forests* 54, 751–767. https://doi.org/10.1007/s11056-021-09898-3

St. Clair, D.A., 2010. Quantitative Disease Resistance and Quantitative Resistance Loci in Breeding. *Annu. Rev. Phytopathol.* 48, 247–268. https://doi.org/10.1146/annurev-phyto-080508-081904

Stocks, J.J. et al., 2019. Genomic basis of European ash tree resistance to ash dieback fungus. *Nat Ecol Evol* 3, 1686–1696. https://doi.org/10.1038/s41559-019-1036-6

Strange, R.N., and Scott, P.R., 2005. Plant Disease: A Threat to Global Food Security. *Annu. Rev. Phytopathol.* 43, 83–116. https://doi.org/10.1146/annurev.phyto.43.113004.133839

Sugano, S. et al., 2013. Induction of resistance to *Phytophthora sojae* in soyabean (*Glycine max*) by salicylic acid and ethylene. *Plant Pathology* 62, 1048–1056. https://doi.org/10.1111/ppa.12011

Tabima, J.F., and Grünwald, N.J., 2019. *effectR* : An Expandable R Package to Predict Candidate RxLR and CRN Effectors in Oomycetes Using Motif Searches. *MPMI* 32, 1067–1076. https://doi.org/10.1094/MPMI-10-18-0279-TA

Tamura, K., Stecher, G., and Kumar, S., 2021. MEGA11: Molecular Evolutionary Genetics Analysis Version 11. *Molecular Biology and Evolution* 38, 3022–3027. https://doi.org/10.1093/molbev/msab120

Telford, A. et al., 2015. Can we protect forests by harnessing variation in resistance to pests and pathogens? *Forestry* 88, 3–12. https://doi.org/10.1093/forestry/cpu012

Teufel, F. et al., 2022. SignalP 6.0 predicts all five types of signal peptides using protein language models. *Nat Biotechnol* 40, 1023–1025. https://doi.org/10.1038/s41587-021-01156-3

Thaler, J.S., Humphrey, P.T., and Whiteman, N.K., 2012. Evolution of jasmonate and salicylate signal crosstalk. *Trends in Plant Science* 17, 260–270. https://doi.org/10.1016/j.tplants.2012.02.010

Thomas, P.A., El-Barghathi, M., and Polwart, A., 2007. Biological Flora of the British Isles: *Juniperus communis L. J Ecology* 95, 1404–1440. https://doi.org/10.1111/j.1365-2745.2007.01308.x

Thomma, B.P.H.J., Nürnberger, T., and Joosten, M.H.A.J., 2011. Of PAMPs and Effectors: The Blurred PTI-ETI Dichotomy. *Plant Cell* 23, 4–15. https://doi.org/10.1105/tpc.110.082602

Thorpe, P. et al., 2021. Draft genome assemblies for tree pathogens *Phytophthora pseudosyringae* and *Phytophthora boehmeriae*. *G3 Genes|Genomes|Genetics* 11, jkab282. https://doi.org/10.1093/g3journal/jkab282

Tian, M. et al., 2004. A Kazal-like Extracellular Serine Protease Inhibitor from Phytophthora infestans Targets the Tomato Pathogenesis-related Protease P69B. *Journal of Biological Chemistry* 279, 26370–26377. https://doi.org/10.1074/jbc.M400941200

Tian, M., Benedetti, B., and Kamoun, S., 2005. A Second Kazal-Like Protease Inhibitor from *Phytophthora infestans* Inhibits and Interacts with the Apoplastic Pathogenesis-Related Protease P69B of Tomato. *Plant Physiology* 138, 1785–1793. https://doi.org/10.1104/pp.105.061226

Törönen, P., and Holm, L., 2022. PANNZER —A practical tool for protein function prediction. *Protein Science* 31, 118–128. https://doi.org/10.1002/pro.4193

Tsuda, K., and Katagiri, F., 2010. Comparing signaling mechanisms engaged in pattern-triggered and effector-triggered immunity. *Current Opinion in Plant Biology* 13, 459–465. https://doi.org/10.1016/j.pbi.2010.04.006

Tsykun, T. et al., 2022. Global invasion history of the emerging plant pathogen Phytophthora multivora. *BMC Genomics* 23, 153. https://doi.org/10.1186/s12864-022-08363-5

Turkensteen, L.J. et al., 2000. Production, survival and infectivity of oospores of *Phytophthora infestans*. *Plant Pathology* 49, 688–696. https://doi.org/10.1046/j.1365-3059.2000.00515.x

Turner, R.S., 2005. After the famine: Plant pathology, Phytophthora infestans, and the late blight of potatoes, 1845–1960. *Historical Studies in the Physical and Biological Sciences* 35, 341–370. https://doi.org/10.1525/hsps.2005.35.2.341

Tyler, B.M., 2007. *Phytophthora sojae* : root rot pathogen of soybean and model oomycete. *Molecular Plant Pathology* 8, 1–8. https://doi.org/10.1111/j.1364-3703.2006.00373.x

Uliano-Silva, M. et al., 2023. MitoHiFi: a python pipeline for mitochondrial genome assembly from PacBio high fidelity reads. *BMC Bioinformatics* 24, 288. https://doi.org/10.1186/s12859-023-05385-y

Van Den Berg, N. et al., 2018. Transcriptome analysis of an incompatible Persea americana-Phytophthora cinnamomi interaction reveals the involvement of SA- and JA-pathways in a successful defense response. *PLoS ONE* 13, e0205705. https://doi.org/10.1371/journal.pone.0205705

van Kleunen, M. et al., 2015. Global exchange and accumulation of non-native plants. *Nature* 525, 100–103. https://doi.org/10.1038/nature14910

van Loon, L.C., Rep, M., and Pieterse, C.M.J., 2006. Significance of Inducible Defense-related Proteins in Infected Plants. *Annu. Rev. Phytopathol.* 44, 135–162. https://doi.org/10.1146/annurev.phyto.44.070505.143425

Van Poucke, K. et al., 2021. Unravelling hybridization in *Phytophthora* using phylogenomics and genome size estimation. *IMA Fungus* 12, 16. https://doi.org/10.1186/s43008-021-00068-w

Velásquez, A.C., Castroverde, C.D.M., and He, S.Y., 2018. Plant–Pathogen Warfare under Changing Climate Conditions. *Current Biology* 28, R619–R634. https://doi.org/10.1016/j.cub.2018.03.054

Vélez, M.L. et al., 2014. Evidence of low levels of genetic diversity for the *Phytophthora austrocedrae* population in Patagonia, Argentina. *Plant Pathol* 63, 212–220.

https://doi.org/10.1111/ppa.12067
Vercauteren, A. et al., 2011. Aberrant genome size and instability of *Phytophthora ramorum* oospore progenies. *Fungal Genetics and Biology* 48, 537–543. https://doi.org/10.1016/j.fgb.2011.01.008
Vleeshouwers, V.G.A.A. et al., 2000. The hypersensitive response is associated with host and nonhost resistance to Phytophthora infestans. *Planta* 210, 853–864. https://doi.org/10.1007/s004250050690
Wang, C. et al., 2015. Insights into the Origin and Evolution of the Plant Hormone Signaling Machinery. *Plant Physiology* 167, 872–886. https://doi.org/10.1104/pp.114.247403
Wang, S. et al., 2023. RxLR Effectors: Master Modulators, Modifiers and Manipulators. *MPMI* 36, 754–763. https://doi.org/10.1094/MPMI-05-23-0054-CR
Wang, Y. et al., 2019. Lack of gene flow between *Phytophthora infestans* populations of two neighboring countries with the largest potato production. *Evolutionary Applications* 13, 318–329. https://doi.org/10.1111/eva.12870
Wang, Yan et al., 2018. Leucine-rich repeat receptor-like gene screen reveals that Nicotiana RXEG1 regulates glycoside hydrolase 12 MAMP detection. *Nat Commun* 9, 594. https://doi.org/10.1038/s41467-018-03010-8
Ward, L.K., 1977. The Conservation of Juniper: The Associated Fauna with Special Reference to Southern England. *The Journal of Applied Ecology* 14, 81. https://doi.org/10.2307/2401829
Weiberg, A. et al., 2013. Fungal Small RNAs Suppress Plant Immunity by Hijacking Host RNA Interference Pathways. *Science* 342, 118–123. https://doi.org/10.1126/science.1239705
Werres, S., Elliot, M., and Greslebin, A., 2014. Phytophthora austrocedrae. *JKI Data Sheets - Plant Diseases and Diagnosis*.
Winkworth, R.C. et al., 2021. The mitogenome of Phytophthora agathidicida: Evidence for a not so recent arrival of the "kauri killing" Phytophthora in New Zealand. *PLoS ONE* 16, e0250422. https://doi.org/10.1371/journal.pone.0250422
Wood, D.E., Lu, J., and Langmead, B., 2019. Improved metagenomic analysis with Kraken 2. *Genome Biol* 20, 257. https://doi.org/10.1186/s13059-019-1891-0
Wu, R., Ma, C.-X., and Casella, G., 2002. A Bivalent Polyploid Model for Linkage Analysis in Outcrossing Tetraploids. *Theoretical Population Biology* 62, 129–151. https://doi.org/10.1006/tpbi.2002.1608
Xu, F. et al., 2015. Allotetraploid and autotetraploid models of linkage analysis. *Briefings in Bioinformatics* 16, 32–38. https://doi.org/10.1093/bib/bbt075
Xu, J. et al., 2021. Genetic variation and inheritance of susceptibility to Neonectria neomacrospora and Christmas tree traits in a progeny test of Nordmann fir. *Annals of Forest Science* 78, 22. https://doi.org/10.1007/s13595-021-01039-2
Yang, B. et al., 2019. The *Phytophthora sojae* RXLR effector Avh238 destabilizes soybean Type2 Gm ACS s to suppress ethylene biosynthesis and promote infection. *New Phytologist* 222, 425–437. https://doi.org/10.1111/nph.15581

Yang, X., Tyler, B.M., and Hong, C., 2017. An expanded phylogeny for the genus Phytophthora. *IMA Fungus* 8, 355–384. https://doi.org/10.5598/imafungus.2017.08.02.09

Yuen, J., 2021. Pathogens which threaten food security: Phytophthora infestans, the potato late blight pathogen. *Food Sec.* 13, 247–253. https://doi.org/10.1007/s12571-021-01141-3

Zelaya-Molina, L.X., Ortega, M.A., and Dorrance, A.E., 2011. Easy and efficient protocol for oomycete DNA extraction suitable for population genetic analysis. *Biotechnol Lett* 33, 715–720. https://doi.org/10.1007/s10529-010-0478-3

Zhan, J. et al., 2021. Disease influences host population growth rates in a natural wild plant–pathogen association over a 30-year period. *J Ecol* 00, 1–12. https://doi.org/10.1111/1365-2745.13794

Zhang, F. et al., 2022. Understanding R Gene Evolution in Brassica. *Agronomy* 12, 1591. https://doi.org/10.3390/agronomy12071591

Zhang, P. et al., 2025. Salicylic acid and jasmonic acid in plant immunity. *Horticulture Research* 12, uhaf082. https://doi.org/10.1093/hr/uhaf082

Zhao, Y. et al., 2022. The *Phytophthora* effector Avh94 manipulates host jasmonic acid signaling to promote infection. *JIPB* 64, 2199–2210. https://doi.org/10.1111/jipb.13358

Zhu, X. et al., 2023. *Phytophthora sojae* effector PsAvh113 associates with the soybean transcription factor GmDPB to inhibit catalase-mediated immunity. *Plant Biotechnology Journal* 21, 1393–1407. https://doi.org/10.1111/pbi.14043

Zipfel, C., 2008. Pattern-recognition receptors in plant innate immunity. *Current Opinion in Immunology* 20, 10–16. https://doi.org/10.1016/j.coi.2007.11.003

Zuluaga, A.P. et al., 2016. Transcriptional dynamics of *Phytophthora infestans* during sequential stages of hemibiotrophic infection of tomato. *Molecular Plant Pathology* 17, 29–41. https://doi.org/10.1111/mpp.12263

Appendices

A. Supplementary material for Chapter 2

Figure S2.1. Representative pictures showing range of lesion sizes underneath the bark in juniper shoots inoculated with *Phytophthora austrocedri* five weeks post-inoculation. Length of lesion in each case is indicated in the bottom right the picture. A standardised scale bar is shown in the bottom left of each picture. A: No lesion development, visually indistinguishable from negative control. B: Medium lesion size. C: Large lesion size.

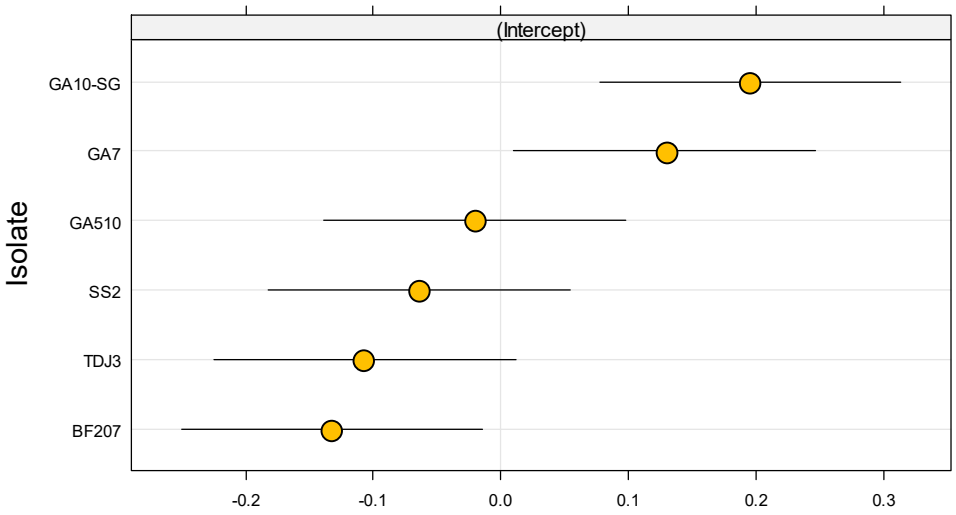

Figure S2.2. Conditional modes for the six *Phytophthora austrocedri* isolates used in the excised shoot inoculation trial, showing the difference between the predicted response for each isolate relative to the average predicted response across all isolates. GA10-SG and GA7 had positive conditional modes, suggesting these two isolates are more virulent than the average isolate.

Table S2.1 Parameter estimates when using a cutoff of 10, 12, 15, 18 or 20 mm in lesion length for defining lesion development as "present" or "absent". The cutoff used in the final analysis was 15 mm. Higher cutoffs increased the estimate of h^2 for lesion length, and lower cutoffs slightly decreased the estimate of h^2 for lesion presence. However, the interpretation of the results would remain unchanged.

		Lesion presence/absence				
		10 mm	12 mm	**15 mm**	18 mm	20 mm
Variance component	**Family**	0.44	0.5	**0.58**	0.6	0.56
	Population	0.16	0.3	**0.3**	0.34	0.18
	Tree_height:Pop	$1x10^{-5}$	$1x10^{-5}$	**$1x10^{-5}$**	$1x10^{-5}$	$1x10^{-5}$
	Block	0.02	0.03	**0.02**	0.03	0.02
Heritability	**h^2**	0.81	0.83	**0.92**	0.91	0.95
		Lesion length				
		10 mm	12 mm	**15 mm**	18 mm	20 mm
Variance component	**Family**	316	265	**234**	316	308
	Population	40.7	28	**22**	17.7	16.5
	Tree_height:Pop	0.01	0.01	**0.006**	0.004	0.004
	Block	141	104	**64**	48	59
Heritability	**h^2**	0.49	0.45	**0.44**	0.62	0.62

Table S2.2. Results of qPCR assays on DNA extractions from phloem/cambium tissue. Assays were multiplexed (using *P. austrocedri* primers and 18S primers) to provide an internal control of DNA extraction success and quality. Primers and qPCR conditions were as described in Mullholland et al. (2013). GH: Greenhouse.

			Ct Value		Call		
Sample	**Technical replicate**	**Run**	**18S**	***P. austrocedri***	**18S**	***P. austrocedri***	**Sample description**
B1.1	1	1	24.910	26.040	Positive	Positive	Inoculated phloem/cambium tissue
B1.1	2	1	25.295	26.414	Positive	Positive	Inoculated phloem/cambium tissue
B1.1	3	1	25.495	26.516	Positive	Positive	Inoculated phloem/cambium tissue
B2.1	1	1	23.282	23.440	Positive	Positive	Inoculated phloem/cambium tissue
B2.1	2	1	23.542	23.538	Positive	Positive	Inoculated phloem/cambium tissue
B2.1	3	1	23.642	23.738	Positive	Positive	Inoculated phloem/cambium tissue
B3.1	1	1	22.162	21.512	Positive	Positive	Inoculated phloem/cambium tissue
B3.1	2	1	22.065	21.383	Positive	Positive	Inoculated phloem/cambium tissue
B3.1	3	1	21.707	21.144	Positive	Positive	Inoculated phloem/cambium tissue
GA7 +ve	1	1	13.530	14.134	Positive	Positive	*P. austrocedri* culture extraction positive
GA7 +ve	2	1	16.271	15.243	Positive	Positive	*P. austrocedri* culture extraction positive
GA7 +ve	3	1	16.902	15.642	Positive	Positive	*P. austrocedri* culture extraction positive
PCR -ve	1	1	Undetermined	Undetermined	Negative	Negative	PCR negative control
PCR -ve	2	1	Undetermined	Undetermined	Negative	Negative	PCR negative control
PCR -ve	3	1	38.020	Undetermined	Negative	Negative	PCR negative control
B1.2	1	2	23.47	32.1	Positive	Positive	Inoculated phloem/cambium tissue
B1.2	2	2	22.99	32.3	Positive	Positive	Inoculated phloem/cambium tissue
B1.2	3	2	22.76	31.94	Positive	Positive	Inoculated phloem/cambium tissue
B1.3	1	2	21.96	25.69	Positive	Positive	Inoculated phloem/cambium tissue
B1.3	2	2	21.35	25.45	Positive	Positive	Inoculated phloem/cambium tissue
B1.3	3	2	20.14	20.48	Positive	Positive	Inoculated phloem/cambium tissue
B1.4	1	2	21.46	25.31	Positive	Positive	Inoculated phloem/cambium tissue
B1.4	2	2	21.1	25.31	Positive	Positive	Inoculated phloem/cambium tissue
B1.4	3	2	20.51	24.88	Positive	Positive	Inoculated phloem/cambium tissue
B1.6	1	2	22.97	24.08	Positive	Positive	Inoculated phloem/cambium tissue
B1.6	2	2	22.35	23.7	Positive	Positive	Inoculated phloem/cambium tissue
B1.6	3	2	22.14	23.26	Positive	Positive	Inoculated phloem/cambium tissue
B2.2	1	2	21.15	27.21	Positive	Positive	Inoculated phloem/cambium tissue
B2.2	2	2	21.52	27.28	Positive	Positive	Inoculated phloem/cambium tissue
B2.2	3	2	21.36	27.15	Positive	Positive	Inoculated phloem/cambium tissue
B2.3	1	2	21.92	35	Positive	Positive	Inoculated phloem/cambium tissue
B2.3	2	2	21.08	34.48	Positive	Positive	Inoculated phloem/cambium tissue
B2.3	3	2	21.61	34.64	Positive	Positive	Inoculated phloem/cambium tissue
B2.4	1	2	22.95	27.13	Positive	Positive	Inoculated phloem/cambium tissue
B2.4	2	2	22.93	27.47	Positive	Positive	Inoculated phloem/cambium tissue
B2.4	3	2	22.97	27.23	Positive	Positive	Inoculated phloem/cambium tissue
B2.7	1	2	21.36	23.03	Positive	Positive	Inoculated phloem/cambium tissue
B2.7	2	2	21.17	23.12	Positive	Positive	Inoculated phloem/cambium tissue
B2.7	3	2	21.06	22.89	Positive	Positive	Inoculated phloem/cambium tissue
B3.2	1	2	19.57	18.81	Positive	Positive	Inoculated phloem/cambium tissue
B3.2	2	2	19.65	19.08	Positive	Positive	Inoculated phloem/cambium tissue
B3.2	3	2	19.48	18.91	Positive	Positive	Inoculated phloem/cambium tissue
B3.3	1	2	17.44	17.48	Positive	Positive	Inoculated phloem/cambium tissue
B3.3	2	2	18.96	17.77	Positive	Positive	Inoculated phloem/cambium tissue
B3.3	3	2	18.91	17.76	Positive	Positive	Inoculated phloem/cambium tissue
B3.4	1	2	19.01	17.64	Positive	Positive	Inoculated phloem/cambium tissue
B3.4	2	2	17.84	17.67	Positive	Positive	Inoculated phloem/cambium tissue
B3.4	3	2	19.42	17.76	Positive	Positive	Inoculated phloem/cambium tissue
B3.6	1	2	19.68	27.76	Positive	Positive	Inoculated phloem/cambium tissue
B3.6	2	2	20.38	28.05	Positive	Positive	Inoculated phloem/cambium tissue
B3.6	3	2	20.5	28.06	Positive	Positive	Inoculated phloem/cambium tissue
GA7 +ve	1	2	14.32	12.09	Positive	Positive	*P. austrocedri* culture extraction positive
GA7 +ve	2	2	13.08	11.05	Positive	Positive	*P. austrocedri* culture extraction positive
GA7 +ve	3	2	14.36	12.37	Positive	Positive	*P. austrocedri* culture extraction positive
B1 GH -ve	1	2	20.62	Undetermined	Positive	Negative	Mock inoculated GH negative control
B1 GH -ve	2	2	19.18	Undetermined	Positive	Negative	Mock inoculated GH negative control
B1 GH -ve	3	2	19.99	Undetermined	Positive	Negative	Mock inoculated GH negative control
B2 GH -ve	1	2	20.1	Undetermined	Positive	Negative	Mock inoculated GH negative control
B2 GH -ve	2	2	22	Undetermined	Positive	Negative	Mock inoculated GH negative control
B2 GH -ve	3	2	20.2	Undetermined	Positive	Negative	Mock inoculated GH negative control
B3 GH -ve	1	2	18.46	39.32	Positive	Negative	Mock inoculated GH negative control
B3 GH -ve	2	2	18.46	Undetermined	Positive	Negative	Mock inoculated GH negative control
B3 GH -ve	3	2	17.59	Undetermined	Positive	Negative	Mock inoculated GH negative control
Blank extraction 1	1	2	Undetermined	Undetermined	Negative	Negative	Blank DNA extraction negative control
Blank extraction 1	2	2	Undetermined	Undetermined	Negative	Negative	Blank DNA extraction negative control
Blank extraction 1	3	2	Undetermined	Undetermined	Negative	Negative	Blank DNA extraction negative control
Blank extraction 2	1	2	Undetermined	Undetermined	Negative	Negative	Blank DNA extraction negative control

Table S2.2 continued

Blank extraction 2	2	2	Undetermined	Undetermined	Negative	Negative	Blank DNA extraction negative control
Blank extraction 2	3	2	Undetermined	39.16	Negative	Negative	Blank DNA extraction negative control
PCR -ve	1	2	Undetermined	Undetermined	Negative	Negative	PCR negative control
PCR -ve	2	2	Undetermined	Undetermined	Negative	Negative	PCR negative control
PCR -ve	3	2	Undetermined	Undetermined	Negative	Negative	PCR negative control
B4.1	1	3	20.36	25.67	Positive	Positive	Inoculated phloem/cambium tissue
B4.1	2	3	19.98	25.41	Positive	Positive	Inoculated phloem/cambium tissue
B4.1	3	3	19.47	25.32	Positive	Positive	Inoculated phloem/cambium tissue
B4.2	1	3	22.14	26.51	Positive	Positive	Inoculated phloem/cambium tissue
B4.2	2	3	21.62	26.49	Positive	Positive	Inoculated phloem/cambium tissue
B4.2	3	3	21.63	26.39	Positive	Positive	Inoculated phloem/cambium tissue
B4.3	1	3	22.52	25.15	Positive	Positive	Inoculated phloem/cambium tissue
B4.3	2	3	21.96	24.94	Positive	Positive	Inoculated phloem/cambium tissue
B4.3	3	3	22.89	26.29	Positive	Positive	Inoculated phloem/cambium tissue
B4.4	1	3	22.07	21.01	Positive	Positive	Inoculated phloem/cambium tissue
B4.4	2	3	22.07	20.74	Positive	Positive	Inoculated phloem/cambium tissue
B4.4	3	3	21.34	20.45	Positive	Positive	Inoculated phloem/cambium tissue
B4.5	1	3	22.28	23.28	Positive	Positive	Inoculated phloem/cambium tissue
B4.5	2	3	21.99	23.14	Positive	Positive	Inoculated phloem/cambium tissue
B4.5	3	3	21.98	23.08	Positive	Positive	Inoculated phloem/cambium tissue
B5.1	1	3	20.16	17.18	Positive	Positive	Inoculated phloem/cambium tissue
B5.1	2	3	19.78	16.29	Positive	Positive	Inoculated phloem/cambium tissue
B5.1	3	3	19.56	17.7	Positive	Positive	Inoculated phloem/cambium tissue
B5.2	1	3	20.23	27.12	Positive	Positive	Inoculated phloem/cambium tissue
B5.2	2	3	19.78	27.07	Positive	Positive	Inoculated phloem/cambium tissue
B5.2	3	3	19.82	27	Positive	Positive	Inoculated phloem/cambium tissue
B5.4	1	3	22.53	21.38	Positive	Positive	Inoculated phloem/cambium tissue
B5.4	2	3	23.06	21.84	Positive	Positive	Inoculated phloem/cambium tissue
B5.4	3	3	22.35	21.08	Positive	Positive	Inoculated phloem/cambium tissue
B5.5	1	3	21.38	25.07	Positive	Positive	Inoculated phloem/cambium tissue
B5.5	2	3	20.88	24.93	Positive	Positive	Inoculated phloem/cambium tissue
B5.5	3	3	21.02	25.04	Positive	Positive	Inoculated phloem/cambium tissue
B5.6	1	3	19.43	15.62	Positive	Positive	Inoculated phloem/cambium tissue
B5.6	2	3	19.44	15.01	Positive	Positive	Inoculated phloem/cambium tissue
B5.6	3	3	19.82	14.97	Positive	Positive	Inoculated phloem/cambium tissue
B6.1	1	3	20.84	22.12	Positive	Positive	Inoculated phloem/cambium tissue
B6.1	2	3	20.72	22.01	Positive	Positive	Inoculated phloem/cambium tissue
B6.1	3	3	20.77	18.78	Positive	Positive	Inoculated phloem/cambium tissue
B6.2	1	3	20.86	19.12	Positive	Positive	Inoculated phloem/cambium tissue
B6.2	2	3	21.05	19.25	Positive	Positive	Inoculated phloem/cambium tissue
B6.2	3	3	21.08	17.34	Positive	Positive	Inoculated phloem/cambium tissue
B6.3	1	3	22.36	23.07	Positive	Positive	Inoculated phloem/cambium tissue
B6.3	2	3	22.35	23.1	Positive	Positive	Inoculated phloem/cambium tissue
B6.3	3	3	22.45	23.25	Positive	Positive	Inoculated phloem/cambium tissue
B6.4	1	3	21.78	22.41	Positive	Positive	Inoculated phloem/cambium tissue
B6.4	2	3	21.42	21.93	Positive	Positive	Inoculated phloem/cambium tissue
B6.4	3	3	21.61	22.07	Positive	Positive	Inoculated phloem/cambium tissue
B6.5	1	3	21.31	21.63	Positive	Positive	Inoculated phloem/cambium tissue
B6.5	2	3	21.54	21.56	Positive	Positive	Inoculated phloem/cambium tissue
B6.5	3	3	21.47	21.75	Positive	Positive	Inoculated phloem/cambium tissue
GA7 +ve	1	3	15.34	7.47	Positive	Positive	*P. austrocedri* culture extraction positive
GA7 +ve	2	3	14.7	7.89	Positive	Positive	*P. austrocedri* culture extraction positive
GA7 +ve	3	3	15.05	11.23	Positive	Positive	*P. austrocedri* culture extraction positive
B4 GH -ve	1	3	21	Undetermined	Positive	Negative	Mock inoculated GH negative control
B4 GH -ve	2	3	20.67	Undetermined	Positive	Negative	Mock inoculated GH negative control
B4 GH -ve	3	3	20.06	Undetermined	Positive	Negative	Mock inoculated GH negative control
B5 GH -ve	1	3	19.42	Undetermined	Positive	Negative	Mock inoculated GH negative control
B5 GH -ve	2	3	19.56	Undetermined	Positive	Negative	Mock inoculated GH negative control
B5 GH -ve	3	3	19.96	Undetermined	Positive	Negative	Mock inoculated GH negative control
B6 GH -ve	1	3	18.73	36	Positive	Positive	Mock inoculated GH negative control
B6 GH -ve	2	3	19.15	37.3	Positive	Positive	Mock inoculated GH negative control
B6 GH -ve	3	3	18.2	37.88	Positive	Positive	Mock inoculated GH negative control
Blank extraction 3	1	3	39.9	Undetermined	Negative	Negative	Blank DNA extraction negative control
Blank extraction 3	2	3	Undetermined	Undetermined	Negative	Negative	Blank DNA extraction negative control
Blank extraction 3	3	3	Undetermined	Undetermined	Negative	Negative	Blank DNA extraction negative control
Blank extraction 4	1	3	Undetermined	Undetermined	Negative	Negative	Blank DNA extraction negative control
Blank extraction 4	2	3	Undetermined	Undetermined	Negative	Negative	Blank DNA extraction negative control
Blank extraction 4	3	3	Undetermined	Undetermined	Negative	Negative	Blank DNA extraction negative control
PCR -ve	1	3	Undetermined	Undetermined	Negative	Negative	PCR negative control
PCR -ve	2	3	Undetermined	Undetermined	Negative	Negative	PCR negative control
PCR -ve	3	3	Undetermined	Undetermined	Negative	Negative	PCR negative control

B. Supplementary material for Chapter 3

B.1 Supplementary methods: DNA extraction protocol to achieve high molecular weight DNA from *Phytophthora* mycelial tissue

- Modified protocol based on Zelaya-Molina et al. (2011) and Schwessinger and Rathjen (2017).
- Extraction buffer is best fresh, no more than 3 months old. Phenol:Chloroform:Isoamylalcohol (P:C:I; 25:24:1) should be very fresh, no more than a few weeks old.
- Any pipetting of sample should be carried out gently using wide-bore tips.

1. Make up extraction buffer as described in Zelaya-Molina et al. (2011): 10 mM Tris/HCl, 50 mM EDTA, 0.5% SDS, 0.5% Triton X-100, 0.5% Tween 20. Autoclave buffer before use.
2. Add 4.8 ml of extraction buffer to a 50 ml falcon tube containing frozen mycelium (ground in liquid nitrogen) from 2-3 colonies (each 2-3 cm in size), and mix by gentle inversion. Heat in a water bath at 55˚C for 30 min, inverting gently every 10 minutes.
3. Add 50 µl of 20 mg/ml Proteinase K to buffer, mix by gentle inversion and heat for another 30 min at 55˚C, inverting every 10 min.
4. Transfer 800 µl aliquots to 2 ml Eppendorf tubes and cool on ice for 5 min.
5. Add 160 µl of KAc 5M, mix by inversion.
6. Working in fume hood, add 1 ml of P:C:I, mix by inversion for 2 min.
7. Centrifuge at 10,000 g for 10 min at 4˚C.
8. Transfer supernatant to a fresh Eppendorf tube and repeat P:C:I step and centrifugation.
9. Transfer supernatant to a fresh Eppendorf tube, add 20 µl RNase A/T1, mix by inversion, and incubate for 30 min at room temperature.
10. Add 100 µl NaAc 3M, mix by inversion.
11. Add 1 ml isopropanol, mix by inversion, and incubate for 30 min at room temperature.
12. Centrifuge at 10,000 g for 30 min at 4˚C.
13. Remove supernatant, leaving only pellet. Wash with 1 ml of 70% EtOH, inverting to dislodge pellet. Centrifuge at 13,000 g for 5 min at room temperature.
14. Remove supernatant and repeat wash with 70% EtOH and centrifugation.
15. Remove supernatant and air-dry pellet until ethanol halo disappears.
16. Add 30-50 µl EB buffer and resuspend pellet by gently flicking tube.
17. Leave overnight at room temperature to resuspend pellet, then store at 4˚C until sequencing can occur, preferably as soon as possible. Do not freeze.

B.2 Supplementary figures

Figure S3.1. K-mer spectra of genomic DNA (PacBio reads) for two *Phytophthora austrocedri* isolates. TDJ3 represents the UK lineage; PHY-211 represents the Argentinian lineage. The presence of more than two distinct peaks suggests their genomes are polyploid. *Phytophthora* are known to have flexible genomes with multiple duplications and deletions, which may be causing the poor model fit. Nevertheless, the best fit (shown in the figures below) suggests that *P. austrocedri* is tetraploid.

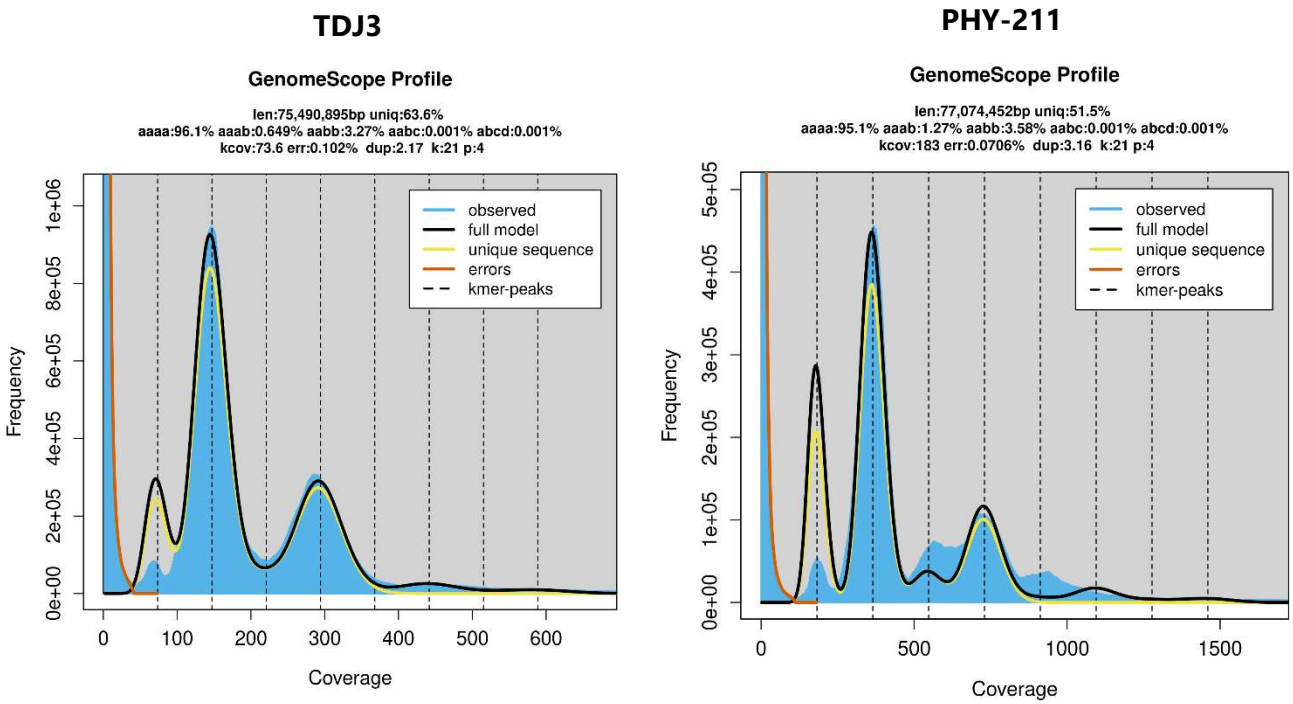

C. Supplementary material for Chapter 4

Figure S4.1. Histograms of sequencing coverage for different kinds of SNP calls. Blue indicates heterozygous calls (0/1) and yellow indicates homozygous alternate SNP calls (1/1). Each plot represents a different isolate, in each case mapped to the reference genome for its own lineage. The top two plots show ARG isolates mapped to the ARG reference; the bottom two plots show UK isolates mapped to the UK reference. All isolates showed a similar pattern, and two isolates for each lineage were chosen arbitrarily. SNPs plotted here were filtered for quality using the parameters described in the main text, but no depth filters were imposed. "Real" SNPs should coincide with a coverage of approx. 60-100, depending on the isolate. This coincides with the peak in homozygous alternate calls, but the heterozygous calls have their main peak at approximately 2x that coverage. Thus, "real" heterozygous SNPs appear to be overwhelmed by paralogs/duplicated regions of the genome. To more accurately analyse genetic diversity across the genome we therefore implemented a hard filter at an individual level for each isolate to remove any SNPs with a coverage of greater than 1.5x the expected values for "real" SNPs for each isolate.

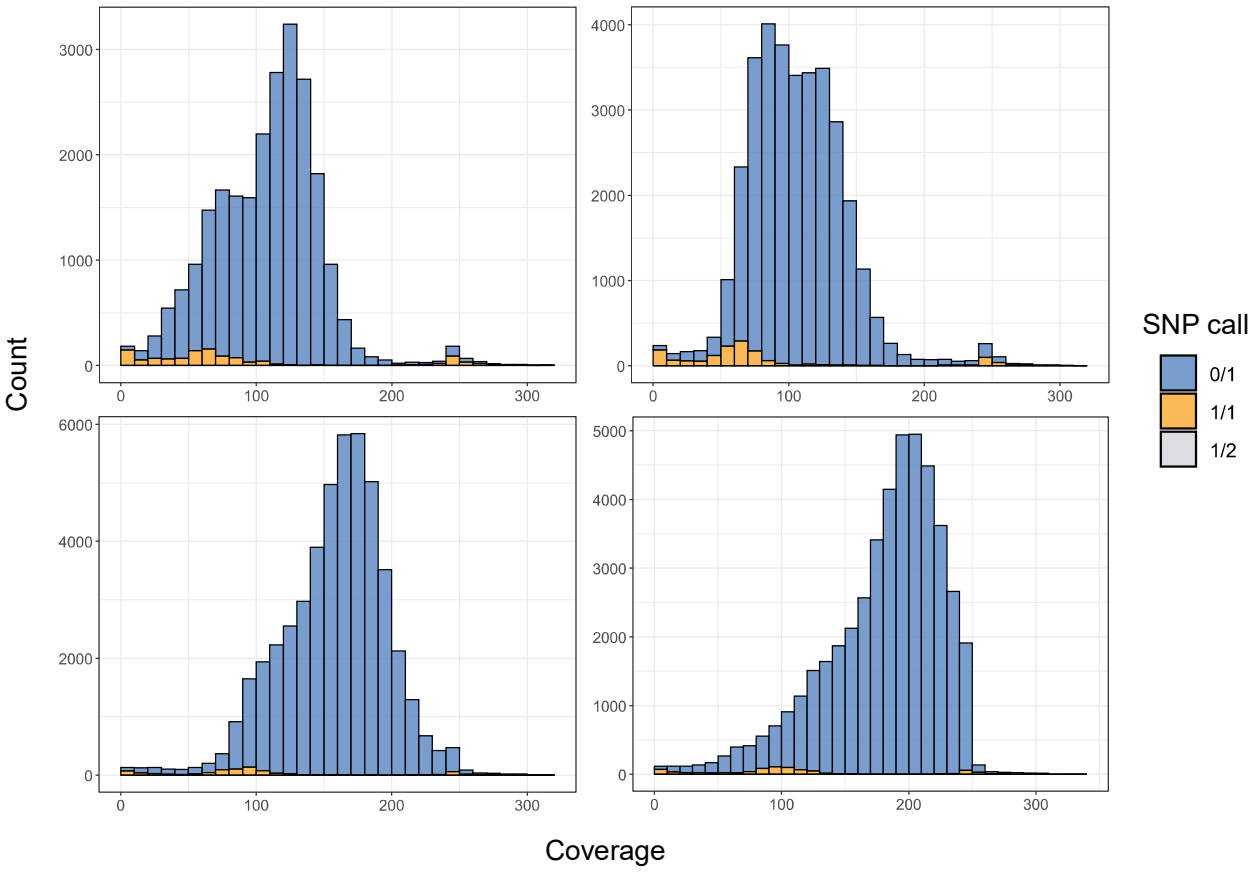

Figure S4.2. Genomescope output showing alternative ploidy fits (diploid, triploid and tetraploid) for isolates that had ambiguous ploidy levels. A: Isolates PHY-215 (top three) and PHY-257 (bottom three). Diploid, triploid and tetraploid models fit similarly well. B: Isolates BT3 (top three) and TDJ6 (bottom three). Diploid and triploid models could not converge on correct peaks, despite numerous attempts at specifying correct monoploid coverage. Tetraploid model correctly identifies 1x and 2x peaks.

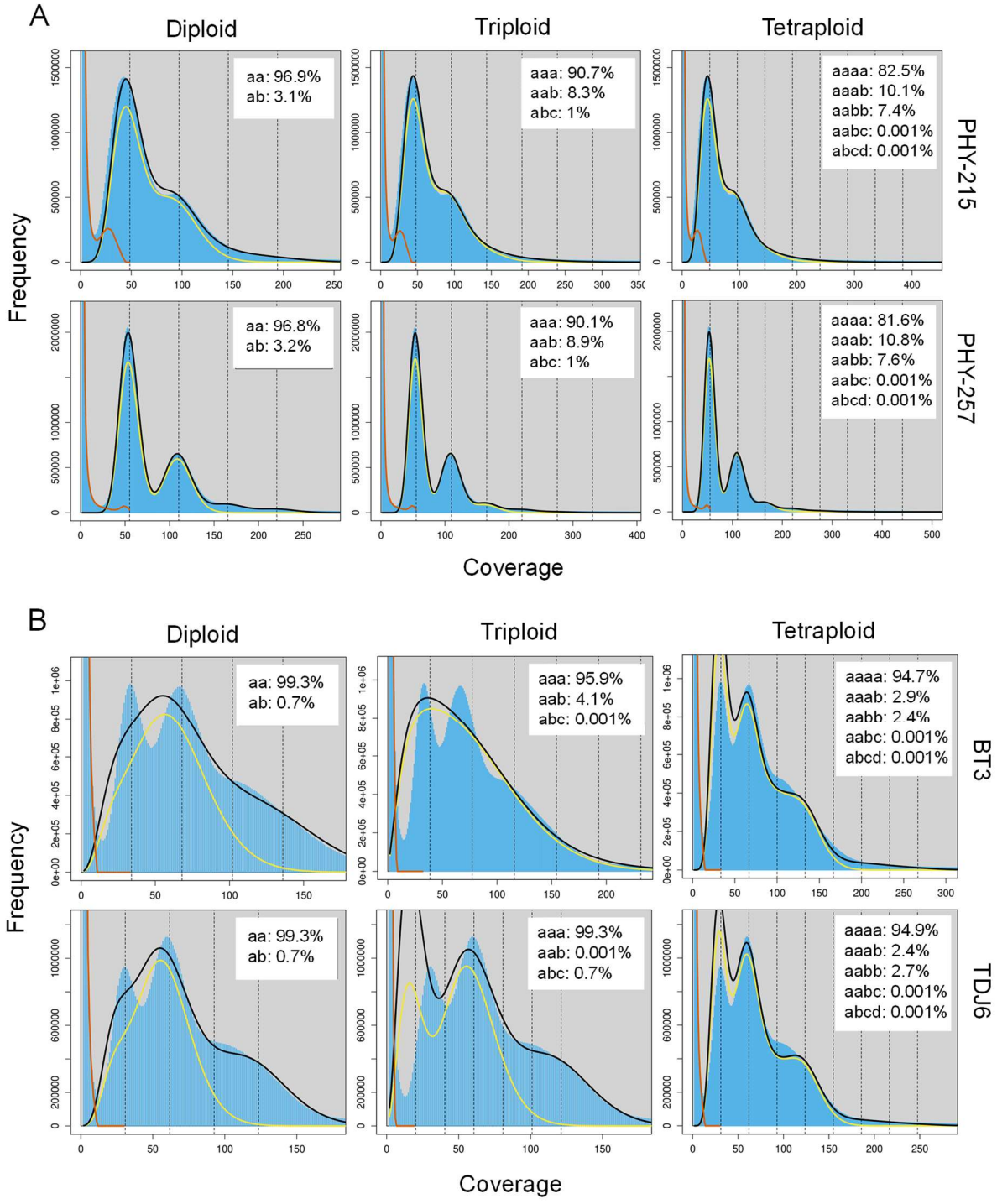

.

Table S4.1. Species designation and accession numbers for the 17 *Phytophthora* reference genomes used in the phylogenetic analysis of homologous genes, along with the two *P. austrocedri* assemblies.

***Phytophthora* species**	**Accession number**
P. agathidicida	GCA_25722995.1
P. cactorum	GCA_16864655.1
P. cambivora	GCA_443045.1
P. capsici	GCA_30324255.1
P. cinnamomi	GCA_18691715.1
P. infestans	GCA_142945.1
P. kernoviae	GCA_8080845.1
P. lateralis	GCA_500205.2
P. multivora	GCA_1314345.1
P. palmivora	GCA_8079305.1
P. pini	GCA_23611945.1
P. pluvialis	GCA_1314425.1
P. ramorum	GCA_20800215.1
P. sojae	GCF_149755.1
P. syringae	GCA_12656105.1
P. x alni	GCA_439335.1
P. x cambivora	GCA_33557925.1

D. Supplementary material for Chapter 5

D.1 Supplementary methods: Microsatellite genotyping

Susceptible juniper were genotyped at four microsatellite markers. A PCR was set up for each of the markers with a forward primer containing a 5'–AGGTTTTCCCAGTCACGACGTT–3' M13 sequence attached at the 5' end for subsequent detection purposes. DNA was amplified in a total volume of 20 µl comprising the following reaction mixture: 1.5 µl DNA, 1X PCR buffer (Bioron, Germany), 5 µM of each primer, 0.2 mM of each dNTP (VWR International), 0.25 µM M13 oligo with a FAM fluorescent dye attached, and 0.25 U Taq DNA polymerase (Bioron). The PCR cycle conditions were as follows: 95°C for 5 min; 10 cycles of 94°C for 30s, 55°C for 60s, 72°C for 30s; 25 cycles of 94°C for 30s, 53°C for 60s, 72°C for 30s; 72°C for 10 min. PCR products were sent to Dundee University Sequencing Service for fragment analysis and the resulting data were analysed using the Geneious software package.

All 30 susceptible juniper individuals genotyped were identical at every microsatellite marker, and were distinct at every marker from the resistant juniper genotype. The probability of the genotype at each marker was calculated using regional allele frequencies (based on 215 juniper individuals from nine populations in Scotland), assuming Hardy-Weinberg equilibrium:

	Type	Frequency allele 1	Frequency allele 2	Frequency of genotype
Marker 1	Heterozygous	0.435	0.005	0.00435
Marker 2	Heterozygous	0.757	0.072	0.109008
Marker 3	Homozygous	0.045		0.002025
Maker 4	Heterozygous	0.052	0.055	0.00572

The probability of a match at all four markers between two juniper individuals occurring by chance was therefore estimated to be 5.5×10^{-9}.

D.2 Supplementary tables

Table S5.1. Significantly enriched GO terms (Biological Process) associated with genes that were differentially expressed between the susceptible juniper genotype inoculated with the less virulent *P. austrocedri* isolate compared to the same genotype's mock-inoculated control at 48 hours post-inoculation.

GO	GO ID	GO Description	p-val	Corrected p-val	Cluster frequency	Total frequency	Direction
BP	6412	translation	6.55E-05	2.00E-02	14/52 26.9%	4607/55204 8.3%	Upregulated
BP	2181	cytoplasmic translation	1.35E-04	2.00E-02	6/52 11.5%	838/55204 1.5%	Upregulated
BP	9772	photosynthetic electron transport in photosystem II	1.38E-04	2.00E-02	3/52 5.7%	105/55204 0.1%	Upregulated
BP	6412	translation	5.98E-31	3.28E-28	67/158 42.4%	4607/55204 8.3%	Downregulated
BP	9765	photosynthesis, light harvesting	3.45E-22	9.46E-20	29/158 18.3%	886/55204 1.6%	Downregulated
BP	15979	photosynthesis	1.45E-20	2.65E-18	43/158 27.2%	2707/55204 4.9%	Downregulated
BP	19684	photosynthesis, light reaction	3.24E-19	4.45E-17	31/158 19.6%	1354/55204 2.4%	Downregulated
BP	10467	gene expression	1.05E-13	1.15E-11	73/158 46.2%	11047/55204 20.0%	Downregulated
BP	9059	macromolecule biosynthetic process	1.16E-11	1.06E-09	73/158 46.2%	12110/55204 21.9%	Downregulated
BP	6091	generation of precursor metabolites and energy	1.34E-09	1.05E-07	34/158 21.5%	3720/55204 6.7%	Downregulated
BP	2182	cytoplasmic translational elongation	5.63E-09	3.87E-07	7/158 4.4%	85/55204 0.1%	Downregulated
BP	19538	protein metabolic process	6.11E-08	3.73E-06	72/158 45.5%	14238/55204 25.7%	Downregulated
BP	8152	metabolic process	4.03E-07	2.21E-05	142/158 89.8%	40728/55204 73.7%	Downregulated
BP	6414	translational elongation	4.49E-07	2.24E-05	9/158 5.6%	323/55204 0.5%	Downregulated
BP	9058	biosynthetic process	3.60E-05	1.65E-03	86/158 54.4%	21272/55204 38.5%	Downregulated
BP	42274	ribosomal small subunit biogenesis	5.09E-04	2.11E-02	7/158 4.4%	482/55204 0.8%	Downregulated
BP	28	ribosomal small subunit assembly	5.39E-04	2.11E-02	4/158 2.5%	129/55204 0.2%	Downregulated
BP	2181	cytoplasmic translation	7.39E-04	2.71E-02	9/158 5.6%	838/55204 1.5%	Downregulated
BP	9768	photosynthesis, light harvesting in photosystem	1.01E-03	3.45E-02	5/158 3.1%	263/55204 0.4%	Downregulated

Table S5.2. Significantly enriched GO terms (Biological Process) associated with genes that were differentially expressed between the susceptible juniper genotype inoculated with the more virulent *P. austrocedri* isolate compared to the same genotype's mock-inoculated control at 48 hours post-inoculation.

GO	GO ID	GO Description	p-val	Corrected p-val	Cluster frequency	Total frequency	Direction
BP	6412	translation	7.44E-09	3.02E-06	23/71 32.3%	4607/55204 8.3%	Upregulated
BP	2181	cytoplasmic translation	1.32E-06	2.68E-04	9/71 12.6%	838/55204 1.5%	Upregulated
BP	10467	gene expression	1.32E-04	1.78E-02	28/71 39.4%	11047/55204 20.0%	Upregulated
BP	9059	macromolecule biosynthetic process	2.61E-04	2.65E-02	29/71 40.8%	12110/55204 21.9%	Upregulated
BP	463	maturation of LSU-rRNA from tricistronic rRNA transcript	3.88E-04	3.15E-02	3/71 4.2%	109/55204 0.1%	Upregulated
BP	6412	translation	4.32E-13	1.14E-10	27/65 41.5%	4607/55204 8.3%	Downregulated
BP	10467	gene expression	1.29E-07	1.71E-05	32/65 49.2%	11047/55204 20.0%	Downregulated
BP	9059	macromolecule biosynthetic process	3.14E-07	2.77E-05	33/65 50.7%	12110/55204 21.9%	Downregulated
BP	19538	protein metabolic process	4.21E-05	2.79E-03	32/65 49.2%	14238/55204 25.7%	Downregulated
BP	2181	cytoplasmic translation	4.64E-04	2.46E-02	6/65 9.2%	838/55204 1.5%	Downregulated
BP	9765	photosynthesis, light harvesting	6.21E-04	2.74E-02	6/65 9.2%	886/55204 1.6%	Downregulated
BP	19684	photosynthesis, light reaction	1.06E-03	4.02E-02	7/65 10.7%	1354/55204 2.4%	Downregulated

Table S5.3. Significantly enriched GO terms (Biological Process) associated with genes that were differentially expressed between the resistant juniper genotype inoculated with the less virulent *P. austrocedri* isolate compared to the same genotype's mock-inoculated control at 48 hours post-inoculation. Where relevant, only the top 50 GO terms have been included for each direction (upregulated and downregulated).

GO	GO ID	GO Description	p-val	Corrected p-val	Cluster frequency	Total frequency	Direction
BP	9723	response to ethylene	2.94E-21	2.20E-18	20/110 18.1%	454/55204 0.8%	Upregulated
BP	9873	ethylene-activated signaling pathway	2.45E-19	9.20E-17	17/110 15.4%	330/55204 0.5%	Upregulated
BP	71369	cellular response to ethylene stimulus	4.49E-19	1.12E-16	17/110 15.4%	342/55204 0.6%	Upregulated
BP	160	phosphorelay signal transduction system	1.06E-17	1.99E-15	17/110 15.4%	413/55204 0.7%	Upregulated
BP	9719	response to endogenous stimulus	4.12E-15	6.17E-13	31/110 28.1%	2847/55204 5.1%	Upregulated
BP	9725	response to hormone	2.28E-14	2.86E-12	30/110 27.2%	2818/55204 5.1%	Upregulated
BP	9755	hormone-mediated signaling pathway	2.06E-13	2.21E-11	23/110 20.9%	1661/55204 3.0%	Upregulated
BP	71495	cellular response to endogenous stimulus	2.38E-13	2.23E-11	24/110 21.8%	1853/55204 3.3%	Upregulated
BP	42221	response to chemical	5.18E-13	4.32E-11	43/110 39.0%	6671/55204 12.0%	Upregulated
BP	44550	secondary metabolite biosynthetic process	1.02E-12	7.64E-11	13/110 11.8%	383/55204 0.6%	Upregulated
BP	32870	cellular response to hormone stimulus	1.38E-12	9.44E-11	23/110 20.9%	1823/55204 3.3%	Upregulated
BP	70887	cellular response to chemical stimulus	4.08E-12	2.55E-10	31/110 28.1%	3698/55204 6.6%	Upregulated
BP	19748	secondary metabolic process	9.69E-12	5.59E-10	14/110 12.7%	569/55204 1.0%	Upregulated
BP	70297	regulation of phosphorelay signal transduction	1.28E-11	6.38E-10	7/110 6.3%	52/55204 0.0%	Upregulated
BP	10104	regulation of ethylene-activated signaling pathway	1.28E-11	6.38E-10	7/110 6.3%	52/55204 0.0%	Upregulated
BP	6952	defense response	1.49E-10	7.00E-09	26/110 23.6%	2990/55204 5.4%	Upregulated
BP	50896	response to stimulus	1.62E-10	7.13E-09	61/110 55.4%	14712/55204 26.6%	Upregulated
BP	35556	intracellular signal transduction	1.97E-10	8.21E-09	18/110 16.3%	1345/55204 2.4%	Upregulated
BP	9699	phenylpropanoid biosynthetic process	3.54E-10	1.40E-08	10/110 9.0%	286/55204 0.5%	Upregulated
BP	6950	response to stress	2.86E-09	1.07E-07	45/110 40.9%	9393/55204 17.0%	Upregulated
BP	9698	phenylpropanoid metabolic process	7.80E-09	2.79E-07	10/110 9.0%	395/55204 0.7%	Upregulated
BP	6355	regulation of DNA-templated transcription	1.46E-08	4.80E-07	21/110 19.0%	2446/55204 4.4%	Upregulated
BP	2001141	regulation of RNA biosynthetic process	1.47E-08	4.80E-07	21/110 19.0%	2447/55204 4.4%	Upregulated
BP	51252	regulation of RNA metabolic process	4.37E-08	1.36E-06	22/110 20.0%	2858/55204 5.1%	Upregulated
BP	120255	olefinic compound biosynthetic process	9.35E-08	2.81E-06	7/110 6.3%	183/55204 0.3%	Upregulated
BP	19219	regulation of nucleobase-containing compound metabolic process	1.80E-07	5.18E-06	22/110 20.0%	3101/55204 5.6%	Upregulated
BP	23052	signaling	2.74E-07	7.62E-06	25/110 22.7%	4021/55204 7.2%	Upregulated
BP	43449	alkene metabolic process	3.36E-07	8.13E-06	5/110 4.5%	71/55204 0.1%	Upregulated
BP	43450	alkene biosynthetic process	3.36E-07	8.13E-06	5/110 4.5%	71/55204 0.1%	Upregulated
BP	9692	ethylene metabolic process	3.36E-07	8.13E-06	5/110 4.5%	71/55204 0.1%	Upregulated
BP	9693	ethylene biosynthetic process	3.36E-07	8.13E-06	5/110 4.5%	71/55204 0.1%	Upregulated
BP	1900673	olefin metabolic process	3.61E-07	8.19E-06	5/110 4.5%	72/55204 0.1%	Upregulated
BP	1900674	olefin biosynthetic process	3.61E-07	8.19E-06	5/110 4.5%	72/55204 0.1%	Upregulated
BP	71456	cellular response to hypoxia	6.36E-07	1.40E-05	7/110 6.3%	243/55204 0.4%	Upregulated
BP	36294	cellular response to decreased oxygen levels	6.71E-07	1.44E-05	7/110 6.3%	245/55204 0.4%	Upregulated
BP	71453	cellular response to oxygen levels	7.48E-07	1.56E-05	7/110 6.3%	249/55204 0.4%	Upregulated
BP	7154	cell communication	1.16E-06	2.20E-05	24/110 21.8%	4047/55204 7.3%	Upregulated
BP	70298	negative regulation of phosphorelay signal transduction system	1.16E-06	2.20E-05	4/110 3.6%	39/55204 0.0%	Upregulated
BP	10105	negative regulation of ethylene-activated signaling pathway	1.16E-06	2.20E-05	4/110 3.6%	39/55204 0.0%	Upregulated
BP	45893	positive regulation of DNA-templated transcription	1.19E-06	2.20E-05	10/110 9.0%	681/55204 1.2%	Upregulated
BP	1902680	positive regulation of RNA biosynthetic process	1.20E-06	2.20E-05	10/110 9.0%	682/55204 1.2%	Upregulated
BP	120254	olefinic compound metabolic process	2.36E-06	4.21E-05	7/110 6.3%	296/55204 0.5%	Upregulated
BP	7165	signal transduction	2.63E-06	4.59E-05	23/110 20.9%	3938/55204 7.1%	Upregulated
BP	51254	positive regulation of RNA metabolic process	3.74E-06	6.38E-05	11/110 10.0%	961/55204 1.7%	Upregulated
BP	80090	regulation of primary metabolic process	5.29E-06	8.82E-05	24/110 21.8%	4417/55204 8.0%	Upregulated
BP	9809	lignin biosynthetic process	6.48E-06	1.06E-04	5/110 4.5%	129/55204 0.2%	Upregulated
BP	45935	positive regulation of nucleobase-containing compound metabolic process	8.38E-06	1.34E-04	11/110 10.0%	1047/55204 1.8%	Upregulated
BP	1666	response to hypoxia	8.62E-06	1.35E-04	7/110 6.3%	361/55204 0.6%	Upregulated
BP	9891	positive regulation of biosynthetic process	1.10E-05	1.68E-04	12/110 10.9%	1292/55204 2.3%	Upregulated
BP	36293	response to decreased oxygen levels	1.31E-05	1.96E-04	7/110 6.3%	385/55204 0.6%	Upregulated

Table S5.3 continued.

BP	6412	translation	1.31E-19	8.94E-17	51/145 35.1%	4607/55204 8.3%	Downregulated
BP	15979	photosynthesis	4.64E-10	1.59E-07	28/145 19.3%	2707/55204 4.9%	Downregulated
BP	2181	cytoplasmic translation	8.67E-10	1.98E-07	16/145 11.0%	838/55204 1.5%	Downregulated
BP	9765	photosynthesis, light harvesting	1.48E-08	2.54E-06	15/145 10.3%	886/55204 1.6%	Downregulated
BP	10467	gene expression	2.65E-08	3.63E-06	58/145 40.0%	11047/55204 20.0%	Downregulated
BP	9059	macromolecule biosynthetic process	1.14E-07	1.30E-05	60/145 41.3%	12110/55204 21.9%	Downregulated
BP	19684	photosynthesis, light reaction	6.28E-07	6.15E-05	16/145 11.0%	1354/55204 2.4%	Downregulated
BP	19538	protein metabolic process	2.93E-06	2.51E-04	63/145 43.4%	14238/55204 25.7%	Downregulated
BP	6091	generation of precursor metabolites and energy	1.34E-05	1.02E-03	25/145 17.2%	3720/55204 6.7%	Downregulated
BP	6414	translational elongation	2.55E-05	1.74E-03	7/145 4.8%	323/55204 0.5%	Downregulated
BP	9058	biosynthetic process	7.00E-05	4.36E-03	79/145 54.4%	21272/55204 38.5%	Downregulated
BP	2182	cytoplasmic translational elongation	7.84E-05	4.47E-03	4/145 2.7%	85/55204 0.1%	Downregulated
BP	7017	microtubule-based process	6.93E-04	3.65E-02	9/145 6.2%	906/55204 1.6%	Downregulated
BP	51607	defense response to virus	9.37E-04	4.58E-02	4/145 2.7%	163/55204 0.2%	Downregulated

Table S5.4. Significantly enriched GO terms (Biological Process) associated with genes that were differentially expressed between the resistant juniper genotype inoculated with the more virulent *P. austrocedri* isolate compared to the same genotype's mock-inoculated control at 48 hours post-inoculation.

GO	GO ID	GO Description	p-val	Corrected p-val	Cluster frequency	Total frequency	Direction
BP	6412	translation	2.42E-05	2.73E-03	15/54 27.7%	4607/55204 8.3%	Upregulated
BP	43449	alkene metabolic process	4.82E-05	2.73E-03	3/54 5.5%	71/55204 0.1%	Upregulated
BP	43450	alkene biosynthetic process	4.82E-05	2.73E-03	3/54 5.5%	71/55204 0.1%	Upregulated
BP	9692	ethylene metabolic process	4.82E-05	2.73E-03	3/54 5.5%	71/55204 0.1%	Upregulated
BP	9693	ethylene biosynthetic process	4.82E-05	2.73E-03	3/54 5.5%	71/55204 0.1%	Upregulated
BP	1900673	olefin metabolic process	5.03E-05	2.73E-03	3/54 5.5%	72/55204 0.1%	Upregulated
BP	1900674	olefin biosynthetic process	5.03E-05	2.73E-03	3/54 5.5%	72/55204 0.1%	Upregulated
BP	9835	fruit ripening	6.39E-05	3.04E-03	3/54 5.5%	78/55204 0.1%	Upregulated
BP	120251	hydrocarbon biosynthetic process	7.48E-04	2.98E-02	3/54 5.5%	180/55204 0.3%	Upregulated
BP	120255	olefinic compound biosynthetic process	7.85E-04	2.98E-02	3/54 5.5%	183/55204 0.3%	Upregulated
BP	1901336	lactone biosynthetic process	9.15E-04	3.16E-02	3/54 5.5%	193/55204 0.3%	Upregulated
BP	10555	response to mannitol	1.35E-03	3.89E-02	2/54 3.7%	55/55204 0.0%	Upregulated
BP	1901334	lactone metabolic process	1.50E-03	3.89E-02	3/54 5.5%	229/55204 0.4%	Upregulated
BP	120252	hydrocarbon metabolic process	1.50E-03	3.89E-02	3/54 5.5%	229/55204 0.4%	Upregulated
BP	21700	developmental maturation	1.54E-03	3.89E-02	4/54 7.4%	506/55204 0.9%	Upregulated
BP	18969	thiocyanate metabolic process	1.96E-03	3.93E-02	1/54 1.8%	2/55204 0.0%	Upregulated
BP	46265	thiocyanate catabolic process	1.96E-03	3.93E-02	1/54 1.8%	2/55204 0.0%	Upregulated
BP	31034	myosin filament assembly	1.96E-03	3.93E-02	1/54 1.8%	2/55204 0.0%	Upregulated
BP	43467	regulation of generation of precursor metabolites and energy	1.96E-03	3.93E-02	3/54 5.5%	252/55204 0.4%	Upregulated
BP	6412	translation	7.64E-11	3.64E-08	25/68 36.7%	4607/55204 8.3%	Downregulated
BP	9765	photosynthesis, light harvesting	1.14E-08	2.72E-06	11/68 16.1%	886/55204 1.6%	Downregulated
BP	19684	photosynthesis, light reaction	9.27E-08	1.47E-05	12/68 17.6%	1354/55204 2.4%	Downregulated
BP	10467	gene expression	5.67E-06	6.76E-04	30/68 44.1%	11047/55204 20.0%	Downregulated
BP	6091	generation of precursor metabolites and energy	8.86E-06	8.45E-04	16/68 23.5%	3720/55204 6.7%	Downregulated
BP	9059	macromolecule biosynthetic process	1.25E-05	9.95E-04	31/68 45.5%	12110/55204 21.9%	Downregulated
BP	15979	photosynthesis	2.30E-05	1.57E-03	13/68 19.1%	2707/55204 4.9%	Downregulated
BP	2181	cytoplasmic translation	5.92E-04	3.53E-02	6/68 8.8%	838/55204 1.5%	Downregulated
BP	6123	mitochondrial electron transport, cytochrome c to oxygen	6.79E-04	3.60E-02	2/68 2.9%	31/55204 0.0%	Downregulated
BP	60600	dichotomous subdivision of an epithelial terminal unit	1.23E-03	4.58E-02	1/68 1.4%	1/55204 0.0%	Downregulated
BP	15988	energy coupled proton transmembrane transport, against electrochemical gradient	1.25E-03	4.58E-02	2/68 2.9%	42/55204 0.0%	Downregulated
BP	15990	electron transport coupled proton transport	1.25E-03	4.58E-02	2/68 2.9%	42/55204 0.0%	Downregulated

Table S5.5. Significantly enriched GO terms (Biological Process) associated with genes that were differentially expressed between the susceptible juniper genotype inoculated with the less virulent *P. austrocedri* isolate compared to the same genotype's mock-inoculated control at one week post-inoculation. Where relevant, only the top 50 GO terms have been included for each direction (upregulated and downregulated).

GO	GO ID	GO Description	p-val	Corrected p-val	Cluster frequency	Total frequency	Direction
BP	6412	translation	4.24E-25	9.67E-22	184/989 18.6%	4607/55204 8.3%	Upregulated
BP	9451	RNA modification	2.43E-24	2.77E-21	119/989 12.0%	2344/55204 4.2%	Upregulated
BP	10467	gene expression	4.93E-15	3.75E-12	300/989 30.3%	11047/55204 20.0%	Upregulated
BP	16556	mRNA modification	6.99E-15	3.99E-12	43/989 4.3%	578/55204 1.0%	Upregulated
BP	9059	macromolecule biosynthetic process	1.30E-13	5.94E-11	316/989 31.9%	12110/55204 21.9%	Upregulated
BP	959	mitochondrial RNA metabolic process	6.87E-11	2.61E-08	30/989 3.0%	400/55204 0.7%	Upregulated
BP	80156	mitochondrial mRNA modification	1.32E-10	4.29E-08	27/989 2.7%	336/55204 0.6%	Upregulated
BP	1900864	mitochondrial RNA modification	3.95E-10	1.13E-07	27/989 2.7%	353/55204 0.6%	Upregulated
BP	9806	lignan metabolic process	1.54E-07	3.51E-05	7/989 0.7%	24/55204 0.0%	Upregulated
BP	9807	lignan biosynthetic process	1.54E-07	3.51E-05	7/989 0.7%	24/55204 0.0%	Upregulated
BP	9699	phenylpropanoid biosynthetic process	3.07E-07	6.36E-05	20/989 2.0%	286/55204 0.5%	Upregulated
BP	16070	RNA metabolic process	1.45E-06	2.70E-04	183/989 18.5%	7301/55204 13.2%	Upregulated
BP	9058	biosynthetic process	1.54E-06	2.70E-04	453/989 45.8%	21272/55204 38.5%	Upregulated
BP	19748	secondary metabolic process	2.07E-06	2.96E-04	28/989 2.8%	569/55204 1.0%	Upregulated
BP	16553	base conversion or substitution editing	2.18E-06	2.96E-04	15/989 1.5%	191/55204 0.3%	Upregulated
BP	16554	cytidine to uridine editing	2.19E-06	2.96E-04	14/989 1.4%	167/55204 0.3%	Upregulated
BP	44550	secondary metabolite biosynthetic process	2.20E-06	2.96E-04	22/989 2.2%	383/55204 0.6%	Upregulated
BP	963	mitochondrial RNA processing	6.31E-06	8.00E-04	12/989 1.2%	135/55204 0.2%	Upregulated
BP	43170	macromolecule metabolic process	1.14E-05	1.37E-03	478/989 48.3%	23000/55204 41.6%	Upregulated
BP	9698	phenylpropanoid metabolic process	1.21E-05	1.38E-03	21/989 2.1%	395/55204 0.7%	Upregulated
BP	45490	pectin catabolic process	2.24E-05	2.43E-03	9/989 0.9%	85/55204 0.1%	Upregulated
BP	42255	ribosome assembly	3.55E-05	3.68E-03	18/989 1.8%	330/55204 0.5%	Upregulated
BP	43412	macromolecule modification	5.43E-05	5.38E-03	171/989 17.2%	7166/55204 12.9%	Upregulated
BP	8202	steroid metabolic process	1.70E-04	1.62E-02	23/989 2.3%	546/55204 0.9%	Upregulated
BP	45488	pectin metabolic process	1.81E-04	1.65E-02	12/989 1.2%	190/55204 0.3%	Upregulated
BP	16094	polyprenol biosynthetic process	1.90E-04	1.67E-02	3/989 0.3%	7/55204 0.0%	Upregulated
BP	42274	ribosomal small subunit biogenesis	2.05E-04	1.73E-02	21/989 2.1%	482/55204 0.8%	Upregulated
BP	10393	galacturonan metabolic process	2.20E-04	1.79E-02	12/989 1.2%	194/55204 0.3%	Upregulated
BP	140694	membraneless organelle assembly	2.49E-04	1.96E-02	20/989 2.0%	454/55204 0.8%	Upregulated
BP	6694	steroid biosynthetic process	2.68E-04	2.04E-02	19/989 1.9%	422/55204 0.7%	Upregulated
BP	6678	glucosylceramide metabolic process	3.21E-04	2.29E-02	2/989 0.2%	2/55204 0.0%	Upregulated
BP	6680	glucosylceramide catabolic process	3.21E-04	2.29E-02	2/989 0.2%	2/55204 0.0%	Upregulated
BP	42254	ribosome biogenesis	3.65E-04	2.53E-02	51/989 5.1%	1717/55204 3.1%	Upregulated
BP	16093	polyprenol metabolic process	4.44E-04	2.98E-02	3/989 0.3%	9/55204 0.0%	Upregulated
BP	72655	establishment of protein localization to mitochondrion	5.86E-04	3.82E-02	9/989 0.9%	130/55204 0.2%	Upregulated
BP	21954	central nervous system neuron development	6.26E-04	3.97E-02	3/989 0.3%	10/55204 0.0%	Upregulated
BP	6119	oxidative phosphorylation	6.94E-04	4.28E-02	16/989 1.6%	351/55204 0.6%	Upregulated
BP	140053	mitochondrial gene expression	7.51E-04	4.51E-02	13/989 1.3%	254/55204 0.4%	Upregulated
BP	50896	response to stimulus	3.62E-43	1.15E-39	738/1780 41.4%	14712/55204 26.6%	Downregulated
BP	65007	biological regulation	1.87E-41	2.97E-38	643/1780 36.1%	12316/55204 22.3%	Downregulated
BP	50789	regulation of biological process	2.70E-40	2.86E-37	615/1780 34.5%	11681/55204 21.1%	Downregulated
BP	9725	response to hormone	2.51E-36	1.99E-33	225/1780 12.6%	2818/55204 5.1%	Downregulated
BP	9719	response to endogenous stimulus	1.16E-35	7.00E-33	225/1780 12.6%	2847/55204 5.1%	Downregulated
BP	50794	regulation of cellular process	1.32E-35	7.00E-33	557/1780 31.2%	10579/55204 19.1%	Downregulated
BP	6355	regulation of DNA-templated transcription	3.71E-33	1.55E-30	199/1780 11.1%	2446/55204 4.4%	Downregulated
BP	2001141	regulation of RNA biosynthetic process	3.91E-33	1.55E-30	199/1780 11.1%	2447/55204 4.4%	Downregulated
BP	6952	defense response	1.08E-31	3.80E-29	223/1780 12.5%	2990/55204 5.4%	Downregulated
BP	9755	hormone-mediated signaling pathway	3.10E-30	9.83E-28	151/1780 8.4%	1661/55204 3.0%	Downregulated
BP	32870	cellular response to hormone stimulus	7.83E-29	2.26E-26	157/1780 8.8%	1823/55204 3.3%	Downregulated
BP	19219	regulation of nucleobase-containing compound metabolic process	2.80E-28	7.40E-26	220/1780 12.3%	3101/55204 5.6%	Downregulated
BP	71495	cellular response to endogenous stimulus	4.55E-28	1.11E-25	157/1780 8.8%	1853/55204 3.3%	Downregulated
BP	23052	signaling	5.72E-27	1.30E-24	259/1780 14.5%	4021/55204 7.2%	Downregulated
BP	7154	cell communication	6.55E-27	1.39E-24	260/1780 14.6%	4047/55204 7.3%	Downregulated
BP	51252	regulation of RNA metabolic process	1.53E-26	3.00E-24	204/1780 11.4%	2858/55204 5.1%	Downregulated
BP	7165	signal transduction	1.61E-26	3.00E-24	254/1780 14.2%	3938/55204 7.1%	Downregulated
BP	9605	response to external stimulus	1.14E-25	2.02E-23	223/1780 12.5%	3310/55204 5.9%	Downregulated
BP	6950	response to stress	2.98E-25	4.98E-23	474/1780 26.6%	9393/55204 17.0%	Downregulated
BP	42221	response to chemical	2.86E-24	4.54E-22	363/1780 20.3%	6671/55204 12.0%	Downregulated
BP	51707	response to other organism	7.92E-23	1.19E-20	191/1780 10.7%	2787/55204 5.0%	Downregulated
BP	43207	response to external biotic stimulus	8.24E-23	1.19E-20	191/1780 10.7%	2788/55204 5.0%	Downregulated
BP	9733	response to auxin	1.62E-22	2.16E-20	79/1780 4.4%	683/55204 1.2%	Downregulated
BP	9607	response to biotic stimulus	1.63E-22	2.16E-20	191/1780 10.7%	2805/55204 5.0%	Downregulated
BP	9889	regulation of biosynthetic process	3.82E-22	4.86E-20	282/1780 15.8%	4888/55204 8.8%	Downregulated
BP	19222	regulation of metabolic process	1.33E-21	1.62E-19	331/1780 18.5%	6117/55204 11.0%	Downregulated
BP	10468	regulation of gene expression	1.83E-21	2.10E-19	260/1780 14.6%	4423/55204 8.0%	Downregulated

Table S5.5 continued.

BP	44419	biological process involved in interspecies interaction between organisms	1.86E-21	2.10E-19	191/1780 10.7%	2867/55204 5.1%	Downregulated
BP	10556	regulation of macromolecule biosynthetic process	3.69E-21	4.04E-19	264/1780 14.8%	4540/55204 8.2%	Downregulated
BP	51716	cellular response to stimulus	3.10E-20	3.28E-18	396/1780 22.2%	7888/55204 14.2%	Downregulated
BP	60255	regulation of macromolecule metabolic process	3.22E-20	3.30E-18	283/1780 15.8%	5068/55204 9.1%	Downregulated
BP	80090	regulation of primary metabolic process	2.00E-19	1.98E-17	253/1780 14.2%	4417/55204 8.0%	Downregulated
BP	48367	shoot system development	3.33E-19	3.20E-17	126/1780 7.0%	1637/55204 2.9%	Downregulated
BP	71365	cellular response to auxin stimulus	4.87E-18	4.55E-16	57/1780 3.2%	459/55204 0.8%	Downregulated
BP	7275	multicellular organism development	3.82E-17	3.47E-15	308/1780 17.3%	5966/55204 10.8%	Downregulated
BP	9734	auxin-activated signaling pathway	1.22E-16	1.05E-14	54/1780 3.0%	447/55204 0.8%	Downregulated
BP	70887	cellular response to chemical stimulus	1.23E-16	1.05E-14	213/1780 11.9%	3698/55204 6.6%	Downregulated
BP	99402	plant organ development	5.66E-16	4.73E-14	137/1780 7.6%	2034/55204 3.6%	Downregulated
BP	48731	system development	1.28E-15	1.04E-13	254/1780 14.2%	4773/55204 8.6%	Downregulated
BP	48856	anatomical structure development	1.51E-15	1.20E-13	343/1780 19.2%	7032/55204 12.7%	Downregulated
BP	32502	developmental process	1.95E-15	1.51E-13	351/1780 19.7%	7253/55204 13.1%	Downregulated
BP	48580	regulation of post-embryonic development	1.54E-14	1.16E-12	69/1780 3.8%	755/55204 1.3%	Downregulated
BP	32501	multicellular organismal process	1.65E-14	1.22E-12	325/1780 18.2%	6686/55204 12.1%	Downregulated
BP	9617	response to bacterium	1.86E-13	1.34E-11	93/1780 5.2%	1258/55204 2.2%	Downregulated
BP	33993	response to lipid	2.21E-13	1.56E-11	130/1780 7.3%	2045/55204 3.7%	Downregulated
BP	1901700	response to oxygen-containing compound	4.47E-13	3.08E-11	222/1780 12.4%	4232/55204 7.6%	Downregulated
BP	48583	regulation of response to stimulus	1.71E-12	1.16E-10	152/1780 8.5%	2607/55204 4.7%	Downregulated
BP	9628	response to abiotic stimulus	2.15E-12	1.42E-10	267/1780 15.0%	5438/55204 9.8%	Downregulated
BP	9791	post-embryonic development	4.60E-12	2.98E-10	178/1780 10.0%	3257/55204 5.8%	Downregulated
BP	90567	reproductive shoot system development	1.01E-11	6.40E-10	71/1780 3.9%	906/55204 1.6%	Downregulated

Table S5.6. Significantly enriched GO terms (Biological Process) associated with genes that were differentially expressed between the susceptible juniper genotype inoculated with the more virulent *P. austrocedri* isolate compared to the same genotype's mock-inoculated control at one week post-inoculation. Where relevant, only the top 50 GO terms have been included for each direction (upregulated and downregulated).

GO	GO ID	GO Description	p-val	Corrected p-val	Cluster frequency	Total frequency	Direction
BP	6412	translation	1.16E-19	2.73E-16	175/1029 17.0%	4607/55204 8.3%	Upregulated
BP	9813	flavonoid biosynthetic process	3.46E-14	4.06E-11	25/1029 2.4%	192/55204 0.3%	Upregulated
BP	9812	flavonoid metabolic process	1.31E-12	1.02E-09	25/1029 2.4%	225/55204 0.4%	Upregulated
BP	9699	phenylpropanoid biosynthetic process	4.52E-11	2.65E-08	26/1029 2.5%	286/55204 0.5%	Upregulated
BP	44550	secondary metabolite biosynthetic process	6.15E-11	2.89E-08	30/1029 2.9%	383/55204 0.6%	Upregulated
BP	6694	steroid biosynthetic process	6.33E-10	2.48E-07	30/1029 2.9%	422/55204 0.7%	Upregulated
BP	9698	phenylpropanoid metabolic process	2.49E-09	8.36E-07	28/1029 2.7%	395/55204 0.7%	Upregulated
BP	19748	secondary metabolic process	4.17E-09	1.22E-06	34/1029 3.3%	569/55204 1.0%	Upregulated
BP	8202	steroid metabolic process	1.86E-08	4.86E-06	32/1029 3.1%	546/55204 0.9%	Upregulated
BP	9806	lignan metabolic process	2.01E-07	3.97E-05	7/1029 0.6%	24/55204 0.0%	Upregulated
BP	9807	lignan biosynthetic process	2.01E-07	3.97E-05	7/1029 0.6%	24/55204 0.0%	Upregulated
BP	9451	RNA modification	2.03E-07	3.97E-05	80/1029 7.7%	2344/55204 4.2%	Upregulated
BP	9058	biosynthetic process	5.62E-07	1.02E-04	473/1029 45.9%	21272/55204 38.5%	Upregulated
BP	19287	isopentenyl diphosphate biosynthetic process, mevalonate pathway	1.40E-05	2.32E-03	4/1029 0.3%	9/55204 0.0%	Upregulated
BP	10467	gene expression	1.48E-05	2.32E-03	261/1029 25.3%	11047/55204 20.0%	Upregulated
BP	42274	ribosomal small subunit biogenesis	1.70E-05	2.49E-03	24/1029 2.3%	482/55204 0.8%	Upregulated
BP	9059	macromolecule biosynthetic process	2.40E-05	3.31E-03	281/1029 27.3%	12110/55204 21.9%	Upregulated
BP	16126	sterol biosynthetic process	9.70E-05	1.26E-02	12/1029 1.1%	171/55204 0.3%	Upregulated
BP	30490	maturation of SSU-rRNA	1.16E-04	1.44E-02	14/1029 1.3%	229/55204 0.4%	Upregulated
BP	10023	proanthocyanidin biosynthetic process	1.39E-04	1.63E-02	4/1029 0.3%	15/55204 0.0%	Upregulated
BP	42775	mitochondrial ATP synthesis coupled electron transport	1.59E-04	1.70E-02	14/1029 1.3%	236/55204 0.4%	Upregulated
BP	6012	galactose metabolic process	1.60E-04	1.70E-02	9/1029 0.8%	105/55204 0.1%	Upregulated
BP	1900366	negative regulation of defense response to insect	1.83E-04	1.86E-02	4/1029 0.3%	16/55204 0.0%	Upregulated
BP	16137	glycoside metabolic process	1.92E-04	1.87E-02	8/1029 0.7%	85/55204 0.1%	Upregulated
BP	16125	sterol metabolic process	2.01E-04	1.87E-02	15/1029 1.4%	271/55204 0.4%	Upregulated
BP	19646	aerobic electron transport chain	2.07E-04	1.87E-02	14/1029 1.3%	242/55204 0.4%	Upregulated
BP	6678	glucosylceramide metabolic process	3.47E-04	2.91E-02	2/1029 0.1%	2/55204 0.0%	Upregulated
BP	6680	glucosylceramide catabolic process	3.47E-04	2.91E-02	2/1029 0.1%	2/55204 0.0%	Upregulated
BP	1902223	erythrose 4-phosphate/phosphoenolpyruvate family amino acid biosynthetic process	4.43E-04	3.59E-02	8/1029 0.7%	96/55204 0.1%	Upregulated
BP	42255	ribosome assembly	5.47E-04	4.28E-02	16/1029 1.5%	330/55204 0.5%	Upregulated
BP	71669	plant-type cell wall organization or biogenesis	6.41E-04	4.71E-02	17/1029 1.6%	368/55204 0.6%	Upregulated
BP	16556	mRNA modification	6.52E-04	4.71E-02	23/1029 2.2%	578/55204 1.0%	Upregulated
BP	462	maturation of SSU-rRNA from tricistronic rRNA transcript (SSU-rRNA, 5.8S rRNA, LSU-rRNA)	6.67E-04	4.71E-02	10/1029 0.9%	154/55204 0.2%	Upregulated
BP	1990961	xenobiotic detoxification by transmembrane export across the plasma membrane	6.93E-04	4.71E-02	7/1029 0.6%	79/55204 0.1%	Upregulated
BP	21954	central nervous system neuron development	7.03E-04	4.71E-02	3/1029 0.2%	10/55204 0.0%	Upregulated
BP	50896	response to stimulus	1.24E-53	3.98E-50	790/1836 43.0%	14712/55204 26.6%	Downregulated
BP	6952	defense response	2.69E-47	4.34E-44	262/1836 14.2%	2990/55204 5.4%	Downregulated
BP	9725	response to hormone	2.88E-39	3.09E-36	236/1836 12.8%	2818/55204 5.1%	Downregulated
BP	9719	response to endogenous stimulus	5.08E-39	4.09E-36	237/1836 12.9%	2847/55204 5.1%	Downregulated
BP	9605	response to external stimulus	2.79E-37	1.80E-34	257/1836 13.9%	3310/55204 5.9%	Downregulated
BP	65007	biological regulation	1.85E-36	9.92E-34	642/1836 34.9%	12316/55204 22.3%	Downregulated
BP	50789	regulation of biological process	8.21E-36	3.78E-33	615/1836 33.4%	11681/55204 21.1%	Downregulated
BP	6950	response to stress	8.21E-34	3.30E-31	517/1836 28.1%	9393/55204 17.0%	Downregulated
BP	9607	response to biotic stimulus	7.58E-33	2.52E-30	221/1836 12.0%	2805/55204 5.0%	Downregulated
BP	51707	response to other organism	8.18E-33	2.52E-30	220/1836 11.9%	2787/55204 5.0%	Downregulated
BP	43207	response to external biotic stimulus	8.61E-33	2.52E-30	220/1836 11.9%	2788/55204 5.0%	Downregulated
BP	44419	biological process involved in interspecies interaction between organisms	1.69E-31	4.52E-29	221/1836 12.0%	2867/55204 5.1%	Downregulated
BP	50794	regulation of cellular process	2.08E-31	5.15E-29	556/1836 30.2%	10579/55204 19.1%	Downregulated
BP	7154	cell communication	4.25E-29	9.77E-27	272/1836 14.8%	4047/55204 7.3%	Downregulated
BP	42221	response to chemical	5.28E-29	1.13E-26	388/1836 21.1%	6671/55204 12.0%	Downregulated
BP	23052	signaling	1.87E-28	3.76E-26	269/1836 14.6%	4021/55204 7.2%	Downregulated
BP	7165	signal transduction	2.09E-28	3.95E-26	265/1836 14.4%	3938/55204 7.1%	Downregulated
BP	9755	hormone-mediated signaling pathway	7.20E-27	1.29E-24	147/1836 8.0%	1661/55204 3.0%	Downregulated
BP	32870	cellular response to hormone stimulus	4.22E-25	7.16E-23	152/1836 8.2%	1823/55204 3.3%	Downregulated
BP	71495	cellular response to endogenous stimulus	7.84E-25	1.26E-22	153/1836 8.3%	1853/55204 3.3%	Downregulated
BP	51716	cellular response to stimulus	1.76E-22	2.69E-20	415/1836 22.6%	7888/55204 14.2%	Downregulated
BP	6355	regulation of DNA-templated transcription	3.05E-22	4.45E-20	177/1836 9.6%	2446/55204 4.4%	Downregulated
BP	2001141	regulation of RNA biosynthetic process	3.18E-22	4.45E-20	177/1836 9.6%	2447/55204 4.4%	Downregulated
BP	9733	response to auxin	4.17E-21	5.59E-19	78/1836 4.2%	683/55204 1.2%	Downregulated

Table S5.6 continued.

BP	19219	regulation of nucleobase-containing compound metabolic process	1.11E-19	1.43E-17	201/1836 10.9%	3101/55204 5.6%	Downregulated
BP	51252	regulation of RNA metabolic process	1.94E-17	2.40E-15	183/1836 9.9%	2858/55204 5.1%	Downregulated
BP	99402	plant organ development	2.01E-17	2.40E-15	144/1836 7.8%	2034/55204 3.6%	Downregulated
BP	70887	cellular response to chemical stimulus	3.25E-17	3.74E-15	220/1836 11.9%	3698/55204 6.6%	Downregulated
BP	48367	shoot system development	6.20E-17	6.89E-15	123/1836 6.6%	1637/55204 2.9%	Downregulated
BP	9617	response to bacterium	8.57E-17	9.19E-15	103/1836 5.6%	1258/55204 2.2%	Downregulated
BP	71365	cellular response to auxin stimulus	3.40E-16	3.53E-14	55/1836 2.9%	459/55204 0.8%	Downregulated
BP	42742	defense response to bacterium	9.59E-16	9.65E-14	80/1836 4.3%	881/55204 1.5%	Downregulated
BP	9889	regulation of biosynthetic process	1.30E-15	1.27E-13	265/1836 14.4%	4888/55204 8.8%	Downregulated
BP	19222	regulation of metabolic process	1.63E-15	1.55E-13	315/1836 17.1%	6117/55204 11.0%	Downregulated
BP	9734	auxin-activated signaling pathway	1.82E-15	1.68E-13	53/1836 2.8%	447/55204 0.8%	Downregulated
BP	33993	response to lipid	4.33E-15	3.87E-13	138/1836 7.5%	2045/55204 3.7%	Downregulated
BP	1901700	response to oxygen-containing compound	1.01E-14	8.77E-13	234/1836 12.7%	4232/55204 7.6%	Downregulated
BP	9626	plant-type hypersensitive response	1.83E-14	1.54E-12	39/1836 2.1%	271/55204 0.4%	Downregulated
BP	10468	regulation of gene expression	1.86E-14	1.54E-12	241/1836 13.1%	4423/55204 8.0%	Downregulated
BP	34050	symbiont-induced defense-related programmed cell death	2.07E-14	1.66E-12	39/1836 2.1%	272/55204 0.4%	Downregulated
BP	9628	response to abiotic stimulus	3.07E-14	2.36E-12	282/1836 15.3%	5438/55204 9.8%	Downregulated
BP	10556	regulation of macromolecule biosynthetic process	3.11E-14	2.36E-12	245/1836 13.3%	4540/55204 8.2%	Downregulated
BP	98542	defense response to other organism	3.15E-14	2.36E-12	75/1836 4.0%	849/55204 1.5%	Downregulated
BP	9620	response to fungus	5.32E-14	3.90E-12	73/1836 3.9%	822/55204 1.4%	Downregulated
BP	60255	regulation of macromolecule metabolic process	1.46E-13	1.05E-11	264/1836 14.3%	5068/55204 9.1%	Downregulated
BP	7275	multicellular organism development	2.02E-12	1.42E-10	295/1836 16.0%	5966/55204 10.8%	Downregulated
BP	45087	innate immune response	2.21E-12	1.51E-10	61/1836 3.3%	670/55204 1.2%	Downregulated
BP	80090	regulation of primary metabolic process	2.53E-12	1.69E-10	232/1836 12.6%	4417/55204 8.0%	Downregulated
BP	5976	polysaccharide metabolic process	4.13E-12	2.71E-10	91/1836 4.9%	1249/55204 2.2%	Downregulated
BP	48731	system development	5.77E-12	3.71E-10	245/1836 13.3%	4773/55204 8.6%	Downregulated

Table S5.7. Significantly enriched GO terms (Biological Process) associated with genes that were differentially expressed between the resistant juniper genotype inoculated with the less virulent *P. austrocedri* isolate compared to the same genotype's mock-inoculated control at one week post-inoculation.

GO	GO ID	GO Description	p-val	Corrected p-val	Cluster frequency	Total frequency	Direction
BP	1901072	glucosamine-containing compound catabolic process	3.82E-21	8.71E-19	12/91 13.1%	74/55204 0.1%	Upregulated
BP	6032	chitin catabolic process	3.82E-21	8.71E-19	12/91 13.1%	74/55204 0.1%	Upregulated
BP	16998	cell wall macromolecule catabolic process	5.89E-21	8.71E-19	11/91 12.0%	51/55204 0.0%	Upregulated
BP	46348	amino sugar catabolic process	7.52E-21	8.71E-19	12/91 13.1%	78/55204 0.1%	Upregulated
BP	6030	chitin metabolic process	7.52E-21	8.71E-19	12/91 13.1%	78/55204 0.1%	Upregulated
BP	6026	aminoglycan catabolic process	1.94E-20	1.87E-18	12/91 13.1%	84/55204 0.1%	Upregulated
BP	1901071	glucosamine-containing compound metabolic process	7.07E-20	5.85E-18	12/91 13.1%	93/55204 0.1%	Upregulated
BP	6022	aminoglycan metabolic process	4.23E-18	3.06E-16	12/91 13.1%	129/55204 0.2%	Upregulated
BP	6040	amino sugar metabolic process	2.50E-17	1.61E-15	12/91 13.1%	149/55204 0.2%	Upregulated
BP	44036	cell wall macromolecule metabolic process	1.61E-15	9.34E-14	11/91 12.0%	150/55204 0.2%	Upregulated
BP	272	polysaccharide catabolic process	3.54E-15	1.86E-13	16/91 17.5%	597/55204 1.0%	Upregulated
BP	16052	carbohydrate catabolic process	1.01E-14	4.88E-13	21/91 23.0%	1395/55204 2.5%	Upregulated
BP	1901136	carbohydrate derivative catabolic process	1.04E-12	4.64E-11	16/91 17.5%	867/55204 1.5%	Upregulated
BP	5976	polysaccharide metabolic process	2.28E-11	9.44E-10	17/91 18.6%	1249/55204 2.2%	Upregulated
BP	5975	carbohydrate metabolic process	1.75E-10	6.76E-09	27/91 29.6%	4025/55204 7.2%	Upregulated
BP	141060	disruption of anatomical structure in another organism	3.94E-09	1.27E-07	5/91 5.4%	36/55204 0.0%	Upregulated
BP	141061	disruption of cell in another organism	3.94E-09	1.27E-07	5/91 5.4%	36/55204 0.0%	Upregulated
BP	31640	killing of cells of another organism	3.94E-09	1.27E-07	5/91 5.4%	36/55204 0.0%	Upregulated
BP	71554	cell wall organization or biogenesis	7.17E-09	2.19E-07	13/91 14.2%	965/55204 1.7%	Upregulated
BP	1906	cell killing	8.83E-09	2.56E-07	5/91 5.4%	42/55204 0.0%	Upregulated
BP	9056	catabolic process	6.57E-07	1.81E-05	30/91 32.9%	7138/55204 12.9%	Upregulated
BP	9057	macromolecule catabolic process	2.40E-06	6.32E-05	18/91 19.7%	3075/55204 5.5%	Upregulated
BP	19320	hexose catabolic process	4.33E-06	1.09E-04	4/91 4.3%	65/55204 0.1%	Upregulated
BP	5996	monosaccharide metabolic process	1.39E-05	3.36E-04	10/91 10.9%	1098/55204 1.9%	Upregulated
BP	46365	monosaccharide catabolic process	1.73E-05	4.00E-04	4/91 4.3%	92/55204 0.1%	Upregulated
BP	1901135	carbohydrate derivative metabolic process	2.51E-05	5.60E-04	17/91 18.6%	3300/55204 5.9%	Upregulated
BP	6952	defense response	2.86E-05	6.12E-04	16/91 17.5%	2990/55204 5.4%	Upregulated
BP	19388	galactose catabolic process	3.51E-05	7.25E-04	3/91 3.2%	38/55204 0.0%	Upregulated
BP	2000068	regulation of defense response to insect	6.67E-05	1.33E-03	3/91 3.2%	47/55204 0.0%	Upregulated
BP	1900366	negative regulation of defense response to insect	3.18E-04	6.13E-03	2/91 2.1%	16/55204 0.0%	Upregulated
BP	19318	hexose metabolic process	4.56E-04	8.52E-03	7/91 7.6%	829/55204 1.5%	Upregulated
BP	33499	galactose catabolic process via UDP-galactose	6.65E-04	1.20E-02	2/91 2.1%	23/55204 0.0%	Upregulated
BP	6012	galactose metabolic process	7.19E-04	1.26E-02	3/91 3.2%	105/55204 0.1%	Upregulated
BP	18874	benzoate metabolic process	1.65E-03	2.81E-02	1/91 1.0%	1/55204 0.0%	Upregulated
BP	44282	small molecule catabolic process	1.88E-03	3.11E-02	9/91 9.8%	1686/55204 3.0%	Upregulated
BP	9620	response to fungus	2.44E-03	3.93E-02	6/91 6.5%	822/55204 1.4%	Upregulated
BP	31034	myosin filament assembly	3.29E-03	4.78E-02	1/91 1.0%	2/55204 0.0%	Upregulated
BP	71497	cellular response to freezing	3.29E-03	4.78E-02	1/91 1.0%	2/55204 0.0%	Upregulated
BP	6076	(1->3)-beta-D-glucan catabolic process	3.29E-03	4.78E-02	1/91 1.0%	2/55204 0.0%	Upregulated
BP	50832	defense response to fungus	3.38E-03	4.78E-02	5/91 5.4%	607/55204 1.0%	Upregulated
BP	6006	glucose metabolic process	3.38E-03	4.78E-02	5/91 5.4%	607/55204 1.0%	Upregulated
BP	9698	phenylpropanoid metabolic process	3.86E-08	1.89E-05	12/206 5.8%	395/55204 0.7%	Downregulated
BP	19748	secondary metabolic process	3.87E-08	1.89E-05	14/206 6.7%	569/55204 1.0%	Downregulated
BP	6412	translation	4.24E-07	1.17E-04	40/206 19.4%	4607/55204 8.3%	Downregulated
BP	9808	lignin metabolic process	4.81E-07	1.17E-04	8/206 3.8%	182/55204 0.3%	Downregulated
BP	44550	secondary metabolite biosynthetic process	2.09E-06	4.08E-04	10/206 4.8%	383/55204 0.6%	Downregulated
BP	9699	phenylpropanoid biosynthetic process	1.36E-05	2.21E-03	8/206 3.8%	286/55204 0.5%	Downregulated
BP	19253	reductive pentose-phosphate cycle	6.93E-05	9.64E-03	8/206 3.8%	360/55204 0.6%	Downregulated
BP	19685	photosynthesis, dark reaction	9.36E-05	1.14E-02	8/206 3.8%	376/55204 0.6%	Downregulated
BP	9809	lignin biosynthetic process	1.30E-04	1.27E-02	5/206 2.4%	129/55204 0.2%	Downregulated
BP	16102	diterpenoid biosynthetic process	1.30E-04	1.27E-02	5/206 2.4%	129/55204 0.2%	Downregulated
BP	15977	carbon fixation	1.72E-04	1.38E-02	8/206 3.8%	411/55204 0.7%	Downregulated
BP	46248	alpha-pinene biosynthetic process	1.74E-04	1.38E-02	3/206 1.4%	29/55204 0.0%	Downregulated
BP	42214	terpene metabolic process	2.04E-04	1.38E-02	5/206 2.4%	142/55204 0.2%	Downregulated
BP	33073	pinene metabolic process	2.13E-04	1.38E-02	3/206 1.4%	31/55204 0.0%	Downregulated
BP	18867	alpha-pinene metabolic process	2.13E-04	1.38E-02	3/206 1.4%	31/55204 0.0%	Downregulated
BP	2181	cytoplasmic translation	3.46E-04	2.10E-02	11/206 5.3%	838/55204 1.5%	Downregulated
BP	9765	photosynthesis, light harvesting	5.49E-04	3.06E-02	11/206 5.3%	886/55204 1.6%	Downregulated
BP	43693	monoterpene biosynthetic process	5.66E-04	3.06E-02	3/206 1.4%	43/55204 0.0%	Downregulated
BP	43692	monoterpene metabolic process	6.47E-04	3.32E-02	3/206 1.4%	45/55204 0.0%	Downregulated
BP	1903601	thermospermine metabolic process	7.45E-04	3.42E-02	2/206 0.9%	11/55204 0.0%	Downregulated
BP	1903602	thermospermine catabolic process	7.45E-04	3.42E-02	2/206 0.9%	11/55204 0.0%	Downregulated
BP	45488	pectin metabolic process	7.72E-04	3.42E-02	5/206 2.4%	190/55204 0.3%	Downregulated
BP	10393	galacturonan metabolic process	8.47E-04	3.59E-02	5/206 2.4%	194/55204 0.3%	Downregulated
BP	16101	diterpenoid metabolic process	1.08E-03	4.39E-02	5/206 2.4%	205/55204 0.3%	Downregulated
BP	16099	monoterpenoid biosynthetic process	1.16E-03	4.51E-02	3/206 1.4%	55/55204 0.0%	Downregulated
BP	46274	lignin catabolic process	1.29E-03	4.51E-02	3/206 1.4%	57/55204 0.1%	Downregulated
BP	16098	monoterpenoid metabolic process	1.29E-03	4.51E-02	3/206 1.4%	57/55204 0.1%	Downregulated
BP	15979	photosynthesis	1.30E-03	4.51E-02	21/206 10.1%	2707/55204 4.9%	Downregulated

Table S5.8. Significantly enriched GO terms (Biological Process) associated with genes that were differentially expressed between the resistant juniper genotype inoculated with the more virulent *P. austrocedri* isolate compared to the same genotype's mock-inoculated control at one week post-inoculation. Where relevant, only the top 50 GO terms have been included for each direction (upregulated and downregulated).

GO	GO ID	GO Description	p-val	Corrected p-val	Cluster frequency	Total frequency	Direction
BP	6952	defense response	2.10E-16	6.78E-13	159/1482 10.7%	2990/55204 5.4%	Upregulated
BP	50896	response to stimulus	9.15E-13	1.48E-09	517/1482 34.8%	14712/55204 26.6%	Upregulated
BP	6950	response to stress	2.01E-11	2.16E-08	351/1482 23.6%	9393/55204 17.0%	Upregulated
BP	16137	glycoside metabolic process	7.82E-09	6.30E-06	15/1482 1.0%	85/55204 0.1%	Upregulated
BP	42221	response to chemical	2.83E-08	1.82E-05	250/1482 16.8%	6671/55204 12.0%	Upregulated
BP	44550	secondary metabolite biosynthetic process	7.05E-08	3.76E-05	31/1482 2.0%	383/55204 0.6%	Upregulated
BP	9699	phenylpropanoid biosynthetic process	8.16E-08	3.76E-05	26/1482 1.7%	286/55204 0.5%	Upregulated
BP	70542	response to fatty acid	1.00E-07	4.04E-05	33/1482 2.2%	431/55204 0.7%	Upregulated
BP	1904550	response to arachidonate	2.43E-07	6.90E-05	7/1482 0.4%	18/55204 0.0%	Upregulated
BP	2000032	regulation of secondary shoot formation	2.44E-07	6.90E-05	12/1482 0.8%	68/55204 0.1%	Upregulated
BP	60688	regulation of morphogenesis of a branching structure	2.44E-07	6.90E-05	12/1482 0.8%	68/55204 0.1%	Upregulated
BP	18158	protein oxidation	2.78E-07	6.90E-05	5/1482 0.3%	7/55204 0.0%	Upregulated
BP	18171	peptidyl-cysteine oxidation	2.78E-07	6.90E-05	5/1482 0.3%	7/55204 0.0%	Upregulated
BP	22603	regulation of anatomical structure morphogenesis	5.29E-07	1.22E-04	29/1482 1.9%	377/55204 0.6%	Upregulated
BP	16138	glycoside biosynthetic process	7.29E-07	1.57E-04	10/1482 0.6%	50/55204 0.0%	Upregulated
BP	1905428	regulation of plant organ formation	9.82E-07	1.98E-04	13/1482 0.8%	91/55204 0.1%	Upregulated
BP	8299	isoprenoid biosynthetic process	1.13E-06	2.14E-04	49/1482 3.3%	865/55204 1.5%	Upregulated
BP	70483	detection of hypoxia	1.60E-06	2.71E-04	5/1482 0.3%	9/55204 0.0%	Upregulated
BP	1901657	glycosyl compound metabolic process	1.60E-06	2.71E-04	25/1482 1.6%	313/55204 0.5%	Upregulated
BP	9806	lignan metabolic process	2.30E-06	3.53E-04	7/1482 0.4%	24/55204 0.0%	Upregulated
BP	9807	lignan biosynthetic process	2.30E-06	3.53E-04	7/1482 0.4%	24/55204 0.0%	Upregulated
BP	1901700	response to oxygen-containing compound	3.42E-06	5.01E-04	162/1482 10.9%	4232/55204 7.6%	Upregulated
BP	33993	response to lipid	4.04E-06	5.09E-04	90/1482 6.0%	2045/55204 3.7%	Upregulated
BP	141060	disruption of anatomical structure in another organism	4.10E-06	5.09E-04	8/1482 0.5%	36/55204 0.0%	Upregulated
BP	141061	disruption of cell in another organism	4.10E-06	5.09E-04	8/1482 0.5%	36/55204 0.0%	Upregulated
BP	31640	killing of cells of another organism	4.10E-06	5.09E-04	8/1482 0.5%	36/55204 0.0%	Upregulated
BP	1901072	glucosamine-containing compound catabolic process	4.47E-06	5.14E-04	11/1482 0.7%	74/55204 0.1%	Upregulated
BP	6032	chitin catabolic process	4.47E-06	5.14E-04	11/1482 0.7%	74/55204 0.1%	Upregulated
BP	6720	isoprenoid metabolic process	5.22E-06	5.81E-04	53/1482 3.5%	1020/55204 1.8%	Upregulated
BP	9620	response to fungus	7.26E-06	7.59E-04	45/1482 3.0%	822/55204 1.4%	Upregulated
BP	46348	amino sugar catabolic process	7.54E-06	7.59E-04	11/1482 0.7%	78/55204 0.1%	Upregulated
BP	6030	chitin metabolic process	7.54E-06	7.59E-04	11/1482 0.7%	78/55204 0.1%	Upregulated
BP	16998	cell wall macromolecule catabolic process	7.79E-06	7.61E-04	9/1482 0.6%	51/55204 0.0%	Upregulated
BP	3032	detection of oxygen	9.37E-06	8.89E-04	5/1482 0.3%	12/55204 0.0%	Upregulated
BP	42773	ATP synthesis coupled electron transport	1.07E-05	9.82E-04	22/1482 1.4%	284/55204 0.5%	Upregulated
BP	71456	cellular response to hypoxia	1.10E-05	9.82E-04	20/1482 1.3%	243/55204 0.4%	Upregulated
BP	9698	phenylpropanoid metabolic process	1.14E-05	9.96E-04	27/1482 1.8%	395/55204 0.7%	Upregulated
BP	6119	oxidative phosphorylation	1.19E-05	1.01E-03	25/1482 1.6%	351/55204 0.6%	Upregulated
BP	36294	cellular response to decreased oxygen levels	1.24E-05	1.02E-03	20/1482 1.3%	245/55204 0.4%	Upregulated
BP	1906	cell killing	1.39E-05	1.12E-03	8/1482 0.5%	42/55204 0.0%	Upregulated
BP	6026	aminoglycan catabolic process	1.55E-05	1.18E-03	11/1482 0.7%	84/55204 0.1%	Upregulated
BP	71453	cellular response to oxygen levels	1.57E-05	1.18E-03	20/1482 1.3%	249/55204 0.4%	Upregulated
BP	19748	secondary metabolic process	1.60E-05	1.18E-03	34/1482 2.2%	569/55204 1.0%	Upregulated
BP	51707	response to other organism	1.66E-05	1.18E-03	112/1482 7.5%	2787/55204 5.0%	Upregulated
BP	1901600	strigolactone metabolic process	1.66E-05	1.18E-03	8/1482 0.5%	43/55204 0.0%	Upregulated
BP	43207	response to external biotic stimulus	1.69E-05	1.18E-03	112/1482 7.5%	2788/55204 5.0%	Upregulated
BP	6629	lipid metabolic process	2.16E-05	1.44E-03	176/1482 11.8%	4830/55204 8.7%	Upregulated
BP	9607	response to biotic stimulus	2.18E-05	1.44E-03	112/1482 7.5%	2805/55204 5.0%	Upregulated
BP	44419	biological process involved in interspecies interaction between organisms	2.19E-05	1.44E-03	114/1482 7.6%	2867/55204 5.1%	Upregulated
BP	18198	peptidyl-cysteine modification	2.27E-05	1.46E-03	5/1482 0.3%	14/55204 0.0%	Upregulated
BP	6952	defense response	6.26E-67	2.22E-63	361/2501 14.4%	2990/55204 5.4%	Downregulated
BP	50789	regulation of biological process	1.15E-64	2.03E-61	889/2501 35.5%	11681/55204 21.1%	Downregulated
BP	65007	biological regulation	1.31E-62	1.54E-59	917/2501 36.6%	12316/55204 22.3%	Downregulated
BP	50896	response to stimulus	4.63E-61	4.10E-58	1038/2501 41.5%	14712/55204 26.6%	Downregulated
BP	7165	signal transduction	4.87E-57	3.45E-54	407/2501 16.2%	3938/55204 7.1%	Downregulated
BP	7154	cell communication	1.32E-55	7.78E-53	411/2501 16.4%	4047/55204 7.3%	Downregulated
BP	23052	signaling	1.70E-55	8.58E-53	409/2501 16.3%	4021/55204 7.2%	Downregulated
BP	50794	regulation of cellular process	1.81E-53	8.01E-51	794/2501 31.7%	10579/55204 19.1%	Downregulated
BP	6468	protein phosphorylation	4.45E-42	1.75E-39	250/2501 9.9%	2175/55204 3.9%	Downregulated
BP	16310	phosphorylation	1.39E-41	4.94E-39	252/2501 10.0%	2217/55204 4.0%	Downregulated
BP	9725	response to hormone	4.22E-40	1.36E-37	291/2501 11.6%	2818/55204 5.1%	Downregulated
BP	9605	response to external stimulus	4.79E-40	1.41E-37	324/2501 12.9%	3310/55204 5.9%	Downregulated
BP	9719	response to endogenous stimulus	2.82E-39	7.68E-37	291/2501 11.6%	2847/55204 5.1%	Downregulated
BP	51707	response to other organism	1.16E-37	2.91E-35	283/2501 11.3%	2787/55204 5.0%	Downregulated
BP	43207	response to external biotic stimulus	1.24E-37	2.91E-35	283/2501 11.3%	2788/55204 5.0%	Downregulated
BP	9607	response to biotic stimulus	3.65E-37	8.07E-35	283/2501 11.3%	2805/55204 5.0%	Downregulated
BP	44419	biological process involved in interspecies interaction between organisms	6.88E-36	1.43E-33	284/2501 11.3%	2867/55204 5.1%	Downregulated
BP	9755	hormone-mediated signaling pathway	1.55E-34	3.06E-32	196/2501 7.8%	1661/55204 3.0%	Downregulated
BP	71555	cell wall organization	4.09E-33	7.62E-31	123/2501 4.9%	789/55204 1.4%	Downregulated
BP	45229	external encapsulating structure organization	2.82E-32	4.99E-30	134/2501 5.3%	932/55204 1.6%	Downregulated

Table S5.8 continued.

BP	32870	cellular response to hormone stimulus	2.19E-31	3.70E-29	201/2501 8.0%	1823/55204 3.3%	Downregulated
BP	71495	cellular response to endogenous stimulus	1.91E-30	3.07E-28	201/2501 8.0%	1853/55204 3.3%	Downregulated
BP	6950	response to stress	6.51E-30	1.00E-27	645/2501 25.7%	9393/55204 17.0%	Downregulated
BP	71554	cell wall organization or biogenesis	1.24E-29	1.83E-27	132/2501 5.2%	965/55204 1.7%	Downregulated
BP	42221	response to chemical	4.72E-28	6.68E-26	489/2501 19.5%	6671/55204 12.0%	Downregulated
BP	48856	anatomical structure development	9.18E-28	1.24E-25	508/2501 20.3%	7032/55204 12.7%	Downregulated
BP	51716	cellular response to stimulus	9.47E-28	1.24E-25	555/2501 22.1%	7888/55204 14.2%	Downregulated
BP	32502	developmental process	1.88E-27	2.38E-25	519/2501 20.7%	7253/55204 13.1%	Downregulated
BP	99402	plant organ development	4.43E-26	5.40E-24	203/2501 8.1%	2034/55204 3.6%	Downregulated
BP	48367	shoot system development	7.21E-26	8.51E-24	175/2501 6.9%	1637/55204 2.9%	Downregulated
BP	7275	multicellular organism development	4.70E-25	5.36E-23	438/2501 17.5%	5966/55204 10.8%	Downregulated
BP	6355	regulation of DNA-templated transcription	1.79E-24	1.98E-22	226/2501 9.0%	2446/55204 4.4%	Downregulated
BP	2001141	regulation of RNA biosynthetic process	1.89E-24	2.03E-22	226/2501 9.0%	2447/55204 4.4%	Downregulated
BP	43412	macromolecule modification	6.04E-24	6.29E-22	500/2501 19.9%	7166/55204 12.9%	Downregulated
BP	9626	plant-type hypersensitive response	3.48E-23	3.52E-21	58/2501 2.3%	271/55204 0.4%	Downregulated
BP	34050	symbiont-induced defense-related programmed cell death	4.23E-23	4.16E-21	58/2501 2.3%	272/55204 0.4%	Downregulated
BP	9733	response to auxin	9.77E-23	9.35E-21	96/2501 3.8%	683/55204 1.2%	Downregulated
BP	42742	defense response to bacterium	3.41E-22	3.17E-20	111/2501 4.4%	881/55204 1.5%	Downregulated
BP	19219	regulation of nucleobase-containing compound metabolic process	9.38E-22	8.51E-20	259/2501 10.3%	3101/55204 5.6%	Downregulated
BP	32501	multicellular organismal process	2.11E-21	1.87E-19	463/2501 18.5%	6686/55204 12.1%	Downregulated
BP	48731	system development	2.59E-21	2.23E-19	356/2501 14.2%	4773/55204 8.6%	Downregulated
BP	36211	protein modification process	4.09E-21	3.44E-19	359/2501 14.3%	4839/55204 8.7%	Downregulated
BP	9889	regulation of biosynthetic process	6.52E-21	5.37E-19	361/2501 14.4%	4888/55204 8.8%	Downregulated
BP	71365	cellular response to auxin stimulus	1.08E-20	8.69E-19	73/2501 2.9%	459/55204 0.8%	Downregulated
BP	51252	regulation of RNA metabolic process	1.75E-20	1.38E-18	240/2501 9.5%	2858/55204 5.1%	Downregulated
BP	10556	regulation of macromolecule biosynthetic process	2.34E-20	1.80E-18	339/2501 13.5%	4540/55204 8.2%	Downregulated
BP	9734	auxin-activated signaling pathway	3.92E-20	2.95E-18	71/2501 2.8%	447/55204 0.8%	Downregulated
BP	70887	cellular response to chemical stimulus	4.74E-20	3.50E-18	289/2501 11.5%	3698/55204 6.6%	Downregulated
BP	10468	regulation of gene expression	9.27E-20	6.69E-18	330/2501 13.1%	4423/55204 8.0%	Downregulated
BP	9617	response to bacterium	1.72E-19	1.22E-17	133/2501 5.3%	1258/55204 2.2%	Downregulated

Table S5.9. Significantly enriched GO terms (Biological Process) associated with genes that were differentially expressed between the resistant juniper genotype compared to the susceptible genotype, in both cases treated with a mock-inoculated control, at 48 hours post-inoculation. Only the top 50 GO terms have been included for each direction (upregulated and downregulated).

GO	GO ID	GO Description	p-val	Corrected p-val	Cluster frequency	Total frequency	Direction
BP	6952	defense response	1.71E-24	4.76E-21	155/1177 13.1%	2990/55204 5.4%	Upregulated
BP	16998	cell wall macromolecule catabolic process	2.59E-16	3.60E-13	17/1177 1.4%	51/55204 0.0%	Upregulated
BP	50832	defense response to fungus	3.09E-15	2.87E-12	49/1177 4.1%	607/55204 1.0%	Upregulated
BP	141060	disruption of anatomical structure in another organism	9.12E-15	4.22E-12	14/1177 1.1%	36/55204 0.0%	Upregulated
BP	141061	disruption of cell in another organism	9.12E-15	4.22E-12	14/1177 1.1%	36/55204 0.0%	Upregulated
BP	31640	killing of cells of another organism	9.12E-15	4.22E-12	14/1177 1.1%	36/55204 0.0%	Upregulated
BP	1901072	glucosamine-containing compound catabolic process	1.72E-14	5.98E-12	18/1177 1.5%	74/55204 0.1%	Upregulated
BP	6032	chitin catabolic process	1.72E-14	5.98E-12	18/1177 1.5%	74/55204 0.1%	Upregulated
BP	46348	amino sugar catabolic process	4.65E-14	1.29E-11	18/1177 1.5%	78/55204 0.1%	Upregulated
BP	6030	chitin metabolic process	4.65E-14	1.29E-11	18/1177 1.5%	78/55204 0.1%	Upregulated
BP	1906	cell killing	1.13E-13	2.85E-11	14/1177 1.1%	42/55204 0.0%	Upregulated
BP	6026	aminoglycan catabolic process	1.84E-13	4.22E-11	18/1177 1.5%	84/55204 0.1%	Upregulated
BP	44419	biological process involved in interspecies interaction between organisms	1.97E-13	4.22E-11	123/1177 10.4%	2867/55204 5.1%	Upregulated
BP	51707	response to other organism	3.15E-13	5.97E-11	120/1177 10.1%	2787/55204 5.0%	Upregulated
BP	43207	response to external biotic stimulus	3.22E-13	5.97E-11	120/1177 10.1%	2788/55204 5.0%	Upregulated
BP	9607	response to biotic stimulus	4.83E-13	8.38E-11	120/1177 10.1%	2805/55204 5.0%	Upregulated
BP	9620	response to fungus	5.46E-13	8.92E-11	54/1177 4.5%	822/55204 1.4%	Upregulated
BP	19677	NAD+ catabolic process	7.65E-13	1.18E-10	21/1177 1.7%	131/55204 0.2%	Upregulated
BP	1901071	glucosamine-containing compound metabolic process	1.18E-12	1.72E-10	18/1177 1.5%	93/55204 0.1%	Upregulated
BP	50896	response to stimulus	2.38E-12	3.31E-10	421/1177 35.7%	14712/55204 26.6%	Upregulated
BP	6950	response to stress	3.41E-11	4.33E-09	288/1177 24.4%	9393/55204 17.0%	Upregulated
BP	9605	response to external stimulus	3.43E-11	4.33E-09	129/1177 10.9%	3310/55204 5.9%	Upregulated
BP	6022	aminoglycan metabolic process	4.33E-11	5.22E-09	19/1177 1.6%	129/55204 0.2%	Upregulated
BP	7165	signal transduction	5.34E-11	6.18E-09	146/1177 12.4%	3938/55204 7.1%	Upregulated
BP	6040	amino sugar metabolic process	7.54E-11	8.14E-09	20/1177 1.6%	149/55204 0.2%	Upregulated
BP	43068	positive regulation of programmed cell death	7.62E-11	8.14E-09	28/1177 2.3%	297/55204 0.5%	Upregulated
BP	7154	cell communication	1.89E-10	1.94E-08	147/1177 12.4%	4047/55204 7.3%	Upregulated
BP	71554	cell wall organization or biogenesis	2.25E-10	2.16E-08	54/1177 4.5%	965/55204 1.7%	Upregulated
BP	23052	signaling	2.25E-10	2.16E-08	146/1177 12.4%	4021/55204 7.2%	Upregulated
BP	9626	plant-type hypersensitive response	1.22E-09	1.13E-07	25/1177 2.1%	271/55204 0.4%	Upregulated
BP	34050	symbiont-induced defense-related programmed cell death	1.32E-09	1.18E-07	25/1177 2.1%	272/55204 0.4%	Upregulated
BP	19674	NAD+ metabolic process	1.75E-09	1.52E-07	24/1177 2.0%	255/55204 0.4%	Upregulated
BP	44036	cell wall macromolecule metabolic process	4.13E-09	3.48E-07	18/1177 1.5%	150/55204 0.2%	Upregulated
BP	5976	polysaccharide metabolic process	1.11E-06	9.06E-05	54/1177 4.5%	1249/55204 2.2%	Upregulated
BP	43067	regulation of programmed cell death	1.55E-06	1.23E-04	32/1177 2.7%	583/55204 1.0%	Upregulated
BP	272	polysaccharide catabolic process	2.55E-06	1.97E-04	32/1177 2.7%	597/55204 1.0%	Upregulated
BP	98542	defense response to other organism	3.69E-06	2.77E-04	40/1177 3.3%	849/55204 1.5%	Upregulated
BP	19748	secondary metabolic process	7.14E-06	5.22E-04	30/1177 2.5%	569/55204 1.0%	Upregulated
BP	6955	immune response	9.56E-06	6.66E-04	35/1177 2.9%	728/55204 1.3%	Upregulated
BP	140546	defense response to symbiont	9.59E-06	6.66E-04	37/1177 3.1%	790/55204 1.4%	Upregulated
BP	45087	innate immune response	1.04E-05	7.07E-04	33/1177 2.8%	670/55204 1.2%	Upregulated
BP	8219	cell death	1.84E-05	1.21E-03	30/1177 2.5%	598/55204 1.0%	Upregulated
BP	12501	programmed cell death	1.92E-05	1.24E-03	28/1177 2.3%	540/55204 0.9%	Upregulated
BP	51716	cellular response to stimulus	2.97E-05	1.88E-03	218/1177 18.5%	7888/55204 14.2%	Upregulated
BP	44550	secondary metabolite biosynthetic process	3.23E-05	2.00E-03	22/1177 1.8%	383/55204 0.6%	Upregulated
BP	71555	cell wall organization	4.97E-05	3.00E-03	35/1177 2.9%	789/55204 1.4%	Upregulated
BP	50789	regulation of biological process	6.11E-05	3.61E-03	304/1177 25.8%	11681/55204 21.1%	Upregulated
BP	19310	inositol catabolic process	8.88E-05	5.14E-03	4/1177 0.3%	12/55204 0.0%	Upregulated
BP	10411	xyloglucan metabolic process	1.02E-04	5.80E-03	9/1177 0.7%	87/55204 0.1%	Upregulated
BP	9765	photosynthesis, light harvesting	1.05E-04	5.85E-03	37/1177 3.1%	886/55204 1.6%	Upregulated
BP	6952	defense response	3.39E-30	7.60E-27	137/853 16.0%	2990/55204 5.4%	Downregulated
BP	7165	signal transduction	7.00E-15	7.78E-12	126/853 14.7%	3938/55204 7.1%	Downregulated
BP	23052	signaling	1.38E-14	7.78E-12	127/853 14.8%	4021/55204 7.2%	Downregulated
BP	50896	response to stimulus	1.39E-14	7.78E-12	329/853 38.5%	14712/55204 26.6%	Downregulated
BP	7154	cell communication	2.19E-14	9.18E-12	127/853 14.8%	4047/55204 7.3%	Downregulated
BP	6950	response to stress	2.45E-14	9.18E-12	233/853 27.3%	9393/55204 17.0%	Downregulated
BP	51707	response to other organism	1.09E-13	3.11E-11	97/853 11.3%	2787/55204 5.0%	Downregulated
BP	43207	response to external biotic stimulus	1.11E-13	3.11E-11	97/853 11.3%	2788/55204 5.0%	Downregulated
BP	9607	response to biotic stimulus	1.59E-13	3.96E-11	97/853 11.3%	2805/55204 5.0%	Downregulated
BP	9626	plant-type hypersensitive response	2.07E-13	4.60E-11	26/853 3.0%	271/55204 0.4%	Downregulated
BP	34050	symbiont-induced defense-related programmed cell death	2.26E-13	4.60E-11	26/853 3.0%	272/55204 0.4%	Downregulated
BP	44419	biological process involved in interspecies interaction between organisms	5.66E-13	1.06E-10	97/853 11.3%	2867/55204 5.1%	Downregulated
BP	19748	secondary metabolic process	1.74E-12	3.00E-10	36/853 4.2%	569/55204 1.0%	Downregulated
BP	19677	NAD+ catabolic process	2.45E-12	3.93E-10	18/853 2.1%	131/55204 0.2%	Downregulated

Table S5.9 continued.

BP	9605	response to external stimulus	1.43E-11	2.14E-09	103/853 12.0%	3310/55204 5.9%	Downregulated
BP	9813	flavonoid biosynthetic process	2.08E-10	2.91E-08	19/853 2.2%	192/55204 0.3%	Downregulated
BP	43068	positive regulation of programmed cell death	3.76E-10	4.95E-08	23/853 2.6%	297/55204 0.5%	Downregulated
BP	6955	immune response	4.44E-10	5.54E-08	37/853 4.3%	728/55204 1.3%	Downregulated
BP	44550	secondary metabolite biosynthetic process	4.76E-10	5.62E-08	26/853 3.0%	383/55204 0.6%	Downregulated
BP	8219	cell death	5.03E-10	5.65E-08	33/853 3.8%	598/55204 1.0%	Downregulated
BP	12501	programmed cell death	6.55E-10	6.99E-08	31/853 3.6%	540/55204 0.9%	Downregulated
BP	16310	phosphorylation	1.65E-09	1.67E-07	73/853 8.5%	2217/55204 4.0%	Downregulated
BP	6468	protein phosphorylation	1.72E-09	1.67E-07	72/853 8.4%	2175/55204 3.9%	Downregulated
BP	45087	innate immune response	2.35E-09	2.19E-07	34/853 3.9%	670/55204 1.2%	Downregulated
BP	51716	cellular response to stimulus	2.78E-09	2.50E-07	185/853 21.6%	7888/55204 14.2%	Downregulated
BP	9812	flavonoid metabolic process	3.02E-09	2.61E-07	19/853 2.2%	225/55204 0.4%	Downregulated
BP	2376	immune system process	7.76E-09	6.44E-07	40/853 4.6%	921/55204 1.6%	Downregulated
BP	9620	response to fungus	1.13E-08	9.04E-07	37/853 4.3%	822/55204 1.4%	Downregulated
BP	19674	NAD+ metabolic process	2.33E-08	1.80E-06	19/853 2.2%	255/55204 0.4%	Downregulated
BP	98542	defense response to other organism	2.59E-08	1.93E-06	37/853 4.3%	849/55204 1.5%	Downregulated
BP	9699	phenylpropanoid biosynthetic process	2.89E-08	2.09E-06	20/853 2.3%	286/55204 0.5%	Downregulated
BP	9838	abscission	3.88E-08	2.72E-06	9/853 1.0%	47/55204 0.0%	Downregulated
BP	140546	defense response to symbiont	4.12E-08	2.80E-06	35/853 4.1%	790/55204 1.4%	Downregulated
BP	10618	aerenchyma formation	9.38E-08	6.19E-06	6/853 0.7%	16/55204 0.0%	Downregulated
BP	65007	biological regulation	1.99E-07	1.27E-05	254/853 29.7%	12316/55204 22.3%	Downregulated
BP	60866	leaf abscission	2.38E-07	1.48E-05	7/853 0.8%	29/55204 0.0%	Downregulated
BP	9698	phenylpropanoid metabolic process	3.26E-07	1.97E-05	22/853 2.5%	395/55204 0.7%	Downregulated
BP	16137	glycoside metabolic process	8.11E-07	4.79E-05	10/853 1.1%	85/55204 0.1%	Downregulated
BP	16138	glycoside biosynthetic process	9.52E-07	5.47E-05	8/853 0.9%	50/55204 0.0%	Downregulated
BP	1666	response to hypoxia	1.20E-06	6.71E-05	20/853 2.3%	361/55204 0.6%	Downregulated
BP	50829	defense response to Gram-negative bacterium	1.35E-06	7.38E-05	9/853 1.0%	70/55204 0.1%	Downregulated
BP	1900378	positive regulation of secondary metabolite biosynthetic process	1.42E-06	7.58E-05	6/853 0.7%	24/55204 0.0%	Downregulated
BP	9751	response to salicylic acid	1.49E-06	7.77E-05	19/853 2.2%	334/55204 0.6%	Downregulated
BP	16104	triterpenoid biosynthetic process	2.05E-06	1.05E-04	7/853 0.8%	39/55204 0.0%	Downregulated
BP	6722	triterpenoid metabolic process	2.45E-06	1.22E-04	7/853 0.8%	40/55204 0.0%	Downregulated
BP	36293	response to decreased oxygen levels	3.18E-06	1.55E-04	20/853 2.3%	385/55204 0.6%	Downregulated
BP	50789	regulation of biological process	3.30E-06	1.57E-04	236/853 27.6%	11681/55204 21.1%	Downregulated
BP	50832	defense response to fungus	4.08E-06	1.91E-04	26/853 3.0%	607/55204 1.0%	Downregulated
BP	43067	regulation of programmed cell death	6.09E-06	2.79E-04	25/853 2.9%	583/55204 1.0%	Downregulated
BP	70482	response to oxygen levels	6.50E-06	2.86E-04	20/853 2.3%	404/55204 0.7%	Downregulated

Table S5.10. Significantly enriched GO terms (Biological Process) associated with genes that were differentially expressed between the resistant juniper genotype compared to the susceptible genotype, in both cases inoculated with the less virulent *P. austrocedri* isolate, at 48 hours post-inoculation. Only the top 50 GO terms have been included for each direction (upregulated and downregulated).

GO	GO ID	GO Description	p-val	Corrected p-val	Cluster frequency	Total frequency	Direction
BP	6952	defense response	3.42E-32	9.54E-29	191/1394 13.7%	2990/55204 5.4%	Upregulated
BP	15979	photosynthesis	1.46E-20	2.04E-17	153/1394 10.9%	2707/55204 4.9%	Upregulated
BP	16998	cell wall macromolecule catabolic process	3.58E-19	3.34E-16	20/1394 1.4%	51/55204 0.0%	Upregulated
BP	9765	photosynthesis, light harvesting	1.79E-18	1.25E-15	73/1394 5.2%	886/55204 1.6%	Upregulated
BP	19684	photosynthesis, light reaction	1.86E-17	1.04E-14	92/1394 6.5%	1354/55204 2.4%	Upregulated
BP	1901072	glucosamine-containing compound catabolic process	1.03E-16	4.10E-14	21/1394 1.5%	74/55204 0.1%	Upregulated
BP	6032	chitin catabolic process	1.03E-16	4.10E-14	21/1394 1.5%	74/55204 0.1%	Upregulated
BP	46348	amino sugar catabolic process	3.37E-16	1.05E-13	21/1394 1.5%	78/55204 0.1%	Upregulated
BP	6030	chitin metabolic process	3.37E-16	1.05E-13	21/1394 1.5%	78/55204 0.1%	Upregulated
BP	6026	aminoglycan catabolic process	1.75E-15	4.88E-13	21/1394 1.5%	84/55204 0.1%	Upregulated
BP	44036	cell wall macromolecule metabolic process	1.08E-14	2.75E-12	26/1394 1.8%	150/55204 0.2%	Upregulated
BP	1901071	glucosamine-containing compound metabolic process	1.59E-14	3.70E-12	21/1394 1.5%	93/55204 0.1%	Upregulated
BP	6950	response to stress	8.04E-14	1.59E-11	345/1394 24.7%	9393/55204 17.0%	Upregulated
BP	141060	disruption of anatomical structure in another organism	9.09E-14	1.59E-11	14/1394 1.0%	36/55204 0.0%	Upregulated
BP	141061	disruption of cell in another organism	9.09E-14	1.59E-11	14/1394 1.0%	36/55204 0.0%	Upregulated
BP	31640	killing of cells of another organism	9.09E-14	1.59E-11	14/1394 1.0%	36/55204 0.0%	Upregulated
BP	50896	response to stimulus	4.07E-13	6.69E-11	492/1394 35.2%	14712/55204 26.6%	Upregulated
BP	44419	biological process involved in interspecies interaction between organisms	8.27E-13	1.28E-10	137/1394 9.8%	2867/55204 5.1%	Upregulated
BP	1906	cell killing	1.10E-12	1.61E-10	14/1394 1.0%	42/55204 0.0%	Upregulated
BP	50832	defense response to fungus	1.61E-12	2.25E-10	49/1394 3.5%	607/55204 1.0%	Upregulated
BP	51707	response to other organism	2.02E-12	2.63E-10	133/1394 9.5%	2787/55204 5.0%	Upregulated
BP	43207	response to external biotic stimulus	2.07E-12	2.63E-10	133/1394 9.5%	2788/55204 5.0%	Upregulated
BP	9607	response to biotic stimulus	3.15E-12	3.83E-10	133/1394 9.5%	2805/55204 5.0%	Upregulated
BP	6040	amino sugar metabolic process	4.49E-12	5.23E-10	23/1394 1.6%	149/55204 0.2%	Upregulated
BP	6022	aminoglycan metabolic process	1.33E-11	1.49E-09	21/1394 1.5%	129/55204 0.2%	Upregulated
BP	9620	response to fungus	3.56E-11	3.83E-09	56/1394 4.0%	822/55204 1.4%	Upregulated
BP	44550	secondary metabolite biosynthetic process	8.70E-11	8.75E-09	35/1394 2.5%	383/55204 0.6%	Upregulated
BP	19748	secondary metabolic process	8.77E-11	8.75E-09	44/1394 3.1%	569/55204 1.0%	Upregulated
BP	9605	response to external stimulus	1.06E-09	1.02E-07	141/1394 10.1%	3310/55204 5.9%	Upregulated
BP	1904550	response to arachidonate	5.66E-09	5.27E-07	8/1394 0.5%	18/55204 0.0%	Upregulated
BP	9699	phenylpropanoid biosynthetic process	5.97E-09	5.38E-07	27/1394 1.9%	286/55204 0.5%	Upregulated
BP	9698	phenylpropanoid metabolic process	1.04E-08	9.12E-07	32/1394 2.2%	395/55204 0.7%	Upregulated
BP	71554	cell wall organization or biogenesis	1.18E-08	9.99E-07	56/1394 4.0%	965/55204 1.7%	Upregulated
BP	71281	cellular response to iron ion	2.46E-08	2.02E-06	8/1394 0.5%	21/55204 0.0%	Upregulated
BP	7154	cell communication	5.93E-08	4.73E-06	157/1394 11.2%	4047/55204 7.3%	Upregulated
BP	23052	signaling	6.54E-08	5.07E-06	156/1394 11.1%	4021/55204 7.2%	Upregulated
BP	7165	signal transduction	8.13E-08	6.14E-06	153/1394 10.9%	3938/55204 7.1%	Upregulated
BP	9805	coumarin biosynthetic process	1.21E-07	8.88E-06	9/1394 0.6%	34/55204 0.0%	Upregulated
BP	106146	sideretin biosynthesis	1.61E-07	1.15E-05	7/1394 0.5%	18/55204 0.0%	Upregulated
BP	9692	ethylene metabolic process	2.08E-07	1.35E-05	12/1394 0.8%	71/55204 0.1%	Upregulated
BP	9693	ethylene biosynthetic process	2.08E-07	1.35E-05	12/1394 0.8%	71/55204 0.1%	Upregulated
BP	43449	alkene metabolic process	2.08E-07	1.35E-05	12/1394 0.8%	71/55204 0.1%	Upregulated
BP	43450	alkene biosynthetic process	2.08E-07	1.35E-05	12/1394 0.8%	71/55204 0.1%	Upregulated
BP	1900673	olefin metabolic process	2.44E-07	1.51E-05	12/1394 0.8%	72/55204 0.1%	Upregulated
BP	1900674	olefin biosynthetic process	2.44E-07	1.51E-05	12/1394 0.8%	72/55204 0.1%	Upregulated
BP	9626	plant-type hypersensitive response	5.24E-07	3.18E-05	23/1394 1.6%	271/55204 0.4%	Upregulated
BP	34050	symbiont-induced defense-related programmed cell death	5.59E-07	3.32E-05	23/1394 1.6%	272/55204 0.4%	Upregulated
BP	19677	NAD+ catabolic process	1.24E-06	7.24E-05	15/1394 1.0%	131/55204 0.2%	Upregulated
BP	120251	hydrocarbon biosynthetic process	3.70E-06	2.11E-04	17/1394 1.2%	180/55204 0.3%	Upregulated
BP	9808	lignin metabolic process	4.30E-06	2.40E-04	17/1394 1.2%	182/55204 0.3%	Upregulated
BP	6952	defense response	5.00E-35	1.33E-31	171/1112 15.3%	2990/55204 5.4%	Downregulated
BP	9607	response to biotic stimulus	3.56E-21	3.03E-18	136/1112 12.2%	2805/55204 5.0%	Downregulated
BP	51707	response to other organism	5.51E-21	3.03E-18	135/1112 12.1%	2787/55204 5.0%	Downregulated
BP	9605	response to external stimulus	5.66E-21	3.03E-18	151/1112 13.5%	3310/55204 5.9%	Downregulated
BP	43207	response to external biotic stimulus	5.68E-21	3.03E-18	135/1112 12.1%	2788/55204 5.0%	Downregulated
BP	44419	biological process involved in interspecies interaction between organisms	2.37E-20	1.05E-17	136/1112 12.2%	2867/55204 5.1%	Downregulated
BP	9626	plant-type hypersensitive response	5.11E-19	1.92E-16	36/1112 3.2%	271/55204 0.4%	Downregulated
BP	34050	symbiont-induced defense-related programmed cell death	5.78E-19	1.92E-16	36/1112 3.2%	272/55204 0.4%	Downregulated
BP	19677	NAD+ catabolic process	2.25E-16	6.18E-14	24/1112 2.1%	131/55204 0.2%	Downregulated
BP	6468	protein phosphorylation	2.32E-16	6.18E-14	105/1112 9.4%	2175/55204 3.9%	Downregulated
BP	16310	phosphorylation	3.15E-16	7.63E-14	106/1112 9.5%	2217/55204 4.0%	Downregulated
BP	6950	response to stress	1.07E-15	2.37E-13	294/1112 26.4%	9393/55204 17.0%	Downregulated

Table S5.10 continued.

BP	50896	response to stimulus	6.93E-15	1.42E-12	413/1112 37.1%	14712/55204 26.6%	Downregulated
BP	7165	signal transduction	4.42E-14	8.40E-12	150/1112 13.4%	3938/55204 7.1%	Downregulated
BP	98542	defense response to other organism	6.01E-14	1.07E-11	55/1112 4.9%	849/55204 1.5%	Downregulated
BP	43068	positive regulation of programmed cell death	1.18E-13	1.96E-11	31/1112 2.7%	297/55204 0.5%	Downregulated
BP	23052	signaling	2.27E-13	3.56E-11	150/1112 13.4%	4021/55204 7.2%	Downregulated
BP	45087	innate immune response	2.47E-13	3.66E-11	47/1112 4.2%	670/55204 1.2%	Downregulated
BP	6955	immune response	3.54E-13	4.96E-11	49/1112 4.4%	728/55204 1.3%	Downregulated
BP	7154	cell communication	3.74E-13	4.98E-11	150/1112 13.4%	4047/55204 7.3%	Downregulated
BP	140546	defense response to symbiont	5.67E-13	7.19E-11	51/1112 4.5%	790/55204 1.4%	Downregulated
BP	12501	programmed cell death	6.72E-13	8.13E-11	41/1112 3.6%	540/55204 0.9%	Downregulated
BP	8219	cell death	4.44E-12	5.15E-10	42/1112 3.7%	598/55204 1.0%	Downregulated
BP	2376	immune system process	4.83E-11	5.36E-09	52/1112 4.6%	921/55204 1.6%	Downregulated
BP	42742	defense response to bacterium	9.52E-11	1.01E-08	50/1112 4.4%	881/55204 1.5%	Downregulated
BP	19674	NAD+ metabolic process	1.06E-10	1.09E-08	25/1112 2.2%	255/55204 0.4%	Downregulated
BP	36211	protein modification process	1.10E-10	1.09E-08	162/1112 14.5%	4839/55204 8.7%	Downregulated
BP	60866	leaf abscission	1.50E-10	1.42E-08	10/1112 0.8%	29/55204 0.0%	Downregulated
BP	9617	response to bacterium	4.61E-10	4.23E-08	61/1112 5.4%	1258/55204 2.2%	Downregulated
BP	50829	defense response to Gram-negative bacterium	1.38E-09	1.22E-07	13/1112 1.1%	70/55204 0.1%	Downregulated
BP	9838	abscission	1.89E-09	1.63E-07	11/1112 0.9%	47/55204 0.0%	Downregulated
BP	9862	systemic acquired resistance, salicylic acid mediated signaling pathway	1.98E-09	1.65E-07	13/1112 1.1%	72/55204 0.1%	Downregulated
BP	43067	regulation of programmed cell death	4.65E-09	3.76E-07	36/1112 3.2%	583/55204 1.0%	Downregulated
BP	9863	salicylic acid mediated signaling pathway	1.08E-08	8.48E-07	15/1112 1.3%	114/55204 0.2%	Downregulated
BP	10618	aerenchyma formation	1.29E-08	9.81E-07	7/1112 0.6%	16/55204 0.0%	Downregulated
BP	1900426	positive regulation of defense response to bacterium	1.81E-08	1.34E-06	12/1112 1.0%	71/55204 0.1%	Downregulated
BP	9620	response to fungus	2.09E-08	1.50E-06	43/1112 3.8%	822/55204 1.4%	Downregulated
BP	48544	recognition of pollen	2.25E-08	1.58E-06	21/1112 1.8%	239/55204 0.4%	Downregulated
BP	71446	cellular response to salicylic acid stimulus	3.44E-08	2.35E-06	15/1112 1.3%	124/55204 0.2%	Downregulated
BP	9751	response to salicylic acid	1.09E-07	7.18E-06	24/1112 2.1%	334/55204 0.6%	Downregulated
BP	51716	cellular response to stimulus	1.10E-07	7.18E-06	222/1112 19.9%	7888/55204 14.2%	Downregulated
BP	1900424	regulation of defense response to bacterium	1.26E-07	8.00E-06	16/1112 1.4%	156/55204 0.2%	Downregulated
BP	8037	cell recognition	1.81E-07	1.12E-05	21/1112 1.8%	270/55204 0.4%	Downregulated
BP	9627	systemic acquired resistance	2.13E-07	1.29E-05	16/1112 1.4%	162/55204 0.2%	Downregulated
BP	1900376	regulation of secondary metabolite biosynthetic process	2.98E-07	1.77E-05	9/1112 0.8%	46/55204 0.0%	Downregulated
BP	1900378	positive regulation of secondary metabolite biosynthetic process	3.39E-07	1.96E-05	7/1112 0.6%	24/55204 0.0%	Downregulated
BP	16138	glycoside biosynthetic process	6.31E-07	3.58E-05	9/1112 0.8%	50/55204 0.0%	Downregulated
BP	2229	defense response to oomycetes	9.86E-07	5.47E-05	15/1112 1.3%	160/55204 0.2%	Downregulated
BP	16137	glycoside metabolic process	1.16E-06	6.28E-05	11/1112 0.9%	85/55204 0.1%	Downregulated
BP	71327	cellular response to trehalose stimulus	1.37E-06	7.31E-05	5/1112 0.4%	11/55204 0.0%	Downregulated

Table S5.11. Significantly enriched GO terms (Biological Process) associated with genes that were differentially expressed between the resistant juniper genotype compared to the susceptible genotype, in both cases inoculated with the more virulent *P. austrocedri* isolate, at 48 hours post-inoculation. Where relevant, only the top 50 GO terms have been included for each direction (upregulated and downregulated).

GO	GO ID	GO Description	p-val	Corrected p-val	Cluster frequency	Total frequency	Direction
BP	6952	defense response	3.85E-34	1.10E-30	180/1227 14.6%	2990/55204 5.4%	Upregulated
BP	44419	biological process involved in interspecies interaction between organisms	4.70E-21	4.58E-18	147/1227 11.9%	2867/55204 5.1%	Upregulated
BP	51707	response to other organism	6.23E-21	4.58E-18	144/1227 11.7%	2787/55204 5.0%	Upregulated
BP	43207	response to external biotic stimulus	6.43E-21	4.58E-18	144/1227 11.7%	2788/55204 5.0%	Upregulated
BP	9607	response to biotic stimulus	1.11E-20	6.33E-18	144/1227 11.7%	2805/55204 5.0%	Upregulated
BP	9605	response to external stimulus	3.98E-18	1.89E-15	154/1227 12.5%	3310/55204 5.9%	Upregulated
BP	16998	cell wall macromolecule catabolic process	5.13E-16	2.09E-13	17/1227 1.3%	51/55204 0.0%	Upregulated
BP	50832	defense response to fungus	1.49E-14	4.16E-12	49/1227 3.9%	607/55204 1.0%	Upregulated
BP	141060	disruption of anatomical structure in another organism	1.61E-14	4.16E-12	14/1227 1.1%	36/55204 0.0%	Upregulated
BP	141061	disruption of cell in another organism	1.61E-14	4.16E-12	14/1227 1.1%	36/55204 0.0%	Upregulated
BP	31640	killing of cells of another organism	1.61E-14	4.16E-12	14/1227 1.1%	36/55204 0.0%	Upregulated
BP	9626	plant-type hypersensitive response	2.15E-14	5.09E-12	32/1227 2.6%	271/55204 0.4%	Upregulated
BP	34050	symbiont-induced defense-related programmed cell death	2.38E-14	5.22E-12	32/1227 2.6%	272/55204 0.4%	Upregulated
BP	1901072	glucosamine-containing compound catabolic process	3.49E-14	6.62E-12	18/1227 1.4%	74/55204 0.1%	Upregulated
BP	6032	chitin catabolic process	3.49E-14	6.62E-12	18/1227 1.4%	74/55204 0.1%	Upregulated
BP	46348	amino sugar catabolic process	9.38E-14	1.57E-11	18/1227 1.4%	78/55204 0.1%	Upregulated
BP	6030	chitin metabolic process	9.38E-14	1.57E-11	18/1227 1.4%	78/55204 0.1%	Upregulated
BP	1906	cell killing	1.98E-13	3.13E-11	14/1227 1.1%	42/55204 0.0%	Upregulated
BP	6026	aminoglycan catabolic process	3.70E-13	5.54E-11	18/1227 1.4%	84/55204 0.1%	Upregulated
BP	7165	signal transduction	8.83E-13	1.26E-10	157/1227 12.7%	3938/55204 7.1%	Upregulated
BP	6950	response to stress	1.28E-12	1.74E-10	305/1227 24.8%	9393/55204 17.0%	Upregulated
BP	19677	NAD+ catabolic process	1.68E-12	2.17E-10	21/1227 1.7%	131/55204 0.2%	Upregulated
BP	50896	response to stimulus	1.88E-12	2.32E-10	437/1227 35.6%	14712/55204 26.6%	Upregulated
BP	7154	cell communication	1.96E-12	2.32E-10	159/1227 12.9%	4047/55204 7.3%	Upregulated
BP	1901071	glucosamine-containing compound metabolic process	2.35E-12	2.67E-10	18/1227 1.4%	93/55204 0.1%	Upregulated
BP	23052	signaling	4.43E-12	4.85E-10	157/1227 12.7%	4021/55204 7.2%	Upregulated
BP	9620	response to fungus	8.68E-12	9.15E-10	53/1227 4.3%	822/55204 1.4%	Upregulated
BP	6022	aminoglycan metabolic process	1.07E-11	1.08E-09	20/1227 1.6%	129/55204 0.2%	Upregulated
BP	6040	amino sugar metabolic process	1.56E-10	1.53E-08	20/1227 1.6%	149/55204 0.2%	Upregulated
BP	19674	NAD+ metabolic process	7.98E-10	7.57E-08	25/1227 2.0%	255/55204 0.4%	Upregulated
BP	98542	defense response to other organism	2.16E-09	1.98E-07	49/1227 3.9%	849/55204 1.5%	Upregulated
BP	44036	cell wall macromolecule metabolic process	7.83E-09	6.97E-07	18/1227 1.4%	150/55204 0.2%	Upregulated
BP	45087	innate immune response	8.68E-09	7.48E-07	41/1227 3.3%	670/55204 1.2%	Upregulated
BP	6955	immune response	1.06E-08	8.89E-07	43/1227 3.5%	728/55204 1.3%	Upregulated
BP	43068	positive regulation of programmed cell death	1.78E-08	1.45E-06	25/1227 2.0%	297/55204 0.5%	Upregulated
BP	48544	recognition of pollen	2.56E-08	1.98E-06	22/1227 1.7%	239/55204 0.4%	Upregulated
BP	12501	programmed cell death	2.57E-08	1.98E-06	35/1227 2.8%	540/55204 0.9%	Upregulated
BP	8219	cell death	3.44E-08	2.58E-06	37/1227 3.0%	598/55204 1.0%	Upregulated
BP	140546	defense response to symbiont	3.95E-08	2.88E-06	44/1227 3.5%	790/55204 1.4%	Upregulated
BP	8037	cell recognition	5.25E-08	3.74E-06	23/1227 1.8%	270/55204 0.4%	Upregulated
BP	51716	cellular response to stimulus	9.12E-07	6.33E-05	236/1227 19.2%	7888/55204 14.2%	Upregulated
BP	9617	response to bacterium	1.03E-06	6.99E-05	56/1227 4.5%	1258/55204 2.2%	Upregulated
BP	2376	immune system process	1.07E-06	7.06E-05	45/1227 3.6%	921/55204 1.6%	Upregulated
BP	71554	cell wall organization or biogenesis	1.58E-06	1.02E-04	46/1227 3.7%	965/55204 1.7%	Upregulated
BP	42742	defense response to bacterium	1.89E-06	1.19E-04	43/1227 3.5%	881/55204 1.5%	Upregulated
BP	9625	response to insect	2.38E-06	1.47E-04	8/1227 0.6%	40/55204 0.0%	Upregulated
BP	10618	aerenchyma formation	1.92E-05	1.16E-03	5/1227 0.4%	16/55204 0.0%	Upregulated
BP	43067	regulation of programmed cell death	2.47E-05	1.46E-03	30/1227 2.4%	583/55204 1.0%	Upregulated
BP	60866	leaf abscission	3.65E-05	2.12E-03	6/1227 0.4%	29/55204 0.0%	Upregulated
BP	6412	translation	7.22E-05	4.11E-03	141/1227 11.4%	4607/55204 8.3%	Upregulated
BP	6952	defense response	2.65E-12	6.02E-09	100/878 11.3%	2990/55204 5.4%	Downregulated
BP	19677	NAD+ catabolic process	3.70E-10	4.21E-07	16/878 1.8%	131/55204 0.2%	Downregulated
BP	19748	secondary metabolic process	5.88E-08	3.84E-05	29/878 3.3%	569/55204 1.0%	Downregulated
BP	43068	positive regulation of programmed cell death	8.57E-08	3.84E-05	20/878 2.2%	297/55204 0.5%	Downregulated
BP	9626	plant-type hypersensitive response	9.56E-08	3.84E-05	19/878 2.1%	271/55204 0.4%	Downregulated
BP	34050	symbiont-induced defense-related programmed cell death	1.01E-07	3.84E-05	19/878 2.1%	272/55204 0.4%	Downregulated
BP	44550	secondary metabolite biosynthetic process	3.13E-07	1.02E-04	22/878 2.5%	383/55204 0.6%	Downregulated
BP	9813	flavonoid biosynthetic process	5.37E-07	1.53E-04	15/878 1.7%	192/55204 0.3%	Downregulated
BP	19674	NAD+ metabolic process	9.01E-07	2.17E-04	17/878 1.9%	255/55204 0.4%	Downregulated
BP	6955	immune response	1.03E-06	2.17E-04	31/878 3.5%	728/55204 1.3%	Downregulated
BP	16137	glycoside metabolic process	1.05E-06	2.17E-04	10/878 1.1%	85/55204 0.1%	Downregulated
BP	16138	glycoside biosynthetic process	1.18E-06	2.24E-04	8/878 0.9%	50/55204 0.0%	Downregulated
BP	9812	flavonoid metabolic process	3.90E-06	6.47E-04	15/878 1.7%	225/55204 0.4%	Downregulated

Table S5.11 continued.

BP	6950	response to stress	4.15E-06	6.47E-04	201/878 22.8%	9393/55204 17.0%	Downregulated
BP	9699	phenylpropanoid biosynthetic process	4.27E-06	6.47E-04	17/878 1.9%	286/55204 0.5%	Downregulated
BP	45087	innate immune response	4.82E-06	6.86E-04	28/878 3.1%	670/55204 1.2%	Downregulated
BP	2376	immune system process	7.10E-06	9.51E-04	34/878 3.8%	921/55204 1.6%	Downregulated
BP	12501	programmed cell death	8.26E-06	1.04E-03	24/878 2.7%	540/55204 0.9%	Downregulated
BP	16134	saponin metabolic process	9.09E-06	1.09E-03	7/878 0.7%	47/55204 0.0%	Downregulated
BP	9698	phenylpropanoid metabolic process	2.42E-05	2.64E-03	19/878 2.1%	395/55204 0.7%	Downregulated
BP	51707	response to other organism	2.53E-05	2.64E-03	73/878 8.3%	2787/55204 5.0%	Downregulated
BP	43207	response to external biotic stimulus	2.56E-05	2.64E-03	73/878 8.3%	2788/55204 5.0%	Downregulated
BP	9607	response to biotic stimulus	3.11E-05	3.02E-03	73/878 8.3%	2805/55204 5.0%	Downregulated
BP	16104	triterpenoid biosynthetic process	3.32E-05	3.02E-03	6/878 0.6%	39/55204 0.0%	Downregulated
BP	48544	recognition of pollen	3.44E-05	3.02E-03	14/878 1.5%	239/55204 0.4%	Downregulated
BP	44419	biological process involved in interspecies interaction between organisms	3.57E-05	3.02E-03	74/878 8.4%	2867/55204 5.1%	Downregulated
BP	140546	defense response to symbiont	3.63E-05	3.02E-03	29/878 3.3%	790/55204 1.4%	Downregulated
BP	6722	triterpenoid metabolic process	3.85E-05	3.02E-03	6/878 0.6%	40/55204 0.0%	Downregulated
BP	16135	saponin biosynthetic process	3.85E-05	3.02E-03	6/878 0.6%	40/55204 0.0%	Downregulated
BP	8219	cell death	4.26E-05	3.23E-03	24/878 2.7%	598/55204 1.0%	Downregulated
BP	15988	energy coupled proton transmembrane transport, against electrochemical gradient	5.12E-05	3.64E-03	6/878 0.6%	42/55204 0.0%	Downregulated
BP	15990	electron transport coupled proton transport	5.12E-05	3.64E-03	6/878 0.6%	42/55204 0.0%	Downregulated
BP	19684	photosynthesis, light reaction	8.41E-05	5.80E-03	41/878 4.6%	1354/55204 2.4%	Downregulated
BP	98542	defense response to other organism	1.26E-04	8.24E-03	29/878 3.3%	849/55204 1.5%	Downregulated
BP	8037	cell recognition	1.27E-04	8.24E-03	14/878 1.5%	270/55204 0.4%	Downregulated
BP	15979	photosynthesis	1.62E-04	1.01E-02	68/878 7.7%	2707/55204 4.9%	Downregulated
BP	50896	response to stimulus	1.64E-04	1.01E-02	282/878 32.1%	14712/55204 26.6%	Downregulated
BP	9620	response to fungus	1.71E-04	1.03E-02	28/878 3.1%	822/55204 1.4%	Downregulated
BP	43067	regulation of programmed cell death	2.08E-04	1.21E-02	22/878 2.5%	583/55204 1.0%	Downregulated
BP	42445	hormone metabolic process	2.38E-04	1.34E-02	16/878 1.8%	358/55204 0.6%	Downregulated
BP	9605	response to external stimulus	2.41E-04	1.34E-02	79/878 8.9%	3310/55204 5.9%	Downregulated
BP	9850	auxin metabolic process	2.78E-04	1.51E-02	9/878 1.0%	132/55204 0.2%	Downregulated
BP	140673	transcription elongation-coupled chromatin remodeling	4.69E-04	2.48E-02	5/878 0.5%	41/55204 0.0%	Downregulated
BP	1900378	positive regulation of secondary metabolite biosynthetic process	5.24E-04	2.71E-02	4/878 0.4%	24/55204 0.0%	Downregulated
BP	7165	signal transduction	5.71E-04	2.88E-02	89/878 10.1%	3938/55204 7.1%	Downregulated
BP	71284	cellular response to lead ion	6.01E-04	2.97E-02	3/878 0.3%	11/55204 0.0%	Downregulated
BP	23052	signaling	7.17E-04	3.47E-02	90/878 10.2%	4021/55204 7.2%	Downregulated
BP	1900376	regulation of secondary metabolite biosynthetic process	8.04E-04	3.81E-02	5/878 0.5%	46/55204 0.0%	Downregulated
BP	7154	cell communication	8.72E-04	4.05E-02	90/878 10.2%	4047/55204 7.3%	Downregulated

Table S5.12. Significantly enriched GO terms (Biological Process) associated with genes that were differentially expressed between the resistant juniper genotype compared to the susceptible genotype, in both cases treated with a mock-inoculated control, at one week post-inoculation. Where relevant, only the top 50 GO terms have been included for each direction (upregulated and downregulated).

GO	GO ID	GO Description	p-val	Corrected p-val	Cluster frequency	Total frequency	Direction
BP	6412	translation	5.68E-25	1.69E-21	271/1711 15.8%	4607/55204 8.3%	Upregulated
BP	19677	NAD+ catabolic process	3.28E-13	4.89E-10	25/1711 1.4%	131/55204 0.2%	Upregulated
BP	15979	photosynthesis	1.45E-12	1.44E-09	152/1711 8.8%	2707/55204 4.9%	Upregulated
BP	9451	RNA modification	2.48E-12	1.85E-09	136/1711 7.9%	2344/55204 4.2%	Upregulated
BP	9765	photosynthesis, light harvesting	8.80E-11	5.25E-08	66/1711 3.8%	886/55204 1.6%	Upregulated
BP	10467	gene expression	1.43E-10	7.13E-08	449/1711 26.2%	11047/55204 20.0%	Upregulated
BP	6952	defense response	3.12E-10	1.33E-07	155/1711 9.0%	2990/55204 5.4%	Upregulated
BP	19684	photosynthesis, light reaction	4.53E-10	1.69E-07	86/1711 5.0%	1354/55204 2.4%	Upregulated
BP	9059	macromolecule biosynthetic process	1.85E-08	5.56E-06	471/1711 27.5%	12110/55204 21.9%	Upregulated
BP	43068	positive regulation of programmed cell death	1.87E-08	5.56E-06	30/1711 1.7%	297/55204 0.5%	Upregulated
BP	16556	mRNA modification	2.33E-08	6.31E-06	45/1711 2.6%	578/55204 1.0%	Upregulated
BP	9626	plant-type hypersensitive response	3.38E-08	7.80E-06	28/1711 1.6%	271/55204 0.4%	Upregulated
BP	19674	NAD+ metabolic process	3.54E-08	7.80E-06	27/1711 1.5%	255/55204 0.4%	Upregulated
BP	34050	symbiont-induced defense-related programmed cell death	3.66E-08	7.80E-06	28/1711 1.6%	272/55204 0.4%	Upregulated
BP	2181	cytoplasmic translation	4.99E-07	9.91E-05	54/1711 3.1%	838/55204 1.5%	Upregulated
BP	7165	signal transduction	2.42E-06	4.51E-04	173/1711 10.1%	3938/55204 7.1%	Upregulated
BP	9808	lignin metabolic process	4.42E-06	7.37E-04	19/1711 1.1%	182/55204 0.3%	Upregulated
BP	19748	secondary metabolic process	4.45E-06	7.37E-04	39/1711 2.2%	569/55204 1.0%	Upregulated
BP	7154	cell communication	5.32E-06	8.12E-04	175/1711 10.2%	4047/55204 7.3%	Upregulated
BP	23052	signaling	5.45E-06	8.12E-04	174/1711 10.1%	4021/55204 7.2%	Upregulated
BP	80156	mitochondrial mRNA modification	7.89E-06	1.12E-03	27/1711 1.5%	336/55204 0.6%	Upregulated
BP	959	mitochondrial RNA metabolic process	9.92E-06	1.35E-03	30/1711 1.7%	400/55204 0.7%	Upregulated
BP	1900864	mitochondrial RNA modification	1.91E-05	2.48E-03	27/1711 1.5%	353/55204 0.6%	Upregulated
BP	16138	glycoside biosynthetic process	2.06E-05	2.56E-03	9/1711 0.5%	50/55204 0.0%	Upregulated
BP	42549	photosystem II stabilization	2.21E-05	2.64E-03	11/1711 0.6%	76/55204 0.1%	Upregulated
BP	44550	secondary metabolite biosynthetic process	3.05E-05	3.50E-03	28/1711 1.6%	383/55204 0.6%	Upregulated
BP	48544	recognition of pollen	6.44E-05	7.12E-03	20/1711 1.1%	239/55204 0.4%	Upregulated
BP	6414	translational elongation	8.48E-05	9.03E-03	24/1711 1.4%	323/55204 0.5%	Upregulated
BP	43067	regulation of programmed cell death	8.88E-05	9.13E-03	36/1711 2.1%	583/55204 1.0%	Upregulated
BP	9698	phenylpropanoid metabolic process	1.29E-04	1.27E-02	27/1711 1.5%	395/55204 0.7%	Upregulated
BP	51707	response to other organism	1.35E-04	1.27E-02	121/1711 7.0%	2787/55204 5.0%	Upregulated
BP	43207	response to external biotic stimulus	1.37E-04	1.27E-02	121/1711 7.0%	2788/55204 5.0%	Upregulated
BP	42254	ribosome biogenesis	1.46E-04	1.28E-02	81/1711 4.7%	1717/55204 3.1%	Upregulated
BP	8219	cell death	1.46E-04	1.28E-02	36/1711 2.1%	598/55204 1.0%	Upregulated
BP	9607	response to biotic stimulus	1.74E-04	1.46E-02	121/1711 7.0%	2805/55204 5.0%	Upregulated
BP	1900865	chloroplast RNA modification	1.76E-04	1.46E-02	12/1711 0.7%	111/55204 0.2%	Upregulated
BP	44419	biological process involved in interspecies interaction between organisms	1.91E-04	1.50E-02	123/1711 7.1%	2867/55204 5.1%	Upregulated
BP	9820	alkaloid metabolic process	1.92E-04	1.50E-02	14/1711 0.8%	146/55204 0.2%	Upregulated
BP	12501	programmed cell death	2.06E-04	1.54E-02	33/1711 1.9%	540/55204 0.9%	Upregulated
BP	16135	saponin biosynthetic process	2.06E-04	1.54E-02	7/1711 0.4%	40/55204 0.0%	Upregulated
BP	98542	defense response to other organism	2.23E-04	1.62E-02	46/1711 2.6%	849/55204 1.5%	Upregulated
BP	45087	innate immune response	3.17E-04	2.24E-02	38/1711 2.2%	670/55204 1.2%	Upregulated
BP	16553	base conversion or substitution editing	3.30E-04	2.24E-02	16/1711 0.9%	191/55204 0.3%	Upregulated
BP	8037	cell recognition	3.30E-04	2.24E-02	20/1711 1.1%	270/55204 0.4%	Upregulated
BP	46274	lignin catabolic process	3.59E-04	2.38E-02	8/1711 0.4%	57/55204 0.1%	Upregulated
BP	6955	immune response	4.21E-04	2.73E-02	40/1711 2.3%	728/55204 1.3%	Upregulated
BP	46484	oxazole or thiazole metabolic process	5.04E-04	3.07E-02	7/1711 0.4%	46/55204 0.0%	Upregulated
BP	52837	thiazole biosynthetic process	5.04E-04	3.07E-02	7/1711 0.4%	46/55204 0.0%	Upregulated
BP	52838	thiazole metabolic process	5.04E-04	3.07E-02	7/1711 0.4%	46/55204 0.0%	Upregulated
BP	35834	indole alkaloid metabolic process	5.25E-04	3.13E-02	4/1711 0.2%	13/55204 0.0%	Upregulated
BP	6952	defense response	3.09E-32	8.33E-29	165/1106 14.9%	2990/55204 5.4%	Downregulated
BP	50896	response to stimulus	9.32E-30	1.26E-26	467/1106 42.2%	14712/55204 26.6%	Downregulated
BP	6950	response to stress	3.33E-26	3.00E-23	329/1106 29.7%	9393/55204 17.0%	Downregulated
BP	9607	response to biotic stimulus	4.26E-20	2.88E-17	133/1106 12.0%	2805/55204 5.0%	Downregulated
BP	51707	response to other organism	6.58E-20	3.05E-17	132/1106 11.9%	2787/55204 5.0%	Downregulated
BP	43207	response to external biotic stimulus	6.78E-20	3.05E-17	132/1106 11.9%	2788/55204 5.0%	Downregulated
BP	44419	biological process involved in interspecies interaction between organisms	6.85E-19	2.64E-16	132/1106 11.9%	2867/55204 5.1%	Downregulated
BP	9605	response to external stimulus	2.04E-18	6.89E-16	144/1106 13.0%	3310/55204 5.9%	Downregulated
BP	9620	response to fungus	1.69E-13	5.05E-11	53/1106 4.7%	822/55204 1.4%	Downregulated
BP	7165	signal transduction	5.23E-13	1.41E-10	146/1106 13.2%	3938/55204 7.1%	Downregulated
BP	23052	signaling	1.24E-12	3.03E-10	147/1106 13.2%	4021/55204 7.2%	Downregulated

Table S5.12 continued.

BP	7154	cell communication	3.97E-12	8.92E-10	146/1106 13.2%	4047/55204 7.3%	Downregulated
BP	19677	NAD+ catabolic process	1.99E-11	4.12E-09	19/1106 1.7%	131/55204 0.2%	Downregulated
BP	42221	response to chemical	5.33E-11	1.03E-08	208/1106 18.8%	6671/55204 12.0%	Downregulated
BP	9626	plant-type hypersensitive response	6.49E-11	1.17E-08	26/1106 2.3%	271/55204 0.4%	Downregulated
BP	34050	symbiont-induced defense-related programmed cell death	7.04E-11	1.19E-08	26/1106 2.3%	272/55204 0.4%	Downregulated
BP	65007	biological regulation	8.43E-11	1.34E-08	338/1106 30.5%	12316/55204 22.3%	Downregulated
BP	2229	defense response to oomycetes	9.38E-11	1.41E-08	20/1106 1.8%	160/55204 0.2%	Downregulated
BP	51716	cellular response to stimulus	2.71E-10	3.85E-08	234/1106 21.1%	7888/55204 14.2%	Downregulated
BP	2239	response to oomycetes	3.28E-10	4.42E-08	21/1106 1.8%	190/55204 0.3%	Downregulated
BP	50789	regulation of biological process	4.47E-10	5.75E-08	320/1106 28.9%	11681/55204 21.1%	Downregulated
BP	19748	secondary metabolic process	6.10E-10	7.47E-08	37/1106 3.3%	569/55204 1.0%	Downregulated
BP	9751	response to salicylic acid	1.30E-09	1.52E-07	27/1106 2.4%	334/55204 0.6%	Downregulated
BP	1666	response to hypoxia	1.63E-09	1.83E-07	28/1106 2.5%	361/55204 0.6%	Downregulated
BP	6468	protein phosphorylation	2.51E-09	2.71E-07	86/1106 7.7%	2175/55204 3.9%	Downregulated
BP	10150	leaf senescence	5.94E-09	6.04E-07	22/1106 1.9%	244/55204 0.4%	Downregulated
BP	16310	phosphorylation	6.05E-09	6.04E-07	86/1106 7.7%	2217/55204 4.0%	Downregulated
BP	36293	response to decreased oxygen levels	6.72E-09	6.47E-07	28/1106 2.5%	385/55204 0.6%	Downregulated
BP	8219	cell death	7.81E-09	7.26E-07	36/1106 3.2%	598/55204 1.0%	Downregulated
BP	42537	benzene-containing compound metabolic process	9.75E-09	8.77E-07	16/1106 1.4%	131/55204 0.2%	Downregulated
BP	9725	response to hormone	1.56E-08	1.35E-06	101/1106 9.1%	2818/55204 5.1%	Downregulated
BP	70482	response to oxygen levels	1.90E-08	1.60E-06	28/1106 2.5%	404/55204 0.7%	Downregulated
BP	44550	secondary metabolite biosynthetic process	2.38E-08	1.95E-06	27/1106 2.4%	383/55204 0.6%	Downregulated
BP	9719	response to endogenous stimulus	2.57E-08	2.04E-06	101/1106 9.1%	2847/55204 5.1%	Downregulated
BP	90693	plant organ senescence	2.66E-08	2.05E-06	22/1106 1.9%	265/55204 0.4%	Downregulated
BP	46244	salicylic acid catabolic process	3.34E-08	2.50E-06	7/1106 0.6%	18/55204 0.0%	Downregulated
BP	43068	positive regulation of programmed cell death	4.69E-08	3.42E-06	23/1106 2.0%	297/55204 0.5%	Downregulated
BP	9696	salicylic acid metabolic process	7.88E-08	5.59E-06	9/1106 0.8%	40/55204 0.0%	Downregulated
BP	70887	cellular response to chemical stimulus	8.65E-08	5.98E-06	121/1106 10.9%	3698/55204 6.6%	Downregulated
BP	9617	response to bacterium	8.87E-08	5.98E-06	55/1106 4.9%	1258/55204 2.2%	Downregulated
BP	48367	shoot system development	9.41E-08	6.19E-06	66/1106 5.9%	1637/55204 2.9%	Downregulated
BP	9699	phenylpropanoid biosynthetic process	1.03E-07	6.59E-06	22/1106 1.9%	286/55204 0.5%	Downregulated
BP	6955	immune response	1.26E-07	7.91E-06	38/1106 3.4%	728/55204 1.3%	Downregulated
BP	9611	response to wounding	1.36E-07	8.33E-06	29/1106 2.6%	471/55204 0.8%	Downregulated
BP	50794	regulation of cellular process	2.33E-07	1.39E-05	280/1106 25.3%	10579/55204 19.1%	Downregulated
BP	12501	programmed cell death	2.38E-07	1.40E-05	31/1106 2.8%	540/55204 0.9%	Downregulated
BP	36211	protein modification process	2.82E-07	1.59E-05	147/1106 13.2%	4839/55204 8.7%	Downregulated
BP	19674	NAD+ metabolic process	2.83E-07	1.59E-05	20/1106 1.8%	255/55204 0.4%	Downregulated
BP	1901700	response to oxygen-containing compound	3.06E-07	1.68E-05	132/1106 11.9%	4232/55204 7.6%	Downregulated
BP	10618	aerenchyma formation	4.30E-07	2.32E-05	6/1106 0.5%	16/55204 0.0%	Downregulated

Table S5.13. Significantly enriched GO terms (Biological Process) associated with genes that were differentially expressed between the resistant juniper genotype compared to the susceptible genotype, in both cases inoculated with the less virulent *P. austrocedri* isolate, at one week post-inoculation. Only the top 50 GO terms have been included for each direction (upregulated and downregulated).

GO	GO ID	GO Description	p-val	Corrected p-val	Cluster frequency	Total frequency	Direction
BP	6952	defense response	6.88E-26	2.21E-22	207/1760 11.7%	2990/55204 5.4%	Upregulated
BP	19684	photosynthesis, light reaction	2.65E-20	4.25E-17	113/1760 6.4%	1354/55204 2.4%	Upregulated
BP	9765	photosynthesis, light harvesting	3.50E-19	3.74E-16	85/1760 4.8%	886/55204 1.6%	Upregulated
BP	50896	response to stimulus	6.90E-18	5.53E-15	630/1760 35.7%	14712/55204 26.6%	Upregulated
BP	15979	photosynthesis	3.52E-17	2.26E-14	170/1760 9.6%	2707/55204 4.9%	Upregulated
BP	6950	response to stress	1.65E-14	7.82E-12	423/1760 24.0%	9393/55204 17.0%	Upregulated
BP	51707	response to other organism	1.89E-14	7.82E-12	165/1760 9.3%	2787/55204 5.0%	Upregulated
BP	43207	response to external biotic stimulus	1.95E-14	7.82E-12	165/1760 9.3%	2788/55204 5.0%	Upregulated
BP	9607	response to biotic stimulus	3.26E-14	1.16E-11	165/1760 9.3%	2805/55204 5.0%	Upregulated
BP	44419	biological process involved in interspecies interaction between organisms	5.17E-14	1.66E-11	167/1760 9.4%	2867/55204 5.1%	Upregulated
BP	19677	NAD+ catabolic process	6.08E-13	1.77E-10	25/1760 1.4%	131/55204 0.2%	Upregulated
BP	9605	response to external stimulus	1.08E-12	2.77E-10	181/1760 10.2%	3310/55204 5.9%	Upregulated
BP	7154	cell communication	1.12E-12	2.77E-10	211/1760 11.9%	4047/55204 7.3%	Upregulated
BP	7165	signal transduction	2.84E-12	6.50E-10	205/1760 11.6%	3938/55204 7.1%	Upregulated
BP	23052	signaling	3.43E-12	7.34E-10	208/1760 11.8%	4021/55204 7.2%	Upregulated
BP	50832	defense response to fungus	6.45E-12	1.29E-09	55/1760 3.1%	607/55204 1.0%	Upregulated
BP	16998	cell wall macromolecule catabolic process	3.65E-11	6.89E-09	15/1760 0.8%	51/55204 0.0%	Upregulated
BP	43068	positive regulation of programmed cell death	3.98E-11	7.09E-09	35/1760 1.9%	297/55204 0.5%	Upregulated
BP	9620	response to fungus	8.69E-11	1.47E-08	64/1760 3.6%	822/55204 1.4%	Upregulated
BP	1901072	glucosamine-containing compound catabolic process	1.05E-08	1.60E-06	15/1760 0.8%	74/55204 0.1%	Upregulated
BP	6032	chitin catabolic process	1.05E-08	1.60E-06	15/1760 0.8%	74/55204 0.1%	Upregulated
BP	9626	plant-type hypersensitive response	1.63E-08	2.28E-06	29/1760 1.6%	271/55204 0.4%	Upregulated
BP	19674	NAD+ metabolic process	1.64E-08	2.28E-06	28/1760 1.5%	255/55204 0.4%	Upregulated
BP	34050	symbiont-induced defense-related programmed cell death	1.77E-08	2.37E-06	29/1760 1.6%	272/55204 0.4%	Upregulated
BP	46348	amino sugar catabolic process	2.23E-08	2.75E-06	15/1760 0.8%	78/55204 0.1%	Upregulated
BP	6030	chitin metabolic process	2.23E-08	2.75E-06	15/1760 0.8%	78/55204 0.1%	Upregulated
BP	1901071	glucosamine-containing compound metabolic process	4.01E-08	4.76E-06	16/1760 0.9%	93/55204 0.1%	Upregulated
BP	6026	aminoglycan catabolic process	6.31E-08	7.24E-06	15/1760 0.8%	84/55204 0.1%	Upregulated
BP	51716	cellular response to stimulus	6.67E-08	7.38E-06	331/1760 18.8%	7888/55204 14.2%	Upregulated
BP	6040	amino sugar metabolic process	1.43E-06	1.53E-04	18/1760 1.0%	149/55204 0.2%	Upregulated
BP	44036	cell wall macromolecule metabolic process	1.58E-06	1.63E-04	18/1760 1.0%	150/55204 0.2%	Upregulated
BP	42742	defense response to bacterium	2.41E-06	2.42E-04	55/1760 3.1%	881/55204 1.5%	Upregulated
BP	43067	regulation of programmed cell death	2.70E-06	2.63E-04	41/1760 2.3%	583/55204 1.0%	Upregulated
BP	98542	defense response to other organism	3.65E-06	3.42E-04	53/1760 3.0%	849/55204 1.5%	Upregulated
BP	6022	aminoglycan metabolic process	3.82E-06	3.42E-04	16/1760 0.9%	129/55204 0.2%	Upregulated
BP	10411	xyloglucan metabolic process	3.84E-06	3.42E-04	13/1760 0.7%	87/55204 0.1%	Upregulated
BP	9813	flavonoid biosynthetic process	3.94E-06	3.42E-04	20/1760 1.1%	192/55204 0.3%	Upregulated
BP	9768	photosynthesis, light harvesting in photosystem I	4.66E-06	3.94E-04	24/1760 1.3%	263/55204 0.4%	Upregulated
BP	42549	photosystem II stabilization	4.99E-06	4.01E-04	12/1760 0.6%	76/55204 0.1%	Upregulated
BP	9733	response to auxin	5.00E-06	4.01E-04	45/1760 2.5%	683/55204 1.2%	Upregulated
BP	9812	flavonoid metabolic process	1.27E-05	9.95E-04	21/1760 1.1%	225/55204 0.4%	Upregulated
BP	727	double-strand break repair via break-induced replication	1.68E-05	1.28E-03	7/1760 0.3%	27/55204 0.0%	Upregulated
BP	71554	cell wall organization or biogenesis	3.16E-05	2.36E-03	55/1760 3.1%	965/55204 1.7%	Upregulated
BP	35834	indole alkaloid metabolic process	3.40E-05	2.48E-03	5/1760 0.2%	13/55204 0.0%	Upregulated
BP	9617	response to bacterium	3.84E-05	2.74E-03	67/1760 3.8%	1258/55204 2.2%	Upregulated
BP	65007	biological regulation	5.21E-05	3.64E-03	461/1760 26.1%	12316/55204 22.3%	Upregulated
BP	45087	innate immune response	6.80E-05	4.65E-03	41/1760 2.3%	670/55204 1.2%	Upregulated
BP	140546	defense response to symbiont	8.27E-05	5.53E-03	46/1760 2.6%	790/55204 1.4%	Upregulated
BP	71365	cellular response to auxin stimulus	8.89E-05	5.82E-03	31/1760 1.7%	459/55204 0.8%	Upregulated
BP	50789	regulation of biological process	9.38E-05	6.02E-03	437/1760 24.8%	11681/55204 21.1%	Upregulated
BP	6952	defense response	8.92E-21	2.08E-17	135/1044 12.9%	2990/55204 5.4%	Downregulated
BP	48544	recognition of pollen	2.22E-14	2.59E-11	28/1044 2.6%	239/55204 0.4%	Downregulated
BP	8037	cell recognition	4.71E-13	2.84E-10	28/1044 2.6%	270/55204 0.4%	Downregulated
BP	19748	secondary metabolic process	4.87E-13	2.84E-10	41/1044 3.9%	569/55204 1.0%	Downregulated
BP	6950	response to stress	5.36E-10	2.04E-07	255/1044 24.4%	9393/55204 17.0%	Downregulated
BP	9626	plant-type hypersensitive response	5.67E-10	2.04E-07	24/1044 2.2%	271/55204 0.4%	Downregulated
BP	34050	symbiont-induced defense-related programmed cell death	6.11E-10	2.04E-07	24/1044 2.2%	272/55204 0.4%	Downregulated
BP	51707	response to other organism	9.05E-10	2.39E-07	100/1044 9.5%	2787/55204 5.0%	Downregulated
BP	43207	response to external biotic stimulus	9.22E-10	2.39E-07	100/1044 9.5%	2788/55204 5.0%	Downregulated
BP	9607	response to biotic stimulus	1.26E-09	2.95E-07	100/1044 9.5%	2805/55204 5.0%	Downregulated
BP	9699	phenylpropanoid biosynthetic process	1.67E-09	3.55E-07	24/1044 2.2%	286/55204 0.5%	Downregulated
BP	50896	response to stimulus	2.22E-09	4.31E-07	364/1044 34.8%	14712/55204 26.6%	Downregulated
BP	9698	phenylpropanoid metabolic process	3.41E-09	6.12E-07	28/1044 2.6%	395/55204 0.7%	Downregulated

Table S5.13 continued.

BP	44419	biological process involved in interspecies interaction between organisms	3.88E-09	6.46E-07	100/1044 9.5%	2867/55204 5.1%	Downregulated
BP	44550	secondary metabolite biosynthetic process	7.26E-09	1.13E-06	27/1044 2.5%	383/55204 0.6%	Downregulated
BP	6468	protein phosphorylation	1.69E-08	2.46E-06	80/1044 7.6%	2175/55204 3.9%	Downregulated
BP	7165	signal transduction	1.91E-08	2.62E-06	124/1044 11.8%	3938/55204 7.1%	Downregulated
BP	9605	response to external stimulus	2.96E-08	3.84E-06	108/1044 10.3%	3310/55204 5.9%	Downregulated
BP	23052	signaling	3.41E-08	4.19E-06	125/1044 11.9%	4021/55204 7.2%	Downregulated
BP	16310	phosphorylation	3.78E-08	4.41E-06	80/1044 7.6%	2217/55204 4.0%	Downregulated
BP	9625	response to insect	4.83E-08	5.37E-06	9/1044 0.8%	40/55204 0.0%	Downregulated
BP	7154	cell communication	8.57E-08	9.09E-06	124/1044 11.8%	4047/55204 7.3%	Downregulated
BP	9800	cinnamic acid biosynthetic process	1.19E-07	1.16E-05	6/1044 0.5%	14/55204 0.0%	Downregulated
BP	9803	cinnamic acid metabolic process	1.19E-07	1.16E-05	6/1044 0.5%	14/55204 0.0%	Downregulated
BP	9404	toxin metabolic process	1.71E-07	1.59E-05	11/1044 1.0%	75/55204 0.1%	Downregulated
BP	9813	flavonoid biosynthetic process	1.80E-07	1.61E-05	17/1044 1.6%	192/55204 0.3%	Downregulated
BP	2000068	regulation of defense response to insect	2.14E-07	1.85E-05	9/1044 0.8%	47/55204 0.0%	Downregulated
BP	10618	aerenchyma formation	3.07E-07	2.56E-05	6/1044 0.5%	16/55204 0.0%	Downregulated
BP	16138	glycoside biosynthetic process	3.74E-07	3.01E-05	9/1044 0.8%	50/55204 0.0%	Downregulated
BP	50829	defense response to Gram-negative bacterium	7.97E-07	6.06E-05	10/1044 0.9%	70/55204 0.1%	Downregulated
BP	8299	isoprenoid biosynthetic process	8.06E-07	6.06E-05	39/1044 3.7%	865/55204 1.5%	Downregulated
BP	1900426	positive regulation of defense response to bacterium	9.12E-07	6.50E-05	10/1044 0.9%	71/55204 0.1%	Downregulated
BP	60866	leaf abscission	9.20E-07	6.50E-05	7/1044 0.6%	29/55204 0.0%	Downregulated
BP	71327	cellular response to trehalose stimulus	1.01E-06	6.91E-05	5/1044 0.4%	11/55204 0.0%	Downregulated
BP	19677	NAD+ catabolic process	1.37E-06	8.78E-05	13/1044 1.2%	131/55204 0.2%	Downregulated
BP	1901183	positive regulation of camalexin biosynthetic process	1.39E-06	8.78E-05	6/1044 0.5%	20/55204 0.0%	Downregulated
BP	52322	positive regulation of phytoalexin biosynthetic process	1.39E-06	8.78E-05	6/1044 0.5%	20/55204 0.0%	Downregulated
BP	9812	flavonoid metabolic process	1.66E-06	1.02E-04	17/1044 1.6%	225/55204 0.4%	Downregulated
BP	10597	green leaf volatile biosynthetic process	1.77E-06	1.06E-04	13/1044 1.2%	134/55204 0.2%	Downregulated
BP	6955	immune response	1.88E-06	1.10E-04	34/1044 3.2%	728/55204 1.3%	Downregulated
BP	2000022	regulation of jasmonic acid mediated signaling pathway	2.47E-06	1.41E-04	9/1044 0.8%	62/55204 0.1%	Downregulated
BP	9838	abscission	2.61E-06	1.45E-04	8/1044 0.7%	47/55204 0.0%	Downregulated
BP	80142	regulation of salicylic acid biosynthetic process	2.72E-06	1.47E-04	5/1044 0.4%	13/55204 0.0%	Downregulated
BP	19372	lipoxygenase pathway	3.39E-06	1.80E-04	13/1044 1.2%	142/55204 0.2%	Downregulated
BP	2376	immune system process	3.60E-06	1.87E-04	39/1044 3.7%	921/55204 1.6%	Downregulated
BP	1900378	positive regulation of secondary metabolite biosynthetic process	4.54E-06	2.30E-04	6/1044 0.5%	24/55204 0.0%	Downregulated
BP	16137	glycoside metabolic process	4.87E-06	2.38E-04	10/1044 0.9%	85/55204 0.1%	Downregulated
BP	43068	positive regulation of programmed cell death	4.91E-06	2.38E-04	19/1044 1.8%	297/55204 0.5%	Downregulated
BP	12501	programmed cell death	6.23E-06	2.96E-04	27/1044 2.5%	540/55204 0.9%	Downregulated
BP	45087	innate immune response	6.35E-06	2.96E-04	31/1044 2.9%	670/55204 1.2%	Downregulated

Table S5.14. Significantly enriched GO terms (Biological Process) associated with genes that were differentially expressed between the resistant juniper genotype compared to the susceptible genotype, in both cases inoculated with the more virulent *P. austrocedri* isolate, at one week post-inoculation. Only the top 50 GO terms have been included for each direction (upregulated and downregulated).

GO	GO ID	GO Description	p-val	Corrected p-val	Cluster frequency	Total frequency	Direction
BP	15979	photosynthesis	1.23E-54	4.48E-51	293/2224 13.1%	2707/55204 4.9%	Upregulated
BP	9765	photosynthesis, light harvesting	1.47E-44	2.69E-41	141/2224 6.3%	886/55204 1.6%	Upregulated
BP	19684	photosynthesis, light reaction	3.89E-44	4.74E-41	178/2224 8.0%	1354/55204 2.4%	Upregulated
BP	6091	generation of precursor metabolites and energy	2.18E-26	1.99E-23	286/2224 12.8%	3720/55204 6.7%	Upregulated
BP	6412	translation	3.81E-23	2.79E-20	323/2224 14.5%	4607/55204 8.3%	Upregulated
BP	2181	cytoplasmic translation	3.80E-15	2.31E-12	86/2224 3.8%	838/55204 1.5%	Upregulated
BP	2182	cytoplasmic translational elongation	2.31E-13	1.21E-10	23/2224 1.0%	85/55204 0.1%	Upregulated
BP	6414	translational elongation	3.02E-11	1.38E-08	42/2224 1.8%	323/55204 0.5%	Upregulated
BP	9768	photosynthesis, light harvesting in photosystem I	1.79E-10	7.27E-08	36/2224 1.6%	263/55204 0.4%	Upregulated
BP	16998	cell wall macromolecule catabolic process	9.22E-10	3.37E-07	15/2224 0.6%	51/55204 0.0%	Upregulated
BP	1901072	glucosamine-containing compound catabolic process	3.35E-08	1.02E-05	16/2224 0.7%	74/55204 0.1%	Upregulated
BP	6032	chitin catabolic process	3.35E-08	1.02E-05	16/2224 0.7%	74/55204 0.1%	Upregulated
BP	46348	amino sugar catabolic process	7.35E-08	1.92E-05	16/2224 0.7%	78/55204 0.1%	Upregulated
BP	6030	chitin metabolic process	7.35E-08	1.92E-05	16/2224 0.7%	78/55204 0.1%	Upregulated
BP	15986	proton motive force-driven ATP synthesis	2.12E-07	4.97E-05	31/2224 1.3%	271/55204 0.4%	Upregulated
BP	6026	aminoglycan catabolic process	2.17E-07	4.97E-05	16/2224 0.7%	84/55204 0.1%	Upregulated
BP	19253	reductive pentose-phosphate cycle	2.36E-07	5.07E-05	37/2224 1.6%	360/55204 0.6%	Upregulated
BP	6754	ATP biosynthetic process	2.71E-07	5.51E-05	31/2224 1.3%	274/55204 0.4%	Upregulated
BP	42549	photosystem II stabilization	3.18E-07	6.12E-05	15/2224 0.6%	76/55204 0.1%	Upregulated
BP	16138	glycoside biosynthetic process	5.18E-07	9.47E-05	12/2224 0.5%	50/55204 0.0%	Upregulated
BP	19685	photosynthesis, dark reaction	6.86E-07	1.19E-04	37/2224 1.6%	376/55204 0.6%	Upregulated
BP	1901071	glucosamine-containing compound metabolic process	9.20E-07	1.53E-04	16/2224 0.7%	93/55204 0.1%	Upregulated
BP	16134	saponin metabolic process	2.02E-06	3.21E-04	11/2224 0.4%	47/55204 0.0%	Upregulated
BP	16135	saponin biosynthetic process	3.09E-06	4.71E-04	10/2224 0.4%	40/55204 0.0%	Upregulated
BP	6022	aminoglycan metabolic process	4.56E-06	6.67E-04	18/2224 0.8%	129/55204 0.2%	Upregulated
BP	15977	carbon fixation	5.54E-06	7.79E-04	37/2224 1.6%	411/55204 0.7%	Upregulated
BP	9206	purine ribonucleoside triphosphate biosynthetic process	6.97E-06	9.34E-04	32/2224 1.4%	335/55204 0.6%	Upregulated
BP	16137	glycoside metabolic process	7.38E-06	9.34E-04	14/2224 0.6%	85/55204 0.1%	Upregulated
BP	9145	purine nucleoside triphosphate biosynthetic process	7.41E-06	9.34E-04	32/2224 1.4%	336/55204 0.6%	Upregulated
BP	6952	defense response	9.22E-06	1.12E-03	168/2224 7.5%	2990/55204 5.4%	Upregulated
BP	6040	amino sugar metabolic process	3.39E-05	3.93E-03	18/2224 0.8%	149/55204 0.2%	Upregulated
BP	42542	response to hydrogen peroxide	3.44E-05	3.93E-03	23/2224 1.0%	221/55204 0.4%	Upregulated
BP	10268	brassinosteroid homeostasis	4.41E-05	4.89E-03	10/2224 0.4%	53/55204 0.0%	Upregulated
BP	9201	ribonucleoside triphosphate biosynthetic process	4.59E-05	4.94E-03	33/2224 1.4%	385/55204 0.6%	Upregulated
BP	42776	proton motive force-driven mitochondrial ATP synthesis	8.43E-05	8.81E-03	10/2224 0.4%	57/55204 0.1%	Upregulated
BP	44036	cell wall macromolecule metabolic process	1.23E-04	1.25E-02	17/2224 0.7%	150/55204 0.2%	Upregulated
BP	9142	nucleoside triphosphate biosynthetic process	2.36E-04	2.33E-02	33/2224 1.4%	420/55204 0.7%	Upregulated
BP	43467	regulation of generation of precursor metabolites and energy	2.50E-04	2.40E-02	23/2224 1.0%	252/55204 0.4%	Upregulated
BP	19677	NAD+ catabolic process	2.69E-04	2.45E-02	15/2224 0.6%	131/55204 0.2%	Upregulated
BP	30072	peptide hormone secretion	2.81E-04	2.45E-02	4/2224 0.1%	9/55204 0.0%	Upregulated
BP	30073	insulin secretion	2.81E-04	2.45E-02	4/2224 0.1%	9/55204 0.0%	Upregulated
BP	46879	hormone secretion	2.81E-04	2.45E-02	4/2224 0.1%	9/55204 0.0%	Upregulated
BP	9772	photosynthetic electron transport in photosystem II	3.15E-04	2.68E-02	13/2224 0.5%	105/55204 0.1%	Upregulated
BP	42548	regulation of photosynthesis, light reaction	3.70E-04	3.08E-02	19/2224 0.8%	195/55204 0.3%	Upregulated
BP	10207	photosystem II assembly	4.26E-04	3.40E-02	20/2224 0.8%	213/55204 0.3%	Upregulated
BP	2790	peptide secretion	4.54E-04	3.40E-02	4/2224 0.1%	10/55204 0.0%	Upregulated
BP	52837	thiazole biosynthetic process	4.55E-04	3.40E-02	8/2224 0.3%	46/55204 0.0%	Upregulated
BP	52838	thiazole metabolic process	4.55E-04	3.40E-02	8/2224 0.3%	46/55204 0.0%	Upregulated
BP	46484	oxazole or thiazole metabolic process	4.55E-04	3.40E-02	8/2224 0.3%	46/55204 0.0%	Upregulated
BP	16131	brassinosteroid metabolic process	4.82E-04	3.53E-02	10/2224 0.4%	70/55204 0.1%	Upregulated
BP	6952	defense response	6.39E-28	1.71E-24	174/1307 13.3%	2990/55204 5.4%	Downregulated
BP	6468	protein phosphorylation	1.37E-17	1.83E-14	120/1307 9.1%	2175/55204 3.9%	Downregulated
BP	16310	phosphorylation	5.67E-17	5.06E-14	120/1307 9.1%	2217/55204 4.0%	Downregulated
BP	9813	flavonoid biosynthetic process	3.40E-16	2.27E-13	30/1307 2.2%	192/55204 0.3%	Downregulated
BP	7165	signal transduction	6.69E-16	3.59E-13	175/1307 13.3%	3938/55204 7.1%	Downregulated
BP	7154	cell communication	9.45E-16	4.10E-13	178/1307 13.6%	4047/55204 7.3%	Downregulated
BP	23052	signaling	1.07E-15	4.10E-13	177/1307 13.5%	4021/55204 7.2%	Downregulated
BP	43412	macromolecule modification	1.99E-15	6.65E-13	271/1307 20.7%	7166/55204 12.9%	Downregulated
BP	48544	recognition of pollen	3.34E-15	9.95E-13	32/1307 2.4%	239/55204 0.4%	Downregulated
BP	9812	flavonoid metabolic process	2.71E-14	7.26E-12	30/1307 2.2%	225/55204 0.4%	Downregulated
BP	50896	response to stimulus	3.06E-14	7.44E-12	471/1307 36.0%	14712/55204 26.6%	Downregulated
BP	19748	secondary metabolic process	5.45E-14	1.22E-11	48/1307 3.6%	569/55204 1.0%	Downregulated
BP	8037	cell recognition	1.06E-13	2.19E-11	32/1307 2.4%	270/55204 0.4%	Downregulated
BP	44550	secondary metabolite biosynthetic process	1.64E-13	3.14E-11	38/1307 2.9%	383/55204 0.6%	Downregulated

Table S5.14 continued.

BP	51707	response to other organism	4.14E-13	7.11E-11	129/1307 9.8%	2787/55204 5.0%	Downregulated
BP	43207	response to external biotic stimulus	4.24E-13	7.11E-11	129/1307 9.8%	2788/55204 5.0%	Downregulated
BP	9699	phenylpropanoid biosynthetic process	5.23E-13	8.24E-11	32/1307 2.4%	286/55204 0.5%	Downregulated
BP	9607	response to biotic stimulus	6.47E-13	9.63E-11	129/1307 9.8%	2805/55204 5.0%	Downregulated
BP	44419	biological process involved in interspecies interaction between organisms	2.89E-12	4.08E-10	129/1307 9.8%	2867/55204 5.1%	Downregulated
BP	9698	phenylpropanoid metabolic process	8.47E-12	1.13E-09	36/1307 2.7%	395/55204 0.7%	Downregulated
BP	9605	response to external stimulus	9.43E-11	1.20E-08	138/1307 10.5%	3310/55204 5.9%	Downregulated
BP	9626	plant-type hypersensitive response	4.68E-10	5.70E-08	27/1307 2.0%	271/55204 0.4%	Downregulated
BP	34050	symbiont-induced defense-related programmed cell death	5.08E-10	5.92E-08	27/1307 2.0%	272/55204 0.4%	Downregulated
BP	71555	cell wall organization	5.30E-10	5.92E-08	50/1307 3.8%	789/55204 1.4%	Downregulated
BP	6950	response to stress	1.40E-09	1.50E-07	306/1307 23.4%	9393/55204 17.0%	Downregulated
BP	16138	glycoside biosynthetic process	1.56E-09	1.61E-07	12/1307 0.9%	50/55204 0.0%	Downregulated
BP	71554	cell wall organization or biogenesis	3.29E-09	3.27E-07	55/1307 4.2%	965/55204 1.7%	Downregulated
BP	2229	defense response to oomycetes	9.94E-09	9.51E-07	19/1307 1.4%	160/55204 0.2%	Downregulated
BP	16137	glycoside metabolic process	1.29E-08	1.19E-06	14/1307 1.0%	85/55204 0.1%	Downregulated
BP	19677	NAD+ catabolic process	1.54E-08	1.38E-06	17/1307 1.3%	131/55204 0.2%	Downregulated
BP	9451	RNA modification	2.71E-08	2.34E-06	99/1307 7.5%	2344/55204 4.2%	Downregulated
BP	2239	response to oomycetes	3.24E-08	2.71E-06	20/1307 1.5%	190/55204 0.3%	Downregulated
BP	36211	protein modification process	5.61E-08	4.51E-06	172/1307 13.1%	4839/55204 8.7%	Downregulated
BP	8219	cell death	5.72E-08	4.51E-06	38/1307 2.9%	598/55204 1.0%	Downregulated
BP	32870	cellular response to hormone stimulus	6.65E-08	5.09E-06	81/1307 6.1%	1823/55204 3.3%	Downregulated
BP	45229	external encapsulating structure organization	1.10E-07	8.18E-06	50/1307 3.8%	932/55204 1.6%	Downregulated
BP	71495	cellular response to endogenous stimulus	1.30E-07	9.43E-06	81/1307 6.1%	1853/55204 3.3%	Downregulated
BP	9725	response to hormone	1.38E-07	9.74E-06	111/1307 8.4%	2818/55204 5.1%	Downregulated
BP	10393	galacturonan metabolic process	2.22E-07	1.49E-05	19/1307 1.4%	194/55204 0.3%	Downregulated
BP	9755	hormone-mediated signaling pathway	2.23E-07	1.49E-05	74/1307 5.6%	1661/55204 3.0%	Downregulated
BP	9719	response to endogenous stimulus	2.29E-07	1.49E-05	111/1307 8.4%	2847/55204 5.1%	Downregulated
BP	9664	plant-type cell wall organization	3.05E-07	1.95E-05	19/1307 1.4%	198/55204 0.3%	Downregulated
BP	5976	polysaccharide metabolic process	6.02E-07	3.75E-05	59/1307 4.5%	1249/55204 2.2%	Downregulated
BP	9620	response to fungus	6.64E-07	4.05E-05	44/1307 3.3%	822/55204 1.4%	Downregulated
BP	45488	pectin metabolic process	7.49E-07	4.41E-05	18/1307 1.3%	190/55204 0.3%	Downregulated
BP	9617	response to bacterium	7.57E-07	4.41E-05	59/1307 4.5%	1258/55204 2.2%	Downregulated
BP	43068	positive regulation of programmed cell death	8.61E-07	4.91E-05	23/1307 1.7%	297/55204 0.5%	Downregulated
BP	16134	saponin metabolic process	1.38E-06	7.70E-05	9/1307 0.6%	47/55204 0.0%	Downregulated
BP	12501	programmed cell death	2.74E-06	1.48E-04	32/1307 2.4%	540/55204 0.9%	Downregulated
BP	6955	immune response	2.76E-06	1.48E-04	39/1307 2.9%	728/55204 1.3%	Downregulated

Table S5.15. Significantly enriched GO terms (Biological Process) associated with genes that significantly upregulated *in planta* compared to in culture for both *P. austrocedri* isolates at 48 hours post-inoculation (in susceptible juniper genotype only). Only the top 50 GO terms have been included.

GO	GO ID	GO Description	p-val	Corrected p-val	Cluster frequency	Total frequency
BP	22613	ribonucleoprotein complex biogenesis	7.31E-93	8.80E-90	203/971 20.9%	502/11729 4.2%
BP	42254	ribosome biogenesis		1.26E-82	173/971 17.8%	394/11729 3.3%
BP	10467	gene expression	2.25E-79	9.04E-77	401/971 41.2%	1992/11729 16.9%
BP	6412	translation	1.02E-74	3.08E-72	186/971 19.1%	516/11729 4.3%
BP	9058	biosynthetic process	1.60E-70	3.85E-68	538/971 55.4%	3440/11729 29.3%
BP	16072	rRNA metabolic process	7.28E-64	1.46E-61	132/971 13.5%	304/11729 2.5%
BP	6364	rRNA processing	8.26E-63	1.42E-60	127/971 13.0%	286/11729 2.4%
BP	9059	macromolecule biosynthetic process	1.27E-60	1.92E-58	414/971 42.6%	2406/11729 20.5%
BP	44085	cellular component biogenesis	1.32E-48	1.77E-46	228/971 23.4%	1024/11729 8.7%
BP	42273	ribosomal large subunit biogenesis	6.98E-31	8.41E-29	51/971 5.2%	94/11729 0.8%
BP	6413	translational initiation	5.01E-29	5.49E-27	55/971 5.6%	117/11729 0.9%
BP	8152	metabolic process	3.04E-26	3.05E-24	729/971 75.0%	6988/11729 59.5%
BP	34654	nucleobase-containing compound biosynthetic process	2.63E-24	2.44E-22	239/971 24.6%	1542/11729 13.1%
BP	44238	primary metabolic process	3.28E-24	2.82E-22	666/971 68.5%	6250/11729 53.2%
BP	6396	RNA processing	9.39E-23	7.55E-21	164/971 16.8%	917/11729 7.8%
BP	32774	RNA biosynthetic process	5.71E-22	4.30E-20	189/971 19.4%	1147/11729 9.7%
BP	16070	RNA metabolic process	1.62E-21	1.15E-19	209/971 21.5%	1336/11729 11.3%
BP	1732	formation of cytoplasmic translation initiation complex	2.27E-21	1.52E-19	22/971 2.2%	25/11729 0.2%
BP	22618	protein-RNA complex assembly	5.38E-20	3.41E-18	55/971 5.6%	167/11729 1.4%
BP	2183	cytoplasmic translational initiation	1.53E-19	9.23E-18	26/971 2.6%	39/11729 0.3%
BP	71826	protein-RNA complex organization	4.63E-19	2.66E-17	55/971 5.6%	174/11729 1.4%
BP	2181	cytoplasmic translation	5.06E-19	2.77E-17	35/971 3.6%	74/11729 0.6%
BP	42274	ribosomal small subunit biogenesis	1.72E-18	9.01E-17	40/971 4.1%	99/11729 0.8%
BP	6164	purine nucleotide biosynthetic process	2.03E-18	1.02E-16	38/971 3.9%	90/11729 0.7%
BP	46390	ribose phosphate biosynthetic process	4.27E-18	2.06E-16	37/971 3.8%	87/11729 0.7%
BP	9260	ribonucleotide biosynthetic process	1.15E-17	5.32E-16	35/971 3.6%	80/11729 0.6%
BP	9152	purine ribonucleotide biosynthetic process	2.25E-17	1.00E-15	31/971 3.1%	64/11729 0.5%
BP	30490	maturation of SSU-rRNA	2.92E-17	1.25E-15	33/971 3.3%	73/11729 0.6%
BP	141187	nucleic acid biosynthetic process	3.01E-17	1.25E-15	192/971 19.7%	1290/11729 10.9%
BP	19693	ribose phosphate metabolic process	5.29E-16	2.12E-14	49/971 5.0%	164/11729 1.3%
BP	9259	ribonucleotide metabolic process	6.36E-16	2.47E-14	47/971 4.8%	153/11729 1.3%
BP	42255	ribosome assembly	1.58E-15	5.95E-14	28/971 2.8%	59/11729 0.5%
BP	9150	purine ribonucleotide metabolic process	4.73E-15	1.73E-13	43/971 4.4%	137/11729 1.1%
BP	9126	purine nucleoside monophosphate metabolic process	1.63E-14	5.61E-13	22/971 2.2%	39/11729 0.3%
BP	9167	purine ribonucleoside monophosphate metabolic process	1.63E-14	5.61E-13	22/971 2.2%	39/11729 0.3%
BP	6163	purine nucleotide metabolic process	1.94E-14	6.50E-13	52/971 5.3%	197/11729 1.6%
BP	43170	macromolecule metabolic process	4.02E-14	1.31E-12	504/971 51.9%	4748/11729 40.4%
BP	9127	purine nucleoside monophosphate biosynthetic process	5.50E-14	1.70E-12	21/971 2.1%	37/11729 0.3%
BP	9168	purine ribonucleoside monophosphate biosynthetic process	5.50E-14	1.70E-12	21/971 2.1%	37/11729 0.3%
BP	462	maturation of SSU-rRNA from tricistronic rRNA transcript (SSU-rRNA, 5.8S rRNA, LSU-rRNA)	6.28E-14	1.89E-12	25/971 2.5%	53/11729 0.4%
BP	71840	cellular component organization or biogenesis	2.97E-13	8.72E-12	286/971 29.4%	2362/11729 20.1%
BP	6189	'de novo' IMP biosynthetic process	7.14E-13	2.05E-11	13/971 1.3%	15/11729 0.1%
BP	72522	purine-containing compound biosynthetic process	1.01E-12	2.84E-11	41/971 4.2%	145/11729 1.2%
BP	9165	nucleotide biosynthetic process	1.46E-12	3.99E-11	46/971 4.7%	178/11729 1.5%
BP	9156	ribonucleoside monophosphate biosynthetic process	2.09E-12	5.61E-11	23/971 2.3%	51/11729 0.4%
BP	460	maturation of 5.8S rRNA	7.09E-12	1.86E-10	22/971 2.2%	49/11729 0.4%
BP	27	ribosomal large subunit assembly	1.81E-11	4.63E-10	19/971 1.9%	38/11729 0.3%
BP	72521	purine-containing compound metabolic process	3.34E-11	8.39E-10	58/971 5.9%	279/11729 2.3%
BP	9117	nucleotide metabolic process	8.49E-11	2.09E-09	61/971 6.2%	308/11729 2.6%
BP	46040	IMP metabolic process	1.11E-10	2.66E-09	14/971 1.4%	22/11729 0.1%

Table S5.16. Significantly enriched GO terms (Biological Process) associated with genes that significantly upregulated *in planta* compared to in culture for both *P. austrocedri* isolates at one week post-inoculation (in susceptible juniper genotype only). Only the top 50 GO terms have been included.

GO	GO ID	GO Description	p-val	Corrected p-val	Cluster frequency	Total frequency
BP	44282	small molecule catabolic process	3.28E-23	3.69E-20	54/575 9.3%	225/11729 1.9%
BP	46395	carboxylic acid catabolic process	1.48E-21	5.55E-19	46/575 8.0%	176/11729 1.5%
BP	16054	organic acid catabolic process	1.48E-21	5.55E-19	46/575 8.0%	176/11729 1.5%
BP	9056	catabolic process	2.93E-20	8.26E-18	146/575 25.3%	1392/11729 11.8%
BP	16042	lipid catabolic process	2.06E-19	4.64E-17	43/575 7.4%	172/11729 1.4%
BP	272	polysaccharide catabolic process	1.70E-18	3.19E-16	51/575 8.8%	252/11729 2.1%
BP	72329	monocarboxylic acid catabolic process	2.63E-18	4.23E-16	29/575 5.0%	80/11729 0.6%
BP	9062	fatty acid catabolic process	4.07E-18	5.74E-16	28/575 4.8%	75/11729 0.6%
BP	16052	carbohydrate catabolic process	2.02E-17	2.53E-15	59/575 10.2%	347/11729 2.9%
BP	5975	carbohydrate metabolic process	1.32E-16	1.48E-14	89/575 15.4%	717/11729 6.1%
BP	6635	fatty acid beta-oxidation	1.73E-16	1.78E-14	25/575 4.3%	66/11729 0.5%
BP	19752	carboxylic acid metabolic process	1.99E-16	1.87E-14	87/575 15.1%	696/11729 5.9%
BP	43436	oxoacid metabolic process	8.04E-16	6.47E-14	87/575 15.1%	712/11729 6.0%
BP	6082	organic acid metabolic process	8.04E-16	6.47E-14	87/575 15.1%	712/11729 6.0%
BP	19395	fatty acid oxidation	8.86E-16	6.66E-14	25/575 4.3%	70/11729 0.5%
BP	44281	small molecule metabolic process	2.26E-15	1.59E-13	122/575 21.2%	1212/11729 10.3%
BP	34440	lipid oxidation	2.77E-15	1.84E-13	25/575 4.3%	73/11729 0.6%
BP	6631	fatty acid metabolic process	8.59E-15	5.38E-13	40/575 6.9%	197/11729 1.6%
BP	5976	polysaccharide metabolic process	4.54E-14	2.70E-12	59/575 10.2%	409/11729 3.4%
BP	6629	lipid metabolic process	1.28E-13	7.23E-12	84/575 14.6%	735/11729 6.2%
BP	32787	monocarboxylic acid metabolic process	1.69E-13	9.07E-12	53/575 9.2%	352/11729 3.0%
BP	6570	tyrosine metabolic process	1.54E-12	7.89E-11	9/575 1.5%	9/11729 0.0%
BP	30258	lipid modification	2.17E-10	1.07E-08	25/575 4.3%	115/11729 0.9%
BP	6572	L-tyrosine catabolic process	6.57E-10	3.09E-08	7/575 1.2%	7/11729 0.0%
BP	9074	aromatic amino acid family catabolic process	1.06E-09	4.77E-08	10/575 1.7%	17/11729 0.1%
BP	10393	galacturonan metabolic process	3.41E-09	1.37E-07	18/575 3.1%	69/11729 0.5%
BP	45488	pectin metabolic process	3.41E-09	1.37E-07	18/575 3.1%	69/11729 0.5%
BP	45490	pectin catabolic process	3.41E-09	1.37E-07	18/575 3.1%	69/11729 0.5%
BP	6559	L-phenylalanine catabolic process	1.32E-08	5.14E-07	8/575 1.3%	12/11729 0.1%
BP	72593	reactive oxygen species metabolic process	2.37E-08	8.89E-07	12/575 2.0%	33/11729 0.2%
BP	1902222	erythrose 4-phosphate/phosphoenolpyruvate family amino acid catabolic process	3.29E-08	1.20E-06	8/575 1.3%	13/11729 0.1%
BP	33540	fatty acid beta-oxidation using acyl-CoA oxidase	5.22E-07	1.84E-05	8/575 1.3%	17/11729 0.1%
BP	6558	L-phenylalanine metabolic process	6.77E-07	2.31E-05	9/575 1.5%	23/11729 0.1%
BP	170035	L-amino acid catabolic process	1.11E-06	3.69E-05	15/575 2.6%	70/11729 0.5%
BP	9063	amino acid catabolic process	2.29E-06	7.38E-05	17/575 2.9%	93/11729 0.7%
BP	170040	proteinogenic amino acid catabolic process	2.80E-06	8.76E-05	15/575 2.6%	75/11729 0.6%
BP	55088	lipid homeostasis	2.94E-06	8.76E-05	11/575 1.9%	41/11729 0.3%
BP	6091	generation of precursor metabolites and energy	2.95E-06	8.76E-05	29/575 5.0%	231/11729 1.9%
BP	6099	tricarboxylic acid cycle	4.90E-06	1.42E-04	11/575 1.9%	43/11729 0.3%
BP	9251	glucan catabolic process	7.62E-06	2.10E-04	15/575 2.6%	81/11729 0.6%
BP	1901606	alpha-amino acid catabolic process	7.62E-06	2.10E-04	15/575 2.6%	81/11729 0.6%
BP	1901568	fatty acid derivative metabolic process	8.10E-06	2.17E-04	8/575 1.3%	23/11729 0.1%
BP	302	response to reactive oxygen species	1.73E-05	4.53E-04	6/575 1.0%	13/11729 0.1%
BP	72522	purine-containing compound biosynthetic process	2.60E-05	6.66E-04	20/575 3.4%	145/11729 1.2%
BP	6164	purine nucleotide biosynthetic process	2.85E-05	7.13E-04	15/575 2.6%	90/11729 0.7%
BP	51275	beta-glucan catabolic process	5.56E-05	1.33E-03	9/575 1.5%	37/11729 0.3%
BP	30245	cellulose catabolic process	5.56E-05	1.33E-03	9/575 1.5%	37/11729 0.3%
BP	42743	hydrogen peroxide metabolic process	5.87E-05	1.35E-03	7/575 1.2%	22/11729 0.1%
BP	42744	hydrogen peroxide catabolic process	5.87E-05	1.35E-03	7/575 1.2%	22/11729 0.1%
BP	9060	aerobic respiration	6.08E-05	1.37E-03	21/575 3.6%	166/11729 1.4%

Table S5.17. Significantly enriched GO terms (Biological Process) associated with *P. austrocedri* genes differentially expressed between timepoints *in planta* (one week versus 48 hours post inoculation). Genes were divided into three clusters based on expression patterns: Cluster 1 was more highly expressed at 48 hours, Cluster 2 was more highly expressed at one week, and Cluster 3 was more highly expressed at one week and in the less virulent isolate growing in the resistant genotype at 48 hours. Where relevant, only the top 50 GO terms have been included for each cluster.

GO	GO ID	GO Description	p-val	Corrected p-val	Cluster frequency	Total frequency	Cluster
BP	42254	ribosome biogenesis	2.54E-134	0.00E+00	206/849 24.2%	394/11729 3.3%	One
BP	22613	ribonucleoprotein complex biogenesis	7.80E-129	0.00E+00	225/849 26.5%	502/11729 4.2%	One
BP	16072	rRNA metabolic process	2.79E-102	1.10E-99	159/849 18.7%	304/11729 2.5%	One
BP	6364	rRNA processing	1.79E-101	5.40E-99	154/849 18.1%	286/11729 2.4%	One
BP	9058	biosynthetic process	1.65E-88	3.98E-86	518/849 61.0%	3440/11729 29.3%	One
BP	10467	gene expression	2.96E-87	5.93E-85	380/849 44.7%	1992/11729 16.9%	One
BP	44085	cellular component biogenesis	1.97E-67	3.38E-65	239/849 28.1%	1024/11729 8.7%	One
BP	9059	macromolecule biosynthetic process	4.13E-67	6.21E-65	389/849 45.8%	2406/11729 20.5%	One
BP	16070	RNA metabolic process	6.65E-52	8.89E-50	252/849 29.6%	1336/11729 11.3%	One
BP	32774	RNA biosynthetic process	1.67E-47	2.01E-45	223/849 26.2%	1147/11729 9.7%	One
BP	34654	nucleobase-containing compound biosynthetic process	1.12E-46	1.22E-44	265/849 31.2%	1542/11729 13.1%	One
BP	6396	RNA processing	1.67E-46	1.67E-44	194/849 22.8%	917/11729 7.8%	One
BP	141187	nucleic acid biosynthetic process	9.15E-40	8.46E-38	225/849 26.5%	1290/11729 10.9%	One
BP	6412	translation	3.25E-38	2.79E-36	129/849 15.1%	516/11729 4.3%	One
BP	42273	ribosomal large subunit biogenesis	5.95E-35	4.77E-33	52/849 6.1%	94/11729 0.8%	One
BP	42274	ribosomal small subunit biogenesis	1.28E-34	9.59E-33	53/849 6.2%	99/11729 0.8%	One
BP	30490	maturation of SSU-rRNA	1.16E-30	8.20E-29	43/849 5.0%	73/11729 0.6%	One
BP	462	maturation of SSU-rRNA from tricistronic rRNA transcript	1.36E-23	9.07E-22	32/849 3.7%	53/11729 0.4%	One
BP	8152	metabolic process	1.77E-23	1.12E-21	639/849 75.2%	6988/11729 59.5%	One
BP	6139	nucleobase-containing compound metabolic process	2.06E-23	1.24E-21	320/849 37.6%	2710/11729 23.1%	One
BP	44238	primary metabolic process	2.88E-23	1.65E-21	589/849 69.3%	6250/11729 53.2%	One
BP	71840	cellular component organization or biogenesis	9.26E-23	5.06E-21	288/849 33.9%	2362/11729 20.1%	One
BP	6520	amino acid metabolic process	5.47E-20	2.86E-18	87/849 10.2%	418/11729 3.5%	One
BP	6413	translational initiation	2.18E-18	1.09E-16	41/849 4.8%	117/11729 0.9%	One
BP	1901605	alpha-amino acid metabolic process	1.58E-16	7.60E-15	65/849 7.6%	294/11729 2.5%	One
BP	8652	amino acid biosynthetic process	1.91E-16	8.83E-15	53/849 6.2%	208/11729 1.7%	One
BP	90304	nucleic acid metabolic process	2.66E-16	1.19E-14	259/849 30.5%	2263/11729 19.2%	One
BP	170039	proteinogenic amino acid metabolic process	1.54E-15	6.62E-14	62/849 7.3%	284/11729 2.4%	One
BP	170038	proteinogenic amino acid biosynthetic process	2.72E-15	1.13E-13	46/849 5.4%	172/11729 1.4%	One
BP	9451	RNA modification	1.23E-14	4.92E-13	53/849 6.2%	228/11729 1.9%	One
BP	470	maturation of LSU-rRNA	1.44E-14	5.60E-13	20/849 2.3%	35/11729 0.2%	One
BP	1732	formation of cytoplasmic translation initiation complex	2.20E-14	8.26E-13	17/849 2.0%	25/11729 0.2%	One
BP	170034	L-amino acid biosynthetic process	2.35E-14	8.58E-13	43/849 5.0%	161/11729 1.3%	One
BP	1901607	alpha-amino acid biosynthetic process	3.36E-14	1.19E-12	48/849 5.6%	197/11729 1.6%	One
BP	460	maturation of 5.8S rRNA	4.23E-14	1.45E-12	23/849 2.7%	49/11729 0.4%	One
BP	170033	L-amino acid metabolic process	9.00E-14	3.01E-12	58/849 6.8%	277/11729 2.3%	One
BP	22618	protein-RNA complex assembly	9.53E-14	3.10E-12	43/849 5.0%	167/11729 1.4%	One
BP	71826	protein-RNA complex organization	4.43E-13	1.40E-11	43/849 5.0%	174/11729 1.4%	One
BP	42255	ribosome assembly	5.89E-13	1.79E-11	24/849 2.8%	59/11729 0.5%	One
BP	43170	macromolecule metabolic process	5.95E-13	1.79E-11	443/849 52.1%	4748/11729 40.4%	One
BP	9127	purine nucleoside monophosphate biosynthetic process	9.00E-13	2.58E-11	19/849 2.2%	37/11729 0.3%	One
BP	9168	purine ribonucleoside monophosphate biosynthetic process	9.00E-13	2.58E-11	19/849 2.2%	37/11729 0.3%	One
BP	46394	carboxylic acid biosynthetic process	1.83E-12	5.01E-11	61/849 7.1%	321/11729 2.7%	One
BP	16053	organic acid biosynthetic process	1.83E-12	5.01E-11	61/849 7.1%	321/11729 2.7%	One
BP	2183	cytoplasmic translational initiation	3.06E-12	7.82E-11	19/849 2.2%	39/11729 0.3%	One
BP	9126	purine nucleoside monophosphate metabolic process	3.06E-12	7.82E-11	19/849 2.2%	39/11729 0.3%	One
BP	9167	purine ribonucleoside monophosphate metabolic process	3.06E-12	7.82E-11	19/849 2.2%	39/11729 0.3%	One
BP	19693	ribose phosphate metabolic process	4.61E-12	1.16E-10	40/849 4.7%	164/11729 1.3%	One
BP	9259	ribonucleotide metabolic process	8.80E-12	2.16E-10	38/849 4.4%	153/11729 1.3%	One
BP	6360	transcription by RNA polymerase I	1.16E-11	2.79E-10	20/849 2.3%	46/11729 0.3%	One
BP	9056	catabolic process	1.34E-11	1.88E-08	169/869 19.4%	1392/11729 11.8%	Two
BP	9074	aromatic amino acid family catabolic process	2.84E-09	2.00E-06	11/869 1.2%	17/11729 0.1%	Two
BP	44282	small molecule catabolic process	6.25E-09	2.61E-06	43/869 4.9%	225/11729 1.9%	Two
BP	6570	tyrosine metabolic process	7.41E-09	2.61E-06	8/869 0.9%	9/11729 0.0%	Two
BP	61919	process utilizing autophagic mechanism	1.00E-07	2.34E-05	23/869 2.6%	90/11729 0.7%	Two
BP	6914	autophagy	1.00E-07	2.34E-05	23/869 2.6%	90/11729 0.7%	Two
BP	46395	carboxylic acid catabolic process	1.86E-07	3.20E-05	34/869 3.9%	176/11729 1.5%	Two
BP	16054	organic acid catabolic process	1.86E-07	3.20E-05	34/869 3.9%	176/11729 1.5%	Two
BP	6558	L-phenylalanine metabolic process	2.05E-07	3.20E-05	11/869 1.2%	23/11729 0.1%	Two
BP	6559	L-phenylalanine catabolic process	3.33E-07	4.68E-05	8/869 0.9%	12/11729 0.1%	Two
BP	1902222	erythrose 4-phosphate/phosphoenolpyruvate family amino acid catabolic process	8.10E-07	1.03E-04	8/869 0.9%	13/11729 0.1%	Two
BP	6572	L-tyrosine catabolic process	1.07E-06	1.25E-04	6/869 0.6%	7/11729 0.0%	Two
BP	16197	endosomal transport	7.13E-06	7.72E-04	26/869 2.9%	137/11729 1.1%	Two
BP	7031	peroxisome organization	7.88E-06	7.92E-04	14/869 1.6%	49/11729 0.4%	Two
BP	170035	L-amino acid catabolic process	9.74E-06	9.13E-04	17/869 1.9%	70/11729 0.5%	Two
BP	9063	amino acid catabolic process	1.19E-05	1.04E-03	20/869 2.3%	93/11729 0.7%	Two
BP	1901606	alpha-amino acid catabolic process	2.01E-05	1.66E-03	18/869 2.0%	81/11729 0.6%	Two

Table S5.17 continued.

BP	170040	proteinogenic amino acid catabolic process	2.58E-05	2.02E-03	17/869 1.9%	75/11729 0.6%	Two
BP	44804	nucleophagy	3.05E-05	2.26E-03	9/869 1.0%	24/11729 0.2%	Two
BP	30163	protein catabolic process	3.54E-05	2.49E-03	56/869 6.4%	437/11729 3.7%	Two
BP	43605	amide catabolic process	5.43E-05	3.64E-03	6/869 0.6%	11/11729 0.0%	Two
BP	7034	vacuolar transport	7.32E-05	4.68E-03	21/869 2.4%	113/11729 0.9%	Two
BP	36211	protein modification process	9.58E-05	5.34E-03	63/869 7.2%	527/11729 4.4%	Two
BP	16192	vesicle-mediated transport	9.90E-05	5.34E-03	65/869 7.4%	549/11729 4.6%	Two
BP	422	autophagy of mitochondrion	1.09E-04	5.34E-03	11/869 1.2%	40/11729 0.3%	Two
BP	16558	protein import into peroxisome matrix	1.10E-04	5.34E-03	8/869 0.9%	22/11729 0.1%	Two
BP	44743	protein transmembrane import into intracellular organelle	1.10E-04	5.34E-03	8/869 0.9%	22/11729 0.1%	Two
BP	16237	microautophagy	1.10E-04	5.34E-03	8/869 0.9%	22/11729 0.1%	Two
BP	34727	piecemeal microautophagy of the nucleus	1.10E-04	5.34E-03	8/869 0.9%	22/11729 0.1%	Two
BP	6012	galactose metabolic process	1.41E-04	6.60E-03	4/869 0.4%	5/11729 0.0%	Two
BP	9072	aromatic amino acid metabolic process	1.97E-04	8.77E-03	14/869 1.6%	64/11729 0.5%	Two
BP	5975	carbohydrate metabolic process	2.02E-04	8.77E-03	79/869 9.0%	717/11729 6.1%	Two
BP	43687	post-translational protein modification	2.06E-04	8.77E-03	54/869 6.2%	445/11729 3.7%	Two
BP	16482	cytosolic transport	2.34E-04	9.67E-03	14/869 1.6%	65/11729 0.5%	Two
BP	16567	protein ubiquitination	2.44E-04	9.78E-03	41/869 4.7%	313/11729 2.6%	Two
BP	43574	peroxisomal transport	2.94E-04	1.12E-02	9/869 1.0%	31/11729 0.2%	Two
BP	15919	peroxisomal membrane transport	2.94E-04	1.12E-02	9/869 1.0%	31/11729 0.2%	Two
BP	51603	proteolysis involved in protein catabolic process	3.79E-04	1.40E-02	51/869 5.8%	424/11729 3.6%	Two
BP	51592	response to calcium ion	4.05E-04	1.43E-02	3/869 0.3%	3/11729 0.0%	Two
BP	71277	cellular response to calcium ion	4.05E-04	1.43E-02	3/869 0.3%	3/11729 0.0%	Two
BP	72663	establishment of protein localization to peroxisome	5.48E-04	1.83E-02	8/869 0.9%	27/11729 0.2%	Two
BP	72662	protein localization to peroxisome	5.48E-04	1.83E-02	8/869 0.9%	27/11729 0.2%	Two
BP	10498	proteasomal protein catabolic process	6.34E-04	2.05E-02	28/869 3.2%	197/11729 1.6%	Two
BP	55088	lipid homeostasis	6.40E-04	2.05E-02	10/869 1.1%	41/11729 0.3%	Two
BP	72329	monocarboxylic acid catabolic process	6.89E-04	2.15E-02	15/869 1.7%	80/11729 0.6%	Two
BP	32446	protein modification by small protein conjugation	7.10E-04	2.17E-02	42/869 4.8%	340/11729 2.8%	Two
BP	209	protein polyubiquitination	7.32E-04	2.19E-02	18/869 2.0%	106/11729 0.9%	Two
BP	70647	protein modification by small protein conjugation or removal	8.06E-04	2.36E-02	51/869 5.8%	438/11729 3.7%	Two
BP	45	autophagosome assembly	1.06E-03	2.97E-02	11/869 1.2%	51/11729 0.4%	Two
BP	1905037	autophagosome organization	1.06E-03	2.97E-02	11/869 1.2%	51/11729 0.4%	Two
BP	44282	small molecule catabolic process	2.90E-22	2.21E-19	57/674 8.4%	225/11729 1.9%	Three
BP	46395	carboxylic acid catabolic process	4.88E-22	2.21E-19	50/674 7.4%	176/11729 1.5%	Three
BP	16054	organic acid catabolic process	4.88E-22	2.21E-19	50/674 7.4%	176/11729 1.5%	Three
BP	9056	catabolic process	1.19E-20	4.05E-18	164/674 24.3%	1392/11729 11.8%	Three
BP	72329	monocarboxylic acid catabolic process	1.56E-19	4.15E-17	32/674 4.7%	80/11729 0.6%	Three
BP	9062	fatty acid catabolic process	1.83E-19	4.15E-17	31/674 4.5%	75/11729 0.6%	Three
BP	16042	lipid catabolic process	2.16E-18	4.20E-16	45/674 6.6%	172/11729 1.4%	Three
BP	19395	fatty acid oxidation	2.54E-18	4.31E-16	29/674 4.3%	70/11729 0.5%	Three
BP	6631	fatty acid metabolic process	3.71E-18	5.60E-16	48/674 7.1%	197/11729 1.6%	Three
BP	34440	lipid oxidation	1.01E-17	1.37E-15	29/674 4.3%	73/11729 0.6%	Three
BP	6635	fatty acid beta-oxidation	5.61E-17	6.92E-15	27/674 4.0%	66/11729 0.5%	Three
BP	32787	monocarboxylic acid metabolic process	2.97E-16	3.36E-14	63/674 9.3%	352/11729 3.0%	Three
BP	30258	lipid modification	4.32E-15	4.51E-13	33/674 4.8%	115/11729 0.9%	Three
BP	6629	lipid metabolic process	9.35E-15	9.07E-13	96/674 14.2%	735/11729 6.2%	Three
BP	19752	carboxylic acid metabolic process	3.50E-13	3.17E-11	89/674 13.2%	696/11729 5.9%	Three
BP	43436	oxoacid metabolic process	4.97E-13	3.97E-11	90/674 13.3%	712/11729 6.0%	Three
BP	6082	organic acid metabolic process	4.97E-13	3.97E-11	90/674 13.3%	712/11729 6.0%	Three
BP	44281	small molecule metabolic process	1.80E-09	1.36E-07	119/674 17.6%	1212/11729 10.3%	Three
BP	45	autophagosome assembly	6.64E-07	4.51E-05	14/674 2.0%	51/11729 0.4%	Three
BP	1905037	autophagosome organization	6.64E-07	4.51E-05	14/674 2.0%	51/11729 0.4%	Three
BP	16236	macroautophagy	1.30E-06	8.39E-05	16/674 2.3%	69/11729 0.5%	Three
BP	61919	process utilizing autophagic mechanism	2.85E-06	1.68E-04	18/674 2.6%	90/11729 0.7%	Three
BP	6914	autophagy	2.85E-06	1.68E-04	18/674 2.6%	90/11729 0.7%	Three
BP	9063	amino acid catabolic process	4.66E-06	2.64E-04	18/674 2.6%	93/11729 0.7%	Three
BP	170035	L-amino acid catabolic process	7.88E-06	4.28E-04	15/674 2.2%	70/11729 0.5%	Three
BP	422	autophagy of mitochondrion	1.04E-05	5.42E-04	11/674 1.6%	40/11729 0.3%	Three
BP	1901606	alpha-amino acid catabolic process	1.19E-05	6.00E-04	16/674 2.3%	81/11729 0.6%	Three
BP	170040	proteinogenic amino acid catabolic process	1.91E-05	9.24E-04	15/674 2.2%	75/11729 0.6%	Three
BP	7033	vacuole organization	2.55E-05	1.17E-03	14/674 2.0%	68/11729 0.5%	Three
BP	9083	branched-chain amino acid catabolic process	2.59E-05	1.17E-03	8/674 1.1%	23/11729 0.1%	Three
BP	9437	carnitine metabolic process	2.99E-05	1.31E-03	5/674 0.7%	8/11729 0.0%	Three
BP	6577	amino-acid betaine metabolic process	1.13E-04	4.78E-03	6/674 0.8%	15/11729 0.1%	Three
BP	51865	protein autoubiquitination	1.48E-04	5.73E-03	4/674 0.5%	6/11729 0.0%	Three
BP	46487	glyoxylate metabolic process	1.48E-04	5.73E-03	4/674 0.5%	6/11729 0.0%	Three
BP	6097	glyoxylate cycle	1.48E-04	5.73E-03	4/674 0.5%	6/11729 0.0%	Three
BP	16237	microautophagy	1.60E-04	5.87E-03	7/674 1.0%	22/11729 0.1%	Three
BP	34727	piecemeal microautophagy of the nucleus	1.60E-04	5.87E-03	7/674 1.0%	22/11729 0.1%	Three
BP	46459	short-chain fatty acid metabolic process	1.89E-04	6.75E-03	3/674 0.4%	3/11729 0.0%	Three
BP	44804	nucleophagy	2.94E-04	1.02E-02	7/674 1.0%	24/11729 0.2%	Three
BP	7031	peroxisome organization	3.92E-04	1.33E-02	10/674 1.4%	49/11729 0.4%	Three

Table S5.17 continued.

BP	43632	modification-dependent macromolecule catabolic process	5.15E-04	1.71E-02	36/674 5.3%	351/11729 2.9%	Three
BP	9080	pyruvate family amino acid catabolic process	6.81E-04	2.20E-02	6/674 0.8%	20/11729 0.1%	Three
BP	16192	vesicle-mediated transport	7.82E-04	2.47E-02	50/674 7.4%	549/11729 4.6%	Three
BP	43328	protein transport to vacuole involved in ubiquitin-dependent protein catabolic process	1.20E-03	3.70E-02	8/674 1.1%	38/11729 0.3%	Three
BP	6511	ubiquitin-dependent protein catabolic process	1.41E-03	4.24E-02	33/674 4.8%	331/11729 2.8%	Three
BP	19941	modification-dependent protein catabolic process	1.55E-03	4.58E-02	33/674 4.8%	333/11729 2.8%	Three
BP	43162	ubiquitin-dependent protein catabolic process via the multivesicular body sorting pathway	1.70E-03	4.80E-02	8/674 1.1%	40/11729 0.3%	Three
BP	16559	peroxisome fission	1.72E-03	4.80E-02	4/674 0.5%	10/11729 0.0%	Three
BP	19563	glycerol catabolic process	1.73E-03	4.80E-02	3/674 0.4%	5/11729 0.0%	Three